

Julius-Maximilian-Universität Wuerzburg



**The SnRK1-C/S1-bZIPs network:
a signalling hub in *Arabidopsis*
energy metabolism regulation**

Dissertation zur Erlangung des
naturwissenschaftlichen Doktorgrades
der Julius-Maximilians-Universität Würzburg

vorgelegt von

Lorenzo Pedrotti

geboren in Rovereto

Würzburg 2015



Eingereicht am:

Mitglieder der Promotionskommission:

Vorsitzender:

Gutachter :

Gutachter:

Tag des Promotionskolloquiums:

Doktorurkunde ausgehändigt am:

Table of contents

Summary	<i>i</i>
Zusammenfassung	<i>iii</i>
Introduction	
1 The low energy signaling network	1
2 SnRK1 and C/S1 bZIPs are important regulators of cellular respiration under Low Energy Stress	15
Results	
3 SnRK1-triggered switch of bZIP63 dimerization mediates the low energy response in plants	31
4 Stress-triggered reprogramming of plant mitochondrial metabolism via SnRK1-bZIP complexes	105
5 Crosstalk between two basic leucine zipper signaling pathways orchestrates salt-induced metabolic reprogramming in <i>Arabidopsis</i> roots	147
6 The crucial metabolic kinase SnRK1 controls lipid degradation to support phase transition from heterotrophy to autotrophy during <i>Arabidopsis</i> seedling establishment	191
General discussion and conclusion	213
Own contribution to the thesis	I
<i>Curriculum vitae</i>	III
Acknowledgment	V
Affidavit	VII

Summary

The control of energy homeostasis is of pivotal importance for all living organisms. In the last years emerged the idea that many stress responses that are apparently unrelated, are actually united by a common increase of the cellular energy demand. Therefore, the so called energy signaling is activated by many kind of stresses and is responsible for the activation of the general stress response. In *Arabidopsis thaliana* the protein family SnF1-related protein kinases (SnRK1) is involved in the regulation of many physiological processes but is more known for its involvement in the regulation of the energy homeostasis in response to various stresses. To the SnRK1 protein family belong SnRK1.1 (also known as KIN10), SnRK1.2 (KIN11), and SnRK1.3 (KIN12). SnRK1 exerts its function regulating directly the activity of metabolic enzymes or those of key transcription factors (TFs). The only TFs regulated by SnRK1 identified so far is the basic leucine zipper (bZIP) 63. bZIP63 belongs to the C group of bZIPs (C-bZIPs) protein family together with bZIP9, bZIP10, and bZIP25. SnRK1.1 phosphorylates bZIP63 on three amino acids residues, serine (S) 29, S294, and S300. The phosphorylation of bZIP63 is strongly related to the energy status of the plant, shifting from almost absent during the normal growth to strongly phosphorylated when the plant is exposed to extended dark. bZIPs normally bind the DNA as dimer in order to regulate the expression of their target genes. C-bZIPs preferentially form dimers with S1-bZIPs, constituting the so called C/S1-bZIPs network. The SnRk1 dependent phosphorylation of bZIP63 regulates its activation potential and its dimerization properties. In particular bZIP63 shift its dimerization preferences according to its phosphorylation status. The non-phosphorylated form of bZIP63 dimerize bZIP1, the phosphorylates ones, instead, forms dimer with bZIP1, bZIP11, and bZIP63 its self. Together with bZIP63, S1-bZIPs are important mediator of part of the huge transcriptional reprogramming induced by SnRK1 in response to extended dark. S1-bZIPs regulate, indeed, the expression of 4'000 of the 10'000 SnRK1-regulated genes in response to energy deprivation. In particular S1-bZIPs are very important for the regulation of many genes encoding for enzymes involved in the amino acid metabolism and for their use as alternative energy source. After the exposition for some hours to extended dark, indeed, the plant make use of every energy substrate and amino acids are considered an important energy source together with lipids and proteins. Interestingly, S1-bZIPs regulate the expression of *ETFQO*. *ETFQO* is a unique protein that convoglia the

electrons provenienti from the branch chain amino acids catabolism into the mitochondrial electron transport chain. The dimer formed between bZIP63 and bZIP2 recruits SnRK1.1 directly on the chromatin of *ETFQO* promoter. The recruitment of SnRK1 on *ETFQO* promoter is associated with its acetylation on the lysine 14 of the histone protein 3 (K14H3). This chromatin modification is normally associated with an euchromatic status of the DNA and therefore with its transcriptional activation. Beside the particular case of the regulation of *ETFQO* gene, S1-bZIPs are involved in the regulation of many other genes activated in response of different stresses. bZIP1 is for example an important mediator of the salt stress response. In particular bZIP1 regulates the primary C- and N-metabolism. The expression of *bZIP1*, in response of both salt and energy stress seems to be regulated by SnRK1, as it is the expression of *bZIP53* and *bZIP63*.

Beside its involvement in the regulation of the energy stress response and salt response, SnRK1 is the primary activators of the lipids metabolism during seed germination. SnRK1, indeed, controls the expression of *CALEOSINs* and *OLEOSINs*. Those proteins are very important for lipids remobilization from oil droplets. Without their expression seed germination and subsequent establishment do not take place because of the absence of fuel to sustain these highly energy costly processes, which entirely depend on the catabolism of seed storages.

Zusammenfassung

Die Kontrolle der Energiehomöostase ist für alle lebenden Organismen von großer Bedeutung. In den letzten Jahren kam die Idee auf, dass viele Stressantworten, die scheinbar unabhängig voneinander sind, durch den Energiebedarf doch miteinander verbunden sind. Das sogenannte Energie-*Signaling* wird von vielen verschiedenen Stress-Arten aktiviert und ist verantwortlich für die Aktivierung der allgemeinen Stressantwort. In *Arabidopsis thaliana* ist die Proteinfamilie der SnF1-verwandten Proteinkinasen (SnRK1) an der Regulation vieler physiologischer Prozesse beteiligt. Auch bei der Regulation der Energiehomöostase als Folge von Stress spielen SnRK1-Kinasen eine wichtige Rolle. Proteine aus der SnRK1-Familie sind SnRK1.1, auch als KIN10 bezeichnet, SnRK1.2 (KIN11) und SnRK1.3 (KIN12). SnRK1-Proteine können die Aktivität von metabolischen Enzyme oder bestimmten Transkriptionsfaktoren (TF) direkt regulieren. Bislang wurde nur für den basischen Leucin-Zipper (bZIP) TF bZIP63 die Regulation durch SnRK1 gezeigt. bZIP63 gehört zur Gruppe C der bZIP Proteinfamilie (C-bZIP). Ebenfalls zu Gruppe C werden bZIP9, bZIP10 und bZIP25 zugeordnet. SnRK1.1 phosphoryliert das bZIP63-Protein an Serin (S) 29, S294 und S300. Der Grad der Phosphorylierung von bZIP63 steht in direktem Zusammenhang mit dem Energiehaushalt der Pflanze. Unter normalen Bedingungen wird bZIP63 kaum phosphoryliert, während bei verlängerter Nacht bZIP63 stark phosphoryliert wird. bZIP TF bilden untereinander Dimere aus und binden so an die DNA um die Expression ihrer Zielgene zu regulieren. C-bZIP TF bilden bevorzugt Dimere mit bZIP TF der Gruppe S1, bekannt als das C/S1-bZIP-Netzwerk. Die SnRK1-abhängige Phosphorylierung von bZIP63 steuert das Aktivierungspotential und die Dimerisierungseigenschaften. Besonders bei bZIP63 ändern sich die Dimerisierungspartner in Abhängigkeit des Phosphorylierungsgrads. Nicht-phosphoryliert dimerisiert bZIP61 mit bZIP1, im phosphorylierten Zustand dagegen bildet bZIP63 Dimere neben bZIP1 auch mit bZIP11 und bZIP63.

S1-bZIP TF sowie bZIP63 sind wichtige Regulatoren der transkriptionellen Reprogrammierung, die durch SnRK1 bei verlängerter Dunkelheit induziert wird. S1-bZIP TF regulieren die Expression von 4'000 der 10'000 durch SnRK1 regulierten Gene in der Energieverarmungsantwort. Besonders S1-bZIP TF sind sehr wichtig für die Regulation vieler Gene, die für Enzyme aus dem Aminosäuremetabolismus codieren und als alternative Energiequelle der Pflanze bekannt sind. Wird die Nacht für einige Stunden

verlängert, greift die Pflanze auf jede mögliche Energiequelle zurück. Als Energiequelle werden besonders Aminosäuren, aber auch Lipiden und Proteinen herangezogen.

Interessanterweise regulieren S1-bZIP TF die Expression von *ETFQO*. *ETFQO* ist ein besonderes Protein, das die Elektronen aus dem Metabolismus verzweigter Aminosäuren in die mitochondriale Elektronentransportkette steuert. Das Dimer aus bZIP63 und bZIP2 rekrutiert SnRK1.1 direkt an das Chromatin des *ETFQO*-Promotors. Dieser Rekrutierung folgt die Acetylierung des Histonproteins 3 (K14H3) am Lysin 14. Diese Modifikation des Chromatins führt normalerweise zu einem euchromatischen Status der DNA und der nachfolgenden transkriptionellen Aktivierung. Neben der Regulation des *ETFQO*-Gens sind S1-bZIP TF auch an der Regulation von vielen anderen Genen in Folge von verschiedenen Stressen beteiligt. bZIP1 ist beispielsweise ein wichtiger Regulator der Antwort auf Salz-Stress. Auch der primäre Kohlenstoff- und Stickstoffmetabolismus werden von bZIP1 reguliert. Es wird angenommen, dass die Expression von *bZIP1* wie auch von *bZIP53* und *bZIP63* in der Antwort auf Salzstress und Energieverarmung durch SnRK1 gesteuert wird. Abgesehen von der Regulation der Antwort auf Energieverarmung und Salzstress spielen SnRK1-Proteine auch bei der Aktivierung des Lipidmetabolismus während der Keimung eine Rolle. SnRK1 kontrolliert die Expression von *CALEOSINs* und *OLEOSINs*. Diese beiden Proteine sind sehr wichtig für die Mobilisierung von Lipiden aus Öltröpfchen. In Abwesenheit von SnRK1 finden aufgrund von Energiemangel weder die Keimung noch die nachfolgende Entwicklung statt.



The low energy signaling network

Filipa Tomé^{1*}, Thomas Nägele², Mattia Adamo³, Abhroop Garg⁴, Carles Marco-Illorca⁴, Ella Nukarinen², Lorenzo Pedrotti⁵, Alessia Peviani⁶, Andrea Simeunovic², Anna Tatkiewicz⁷, Monika Tomar⁸ and Magdalena Gamm⁸

¹ Bayer CropScience NV, Innovation Center, Ghent, Belgium

² Department of Ecogenomics and Systems Biology, University of Vienna, Vienna, Austria

³ Instituto Gulbenkian de Ciência, Oeiras, Portugal

⁴ Zentrum für Molekularbiologie der Pflanzen, Eberhard Karls Universität Tübingen, Tübingen, Germany

⁵ Julius-von-Sachs-Institut, Julius-Maximilians-Universität Würzburg, Würzburg, Germany

⁶ Theoretical Biology and Bioinformatics, Department of Biology, Faculty of Science, Utrecht University, Utrecht, Netherlands

⁷ Universidad Politécnica de Madrid–Instituto Nacional de Investigación y Tecnología Agraria y Alimentaria, Centro de Biotecnología y Genómica de Plantas, Universidad Politécnica de Madrid, Madrid, Spain

⁸ Molecular Plant Physiology, Institute of Environmental Biology, Utrecht University, Utrecht, Netherlands

Edited by:

Matthew Gilliam, University of Adelaide, Australia

Reviewed by:

Julia Bailey-Serres, UC Riverside, USA
Patricia Coello, Universidad Nacional Autónoma de México, México

*Correspondence:

Filipa Tomé, Bayer CropScience NV, Innovation Center, Technologiepark 38, 9052 Zwijnaarde (Ghent), Belgium
e-mail: filipa.tome@bayer.com

Stress impacts negatively on plant growth and crop productivity, causing extensive losses to agricultural production worldwide. Throughout their life, plants are often confronted with multiple types of stress that affect overall cellular energy status and activate energy-saving responses. The resulting low energy syndrome (LES) includes transcriptional, translational, and metabolic reprogramming and is essential for stress adaptation. The conserved kinases sucrose-non-fermenting-1-related protein kinase-1 (SnRK1) and target of rapamycin (TOR) play central roles in the regulation of LES in response to stress conditions, affecting cellular processes and leading to growth arrest and metabolic reprogramming. We review the current understanding of how TOR and SnRK1 are involved in regulating the response of plants to low energy conditions. The central role in the regulation of cellular processes, the reprogramming of metabolism, and the phenotypic consequences of these two kinases will be discussed in light of current knowledge and potential future developments.

Keywords: energy signaling, TOR, SnRK1, bZIP/T6P, stress, metabolism

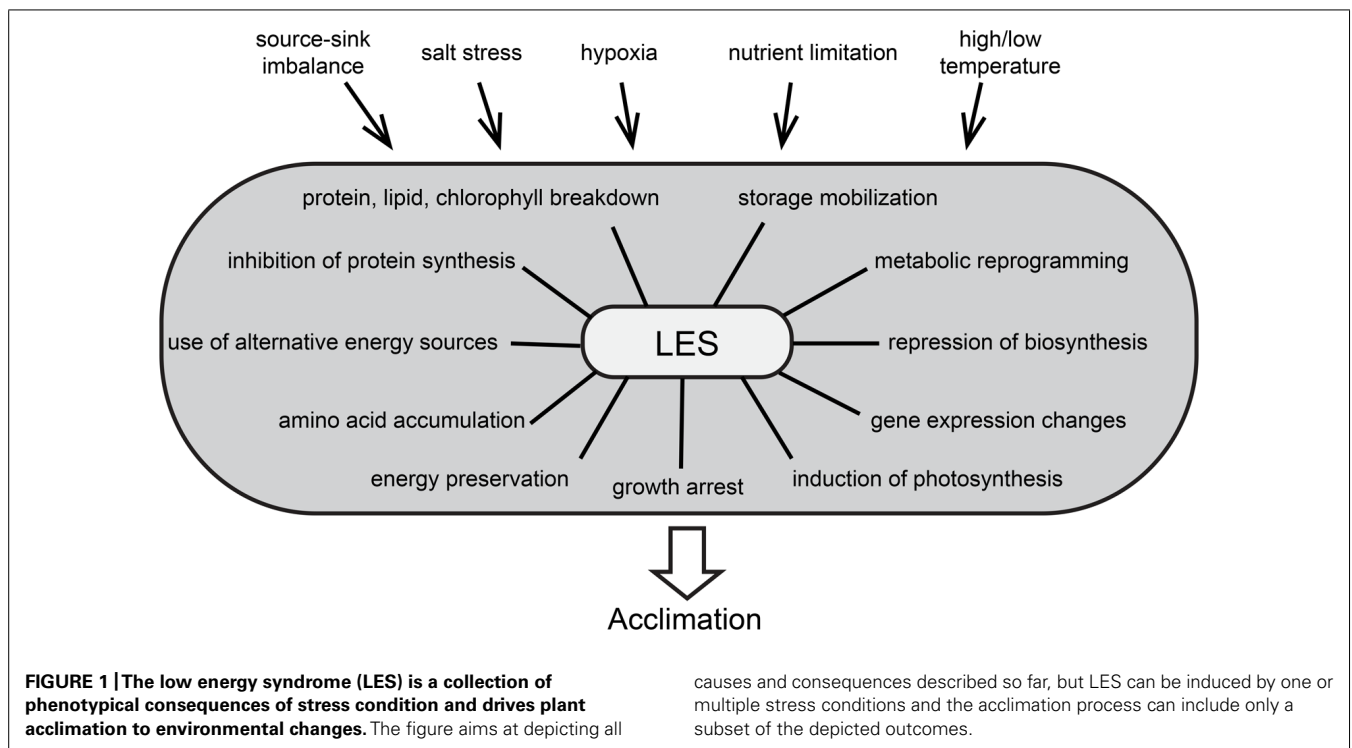
INTRODUCTION

Suboptimal growth conditions related to temperature, light, water supply, and soil characteristics are among the most limiting factors for crop yield worldwide. Fruit and seeds constitute about 75% of world crop production (Liu et al., 2013a). They rely on the supply of carbohydrates from photosynthetic source tissues to sustain growth and development (Rolland et al., 2006) and this fine-tuned balance can be severely disturbed at different levels under biotic and abiotic stress conditions (Lemoine et al., 2013). In general, stress conditions cause the alteration of a set of processes and biochemical reactions. These changes can be encompassed by the term low energy syndrome (LES) and play a major role in the adaptation to stress conditions (Figure 1). In this review we summarize recent advances in the understanding of LES and the different signaling pathway components from energy deficiency toward adaptation, focusing on *Arabidopsis thaliana* as a plant model.

THE LOW ENERGY SYNDROME IS PART OF STRESS ADAPTATION

Controlling energy homeostasis is a challenge for all organisms, as they must constantly sense and integrate internal and external signals to optimize growth and development, often under suboptimal conditions (Polge and Thomas, 2007). This is particularly critical for plants as they are sessile organisms, so it is

very interesting to understand how they have evolved to overcome these constraints and how they respond differently to stresses when compared to other organisms. Their adaptation and survival depend on their capacity to efficiently manage energy resources in all tissues, and to coordinate energy consumption and preservation (Baena-González et al., 2007; Baena-González, 2010). Stress conditions affect source and sink tissues differently. In plants exposed to stress, sink organs like seeds or tubers often suffer from reduced sugar import and are impaired in biomass production (Pinheiro et al., 2001; Cuellar-Ortiz et al., 2008). Accordingly, stress factors like nutrient limitation, hypoxia, excess of salt, and low or high temperatures were discussed to impair fruit and seed development by interfering with the source-sink balance (Gibon et al., 2002; Geigenberger, 2003; Bailey-Serres et al., 2012; Lemoine et al., 2013; Liu et al., 2013b). Furthermore, stress conditions often affect photosynthesis and respiration in source leaves and this can accentuate the source-sink imbalance. The resulting energy deprivation was suggested to be common to most types of stress and to trigger specific responses (Baena-González and Sheen, 2008), leading to the massive alteration of cellular processes, referred to as LES. This includes growth arrest and metabolic reprogramming, comprising the repression of biosynthetic activities and sugar storage, as well as the induction of catabolic processes, photosynthesis, and sugar remobilization (Paul and Pellny, 2003; Gibon et al., 2006). In addition, the expression of thousands of genes is altered (Usadel



et al., 2008). These genes were described to form a network that regulates plant metabolism under stress conditions for the purpose of energy preservation (Avin-Wittenberg et al., 2012). At the same time, metabolic reprogramming favors catabolic processes of molecules other than carbohydrates, resulting in protein, lipid and chlorophyll breakdown (Contento et al., 2004; Thimm et al., 2004). Accordingly, metabolomics data show an increase in amino acids coming from protein degradation (Caldana et al., 2011), which may contribute to sustain levels of TCA cycle intermediates (Araújo et al., 2012). Furthermore, translation rates decrease dramatically (Kawaguchi et al., 2003, 2004; Branco-Price et al., 2005, 2008; Nicolai et al., 2006; Mustroph et al., 2009), although often without alteration of specific mRNA levels, which allows a rapid recovery after removal of the stress (Piques et al., 2009; Juntawong and Bailey-Serres, 2012).

These massive alterations on all cellular levels that comprise LES occur during many different stress situations and are therefore discussed as central processes necessary for adaptation. Even though LES involves a collection of phenotypic outcomes, their interconnection and regulation remain to be fully described. Generally, stress adaptation involves both universal and stress specific reactions, indicating that plants perceive multiple stresses and transduces the signal through pathways which may cross-talk at various levels (Chinnusamy et al., 2004). A number of signaling pathways are involved in the regulation of energy utilization and can be linked to the adaptation to stress conditions. Key players of energy signaling are the evolutionary conserved protein kinases sucrose-non-fermenting-1-related protein kinase-1 (SnRK1) and target of rapamycin (TOR). They are proposed to be antagonists in the coordination of energy consumption and preservation (Robaglia et al., 2012) and the balance of their

activities might be essential to the regulation of LES in stress adaptation.

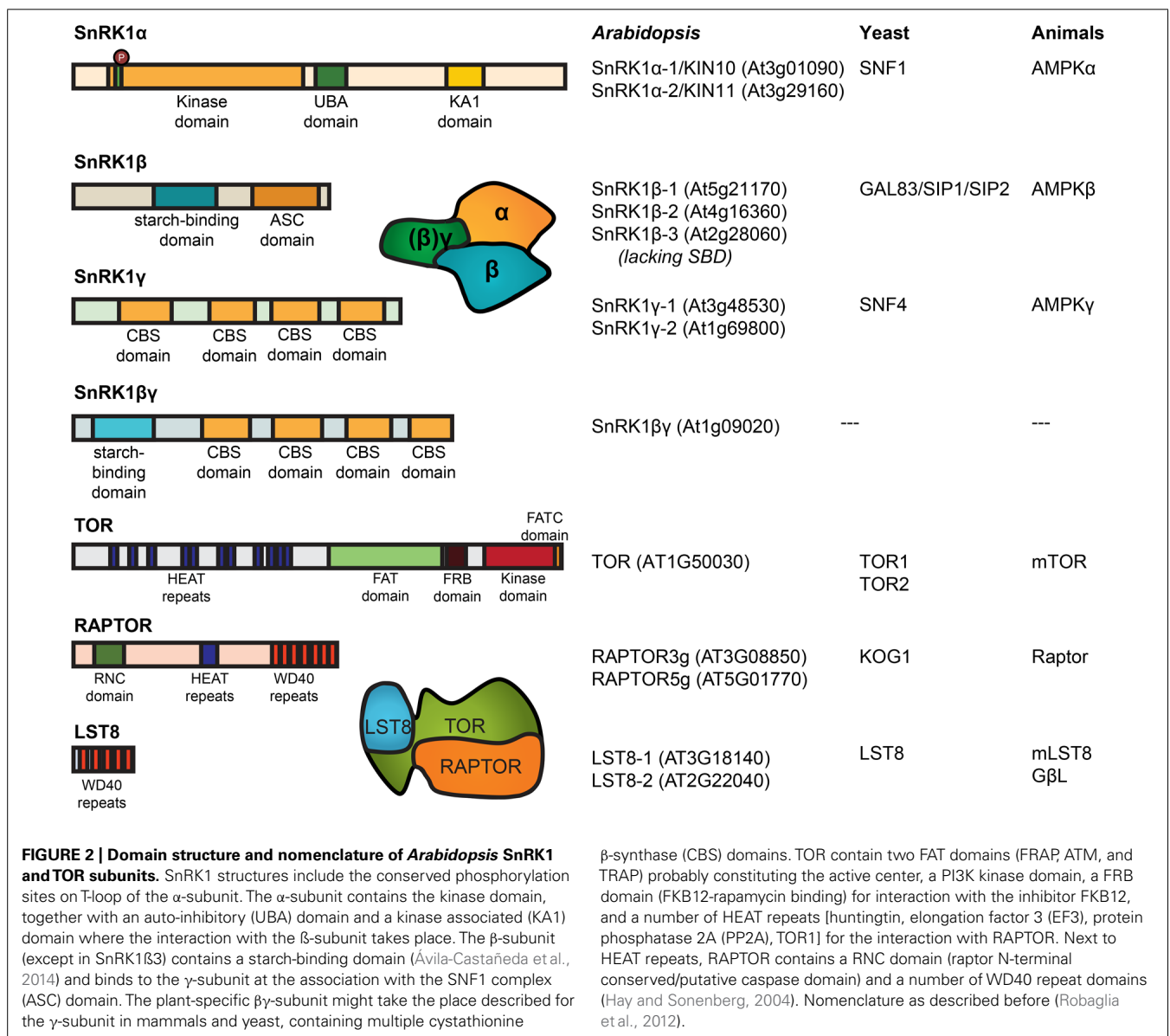
SnRK1 IS A METABOLIC SENSOR KINASE

Sucrose-non-fermenting-1-related protein kinase-1 is a metabolic sensor that can decode energy deficiency signals and induce an extensive metabolic reprogramming. This is mediated by a number of transcription factors and downstream targets that start an energy-saving program at several levels, including transcription, translation or direct phosphorylation of targets (Baena-González et al., 2007). SnRK1 is the plant homolog of the yeast sucrose non-fermenting-1 (SNF1) and the animal AMP-activated protein kinase (AMPK; Halford et al., 2004). SNF1-related protein kinases show close to 50% identity, rising to 65% for the kinase domains (Polge and Thomas, 2007). Their primary role is the integration of nutrient availability, stress signals, and energy expenditure, to be able to activate the required adaptations for homeostasis and survival (Halford and Hardie, 1998; Hardie et al., 1998; Ghillebert et al., 2011). Plants contain two other subfamilies, SnRK2 and SnRK3. They are less similar to SNF1 and AMPK and unique to plants (Halford et al., 2004), and are also involved in plant responses to several stresses (Coello et al., 2011). SnRK2 is involved in ABA signaling, responses to cold, and was shown to improve drought tolerance when overexpressed (Fujita et al., 2009; Halford and Hey, 2009; Yoshida et al., 2014). The SnRK3 family includes *SOS2* (salt overly sensitive 2), involved in conferring salt tolerance (Liu et al., 2000). There is no evidence of redundancy between the different SnRK families and SnRK2 and SnRK3 do not complement the yeast *snf1Δ* deletion mutant growth phenotype (Hrabak et al., 2003). It is clear that they cannot fulfill the role of SnRK1 (Halford and Hey, 2009), even though there is some

similarity in target recognition (Zhang et al., 2008). It was suggested that SnRK2 and SnRK3 arose in plants by duplication of SnRK1 and then diverged rapidly during plant evolution to meet new needs related to networks linking stress and ABA signaling with metabolic signaling (Halford and Hey, 2009).

The SnRK1/SNF1/AMPK kinases typically function as heterotrimeric complexes and require a catalytic α -subunit, KIN10 and KIN11 in plants, and regulatory β and γ subunits (Figure 2). The non-catalytic subunits are also conserved among the SnRK1/SNF1/AMPK complex. They are likely involved in substrate recognition, subcellular localization, and regulation of the complex activity (Polge and Thomas, 2007; Ghillebert et al., 2011). Interestingly, the *Arabidopsis* AKIN β 1, AKIN β 2, and AKIN β 3 have markedly different expression patterns, which suggests a level of regulation based on interactions targeting the β subunits in response to different signals (Bouly et al., 1999; Gissot et al., 2004).

The activity of SnRK1 depends on phosphorylation in the highly conserved T-loop by upstream kinases (Sugden et al., 1999). In *Arabidopsis*, the protein kinases SnRK1-activating kinase 1 and 2 (AtSnAK1 and AtSnAK2) were shown to complement a yeast triple kinase mutant by restoring SNF1 upstream kinase activity (Shen and Hanley-Bowdoin, 2006). In addition, they phosphorylate non-truncated AtSnRK1 catalytic subunits *in vitro*, making them putative candidates as SnRK1 physiological upstream kinases (Crozet et al., 2010). Even though it is known that SnRK1 activation requires phosphorylation, it has not been clarified how it is affected by the cellular energy level. In contrast to the mammalian AMPK, SnRK1 is not allosterically activated by AMP, but it was shown that T-loop dephosphorylation and the resulting inactivation of the kinase are inhibited by low concentrations of AMP (Sugden et al., 1999). Furthermore, SnRK1 activity is modulated by



specific phosphatases. Two clade A type 2C protein phosphatases (PP2C) were recently shown to dephosphorylate and inactivate SnRK1 through interaction with the catalytic subunit (Rodrigues et al., 2013).

The activity of SnRK1 is also inhibited by trehalose-6-phosphate (T6P). The association between trehalose metabolism and sugar-sensing in plants has recently become more evident (Tsai and Gazzarrini, 2014). Despite its role as a carbon source and in stress protection in resurrection plants, fungi, bacteria, and non-vertebrate animals (Elbein et al., 2003; Paul et al., 2008), the amount of trehalose in the majority of plants is too low to perform this function. It was suggested that trehalose has a major role on metabolism, growth, and development, acting as a signal of sugar availability (Schluepmann et al., 2003; Ramon and Rolland, 2007; Gómez et al., 2010). Trehalose is synthesized from UDP-glucose and glucose-6P via the intermediate T6P in a two-step pathway involving trehalose phosphate synthase (TPS) and trehalose phosphate phosphatase (TPP), and degraded by trehalase (Paul et al., 2008). T6P has a distinctive role in metabolic signaling, and class II TPSs, that include AtTPS5-11, are targets of phosphorylation by SnRK1 (Glinski and Weckwerth, 2005). AtTPS5 is induced by sugars and repressed by starvation (Schluepmann et al., 2004), while the opposite is true for AtTPS8-10 (Osuna et al., 2007).

Trehalose-6-phosphate inhibits the catalytic activity of SnRK1 *in vitro* at physiological concentrations, causing expression changes of KIN10 marker genes consistent with an inactivation of SnRK1 (Zhang et al., 2009), while *Arabidopsis* seedlings overexpressing SnRK1 show a glucose-hypersensitive phenotype (Cho et al., 2012), similar to seedlings with low T6P (Schluepmann et al., 2003). However, even though T6P inhibits the growth of *Arabidopsis* seedlings, it does not inhibit SnRK1 catalytic activity in extracts of mature leaves (Zhang et al., 2009), suggesting that an intermediary factor is needed for SnRK1 inhibition by T6P. Recently, it was suggested that T6P and SnRK1 might act through different, but interacting signaling pathways (Lunn et al., 2014) and can play antagonistic roles during stress responses (O'Hara et al., 2013). This is particularly important in stress conditions that negatively affect carbon levels, leading to an activation of starvation responses through SnRK1. For example, T6P levels are much lower in rosettes harvested in the dark and in carbon-starved seedlings (Lunn et al., 2006; Carillo et al., 2013; Yadav et al., 2014). However, stress conditions do not necessarily lead to carbon depletion. For example, under moderate drought or cold stress, a wide range of carbohydrates accumulate in *Arabidopsis* (Muller et al., 2011), including abundant sugars such as hexoses and sucrose, other sugars such as trehalose or mannitol, amino acids, organic acids, structural C-rich compounds like cellulose, among others. In grapevine, sucrose and T6P contents increase in response to chilling (Fernandez et al., 2012). T6P may therefore play a role in the inhibition of SnRK1 under conditions where carbon sources are not limited (Lunn et al., 2014). The cross-talk between SnRK1 and T6P when growth is limited by sink capacity was recently studied by varying temperature and nutrient supply to induce sink limitation, and feed sucrose and glucose at physiological levels (Nunes et al., 2013). In these conditions, T6P responds specifically to sucrose, even at different growth rates. Moreover,

there was a strong correlation between T6P- and SnRK1-regulated gene expression, but not between T6P and relative growth rate. It appears that SnRK1 marker gene expression is related to T6P content regardless of the growth outcome, but further investigations will hopefully elucidate the relationship between SnRK1 and T6P.

SnRK1 REGULATES STRESS RESPONSES UPON LOW ENERGY

The activation of SnRK1 initiates massive transcriptional changes, possibly by affecting a number of transcription factors (Baena-González et al., 2007). The gene expression profile mediated by the SnRK1 subunit KIN10 is positively correlated with the one induced by deprivation of sugar and carbon, and negatively correlated with that controlled by sugars. This places KIN10 as a regulator of gene expression upon starvation and stress conditions. The most prominent KIN10-activated genes represent a variety of major catabolic pathways, including degradation of cell wall, starch, sucrose, amino acid, lipid, and proteins which provide alternative sources of energy and metabolites. Additionally, a large set of genes involved in energy-consuming ribosome biogenesis and anabolism are repressed.

From the possible mechanisms by which SnRK1 affects transcription, the members of the S1 class of the basic leucine zipper (bZIP) transcription factors are probably the best described (Figure 3). They belong to a large family of several classes in eukaryotes (Reinke et al., 2013) and function as homo- or heterodimers, which increases their potential for regulation (Jakoby et al., 2002; Corrêa et al., 2008; Schütze et al., 2008). From the bZIP family, bZIP1, bZIP11, and bZIP53 were proposed to mediate some of the transcriptional changes induced by the SnRK1 signaling pathway (Baena-González et al., 2007) and could be linked to the regulation of LES. In the presence of sucrose and glucose, the transcript levels of bZIP1 and bZIP53 decrease, and energy availability also seems to affect the phenotypes of their mutants. bZIP53 overexpression results in reduced plant size,

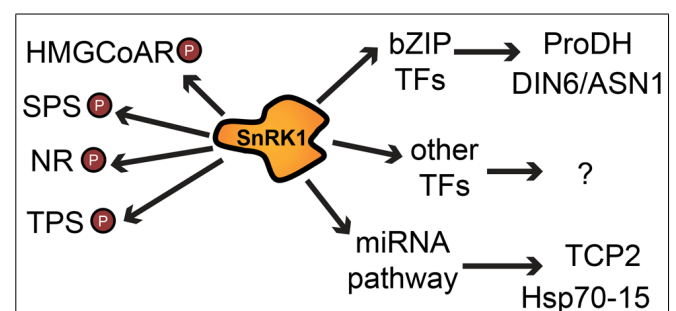


FIGURE 3 | Simplified summary of SnRK1 effects on cellular processes by direct phosphorylation of target proteins and by alteration of mRNA levels of many genes via transcription factors or the miRNA machinery. Arrows indicate a positive or negative regulatory effect; P denotes phosphorylation. Abbreviations: HMGCAR, 3-hydroxy-3-methylglutaryl-coenzyme A reductase; SPS, sucrose phosphate synthase; NR, nitrate reductase; TPS, trehalose phosphate synthase; bZIP TF, basic leucine zipper transcription factor; ProDH, proline dehydrogenase; DIN6/ASN1, dark inducible 6/asparagine synthetase 1; TCP2, teosinte branched 1, cycloidea and PCF transcription factor 2; Hsp70-15, heat shock protein 70-15.

delayed bolting and expression of seed-specific genes in leaves (Alonso et al., 2009). bZIP1 knockout plants were shown to grow faster than wild type on medium lacking glucose (Kang et al., 2010), while a plant overexpressing bZIP1 showed a stronger starvation response indicated by faster leaf-yellowing in extended night conditions (Dietrich et al., 2011). Under ambient growth conditions, bZIP1 gene expression is limited to sink tissue like pollen or young leaves (Weltmeier et al., 2009), but transcript levels were shown to be increased in source leaves after sugar starvation induced by extended night (Dietrich et al., 2011), while bZIP11 transcript levels increase in the presence of glucose and sucrose (Rook et al., 1998). On the other hand, bZIP11 translation is repressed by sucrose mediated by an upstream open reading frame (Wiese et al., 2004; Rahmani et al., 2009). This decrease is observed at physiological sucrose levels in most tissues, restricting bZIP11 activity to conditions of low energy availability (Wiese et al., 2004). Transgenic plants overexpressing bZIP11 show reduced plant size, seed production, viability and a wide effect on gene regulation and metabolism as demonstrated by microarray analysis of these plants (Hanson et al., 2008).

Several gene expression studies identified putative target genes of these transcription factors and there is considerable overlap between their targets and genes regulated by SnRK1. bZIP11 targets include several genes associated with LES, involved in the regulation of trehalose and other minor regulatory carbohydrates, such as myo-inositol and raffinose (Ma et al., 2011). bZIP11 also induces *GDH1* and *GDH2*, genes encoding glutamate dehydrogenase (Hanson et al., 2008). The double mutant *gdh1gdh2* was shown to be more susceptible to extended night, likely due to the role of these enzymes in amino acid degradation (Miyashita and Good, 2008a,b). Other genes involved in amino acid metabolism were shown to be regulated by bZIP transcription factors. Members of the S1 class specifically activate the G-box containing promoter of the SnRK1 regulated gene *DIN6/ASN1* (Baena-González et al., 2007). They were also shown to activate gene expression of proline dehydrogenase (ProDH; Satoh et al., 2004) by binding to G-boxes contained in the promoter region (Weltmeier et al., 2006; Dietrich et al., 2011). While ProDH is thought to be involved in stress recovery (Weltmeier et al., 2006), the accumulation of asparagine and other amino acids during dark-induced starvation was proposed to result from protein degradation in order to provide an alternative to carbon as energy source (Caldana et al., 2011; Dietrich et al., 2011).

Basic leucine zipper transcription factors mediate many, but not all SnRK1 effects on transcription. It remains to be studied which factors mediate the first, direct effect on gene expression and which genes are regulated by secondary mechanisms. Further studies will hopefully reveal a number of additional transcription factors involved in SnRK1 regulation of gene expression.

Sucrose-non-fermenting-1-related protein kinase-1 also affects enzymes by direct phosphorylation. For example, it inhibits the activity of HMG-CoA reductase, the rate-limiting step in sterol synthesis (Clarke and Hardie, 1990; Mackintosh et al., 1992). Two other enzymes were shown to be substrates of SnRK1, sucrose phosphate synthase (SPS), and nitrate reductase (NR; McMichael et al., 1995; Douglas et al., 1997) which are key biosynthetic

enzymes involved in the control of nitrogen assimilation and sucrose synthesis (Figure 3).

In addition to transcriptional changes and direct phosphorylation, SnRK1 was recently shown to activate a miRNA pathway (Confraria et al., 2013). Some of the candidate miRNA targets can be connected to the SnRK1 pathway and miRNAs can therefore be placed as components of the SnRK1 signaling pathway, as they regulate mRNA targets and possibly tune down specific cellular processes during the stress response (Figure 3). Most of the affected genes correspond to genes related to ribosomal proteins (RPs) and translation, which is in accordance with the role of SnRK1 as a repressor of biosynthetic processes and as a modulator of energy metabolism (Baena-González et al., 2007; Baena-González and Sheen, 2008). In animals there seems to be a link between miRNAs and metabolism: AMPK activation was recently reported to induce the differential accumulation of multiple miRNAs (Liu et al., 2013a), suggesting that miRNAs could be possible common elements in diverse organisms for restoring homeostasis following stress (Confraria et al., 2013). A recent paper supports this view by showing a strong connection between the regulation of miRNA expression and glucose-mediated regulatory responses (Duarte et al., 2013). These recent findings make it clear that SnRK1 mode of action goes beyond direct phosphorylation or modulation of transcription and promise new discoveries to come on the interplay between multiple pathways in the regulation of the LES.

THE TOR KINASE IS INVOLVED IN LES

Another key component in this network is the serine/threonine kinase TOR. TOR kinase genes are present in every eukaryote genome analyzed so far and they share 40–60% sequence identity (De Virgilio and Loewith, 2006; Wullschleger et al., 2006). These large proteins are well described for their central roles in the energy signaling pathways of yeast, mammals and plants (Wullschleger et al., 2006; Robaglia et al., 2012). TOR is activated, in both yeast and mammals, by high amino acid levels, but inactivated under amino acid starvation (Jewell et al., 2013). In plants, TOR activity has been linked to cell and organ size, seed yield, and stress resistance (Ren et al., 2012) and it was suggested to play a role in the regulation of carbon partitioning and growth (Zhang et al., 2013). Furthermore, it has been shown that TOR and SnRK1 interact closely and act in opposite ways in the regulation of nutrient-driven processes like autophagy (Robaglia et al., 2012).

In yeast and mammals, TOR functions in two complexes with distinct functions, TOR complex 1 (TORC1) and TORC2, characterized by different interaction partners. Of these, only subunits of TORC1 (TOR, LST8/GbetaL and KOG1/RAPTOR) are present in the *Arabidopsis* genome (Figure 2; van Dam et al., 2011). Mutations that disrupt TOR or RAPTOR genes were shown to be embryo lethal (Menand et al., 2002; Deprout et al., 2005). In addition, the low sensitivity of the *Arabidopsis* TOR toward rapamycin (Xiong and Sheen, 2012; Caldana et al., 2013) makes the study of TOR signaling in plants more difficult than in other organisms, where the inhibitor was extensively used to study TOR functions (Wullschleger et al., 2006).

Alternative approaches were developed including the expression of a yeast FKBP12 protein which confers rapamycin sensitivity (Sormani et al., 2007; Ren et al., 2012), modulation of TOR expression by overexpressor or RNA interference constructs (Deprost et al., 2007; Ren et al., 2011) and the expression of an inducible artificial microRNA targeting TOR (Caldana et al., 2013).

The *Arabidopsis* TOR promoter is active in root and apical primary meristems, embryo and endosperm, but not in source leaves or differentiated cells (Menand et al., 2002). TOR acts on cell cycle control in *Arabidopsis* root meristems by directly phosphorylating the transcription factor E2Fa that regulates S-phase gene expression (Xiong et al., 2013). It was proposed as a potential integrator of cell cycle, cell expansion and cytoplasmic growth (Sablowski and Carnier Dornelas, 2014) and could thus be responsible for the activation of growth in the meristems in response to sugars provided by the photosynthetic source tissues (Xiong et al., 2013). Furthermore, TOR inhibition leads to a reduction of the length of the root meristematic zone and the division zone therein (Montané and Menand, 2013). Recently, TOR was shown to be activated by the growth hormone auxin and is involved in the regulation of translation of auxin responsive genes (Bögre et al., 2013; Schepetilnikov et al., 2013). Accordingly, reduction of TOR expression in *Arabidopsis* results in severe growth arrest with plants displaying decreased cell size, whereas TOR overexpression leads to an increase in shoot and root growth (Deprost et al., 2007).

TOR complex 1 was described to be involved in the control of transcription, protein synthesis, and autophagy in yeast and mammals (Martin and Hall, 2005; De Virgilio and Loewith, 2006; Wang and Proud, 2011). In *Arabidopsis*, massive transcriptional changes induced by glucose in seedlings are dependent on TOR signaling. The genes activated by this signaling pathway are involved in amino acid synthesis, translation, glycolysis and the TCA cycle, cell wall synthesis and modification, whereas genes involved in protein and amino acid degradation and autophagy regulation were downregulated (Xiong et al., 2013). The role of TOR signaling in the induction of biosynthesis and the repression of catabolic pathways was underlined by RNA sequencing and microarray analysis studying gene expression changes in response to TOR inactivation (Ren et al., 2012; Caldana et al., 2013). These transcriptional changes were shown to be accompanied by an increase in starch content (Moreau et al., 2012) and an accumulation of organic and amino acids (Ren et al., 2012; Caldana et al., 2013), as well as a decrease in galactinol and raffinose levels (Moreau et al., 2012). This led to the conclusion that TOR downregulation mimics starvation (Caldana et al., 2013) and strengthens the importance of the TOR pathway in starvation responses.

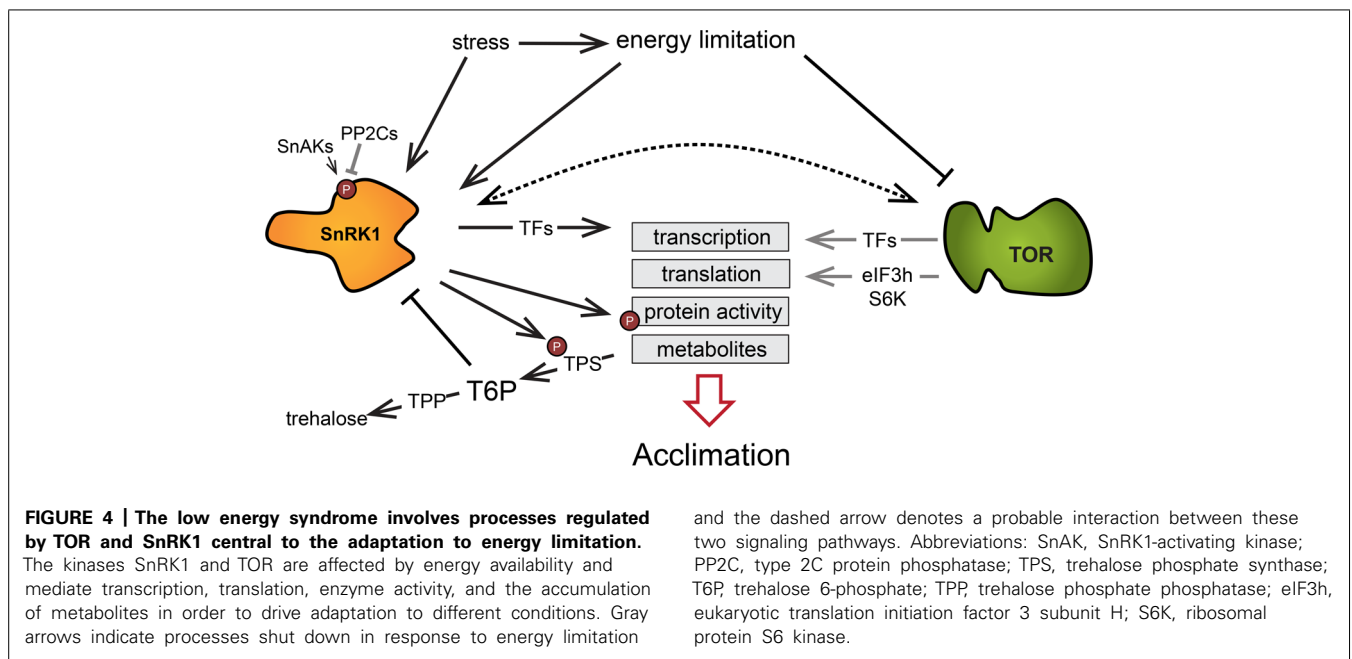
Furthermore, the TOR kinase was implicated in sugar signaling pathways to control translation. Protein synthesis is a very energy demanding process and therefore needs to be tightly regulated in function of the cellular energy availability. In mammals and yeast, TORC1 affects the level of rRNA (Claypool et al., 2004; Mayer et al., 2004; Li et al., 2006a; Tsang et al., 2010) and RP gene expression (Jorgensen et al., 2004; Martin et al., 2004; Rudra and Warner, 2004), as well as cap-dependent translation (Ma and Blenis, 2009)

and scanning along structured 5'-UTRs (Meyuhas and Dreazen, 2009).

The tight regulation of translation according to energy availability also occurs in plants (Pal et al., 2013; Lastdrager et al., 2014). For some of the well described pathway components, like the phosphorylation of 4E-BP, evidence in plants is lacking (Van Der Kelen et al., 2009; Ren et al., 2011). Nevertheless, plants expressing RNAi constructs for TOR or its positive downstream effector TAP46 displayed a significant decrease in polysomal loading and in protein synthesis (Ahn et al., 2011). The transcription of RP genes is induced after sugar treatment and seems to be dependent on the diurnal cycle (Bläsing et al., 2005; Usadel et al., 2008; Baerenfaller et al., 2012) and glucose induction of RP gene expression was shown to depend on TOR activity (Xiong et al., 2013). Furthermore, TOR overexpression was shown to induce rRNA production and ChIP experiments showed that TOR binds directly to the 45S promoter region (Ren et al., 2011). TOR mediated ribosomal protein S6 kinase (S6K) activity was proposed to be important to maintain eukaryotic translation initiation factor 3 subunit H (eIF3h) phosphorylation, which is needed for translation reinitiation and thus for translation of uORF containing mRNAs (Schepetilnikov et al., 2013). Starvation inhibits the TOR kinase and therefore allows energy costly ribosome biogenesis and translation processes to be reduced in growth limiting conditions (Ma and Blenis, 2009; Robaglia et al., 2012).

INTERACTION BETWEEN SnRK1 AND TOR SIGNALING

The TOR and SnRK1 signaling pathways have emerged as crucial in regulating the perception and responses to nutrient and energy levels. The TOR kinase is activated in favorable nutritional and energy conditions, while SnRK1 is stimulated upon nutrient and energy starvation. It is becoming increasingly clear that they act in opposite ways in the regulation of nutrient-driven processes, such as autophagy. For example, SnRK1 induces autophagy to promote recycling of cytosolic components in response to situations where C or N metabolites are in short supply. Conversely, TOR restrains autophagy in energy-replete conditions and is involved in the regulation of N assimilation and in the synthesis of C metabolites like starch or raffinose (Robaglia et al., 2012). They both regulate many similar processes in the context of LES (**Figure 4**) and massively affect the transcription of a number of genes. By comparing the expression of genes targeted by SnRK1/KIN10 (Baena-González et al., 2007) and TOR (Xiong et al., 2013) in two available transcriptional datasets (data was acquired from protoplast and seedlings, respectively), we found that there was a significant overlap in the genes affected by both TOR and SnRK1. More than half of the genes (294 out of 507) described as KIN10 upregulated target genes were found to be downregulated by glucose in a TOR-dependent manner. Interestingly, 47 genes which were oppositely affected by TOR and SnRK1 are annotated to encode RPs or proteins related to translation. Furthermore, a similar proportion of genes found to be downregulated by KIN10 (260 of 515 genes) were among the putative upregulated targets of the TOR kinase, including genes annotated to be involved in amino acid metabolism and involved in carbohydrate metabolism. This underlines the hypothesis that TOR and SnRK1 act antagonistically in the regulation of central processes such as translation and carbohydrate and amino



acid metabolism, a role that is likely to be crucial during the establishment of stress responses.

Target of rapamycin and SnRK1 are both evolutionary conserved and have been shown to interact in mammalian systems. AMPK is described to regulate the mTOR complex 1 in different ways, by phosphorylating components of the mTOR signaling pathway (Xu et al., 2012). The phosphorylation of the TSC2/TSC1 complex by AMPK leads to the inactivation of Rheb, a GTPase that activates mTORC1. Furthermore, AMPK has been described to directly regulate the Raptor subunit of the mTORC1 complex (Inoki et al., 2012). mTOR and AMPK have opposite roles in the regulation of autophagy by targeting different phosphorylation sites of ULK1 (Kim et al., 2011). Under nutrient limitation, AMPK activates ULK1 and autophagy, whereas mTORC1 inactivates ULK1 in nutrient-rich conditions (Inoki et al., 2012). In plants, some of the described factors are present, including the *Arabidopsis* TCTP that was proposed as a regulator of Rheb in TOR signaling (Berkowitz et al., 2008) and the AMPK phosphorylation site in Raptor (Robaglia et al., 2012). However, their role in the interaction between the TOR and SnRK1 signaling pathways remains to be further analyzed. Additionally, many of the described genes are missing in *Arabidopsis*, such as Rheb itself, TSC1, and TSC2 (van Dam et al., 2011). Their functions were taken over by other factors, indicating that plants evolved energy signaling pathways different from mammals or yeast that remain to be fully described (Xiong and Sheen, 2014).

TOWARD A BETTER UNDERSTANDING OF LES

The studies discussed above underline the central role of the energy signaling network composed of TOR, SnRK1, bZIP transcription factors, and T6P in the control of growth and development. Exposure of plants to conditions that challenge their energy homeostasis results in significant metabolic reprogramming to prevent damage to cells, tissue, and organs. LES involves

various changes in transcription, translation, enzymatic activities, and metabolite levels ultimately aiming at the adaptation to energy deprivation (Figure 4). Amongst others, this leads to protein, lipid, and chlorophyll breakdown (Contento et al., 2004; Thimm et al., 2004), while in parallel, carbon utilization is inhibited, which, taken together, severely affects growth (Gibon et al., 2004).

Even though much is already known about the LES network, there are still many open questions. More experimental data is needed to unravel unknown mechanisms behind LES, but several experimental limitations may be restraining new discoveries. For example, most studies were conducted in protoplasts, whole seedlings or plant tissue without distinguishing source and sink organs. Since the interplay of molecules is complex and coordinated in both time and space, increasing spatial resolution of metabolites with the use of better techniques, like subcellular fractionation (Nägele and Heyer, 2013), is necessary to enable a better understanding of regulation of stress conditions by allowing tissue-, cell-, and compartment specific analyses of metabolic changes. Furthermore, the pleiotropic nature of SnRK1 and TOR limits the use of mutants as mutations result in undesired effects that can hardly be precluded. The use of constitutive promoters for overexpression leads to the loss of information about the localization of the expression of a certain gene. This information is very important as many of the discussed genes are differentially expressed between source or sink tissues, which likely impacts on their role and function. It would thus be useful to develop additional mutants, especially including organ and temporal specific promoters, to overcome these current issues. The use of inducible systems is of high interest for both SnRK1 and TOR, but particularly for the latter since knock-out mutants are not available due to lethality. Hence, the uses of inducible artificial microRNAs are a valuable option to down-regulate its expression.

The study of networks like LES requires the analysis of complex datasets. It is important to realize that the challenge is not only the acquisition of more and better experimental data, but especially to be able to integrate it to facilitate its interpretation via methods often referred to as systems biology or omics-based approaches. To improve upon current approaches, theoretical methods of uni- and multivariate statistics and mathematical modeling have been developed which now allow large scale analysis of biological networks (Nägele and Weckwerth, 2012). Several problems related to plant science are being addressed using these approaches, including responses to stress, (Yamaguchi-Shinozaki and Shinozaki, 2006), plant defense (Li et al., 2006b) and the identification of new players, such as transcription factors (Hirai et al., 2007).

Low energy signaling is a complex network that integrates multiple cellular and environmental signals and comprises several cellular changes. To avoid limitation in the interpretation of the biological events, it is important to study this pathway on all possible levels, comprising the gene, transcript, protein, and metabolite levels. Limitations can arise, for example, from the consideration of only transcriptomic data. With this type of data, differences in transcription and RNA stability cannot be distinguished. Also, changes in transcript levels often do not reflect changes in protein or metabolic levels and little information is obtained at this level. Substantial contributions have been made mainly concerning the integration of transcript and metabolite data for *A. thaliana* (Hirai et al., 2004, 2005; Tohge et al., 2005). By combining data from different molecular levels, a better understanding of pathway regulation being affected under low energy conditions and contributing to the acclimatory response will be significantly promoted. One type of systems biology approach is based on the collection of data from different platforms followed by data driven integration using advanced statistical models to study the dynamic interactions between components (Yuan et al., 2008; Fukushima et al., 2009; Keurentjes, 2009). Another more targeted approach where a specific regulatory model involving all known molecular players is built uses mathematical modeling to advance understanding of biological processes (Pokhilko et al., 2010, 2012, 2013; Gould et al., 2013; Seaton et al., 2014). The interaction between predictive models and experimental confirmation can be very effective, as having a more directed approach in a given experiment could enable the achievement of faster and more targeted results. Furthermore, unknown components of the studied system can be discovered (Dalchau et al., 2011). Some of the components that comprise the LES network may still be unknown, but this type of approach could provide very useful information especially in the connection between TOR and SnRK1.

The use of systems biology is limited by the availability of data and requires generalization, simplification, and assumptions. However, it clearly has great potential to increasingly contribute to the understanding of biological networks, including the LES pathway, in combination with other approaches that involve cell biology, biochemistry, or genetics. TOR and SnRK1 are related in the processes they regulate and are activated under opposite conditions, but so far there is no indication in plants that they or their targets interact directly to optimize the activation and repression

of certain processes. While in mammals AMPK phosphorylates the TSC2/TSC1 complex and Raptor, TSC2 and the AMPK phosphorylation site in Raptor are missing in *Arabidopsis* and it is not yet clear whether TOR and SnRK1 pathways interact in a similar way. It is possible that despite their connection, TOR down-regulation is just another way to limit energy use, independent from SnRK1. However, given the complexity of the network and the interconnections seen so far, not only in plants but also in other systems, it seems more likely that additional links or factors are yet to be unraveled. It is crucial to establish if there is a direct interaction between TOR and SnRK1, or if they act independently. In this context, a better understanding of their (sub-)cellular localization could provide insights to their mode of action and possible interaction. Protein interaction studies may uncover novel interactions between known LES components or even unravel new components of the network. Their role in the metabolic reprogramming induced by energy deprivation may then be tested by metabolomics studies which directly give information about changes in the concentrations of central metabolite pools. A multidisciplinary approach on various levels of cellular and organismal organization is needed to be able to draw a comprehensive picture about low energy induced metabolic reprogramming.

AUTHOR CONTRIBUTIONS

Filipa Tomé is first author, Thomas Nägele is second author, Magdalena Gamm is last author, and all other authors contributed equally to the work.

ACKNOWLEDGMENTS

The authors would like to thank Johannes Hanson and Matthew Hannah for critical reading and helpful comments. Furthermore, we are grateful to Elena Baena-González, Christina Chaban, Wolfgang Dröge-Laser, Berend Snel, Markus Teige, Jesus V. Carbajosa, Wolfram Weckwerth, and Ulrike Zentgraf for their ideas and support. All authors are part of the Marie Curie ITN project MERIT, Grant Agreement number 264474, from where financial support was obtained. The authors would like to thank the reviewers for their comments which helped to improve this manuscript.

REFERENCES

- Ahn, C. S., Han, J.-A., Lee, H.-S., Lee, S., and Pai, H.-S. (2011). The PP2A regulatory subunit Tap46, a component of the TOR signaling pathway, modulates growth and metabolism in plants. *Plant Cell* 23, 185–209. doi: 10.1105/tpc.110.074005
- Alonso, R., Oñate-Sánchez, L., Weltmeier, F., Ehlert, A., Diaz, I., Dietrich, K., et al. (2009). A pivotal role of the basic leucine zipper transcription factor bZIP53 in the regulation of *Arabidopsis* seed maturation gene expression based on heterodimerization and protein complex formation. *Plant Cell* 21, 1747–1761. doi: 10.1105/tpc.108.062968
- Araújo, W. L., Nunes-Nesi, A., Nikoloski, Z., Sweetlove, L. J., and Fernie, A. R. (2012). Metabolic control and regulation of the tricarboxylic acid cycle in photosynthetic and heterotrophic plant tissues. *Plant Cell Environ.* 35, 1–21. doi: 10.1111/j.1365-3040.2011.02332.x
- Ávila-Castañeda, A., Gutiérrez-Granados, N., Ruiz-Gayosso, A., Sosa-Peinado, A., Martínez-Barajas, E., and Coello, P. (2014). Structural and functional basis for starch binding in the SnRK1 subunits AKINβ2 and AKINβγ. *Front. Plant Sci.* 5:1–8. doi: 10.3389/fpls.2014.00199
- Ávin-Wittenberg, T., Tzin, V., Angelovici, R., Less, H., and Galili, G. (2012). Deciphering energy-associated gene networks operating in the response of *Arabidopsis* plants to stress and nutritional cues. *Plant J.* 70, 954–966. doi: 10.1111/j.1365-313X.2012.04926.x

- Baena-González, E. (2010). Energy signaling in the regulation of gene expression during stress. *Mol. Plant* 3, 300–313. doi: 10.1093/mp/ssp113
- Baena-González, E., Rolland, F., Thevelein, J. M., and Sheen, J. (2007). A central integrator of transcription networks in plant stress and energy signaling. *Nature* 448, 938–942. doi: 10.1038/nature06069
- Baena-González, E., and Sheen, J. (2008). Convergent energy and stress signaling. *Trends Plant Sci.* 13, 474–482. doi: 10.1016/j.tplants.2008.06.006
- Baerenfaller, K., Massonnet, C., Walsh, S., Baginsky, S., Bühlmann, P., Hennig, L., et al. (2012). Systems-based analysis of *Arabidopsis* leaf growth reveals adaptation to water deficit. *Mol. Syst. Biol.* 8:606. doi: 10.1038/msb.2012.39
- Bailey-Serres, J., Fukao, T., Gibbs, D. J., Holdsworth, M. J., Lee, S. C., Licausi, F., et al. (2012). Making sense of low oxygen sensing. *Trends Plant Sci.* 17, 129–138. doi: 10.1016/j.tplants.2011.12.004
- Berkowitz, O., Jost, R., Pollmann, S., and Masle, J. (2008). Characterization of TCTP, the translationally controlled tumor protein, from *Arabidopsis thaliana*. *Plant Cell* 20, 3430–3447. doi: 10.1105/tpc.108.061010
- Bläsing, O., Gibon, Y., Günther, M., Höhne, M., Morcuende, R., Osuna, D., et al. (2005). Sugars and circadian regulation make major contributions to the global regulation of diurnal gene expression in *Arabidopsis*. *Plant Cell* 17, 3257–3281. doi: 10.1105/tpc.105.035261.1
- Bögre, L., Henriques, R., and Magyar, Z. (2013). TOR tour to auxin. *EMBO J.* 32, 1069–1071. doi: 10.1038/emboj.2013.69
- Bouly, J., Gissot, L., Lessard, P., Kreis, M., and Thomas, M. (1999). *Arabidopsis thaliana* proteins related to the yeast SIP and SNF4 interact with AKINa1, an SNF1-like protein kinase. *Plant J.* 18, 541–550. doi: 10.1046/j.1365-313X.1999.00476.x
- Branco-Price, C., Kaiser, K. A., Jang, C. J., Larive, C. K., and Bailey-Serres, J. (2008). Selective mRNA translation coordinates energetic and metabolic adjustments to cellular oxygen deprivation and reoxygenation in *Arabidopsis thaliana*. *Plant J.* 56, 743–755. doi: 10.1111/j.1365-313X.2008.03642.x
- Branco-Price, C., Kawaguchi, R., Ferreira, R. B., and Bailey-Serres, J. (2005). Genome-wide analysis of transcript abundance and translation in *Arabidopsis* seedlings subjected to oxygen deprivation. *Ann. Bot.* 96, 647–660. doi: 10.1093/aob/mci217
- Caldana, C., Degenkolbe, T., Cuadros-Inostroza, A., Klie, S., Sulpice, R., Leisse, A., et al. (2011). High-density kinetic analysis of the metabolomic and transcriptomic response of *Arabidopsis* to eight environmental conditions. *Plant J.* 67, 869–884. doi: 10.1111/j.1365-313X.2011.04640.x
- Caldana, C., Li, Y., Leisse, A., Zhang, Y., Bartholomaeus, L., Fernie, A. R., et al. (2013). Systemic analysis of inducible target of rapamycin mutants reveal a general metabolic switch controlling growth in *Arabidopsis thaliana*. *Plant J.* 73, 897–909. doi: 10.1111/tpj.12080
- Carillo, P., Feil, R., Gibon, Y., Satoh-Nagasawa, N., Jackson, D., Bläsing, O. E., et al. (2013). A fluorometric assay for trehalose in the picomole range. *Plant Methods* 9:21. doi: 10.1186/1746-4811-9-21
- Chinnusamy, V., Schumaker, K., and Zhu, J.-K. (2004). Molecular genetic perspectives on cross-talk and specificity in abiotic stress signaling in plants. *J. Exp. Bot.* 55, 225–236. doi: 10.1093/jxb/erh005
- Cho, Y.-H., Hong, J.-W., Kim, E.-C., and Yoo, S.-D. (2012). Regulatory functions of SnRK1 in stress-responsive gene expression and in plant growth and development. *Plant Physiol.* 158, 1955–1964. doi: 10.1104/pp.111.189829
- Clarke, P. R., and Hardie, D. G. (1990). Regulation of HMG-CoA reductase: identification of the site phosphorylated by the AMP-activated protein kinase *in vitro* and in intact rat liver. *EMBO J.* 9, 2439–2446.
- Claypool, J. A., French, S. L., Johzuka, K., Eliason, K., Vu, L., Dodd, J. A., et al. (2004). Tor pathway regulates Rrn3p-dependent recruitment of yeast RNA polymerase I to the promoter but does not participate in alteration of the number of active genes. *Mol. Biol. Cell* 15, 946–956. doi: 10.1091/mbc.E03
- Coello, P., Hey, S. J., and Halford, N. G. (2011). The sucrose non-fermenting-1-related (SnRK) family of protein kinases: potential for manipulation to improve stress tolerance and increase yield. *J. Exp. Bot.* 62, 883–893. doi: 10.1093/jxb/erq331
- Confraria, A., Martinho, C., Elias, A., Rubio-Somoza, I., and Baena-González, E. (2013). miRNAs mediate SnRK1-dependent energy signaling in *Arabidopsis*. *Front. Plant Sci.* 4:197. doi: 10.3389/fpls.2013.00197
- Contento, A. L., Kim, S., and Bassham, D. C. (2004). Transcriptome profiling of the response of *Arabidopsis* suspension culture cells to Suc starvation. *Plant Physiol.* 135, 2330–2347. doi: 10.1104/pp.104.044362.2330
- Corrêa, L. G. G., Riaño-Pachón, D. M., Schrago, C. G., dos Santos, R. V., Mueller-Roeber, B., and Vincentz, M. (2008). The role of bZIP transcription factors in green plant evolution: adaptive features emerging from four founder genes. *PLoS ONE* 3:e2944. doi: 10.1371/journal.pone.0002944
- Crozet, P., Jammes, F., Valot, B., Ambard-Bretteville, F., Nessler, S., Hodges, M., et al. (2010). Cross-phosphorylation between *Arabidopsis thaliana* sucrose nonfermenting 1-related protein kinase 1 (AtSnRK1) and its activating kinase (AtSnAK) determines their catalytic activities. *J. Biol. Chem.* 285, 12071–12077. doi: 10.1074/jbc.M109.079194
- Cuellar-Ortiz, S. M., De La Paz Arrieta-Montiel, M., Acosta-Gallegos, J., and Covarrubias, A. (2008). Relationship between carbohydrate partitioning and drought resistance in common bean. *Plant Cell Environ.* 31, 1399–1409. doi: 10.1111/j.1365-3040.2008.01853.x
- Dalchau, N., Baek, S. J., Briggs, H. M., Robertson, F. C., Dodd, A. N., Gardner, M. J., et al. (2011). The circadian oscillator gene GIGANTEA mediates a long-term response of the *Arabidopsis thaliana* circadian clock to sucrose. *Proc. Natl. Acad. Sci. U.S.A.* 108, 5104–5109. doi: 10.1073/pnas.1015452108
- Deprost, D., Truong, H.-N., Robaglia, C., and Meyer, C. (2005). An *Arabidopsis* homolog of RAPTOR/KOG1 is essential for early embryo development. *Biochem. Biophys. Res. Commun.* 326, 844–850. doi: 10.1016/j.bbrc.2004.11.117
- Deprost, D., Yao, L., Sormani, R., Moreau, M., Leterreux, G., Nicolai, M., et al. (2007). The *Arabidopsis* TOR kinase links plant growth, yield, stress resistance and mRNA translation. *EMBO Rep.* 8, 864–870. doi: 10.1038/sj.embor.7401043
- De Virgilio, C., and Loewith, R. (2006). The TOR signaling network from yeast to man. *Int. J. Biochem. Cell Biol.* 38, 1476–1481. doi: 10.1016/j.biocel.2006.02.013
- Dietrich, K., Weltmeier, F., Ehlert, A., Weiste, C., Stahl, M., Harter, K., et al. (2011). Heterodimers of the *Arabidopsis* transcription factors bZIP1 and bZIP53 reprogram amino acid metabolism during low energy stress. *Plant Cell* 23, 381–395. doi: 10.1105/tpc.110.075390
- Douglas, P., Pigaglio, E., Ferrer, A., Halford, N. G., and MacKintosh, C. (1997). Three spinach leaf nitrate reductase-3-hydroxy-3-methylglutaryl-CoA reductase kinases that are regulated by reversible phosphorylation and/or Ca²⁺ ions. *Biochem. J.* 325, 101–109.
- Duarte, G. T., Matioli, C. C., Pant, B. D., Schlereth, A., Scheible, W.-R., Stitt, M., et al. (2013). Involvement of microRNA-related regulatory pathways in the glucose-mediated control of *Arabidopsis* early seedling development. *J. Exp. Bot.* 64, 4301–4312. doi: 10.1093/jxb/ert239
- Elbein, A. D., Pan, Y. T., Pastuszak, I., and Carroll, D. (2003). New insights on trehalose: a multifunctional molecule. *Glycobiology* 13, 17R–27R. doi: 10.1093/glycob/cwg047
- Fernandez, O., Vandesteene, L., Feil, R., Baillieux, F., Lunn, J. E., and Clément, C. (2012). Trehalose metabolism is activated upon chilling in grapevine and might participate in *Burkholderia phytofirmans* induced chilling tolerance. *Planta* 236, 355–369. doi: 10.1007/s00425-012-1611-4
- Fujita, Y., Nakashima, K., Yoshida, T., Katagiri, T., Kidokoro, S., Kanamori, N., et al. (2009). Three SnRK2 protein kinases are the main positive regulators of abscisic acid signaling in response to water stress in *Arabidopsis*. *Plant Cell Physiol.* 50, 2123–2132. doi: 10.1093/pcp/pcp147
- Fukushima, A., Kusano, M., Redestig, H., Arita, M., and Saito, K. (2009). Integrated omics approaches in plant systems biology. *Curr. Opin. Chem. Biol.* 13, 532–538. doi: 10.1016/j.cbpa.2009.09.022
- Geigenberger, P. (2003). Response of plant metabolism to too little oxygen. *Curr. Opin. Plant Biol.* 6, 247–256. doi: 10.1016/S1369-5266(03)00038-4
- Ghillebert, R., Swinnen, E., Wen, J., Vandesteene, L., Ramon, M., Norga, K., et al. (2011). The AMPK/SNF1/SnRK1 fuel gauge and energy regulator: structure, function and regulation. *FEBS J.* 278, 3978–3990. doi: 10.1111/j.1742-4658.2011.08315.x
- Gibon, Y., Bläsing, O. E., Palacios-Rojas, N., Pankovic, D., Hendriks, J. H. M., Fisanh, J., et al. (2004). Adjustment of diurnal starch turnover to short days: depletion of sugar during the night leads to a temporary inhibition of carbohydrate utilization, accumulation of sugars and post-translational activation of ADP-glucose pyrophosphorylase in the followin. *Plant J.* 39, 847–862. doi: 10.1111/j.1365-313X.2004.02173.x
- Gibon, Y., Usadel, B., Bläsing, O. E., Kamlage, B., Hoehne, M., Trethewey, R., et al. (2006). Integration of metabolite with transcript and enzyme activity profiling

- during diurnal cycles in *Arabidopsis* rosettes. *Genome Biol.* 7:R76. doi: 10.1186/gb-2006-7-8-r76
- Gibon, Y., Vigeolas, H., Tiessen, A., Geigenberger, P., and Stitt, M. (2002). Sensitive and high throughput metabolite assays for inorganic pyrophosphate, ADPGlc, nucleotide phosphates, and glycolytic intermediates based on a novel enzymic cycling system. *Plant J.* 30, 221–235. doi: 10.1046/j.1365-313X.2001.01278.x
- Gissot, L., Polge, C., Bouly, J., Lemaitre, T., Kreis, M., and Thomas, M. (2004). AKIN3, a plant specific SnRK1 protein, is lacking domains present in yeast and mammals non-catalytic β -subunits. *Plant Mol. Biol.* 56, 747–759. doi: 10.1007/s11103-004-5111-1
- Glinski, M., and Weckwerth, W. (2005). Differential multisite phosphorylation of the trehalose-6-phosphate synthase gene family in *Arabidopsis thaliana*: a mass spectrometry-based process for multiparallel peptide library phosphorylation analysis. *Mol. Cell. Proteomics* 4, 1614–1625. doi: 10.1074/mcp.M500134-MCP200
- Gómez, L. D., Gilday, A., Feil, R., Lunn, J. E., and Graham, I. A. (2010). AtTPS1-mediated trehalose 6-phosphate synthesis is essential for embryogenic and vegetative growth and responsiveness to ABA in germinating seeds and stomatal guard cells. *Plant J.* 64, 1–13. doi: 10.1111/j.1365-313X.2010.04312.x
- Gould, P. D., Ugarte, N., Domijan, M., Costa, M., Foreman, J., Macgregor, D., et al. (2013). Network balance via CRY signaling controls the *Arabidopsis* circadian clock over ambient temperatures. *Mol. Syst. Biol.* 9:650. doi: 10.1038/msb.2013.7
- Halford, N. G., and Hardie, D. G. (1998). SNF1-related protein kinases: global regulators of carbon metabolism in plants? *Plant Mol. Biol.* 37, 735–748. doi: 10.1023/A:1006024231305
- Halford, N. G., and Hey, S. J. (2009). Snf1-related protein kinases (SnRKs) act within an intricate network that links metabolic and stress signaling in plants. *Biochem. J.* 419, 247–259. doi: 10.1042/BJ20082408
- Halford, N. G., Hey, S., Jhurreea, D., Laurie, S., McKibbin, R. S., Zhang, Y., et al. (2004). Highly conserved protein kinases involved in the regulation of carbon and amino acid metabolism. *J. Exp. Bot.* 55, 35–42. doi: 10.1093/jxb/erh019
- Hanson, J., Hanssen, M., Wiese, A., Hendriks, M. M., and Smeekens, S. (2008). The sucrose regulated transcription factor bZIP11 affects amino acid metabolism by regulating the expression of ASPARAGINE SYNTHETASE1 and PROLINE DEHYDROGENASE2. *Plant J.* 53, 935–949. doi: 10.1111/j.1365-313X.2007.03385.x
- Hardie, D. G., Carling, D., and Carlson, M. (1998). The AMP-activated/SNF1 protein kinase subfamily: metabolic sensors of the eukaryotic cell? *Annu. Rev. Biochem.* 67, 821–855. doi: 10.1146/annurev.biochem.67.1.821
- Hay, N., and Sonenberg, N. (2004). Upstream and downstream of mTOR. *Genes Dev.* 18, 1926–1945. doi: 10.1101/gad.1212704
- Hirai, M. Y., Klein, M., Fujikawa, Y., Yano, M., Goodenowe, D. B., Yamazaki, Y., et al. (2005). Elucidation of gene-to-gene and metabolite-to-gene networks in *Arabidopsis* by integration of metabolomics and transcriptomics. *J. Biol. Chem.* 280, 25590–25595. doi: 10.1074/jbc.M502332200
- Hirai, M. Y., Sugiyama, K., Sawada, Y., Tohge, T., Obayashi, T., Suzuki, A., et al. (2007). Omics-based identification of *Arabidopsis* Myb transcription factors regulating aliphatic glucosinolate biosynthesis. *Proc. Natl. Acad. Sci. U.S.A.* 104, 6478–6483. doi: 10.1073/pnas.0611629104
- Hirai, M. Y., Yano, M., Goodenowe, D. B., Kanaya, S., Kimura, T., Awazuhara, M., et al. (2004). Integration of transcriptomics and metabolomics for understanding of global responses to nutritional stresses in *Arabidopsis thaliana*. *Proc. Natl. Acad. Sci. U.S.A.* 101, 10205–10210. doi: 10.1073/pnas.0403218101
- Hrabak, E. M., Chan, C. W. M., Gribskov, M., Harper, J. F., Choi, J. H., Halford, N., et al. (2003). The *Arabidopsis* CDPK-SnRK superfamily of protein kinases. *Plant Physiol.* 132, 666–680. doi: 10.1104/pp.102.011999.666
- Inoki, K., Kim, J., and Guan, K.-L. (2012). AMPK and mTOR in cellular energy homeostasis and drug targets. *Annu. Rev. Pharmacol. Toxicol.* 52, 381–400. doi: 10.1146/annurev-pharmtox-010611-134537
- Jakoby, M., Weisshaar, B., Dröge-Laser, W., Vicente-Carbajosa, J., Tiedemann, J., Kroj, T., et al. (2002). bZIP transcription factors in *Arabidopsis*. *Trends Plant Sci.* 7, 106–111. doi: 10.1016/S1360-1385(01)02223-3
- Jewell, J. L., Russell, R. C., and Guan, K.-L. (2013). Amino acid signaling upstream of mTOR. *Nat. Rev. Mol. Cell Biol.* 14, 133–139. doi: 10.1038/nrm3522
- Jorgensen, P., Rupeš, I., Sharom, J. R., Schnepfer, L., Broach, J. R., and Tyers, M. (2004). A dynamic transcriptional network communicates growth potential to ribosome synthesis and critical cell size. *Genes Dev.* 18, 2491–2505. doi: 10.1101/gad.1228804
- Juntawong, P., and Bailey-Serres, J. (2012). Dynamic light regulation of translation status in *Arabidopsis thaliana*. *Front. Plant Sci.* 3:66. doi: 10.3389/fpls.2012.00066
- Kang, S. G., Price, J., Lin, P.-C., Hong, J. C., and Jang, J.-C. (2010). The *Arabidopsis* bZIP1 transcription factor is involved in sugar signaling, protein networking, and DNA binding. *Mol. Plant* 3, 361–373. doi: 10.1093/mp/ssp115
- Kawaguchi, R., Girke, T., Bray, E. A., and Bailey-Serres, J. (2004). Differential mRNA translation contributes to gene regulation under non-stress and dehydration stress conditions in *Arabidopsis thaliana*. *Plant J.* 38, 823–839. doi: 10.1111/j.1365-313X.2004.02090.x
- Kawaguchi, R., Williams, A. J., Bray, E. A., and Bailey-Serres, J. (2003). Water-deficit-induced translational control in *Nicotiana tabacum*. *Plant Cell Environ.* 26, 221–229. doi: 10.1046/j.1365-3040.2003.00952.x
- Keurentjes, J. J. B. (2009). Genetical metabolomics: closing in on phenotypes. *Curr. Opin. Plant Biol.* 12, 223–230. doi: 10.1016/j.pbi.2008.12.003
- Kim, J., Kundu, M., Viollet, B., and Guan, K.-L. (2011). AMPK and mTOR regulate autophagy through direct phosphorylation of Ulk1. *Nat. Cell Biol.* 13, 132–141. doi: 10.1038/ncb2152
- Lastdrager, J., Hanson, J., and Smeekens, S. (2014). Sugar signals and the control of plant growth and development. *J. Exp. Bot.* 65, 799–807. doi: 10.1093/jxb/ert474
- Lemoine, R., La Camera, S., Atanassova, R., Dédaldéchamp, F., Allario, T., Pourtau, N., et al. (2013). Source-to-sink transport of sugar and regulation by environmental factors. *Front. Plant Sci.* 4:272. doi: 10.3389/fpls.2013.00272
- Li, H., Tsang, C. K., Watkins, M., Bertram, P. G., and Zheng, X. F. S. (2006a). Nutrient regulates Tor1 nuclear localization and association with rDNA promoter. *Nature* 442, 1058–1061. doi: 10.1038/nature05020
- Li, S., Assmann, S. M., and Albert, R. (2006b). Predicting essential components of signal transduction networks: a dynamic model of guard cell abscisic acid signaling. *PLoS Biol.* 4:e312. doi: 10.1371/journal.pbio.0040312
- Liu, J., Ishitani, M., Halfter, U., Kim, C. S., and Zhu, J. K. (2000). The *Arabidopsis thaliana* SOS2 gene encodes a protein kinase that is required for salt tolerance. *Proc. Natl. Acad. Sci. U.S.A.* 97, 3730–3734. doi: 10.1073/pnas.060034197
- Liu, J., Liu, W., Ying, H., Zhao, W., and Zhang, H. (2013a). Analysis of microRNA expression profile induced by AICAR in mouse hepatocytes. *Gene* 512, 364–372. doi: 10.1016/j.gene.2012.09.118
- Liu, Y.-H., Offler, C. E., and Ruan, Y.-L. (2013b). Regulation of fruit and seed response to heat and drought by sugars as nutrients and signals. *Front. Plant Sci.* 4:282. doi: 10.3389/fpls.2013.00282
- Lunn, J. E., Delorge, I., Figueroa, C. M., Van Dijck, P., and Stitt, M. (2014). Trehalose metabolism in plants. *Plant J.* doi: 10.1111/tpj.12509 [Epub ahead of print].
- Lunn, J. E., Feil, R., Hendriks, J. H. M., Gibon, Y., Morcuende, R., Osuna, D., et al. (2006). Sugar-induced increases in trehalose 6-phosphate are correlated with redox activation of ADPGlucose pyrophosphorylase and higher rates of starch synthesis in *Arabidopsis thaliana*. *Biochem. J.* 397, 139–148. doi: 10.1042/BJ20060083
- Ma, J., Hanssen, M., Lundgren, K., Hernández, L., Delatte, T., Ehlert, A., et al. (2011). The sucrose-regulated *Arabidopsis* transcription factor bZIP11 reprograms metabolism and regulates trehalose metabolism. *New Phytol.* 191, 733–745. doi: 10.1111/j.1469-8137.2011.03735.x
- Ma, X. M., and Blenis, J. (2009). Molecular mechanisms of mTOR-mediated translational control. *Nat. Rev. Mol. Cell Biol.* 10, 307–318. doi: 10.1038/nrm2672
- Mackintosh, R. W., Davies, S. P., Clarke, P. R., Weekes, J., Gillespie, J. G., Gibb, B. J., et al. (1992). Evidence for a protein kinase cascade in higher plants 3-hydroxy-3-methylglutaryl-CoA reductase kinase. *Eur. J. Biochem.* 209, 923–931. doi: 10.1111/j.1432-1033.1992.tb17364.x
- Martin, D. E., and Hall, M. N. (2005). The expanding TOR signaling network. *Curr. Opin. Cell Biol.* 17, 158–166. doi: 10.1016/j.ceb.2005.02.008

- Martin, D. E., Souldard, A., and Hall, M. N. (2004). TOR regulates ribosomal protein gene expression via PKA and the Forkhead transcription factor FHL1. *Cell* 119, 969–979. doi: 10.1016/j.cell.2004.11.047
- Mayer, C., Zhao, J., Yuan, X., and Grummt, I. (2004). mTOR-dependent activation of the transcription factor TIF-IA links rRNA synthesis to nutrient availability. *Genes Dev.* 18, 423–434. doi: 10.1101/gad.285504
- McMichael, R. W., Bachmann, M., and Huber, S. C. (1995). Spinach leaf sucrose-phosphate synthase and nitrate reductase are phosphorylated/inactivated by multiple protein kinases in vitro. *Plant Physiol.* 108, 1077–1082.
- Menand, B., Desnos, T., Nussaume, L., Berger, F., Bouchez, D., Meyer, C., et al. (2002). Expression and disruption of the *Arabidopsis* TOR (target of rapamycin) gene. *Proc. Natl. Acad. Sci. U.S.A.* 99, 6422–6427. doi: 10.1073/pnas.092141899
- Meyuhas, O., and Dreazen, A. (2009). Ribosomal protein S6 kinase from TOP mRNAs to cell size. *Prog. Mol. Biol. Transl. Sci.* 90, 109–153. doi: 10.1016/S1877-1173(09)90003-5
- Miyashita, Y., and Good, A. G. (2008a). Glutamate deamination by glutamate dehydrogenase plays a central role in amino acid catabolism in plants. *Plant Signal. Behav.* 3, 842–843. doi: 10.1093/jxb/erm340.842
- Miyashita, Y., and Good, A. G. (2008b). NAD(H)-dependent glutamate dehydrogenase is essential for the survival of *Arabidopsis thaliana* during dark-induced carbon starvation. *J. Exp. Bot.* 59, 667–680. doi: 10.1093/jxb/erm340
- Montané, M.-H., and Menand, B. (2013). ATP-competitive mTOR kinase inhibitors delay plant growth by triggering early differentiation of meristematic cells but no developmental patterning change. *J. Exp. Bot.* 64, 4361–4374. doi: 10.1093/jxb/ert242
- Moreau, M., Azzopardi, M., Clément, G., Dobrenel, T., Marchive, C., Renne, C., et al. (2012). Mutations in the *Arabidopsis* homolog of LST8 / GbL, a partner of the target of rapamycin kinase, impair plant growth, flowering, and metabolic adaptation to long days. *Plant Cell* 24, 463–481. doi: 10.1105/tpc.111.091306
- Muller, B., Pantin, F., Génard, M., Turc, O., Freixes, S., Piques, M., et al. (2011). Water deficits uncouple growth from photosynthesis, increase C content, and modify the relationships between C and growth in sink organs. *J. Exp. Bot.* 62, 1715–1729. doi: 10.1093/jxb/erq438
- Mustroph, A., Zanetti, M. E., Jang, C. J. H., Holtan, H. E., Repetti, P. P., Galbraith, D. W., et al. (2009). Profiling transcriptomes of discrete cell populations resolves altered cellular priorities during hypoxia in *Arabidopsis*. *Proc. Natl. Acad. Sci. U.S.A.* 106, 18843–18848. doi: 10.1073/pnas.0906131106
- Nägele, T., and Heyer, A. G. (2013). Approximating subcellular organisation of carbohydrate metabolism during cold acclimation in different natural accessions of *Arabidopsis thaliana*. *New Phytol.* 198, 777–787. doi: 10.1111/nph.12201
- Nägele, T., and Weckwerth, W. (2012). Mathematical modeling of plant metabolism—from reconstruction to prediction. *Metabolites* 2, 553–566. doi: 10.3390/metabo2030553
- Nicolai, M., Roncato, M. A., Canoy, A. S., Rouquié, D., Sarda, X., Freyssinet, G., et al. (2006). Large-scale analysis of mRNA translation states during sucrose starvation in *Arabidopsis* cells identifies cell proliferation and chromatin structure as targets of translational control. *Plant Physiol.* 141, 663–673. doi: 10.1104/pp.106.079418.1
- Nunes, C., O'Hara, L. E., Primavesi, L. F., Delatte, T. L., Schlupepmann, H., Somsen, G. W., et al. (2013). The trehalose 6-phosphate/SnRK1 signaling pathway primes growth recovery following relief of sink limitation. *Plant Physiol.* 162, 1720–1732. doi: 10.1104/pp.113.220657
- O'Hara, L. E., Paul, M. J., and Winkler, A. (2013). How do sugars regulate plant growth and development? New insight into the role of trehalose-6-phosphate. *Mol. Plant* 6, 261–274. doi: 10.1093/mp/sss120
- Osuna, D., Usadel, B., Morcuende, R., Gibon, Y., Bläsing, O. E., Höhne, M., et al. (2007). Temporal responses of transcripts, enzyme activities and metabolites after adding sucrose to carbon-deprived *Arabidopsis* seedlings. *Plant J.* 49, 463–491. doi: 10.1111/j.1365-313X.2006.02979.x
- Pal, S. K., Liput, M., Piques, M., Ishihara, H., Obata, T., Martins, M. C. M., et al. (2013). Diurnal changes of polysome loading track sucrose content in the rosette of wild-type *Arabidopsis* and the starchless pgm mutant. *Plant Physiol.* 162, 1246–1265. doi: 10.1104/pp.112.212258
- Paul, M. J., and Pellny, T. K. (2003). Carbon metabolite feedback regulation of leaf photosynthesis and development. *J. Exp. Bot.* 54, 539–547. doi: 10.1093/jxb/erg052
- Paul, M. J., Primavesi, L. F., Jhurreea, D., and Zhang, Y. (2008). Trehalose metabolism and signaling. *Annu. Rev. Plant Biol.* 59, 417–441. doi: 10.1146/annurev.arplant.59.032607.092945
- Pinheiro, C., Chaves, M. M., and Ricardo, C. P. (2001). Alterations in carbon and nitrogen metabolism induced by water deficit in the stems and leaves of *Lupinus albus* L. *J. Exp. Bot.* 52, 1063–1070. doi: 10.1093/jxb/52.358.1063
- Piques, M., Schulze, W. X., Höhne, M., Usadel, B., Gibon, Y., Rohwer, J., et al. (2009). Ribosome and transcript copy numbers, polysome occupancy and enzyme dynamics in *Arabidopsis*. *Mol. Syst. Biol.* 5:314. doi: 10.1038/msb.2009.68
- Pokhilko, A., Fernández, A. P., Edwards, K. D., Southern, M. M., Halliday, K. J., and Millar, A. J. (2012). The clock gene circuit in *Arabidopsis* includes a repressilator with additional feedback loops. *Mol. Syst. Biol.* 8:574. doi: 10.1038/msb.2012.6
- Pokhilko, A., Hodge, S. K., Stratford, K., Knox, K., Edwards, K. D., Thomson, A. W., et al. (2010). Data assimilation constrains new connections and components in a complex, eukaryotic circadian clock model. *Mol. Syst. Biol.* 6:416. doi: 10.1038/msb.2010.69
- Pokhilko, A., Mas, P., and Millar, A. J. (2013). Modelling the widespread effects of TOC1 signaling on the plant circadian clock and its outputs. *BMC Syst. Biol.* 7:23. doi: 10.1186/1752-0509-7-23
- Polge, C., and Thomas, M. (2007). SNF1/AMPK/SnRK1 kinases, global regulators at the heart of energy control? *Trends Plant Sci.* 12, 20–28. doi: 10.1016/j.tplants.2006.11.005
- Rahmani, F., Hummel, M., Schuurmans, J., Wiese-Klinkenberg, A., Smeekens, S., and Hanson, J. (2009). Sucrose control of translation mediated by an upstream open reading frame-encoded peptide. *Plant Physiol.* 150, 1356–1367. doi: 10.1104/pp.109.136036
- Ramon, M., and Rolland, E. (2007). Plant development: introducing trehalose metabolism. *Trends Plant Sci.* 12, 185–188. doi: 10.1016/j.tplants.2007.03.007
- Reinke, A. W., Baek, J., Ashenberg, O., and Keating, A. E. (2013). Networks of bZIP protein-protein interactions diversified over a billion years of evolution. *Science* 340, 730–734. doi: 10.1126/science.1233465
- Ren, M., Qiu, S., Venglat, P., Xiang, D., Feng, L., Selvaraj, G., et al. (2011). Target of rapamycin regulates development and ribosomal RNA expression through kinase domain in *Arabidopsis*. *Plant Physiol.* 155, 1367–1382. doi: 10.1104/pp.110.169045
- Ren, M., Venglat, P., Qiu, S., Feng, L., Cao, Y., Wang, E., et al. (2012). Target of rapamycin signaling regulates metabolism, growth, and life span in *Arabidopsis*. *Plant Cell* 24, 4850–4874. doi: 10.1105/tpc.112.107144
- Robaglia, C., Thomas, M., and Meyer, C. (2012). Sensing nutrient and energy status by SnRK1 and TOR kinases. *Curr. Opin. Plant Biol.* 15, 301–307. doi: 10.1016/j.pbi.2012.01.012
- Rodrigues, A., Adamo, M., Crozet, P., Margalha, L., Confraria, A., Martinho, C., et al. (2013). ABI1 and PP2CA phosphatases are negative regulators of Snf1-related protein kinase1 signaling in *Arabidopsis*. *Plant Cell* 1–15. doi: 10.1105/tpc.113.114066
- Rolland, E., Baena-Gonzalez, E., and Sheen, J. (2006). Sugar sensing and signaling in plants: conserved and novel mechanisms. *Annu. Rev. Plant Biol.* 57, 675–709. doi: 10.1146/annurev.arplant.57.032905.105441
- Rook, F., Gerrits, N., Kortstee, A., van Kampen, M., Borrias, M., Weisbeek, P., et al. (1998). Sucrose-specific signaling represses translation of the *Arabidopsis* ATB2 bZIP transcription factor gene. *Plant J.* 15, 253–263. doi: 10.1046/j.1365-313X.1998.00205.x
- Rudra, D., and Warner, J. R. (2004). What better measure than ribosome synthesis? *Genes Dev.* 18, 2431–2436. doi: 10.1101/gad.1256704
- Sablowski, R., and Carnier Dornelas, M. (2014). Interplay between cell growth and cell cycle in plants. *J. Exp. Bot.* 65, 2703–2714. doi: 10.1093/jxb/ert354
- Satoh, R., Fujita, Y., Nakashima, K., Shinozaki, K., and Yamaguchi-Shinozaki, K. (2004). A novel subgroup of bZIP proteins functions as transcriptional activators in hypoosmolarity-responsive expression of the ProDH gene in *Arabidopsis*. *Plant Cell Physiol.* 45, 309–317. doi: 10.1093/pcp/pch036
- Schepetilnikov, M., Dimitrova, M., Mancera-Martínez, E., Geldreich, A., Keller, M., and Ryabova, L. (2013). TOR and S6K1 promote translation reinitiation of

- uORF-containing mRNAs via phosphorylation of eIF3h. *EMBO J.* 32, 1087–1102. doi: 10.1038/emboj.2013.61
- Schluepmann, H., Dijken, A., Van Aghdasi, M., Wobbes, B., and Paul, M. (2004). Trehalose mediated growth inhibition of *Arabidopsis* seedlings is due to trehalose-6-phosphate accumulation. *Plant Physiol.* 135, 879–890. doi: 10.1104/pp.104.039503.1
- Schluepmann, H., Pellny, T., van Dijken, A., Smeekens, S., and Paul, M. (2003). Trehalose 6-phosphate is indispensable for carbohydrate utilization and growth in *Arabidopsis thaliana*. *Proc. Natl. Acad. Sci. U.S.A.* 100, 6849–6854. doi: 10.1073/pnas.1132018100
- Schütze, K., Harter, K., and Chaban, C. (2008). Post-translational regulation of plant bZIP factors. *Trends Plant Sci.* 13, 247–255. doi: 10.1016/j.tplants.2008.03.002
- Seaton, D. D., Ebenhöf, O., Millar, A. J., and Pokhilko, A. (2014). Regulatory principles and experimental approaches to the circadian control of starch turnover. *J. R. Soc. Interface* 11:20130979. doi: 10.1098/rsif.2013.0979
- Shen, W., and Hanley-Bowdoin, L. (2006). Geminivirus infection up-regulates the expression of two *Arabidopsis* protein kinases related to yeast SNF1- and mammalian AMPK-activating kinases. *Plant Physiol.* 142, 1642–1655. doi: 10.1104/pp.106.088476
- Sormani, R., Yao, L., Menand, B., Ennar, N., Lecampion, C., Meyer, C., et al. (2007). Saccharomyces cerevisiae FKBP12 binds *Arabidopsis thaliana* TOR and its expression in plants leads to rapamycin susceptibility. *BMC Plant Biol.* 7:26. doi: 10.1186/1471-2229-7-26
- Sugden, C., Crawford, R. M., Halford, N. G., and Hardie, D. G. (1999). Regulation of spinach SNF1-related (SnRK1) kinases by protein kinases and phosphatases is associated with phosphorylation of the T loop and is regulated by 5'-AMP. *Plant J.* 19, 433–439. doi: 10.1046/j.1365-313X.1999.00532.x
- Thimm, O., Bläsing, O., Gibon, Y., Nagel, A., Meyer, S., Krüger, P., et al. (2004). Mapman: a user-driven tool to display genomics data sets onto diagrams of metabolic pathways and other biological processes. *Plant J.* 37, 914–939. doi: 10.1111/j.1365-313X.2004.02016.x
- Tohge, T., Nishiyama, Y., Hirai, M. Y., Yano, M., Nakajima, J., Awazu, M., et al. (2005). Functional genomics by integrated analysis of metabolome and transcriptome of *Arabidopsis* plants over-expressing an MYB transcription factor. *Plant J.* 42, 218–235. doi: 10.1111/j.1365-313X.2005.02371.x
- Tsai, A. Y.-L., and Gazzarrini, S. (2014). Trehalose-6-phosphate and SnRK1 kinases in plant development and signaling: the emerging picture. *Front. Plant Sci.* 5:1119. doi: 10.3389/fpls.2014.00119
- Tsang, C. K., Liu, H., and Zheng, X. F. S. (2010). mTOR binds to the promoters of RNA polymerase I- and III- transcribed genes. *Cell Cycle* 9, 953–957. doi: 10.4161/cc.9.5.10876
- Usadel, B., Bläsing, O. E., Gibon, Y., Retzlaff, K., Höhne, M., Günther, M., et al. (2008). Global transcript levels respond to small changes of the carbon status during progressive exhaustion of carbohydrates in *Arabidopsis* rosettes. *Plant Physiol.* 146, 1834–1861. doi: 10.1104/pp.107.115592
- van Dam, T. J. P., Zwartkruis, F. J. T., Bos, J. L., and Snel, B. (2011). Evolution of the TOR pathway. *J. Mol. Evol.* 73, 209–220. doi: 10.1007/s00239-011-9469-9
- Van Der Kelen, K., Beyaert, R., Inzé, D., and De Veylder, L. (2009). Translational control of eukaryotic gene expression. *Crit. Rev. Biochem. Mol. Biol.* 44, 143–168. doi: 10.1080/10409230902882090
- Wang, X., and Proud, C. G. (2011). mTORC1 signaling: what we still don't know. *J. Mol. Cell Biol.* 3, 206–220. doi: 10.1093/jmcb/mjq038
- Weltmeier, F., Ehlert, A., Mayer, C. S., Dietrich, K., Wang, X., Schütze, K., et al. (2006). Combinatorial control of *Arabidopsis* proline dehydrogenase transcription by specific heterodimerisation of bZIP transcription factors. *EMBO J.* 25, 3133–3143. doi: 10.1038/sj.emboj.7601206
- Weltmeier, F., Rahmani, F., Ehlert, A., Dietrich, K., Schütze, K., Wang, X., et al. (2009). Expression patterns within the *Arabidopsis* C/S1 bZIP transcription factor network: availability of heterodimerization partners controls gene expression during stress response and development. *Plant Mol. Biol.* 69, 107–119. doi: 10.1007/s11103-008-9410-9
- Wiese, A., Elzinga, N., Wobbes, B., and Smeekens, S. (2004). A conserved upstream open reading frame mediates sucrose-induced repression of translation. *Plant Cell* 16, 1717–1729. doi: 10.1105/tpc.019349
- Wullschlegel, S., Loewith, R., and Hall, M. N. (2006). TOR signaling in growth and metabolism. *Cell* 124, 471–484. doi: 10.1016/j.cell.2006.01.016
- Xiong, Y., McCormack, M., Li, L., Hall, Q., Xiang, C., and Sheen, J. (2013). Glucose-TOR signaling reprograms the transcriptome and activates meristems. *Nature* 496, 181–186. doi: 10.1038/nature12030
- Xiong, Y., and Sheen, J. (2012). Rapamycin and glucose-target of rapamycin (TOR) protein signaling in plants. *J. Biol. Chem.* 287, 2836–2842. doi: 10.1074/jbc.M111.300749
- Xiong, Y., and Sheen, J. (2014). TOR signaling networks in plant growth and metabolism. *Plant Physiol.* 164, 499–512. doi: 10.1104/pp.113.229948
- Xu, J., Ji, J., and Yan, X.-H. (2012). Cross-talk between AMPK and mTOR in regulating energy balance. *Crit. Rev. Food Sci. Nutr.* 52, 373–381. doi: 10.1080/10408398.2010.500245
- Yadav, U. P., Ivakov, A., Feil, R., Duan, G. Y., Walther, D., Giavalisco, P., et al. (2014). The sucrose-trehalose 6-phosphate (Tre6P) nexus: specificity and mechanisms of sucrose signaling by Tre6P. *J. Exp. Bot.* 65, 1051–1068. doi: 10.1093/jxb/ert457
- Yamaguchi-Shinozaki, K., and Shinozaki, K. (2006). Transcriptional regulatory networks in cellular responses and tolerance to dehydration and cold stresses. *Annu. Rev. Plant Biol.* 57, 781–803. doi: 10.1146/annurev.arplant.57.032905.105444
- Yoshida, T., Fujita, Y., Maruyama, K., Mogami, J., Todaka, D., Shinozaki, K., et al. (2014). Four *Arabidopsis* AREB/ABF transcription factors function predominantly in gene expression downstream of SnRK2 kinases in abscisic-acid signaling in response to osmotic stress. *Plant. Cell Environ.* doi: 10.1111/pce.12351 [Epub ahead of print].
- Yuan, J. S., Galbraith, D. W., Dai, S. Y., Griffin, P., and Stewart, C. N. (2008). Plant systems biology comes of age. *Trends Plant Sci.* 13, 165–171. doi: 10.1016/j.tplants.2008.02.003
- Zhang, Y., Andralojc, P. J., Hey, S. J., Primavesi, L. F., Specht, M., Koehler, J., et al. (2008). *Arabidopsis* sucrose non-fermenting-1-related protein kinase-1 and calcium-dependent protein kinase phosphorylate conserved target sites in ABA response element binding proteins. *Ann. Appl. Biol.* 153, 401–409. doi: 10.1111/j.1744-7348.2008.00302.x
- Zhang, Y., Persson, S., and Giavalisco, P. (2013). Differential regulation of carbon partitioning by the central growth regulator Target of Rapamycin (TOR). *Mol. Plant* 6, 1731–1733. doi: 10.1093/mp/ss094
- Zhang, Y., Primavesi, L. F., Jhurrea, D., Andralojc, P. J., Mitchell, R. A. C., Powers, S. J., et al. (2009). Inhibition of SNF1-related protein kinase1 activity and regulation of metabolic pathways by trehalose-6-phosphate. *Plant Physiol.* 149, 1860–1871. doi: 10.1104/pp.108.133934

Conflict of Interest Statement: The authors declare that the research was conducted in the absence of any commercial or financial relationships that could be construed as a potential conflict of interest.

Received: 16 May 2014; accepted: 02 July 2014; published online: 17 July 2014.

Citation: Tomé F, Nägele T, Adamo M, Garg A, Marco-Illorca C, Nukarinen E, Pedrotti L, Peviani A, Simeunovic A, Tatkievicz A, Tomar M and Gamm M (2014) The low energy signaling network. *Front. Plant Sci.* 5:353. doi: 10.3389/fpls.2014.00353

This article was submitted to *Plant Physiology*, a section of the journal *Frontiers in Plant Science*.

Copyright © 2014 Tomé, Nägele, Adamo, Garg, Marco-Illorca, Nukarinen, Pedrotti, Peviani, Simeunovic, Tatkievicz, Tomar and Gamm. This is an open-access article distributed under the terms of the Creative Commons Attribution License (CC BY). The use, distribution or reproduction in other forums is permitted, provided the original author(s) or licensor are credited and that the original publication in this journal is cited, in accordance with accepted academic practice. No use, distribution or reproduction is permitted which does not comply with these terms.

Chapter 2: SnRK1 and C/S1 bZIPs are important regulators of cellular respiration under Low Energy Stress

INTRODUCTION

Being autotrophic organisms, plants base their growth and development on the supply of carbohydrates from photosynthetic activity. Although most of the energy required by the plant is provided by the photosynthesis, there are several situations when plants should exploit their catabolic potential, as alternative energy provider. At the very early stage of their life, plants consume all the resources accumulated in the seeds to germinate and reach the autotrophic stage. This developmental stage is probably the most hazardous span in the plant life because the successful establishment of a new plant life depends entirely on the catabolism of resources present in the seeds. Another important situation when catabolism is indispensable to ensure plant life is represented by stresses: several environmental perturbations, indeed, require a strong effort, which has an impact on the energy status of the plant. Many stresses, indeed, influence either on light absorption, carbon fixation, or directly increase the cellular energy demand (Baena-González & Sheen, 2008). Fight against the increased energy demand seems to be shared by different and apparently unrelated kinds of stresses (Baena-González, 2010). In recent years is emerging the idea that the response to any stress is composed by a stress-specific component and a general response (Kültz, 2005), the last seems to be decoded as an energy-deficiency signal. F. Tomé and colleagues (Tomé et al., 2014) have recently reviewed the energy-related plant response to stresses. They named Low Energy Syndrome (LES) all the transcriptional, translational, and metabolic reprogramming essential for plant survival under stress situations. LES includes, among the others, the repression of biosynthetic activities and sugar storage, as well as the induction of catabolic processes and sugar remobilization. Therefore, catabolism could represent the unique source of energy to support both early plant development and higher energy demand under stress situation. Sugar metabolism is the major contributor to the cellular energy demand, however, lipids, proteins, and amino acids metabolism could be exploited in particular situations.

Based on recent findings, it seems that all these pathways are under the control of Sucrose non Fermenting Related Protein Kinase 1 (SnRK1). SnRK1 indeed, are one of the most important regulators of LES and, although they have several functions in the plant, in our

context they could be seen as moderator of the unnecessary anabolic activity of the cell and strong promoter of the energy-producing catabolism. SnRK1 contribute to the huge metabolic reprogramming during low energy stress regulating directly the activity of crucial metabolic enzymes or indirectly via the transcriptional control of key genes. SnRK1 and bZIP TFs of the S1 and C group (S1-bZIPs and C-bZIPs) constitute a central regulatory network, responsible of the regulation of the expression of many genes involved in the metabolism of alternative source of energy.

In this work we will briefly introduce the SnRK1 and C/S1-bZIPs and we will describe the major pathways for the utilization “energy” substrates, focusing particularly on their regulation.

SnRK1 (from “the low energy signaling network”)(Tomé et al., 2014)

Sucrose-non-fermenting-1-related protein kinase-1 is a metabolic sensor that can decode energy deficiency signals and induce an extensive metabolic reprogramming. This is mediated by a number of transcription factors and downstream targets that start an energy-saving program at several levels, including transcription, translation or direct phosphorylation of targets (Baena-González et al., 2007). SnRK1 is the plant homolog of the yeast sucrose non-fermenting-1 (SNF1) and the animal AMP-activated protein kinase (AMPK;Halford et al., 2004). SNF1-related protein kinases show close to 50% identity, rising to 65% for the kinase domains (Polge and Thomas, 2007). Their primary role is the integration of nutrient availability, stress signals, and energy expenditure, to be able to activate the required adaptations for homeostasis and survival (Halford and Hardie, 1998; Hardie et al., 1998; Ghillebert et al., 2011). Plants contain two other subfamilies, SnRK2 and SnRK3. They are less similar to SNF1 and AMPK and unique to plants (Halford et al., 2004), and are also involved in plant responses to several stresses (Coello et al.,2011). SnRK2is involved in ABA signaling, responses to cold, and was shown to improve drought tolerance when overexpressed (Fujita et al., 2009; Halford and Hey, 2009; Yoshida et al., 2014). The SnRK3 family includes SOS2 (salt overly sensitive 2), involved in conferring salt tolerance (Liu et al., 2000). There is no evidence of redundancy between the different SnRK families and SnRK2 and SnRK3 do not complement the yeast *snf1*? deletion mutant growth phenotype (Hrabak et al., 2003). It is clear that they cannot fulfill the role of SnRK1 (Halford andHey, 2009), even though there is some similarity in target recognition (Zhang et al., 2008). It was suggested that SnRK2 and SnRK3 arose in plants by

duplication of SnRK1 and then diverged rapidly during plant evolution to meet new needs related to networks linking stress and ABA signaling with metabolic signaling (Halford and Hey, 2009). The SnRK1/SNF1/AMPK kinases typically function as heterotrimeric complexes and require a catalytic α -subunit, KIN10 and KIN11 in plants, and regulatory β and γ subunits (Figure 2). The non-catalytic subunits are also conserved among the SnRK1/SNF1/AMPK complex. They are likely involved in substrate recognition, subcellular localization, and regulation of the complex activity (Polge and Thomas, 2007; Ghillebert et al., 2011). Interestingly, the Arabidopsis AKIN β 1, AKIN β 2, and AKIN β 3 have markedly different expression patterns, which suggests a level of regulation based on interactions targeting the β subunits in response to different signals (Bouly et al., 1999; Gissot et al., 2004).

The activity of SnRK1 depends on phosphorylation in the highly conserved T-loop by upstream kinases (Sugden et al., 1999). In Arabidopsis, the protein kinases SnRK1-activating kinase 1 and 2 (AtSnAK1 and AtSnAK2) were shown to complement a yeast triple kinase mutant by restoring SNF1 upstream kinase activity (Shen and Hanley-Bowdoin, 2006). In addition, they phosphorylate non-truncated AtSnRK1 catalytic subunits in vitro, making them putative candidates as SnRK1 physiological upstream kinases (Crozet et al., 2010). Even though it is known that SnRK1 activation requires phosphorylation, it has not been clarified how it is affected by the cellular energy level. In contrast to the mammalian AMPK, SnRK1 is not allosterically activated by AMP, but it was shown that T-loop dephosphorylation and the resulting inactivation of the kinase are inhibited by low concentrations of AMP (Sugden et al., 1999). Furthermore, SnRK1 activity is modulated by specific phosphatases. Two clade A type 2C protein phosphatases (PP2C) were recently shown to dephosphorylate and inactivate SnRK1 through interaction with the catalytic subunit (Rodrigues et al., 2013). The activity of SnRK1 is also inhibited by trehalose-6-phosphate (T6P). The association between trehalose metabolism and sugar-sensing in plants has recently become more evident (Tsai and Gazzarrini, 2014). Despite its role as a carbon source and in stress protection in resurrection plants, fungi, bacteria, and non-vertebrate animals (Elbein et al., 2003; Paul et al., 2008), the amount of trehalose in the majority of plants is too low to perform this function. It was suggested that trehalose has a major role on metabolism, growth, and development, acting as a signal of sugar availability (Schluepmann et al., 2003; Ramon and Rolland, 2007; Gómez et al., 2010).

Trehalose is synthesized from UDP-glucose and glucose-6P via the intermediate T6P in a two-step pathway involving trehalose phosphate synthase (TPS) and trehalose phosphate phosphatase (TPP), and degraded by trehalase (Paul et al., 2008). T6P has a distinctive role in metabolic signaling, and class II TPSs, that include AtTPS5-11, are targets of phosphorylation by SnRK1 (Glinski and Weckwerth, 2005). AtTPS5 is induced by sugars and repressed by starvation (Schluepmann et al., 2004), while the opposite is true for AtTPS8-10 (Osuna et al., 2007). Trehalose-6-phosphate inhibits the catalytic activity of SnRK1 in vitro at physiological concentrations, causing expression changes of KIN10 marker genes consistent with an inactivation of SnRK1 (Zhang et al., 2009), while Arabidopsis seedlings overexpressing SnRK1 show a glucose-hypersensitive phenotype (Cho et al., 2012), similar to seedlings with low T6P (Schluepmann et al., 2003). However, even though T6P inhibits the growth of Arabidopsis seedlings, it does not inhibit SnRK1 catalytic activity in extracts of mature leaves (Zhang et al., 2009), suggesting that an intermediary factor is needed for SnRK1 inhibition by T6P. Recently, it was suggested that T6P and SnRK1 might act through different, but interacting signaling pathways (Lunn et al., 2014) and can play antagonistic roles during stress responses (O'Hara et al., 2013). This is particularly important in stress conditions that negatively affect carbon levels, leading to an activation of starvation responses through SnRK1. For example, T6P levels are much lower in rosettes harvested in the dark and in carbon-starved seedlings (Lunn et al., 2006; Carillo et al., 2013; Yadav et al., 2014). However, stress conditions do not necessarily lead to carbon depletion. For example, under moderate drought or cold stress, a wide range of carbohydrates accumulate in Arabidopsis (Muller et al., 2011), including abundant sugars such as hexoses and sucrose, other sugars such as trehalose or mannitol, amino acids, organic acids, structural C-rich compounds like cellulose, among others. In grapevine, sucrose and T6P contents increase in response to chilling (Fernandez et al., 2012). T6P may therefore play a role in the inhibition of SnRK1 under conditions where carbon sources are not limited (Lunn et al., 2014). The cross-talk between SnRK1 and T6P when growth is limited by sink capacity was recently studied by varying temperature and nutrient supply to induce sink limitation, and feed sucrose and glucose at physiological levels (Nunes et al., 2013). In these conditions, T6P responds specifically to sucrose, even at different growth rates. Moreover, there was a strong correlation between T6P- and SnRK1-regulated gene expression, but not between T6P and relative growth rate.

It appears that SnRK1 marker gene expression is related to T6P content regardless of the growth outcome, but further investigations will hopefully elucidate the relationship between SnRK1 and T6P.

The C/S1-bZIPs network

Being a kinase without DNA binding activity, SnRK1 cannot reprogram plant transcriptome its self. Many target of SnRK1 are transcription factors, therefore, it is likely to be that SnRK1 plays on transcription factors activity to regulate the transcriptional reprogramming in response to plant stress (Mair et al., in preparation). bZIP transcription factors have been proved to be important mediator of the SnRK1-driven plant response to stress (Baena-González, Rolland, Thevelein, & Sheen, 2007)Mair et al, in preparation; Pedrotti et al., in preparation). In *Arabidopsis* ca. 82 genes encoding for bZIP TF have been identified(Corrêa et al., 2008). The structure of bZIPs is characterized by the presence of a basic DNA-binding domain flanked by a nuclear localization signal and a leucine zipper domain. The leucine zipper domain is a protein-protein interaction interface, which allow bZIPs to form dimers. At the moment, the function of dimerization is still unclear. Indeed, bZIPs could bind the DNA also as monomer. It is likely the case that dimerization add a further degree of regulation. Recently, it has been speculate that different dimers regulate the expression of different gene subsets or that different dimers are present only in specific situations (Dietrich et al., 2011; Ehlert et al., 2006; Weltmeier et al., 2009).

Based on their homology bZIPs were classified in 10 groups, named with letters from A to I and S (Jakoby et al., 2002). Above all, the S1 subgroup (bZIP1, bZIP2, bZIP11, bZIP44, and bZIP53) have been related to the energy metabolism and in particular with those of alternative energy sources. Several studies pointed out the importance of S1-bZIPs in the regulation of amino acids, starch and sugars metabolism (Dietrich et al., 2011; Hanson, Hanssen, Wiese, Hendriks, & Smeekens, 2008; Ma et al., 2011; Weiste & Dröge-Laser, 2014). Energy availability seems to affect also the phenotype of *s1-bzips* mutant. bZIP53 overexpression results in reduced plant size, delayed bolting and expression of seed-specific genes in leaves (Alonso et al., 2009). *bZIP1* knockout plants were shown to grow faster than wild type on medium lacking glucose (Kang et al., 2010), while a plant overexpressing bZIP1 showed a stronger starvation response indicated by faster leaf-yellowing in extended night conditions (Dietrich et al., 2011). Transgenic plants overexpressing bZIP11 show reduced plant size, seed production, and viability (Hanson et

al., 2008).

Interestingly S1-bZIPs are also regulated by the energy status of the cell. All S1-bZIPs share an exceptionally long 5'-UTR which harbour a 5'-uORF that mediates a sucrose dependent repression of their translation. This mechanism has been described as Sucrose Induced Repression of Translation (SIRT) (Rahmani et al., 2009). The expression of some S1-bZIPs have also been reported to be strongly induced by stresses that could affect the energy status of the cell. It is the case for example of bZIP1 and bZIP53 whose expression is strongly induced by extended dark or salt treatment (Dietrich et al., 2011). Interestingly, we observed that the expression of *bZIP1* and *bZIP53* in the *snrk1.1/1.2* mutant exposed to 6h of extended dark, was not as strong as in WT plants. This indicate that bZIP1 and bZIP53 expression is controlled by a SnRK1-dependent mechanism. The details of this regulation, however, are still unknown.

Another interesting feature of S1-bZIPs is their ability to form dimers with bZIP members of the C-group (bZIP9, bZIP10, bZIP25, and bZIP63) (Ehlert et al., 2006). This intricate net of interactions has been referred as the C/S1 network. Although the regulation of the network are still unknown, several works reported the importance of the dimerization. In the work of Dietrich and colleagues, for example, it is clear that the absence of bZIP1 and/or bZIP53 reduces only partially the expression of *ASN1* and *PRODH* and only in the quadruple mutant (*bzip1/53/9/63* or *bzip1/53/10/25*) the expression of those genes is strongly reduced (Dietrich et al., 2011). Other example can be seen in the work of Hartmann and colleagues (Hartmann et al., in preparation).

Starch metabolism

Arabidopsis typically invests 30 to 50% of its photoassimilates into transitory stored starch. Starch is therefore the major storage metabolite in *Arabidopsis* and it is considered the major integrator of plant growth (Stitt & Zeeman, 2012; Sulpice et al., 2009). Changes in the photosynthetic activity or in the energy demand of the plant could, indeed, be firstly buffered by accumulation and remobilization of starch. Whereas plant growth during the day mostly relies on sugar produced by photosynthetic activity, leaf starch remobilization during the night continuously support respiration, sucrose export and growth. Accordingly, starch accumulation is regulated on a daily base by the circadian clock: leaf starch reaches its maximum accumulation at the end of the light phase and is almost but not completely consumed at dawn (Geiger & Servaites 1994; Smith, Denyer & Martin 1997; Geiger et al.

2000; Stitt et al. 2007). Regulation of starch metabolism is very important for the plant, *Arabidopsis* mutants defective in either starch synthesis or degradation are dwarf (Caspar et al., 1985, 1991; Lin et al., 1988a, 1988b; Yu et al., 2001; Schneider et al., 2002; Niittylä et al., 2004; Stitt and Zeeman, 2012). The control of starch metabolism is obtained via the regulation of both starch biosynthesis and degradation. Although the expression of many genes encoding enzymes involved in starch metabolism show large and coordinate diurnal changes, these changes are poorly associated with differences in protein levels or enzymes activity (Geigenberger, 2011; Stitt & Zeeman, 2012). Thus, changes of transcription probably serve to adjust starch turnover to mid- or long-term conditions. Redox regulation, protein modification, and allosteric regulation seem to be responsible for the momentary changes to adjust to sudden environment alteration (Stitt & Zeeman, 2012). A well studied example is the control of ATPase activity, which controls the flux of carbon into transitory starch (Geigenberger, 2011). The activity of AGPase is effectively switched off during the night by a redox regulatory mechanism. AGPase activity is also allosterically activated by glycerate-3-phosphate and inhibited by Pi. Reduction of AGPase leads to dramatic alterations in the kinetic properties of the enzyme, resulting in an increase of the substrate affinities and the sensitivity to the allosteric activator glycerate-3-phosphate, while the sensitivity to inhibition by Pi is decreased (Tiessen et al., 2002). Similar to AGPase, several starch synthases and starch-branching-enzymes have been found to be redox regulated, such as SS1, SS3, and BE2 (Glaring et al., 2012). It has been shown that also enzymes involved in starch degradation are redox regulated. In particular GW1 and BAM1 are activated by reduction and therefore play a role in the control of starch degradation at night.

SnRK1 is definitely related to starch metabolism. Overexpression of SnRK1 resulted in an increased expression of SUS4 (the sucrose synthase expressed in potato tubers) and ADP-glucose pyrophosphorylase, leading to high starch accumulation and low free sugars concentration (Mc Kibbin et al., 2006). Viceversa, the expression of an antisense SnRK1 prevents starch mobilization (Baena-González et al., 2007). The β -subunit of SnRK1 possesses a Starch Binding Domain (SBD) similar to that one of AMPK (Avila-Castañeda et al., 2014). Although with debates (Emanuelle et al., 2015), it has been recently demonstrated that SnRK1 localizes in close proximity with chloroplastic starch and it could actually bind to starch granules. The authors of this work noticed that the activity of

SnRK1 was inhibited by the presence of starch, suggesting that the SBD could act as an inhibitory domain, similarly to what observed for AMPK and its Glycogen Binding Domain. SnRK1 has been suggested to be a starch sensor, activated only when starch reserves are below a certain threshold.

S1-bZIPs are also involved in the regulation of starch metabolism. In particular, it has been shown that bZIP53 overexpressor plants accumulate more starch than WT plants. In bZIP53 o.e. plant, starch is degraded during the night, to sustain plant growth. However, in the light phase, starch accumulates stronger and faster than in WT plants. It seems that bZIP53 o.e. channels sugars into starch biosynthesis at the expense of plant growth (Dietrich K., PhD thesis). Interestingly, in bZIP53 o.e. plants, the expression of *b-amilase 5 (BAM5)* is strongly reduced than in WT plants (Dietrich K., PhD thesis). Accordingly with a defective starch metabolism, bZIP53 o.e. plants show a dwarf phenotype. *bzip53* mutant or *bzip1/bzip53* double ko mutants do not show any starch related phenotype. However, in a transcriptome profiling experiment, *BAM5* was found to be more expressed in *bzip1/bzip53* double ko mutant and in bZIP1 o.e. plants.

SnRK1 and S1-bZIPs control the expression of several genes involved in the metabolism of alternative energy sources

Respiration in plants, as in every other organism, is essential to provide metabolic energy and carbon skeleton for growth and maintenance. The respiratory metabolism includes the reactions of three pathways: glycolysis, the tricarboxylic acid (TCA) cycle, and the mitochondrial electron transport chain. During the glycolysis, a molecule of glucose is broken down into two molecules of pyruvate, which are subsequently interconverted in the reaction of the TCA-cycle, producing energy (ATP) and reducing power (NAD(P)H). The reducing equivalents are used by the mitochondrial electron transport chain to power the synthesis of ATP. Many reaction and enzymes involved in plant respiration present similarities with the animal and bacteria counterparts. However, plant respiration presents several features which make it very flexible and unique: substrates for the TCA cycle reactions or electrons for the mitochondrial electron transport chain can be supplied by various other substrates, such as starch, sucrose, lipids, and amino acids (Ishizaki et al., 2005, 2006; Araújo et al., 2010); the presence of alternative oxidases (Rasmusson et al., 2009) and external NAD(P)H dehydrogenases (Sweetlove et al., 2006; Rasmusson et al., 2008); operation of the TCA cycle in a non-cyclic mode under stress conditions, such as

hypoxia (Rocha et al., 2010a; Sweetlove et al., 2010).

The respiration of substrates other than sugars: proteins, lipids, and chlorophyll

Several stresses could interfere with the light/dark cycle, photosynthesis rate, carbon availability or energy demand. These could be buffered by accumulation and remobilization of starch as carbon reserve, integrating changes in the balance between carbon supply and growth (Gibon et al., 2009; Sulpice et al., 2009; Stitt et al., 2010). However, could happened that starch is not enough to supply the stress and plant needs to make use of alternative source of energy. Under these circumstances, the metabolism of plant cell is modified and different enzymatic pathways are induced to break down alternative respiratory substrates. Proteins and lipids are used as alternative substrates under stress situations.

Protein and amino acids catabolism

The first step in protein degradation is their ubiquitination. During the process of ubiquitination three enzyme complexes, namely E1 (ubiquitin activating enzymes), E2 (ubiquitin conjugating enzymes) and E3 (ubiquitin ligase), flag the target protein with a polimer of ubiquitin. The flagged proteins are then recognized by the proteasome for degradation. In this situation, proteolysis and downstream metabolism, leads to the production of amino acids, which can be recycled for the production of energy and carbon skeleton.

Amino acids produced by protein degradation can then follow three different fate: (i) conversion in other amino acids; (ii) degradation into isovaleryl-CoA or hydroxyglutarate; (iii) processed by the TCA cycle. In the last case, they might enter directly into the TCA cycle by beeing converted in pyruvate or acetyl-CoA or indirectly, after beeing converted in 2-oxoglutarate, an intermediate of this pathway. In this case, they can supply electrons directly to the mitochondrial electron transport chain. Differently, electrons produced by the degradation of branched chain, aromatic amino acids and lysine are transferred to the mitochondrial electron transport chain through the ubiquinol pool via the ETF/ETFQO system. Isovaleryl-CoA dehydrogenase and D-2-hydroxyglutarate dehydrogenase were identified as the key plant enzymes capable of providing electrons to the ubiquinone pool via the ETF complex [84]. By the mechanisms described above, the degradation of amino acid provides a double boost to the mitochondrial electron transport chain. The expression of *IVD*, *MCCA* and *MCCB* and *ETFQO* is strongly induced by extended dark or under

carbohydrate starvation. This observation clearly indicates an important function for the BCCA catabolism under those conditions. The *ivd* and *etfqo* *ko* mutants show an accelerated senescence phenotype under extended dark conditions (Araújo et al., 2010; Ishizaki et al., 2005, 2006).

When activated, SnRK1 strongly reduces protein biosynthesis (Lastdrager, Hanson, & Smeekens, 2014; Tomé et al., 2014) and at the same time induces amino acids degradation (Baena-González et al., 2007). From the work of Baena-Gonzalez and colleagues, the o.e. of SnRK1.1 induces the expression of more than 20 genes with a logFC > 2 involved in amino acids degradation. Several genes encoding for protein involved in the metabolism of branched chain amino acids are positively regulated by SnRK1. Among the others, *METHYLCROTONYL COA CARBOXYLASE* (*MCCA* and *MCCB*), *BRANCHED CHAIN TRANSAMINASE2* (*BCAT2*), *GLUTAMINE DEPENDENT ASPARAGINE SYNTHETASE* (*ASN1*), *PROLINE DEHYDROGENASE* (*PRODH1*) have to be mentioned here because they are also target genes of S1-bZIPs. In the *bzip1/53* double mutant, *bzip1/53/9/63* and *bzip1/53/10/25* quadruple mutants, indeed, the expression of *PRODH*, *ASN1*, *BCAT2*, *MCCA*, and *MCCB* is not induced in response to extended dark (Dietrich et al., 2011). Vice versa, the expression of these genes is strongly upregulated by bZIP1 and bZIP53 o.e. in transgenic plants or protoplasts (K. Dietrich, PhD thesis). Beside bZIP1 and bZIP53, also bZIP11 is involved in the control of amino acids metabolism. Hanson and colleagues demonstrated that bZIP11 exerts a strong control on the expression of *PRODH* and *ASN1* (Hanson et al., 2008). Accordingly to a role of S1-bZIPs in the control of amino acids metabolism, the different *S1-bzips* mutant show an altered amino acids profile. For example, the bZIP1 o.e. mutant used by Dietrich and colleagues showed a reduce content of Leucine, Isoleucine, Valine, and Asparagine when exposed to extended dark for 6 days. The o.e. of bZIP53 had similar effects on Leucine, Isoleucine, and Valine but not on Asparagine, which was higher than in WT plants (Dietrich et al., 2011).

Lipids metabolism

Carbon storage in the form of triacylglycerol (TAG) is a ubiquitous feature of seed plants. TAGs stored within lipid droplets serve as an essential physiological energy and carbon reserve during postgerminative growth. TAG is an extremely compact energy store, since complete oxidation yields more than twice the energy of protein or carbohydrate. TAG can account for up to 60% of a seed's weight. TAGs are not important only during seed

germination but throughout the complete plant life. Leaves, flower and fruits, indeed, synthesize and store TAGs.

TAGs degradation begins with their remobilization from oil bodies. Oil bodies are relatively simple organelles where TAGs are packed and enveloped by a monolayer of phospholipids embedding several proteins. Proteins have the function to prevent coalescence of oil droplets, in many cases the size of oil bodies is correlated with oleosin protein level and *Arabidopsis* mutant with altered oleosins level show a delayed germination or an abnormal TAGs storage. It still have to be elucidated whether caleosin and oleosin actively participate in the removal of TAGs from oil bodies or whether they facilitate the activity of lipases by keeping a high surface-to-volume ratio. Lipases are interfacial enzymes that cleave mono-, di-, and triacylglycerol into free FAs and glycerol at the oil/water interface. The glycerol produced is then predominantly converted in glycerol-3-phosphate by glycerol kinase (GLI1). although relatively small, the contribution of carbon skeletons from the glycerol kinase pathway is essential in the absence of a functional glyoxylate cycle. Fatty acids released by lipolysis are subsequently transported into the peroxisomes, where they are activated by acyl-CoA synthase and further degraded by β -oxidation.

Not so much is known about the regulation by SnRK1 and S1-bZIPs on the lipid metabolism. In the work of Baena-Gonzalez and colleagues it is clearly shown that lipid catabolism is activated by the o.e. of SnRK1 (Baena-González et al., 2007). Preliminary data suggest that S1-bZIPs control the expression of some oleosin and caleosin related genes, as well as those of some lipases (K. Dietrich, PhD thesis).

Outline and objectives of the thesis

It is now clear that SnRK1 and S1-bZIPs are involved in the regulation of the plant energy homeostasis, in particular under situations when a metabolic re-adaptation is needed for survival. This could be the case of a stress, both of biotic or abiotic nature, or during a developmental stage transition. SnRK1 and S1-bZIPs are involved in the regulation of the expression of key enzymes of the primary metabolism, such those of carbohydrates, amino acids and lipids. From the data present in the literature, we could deduce that there is a substantial overlap between genes regulated by SnRK1 and those regulated by S1-bZIPs. It was within the aim of this thesis to demonstrate the functional relation between SnRK1 and S1-bZIPs.

REFERENCES

- Alonso, R., Oñate-Sánchez, L., Weltmeier, F., Ehlert, A., Diaz, I., Dietrich, K., ... Dröge-Laser, W. (2009). A pivotal role of the basic leucine zipper transcription factor bZIP53 in the regulation of Arabidopsis seed maturation gene expression based on heterodimerization and protein complex formation. *The Plant Cell*, 21(6), 1747–61. doi:10.1105/tpc.108.062968
- Araújo, W. L., Ishizaki, K., Nunes-Nesi, A., Larson, T. R., Tohge, T., Krahnert, I., ... Fernie, A. R. (2010). Identification of the 2-hydroxyglutarate and isovaleryl-CoA dehydrogenases as alternative electron donors linking lysine catabolism to the electron transport chain of Arabidopsis mitochondria. *The Plant Cell*, 22(5), 1549–63. doi:10.1105/tpc.110.075630
- Avila-Castañeda, A., Gutiérrez-Granados, N., Ruiz-Gayosso, A., Sosa-Peinado, A., Martínez-Barajas, E., & Coello, P. (2014). Structural and functional basis for starch binding in the SnRK1 subunits AKIN β 2 and AKIN β γ . *Frontiers in Plant Science*, 5(May), 199. doi:10.3389/fpls.2014.00199
- Baena-González, E. (2010). Energy signaling in the regulation of gene expression during stress. *Molecular Plant*, 3(2), 300–13. doi:10.1093/mp/ssp113
- Baena-González, E., Rolland, F., Thevelein, J. M., & Sheen, J. (2007). A central integrator of transcription networks in plant stress and energy signalling. *Nature*, 448(7156), 938–42. doi:10.1038/nature06069
- Baena-González, E., & Sheen, J. (2008). Convergent energy and stress signaling. *Trends in Plant Science*, 13(9), 474–82. doi:10.1016/j.tplants.2008.06.006
- Corrêa, L. G. G., Riaño-Pachón, D. M., Schrago, C. G., dos Santos, R. V., Mueller-Roeber, B., & Vincentz, M. (2008). The role of bZIP transcription factors in green plant evolution: adaptive features emerging from four founder genes. *PloS One*, 3(8), e2944. doi:10.1371/journal.pone.0002944
- Dietrich, K., Weltmeier, F., Ehlert, A., Weiste, C., Stahl, M., Harter, K., ... Dröge-Laser, W. (2011). Heterodimers of the Arabidopsis Transcription Factors bZIP1 and bZIP53 Reprogram Amino Acid Metabolism during Low Energy Stress. *The Plant Cell Online*, 23(January), 381–395. doi:10.1105/tpc.110.075390
- Ehlert, A., Weltmeier, F., Wang, X., Mayer, C. S., Smeekens, S., Vicente-Carbajosa, J., & Dröge-Laser, W. (2006). Two-hybrid protein-protein interaction analysis in Arabidopsis

- protoplasts: establishment of a heterodimerization map of group C and group S bZIP transcription factors. *The Plant Journal : For Cell and Molecular Biology*, 46(5), 890–900. doi:10.1111/j.1365-313X.2006.02731.x
- Emanuelle, S., Hossain, M. I., Moller, I. E., Pedersen, H. L., van de Meene, A. M. L., Doblin, M. S., ... Stapleton, D. (2015). SnRK1 from *Arabidopsis thaliana* is an atypical AMPK. *The Plant Journal*, n/a–n/a. doi:10.1111/tpj.12813
- Geigenberger, P. (2011). Regulation of starch biosynthesis in response to a fluctuating environment. *Plant Physiology*, 155(April), 1566–1577. doi:10.1104/pp.110.170399
- Hanson, J., Hanssen, M., Wiese, A., Hendriks, M. M. W. B., & Smeekens, S. (2008). The sucrose regulated transcription factor bZIP11 affects amino acid metabolism by regulating the expression of ASPARAGINE SYNTHETASE1 and PROLINE DEHYDROGENASE2. *The Plant Journal : For Cell and Molecular Biology*, 53(6), 935–49. doi:10.1111/j.1365-313X.2007.03385.x
- Ishizaki, K., Larson, T. R., Schauer, N., Fernie, A. R., Graham, I. A., & Leaver, C. J. (2005). The Critical Role of *Arabidopsis* Electron-Transfer Flavoprotein:Ubiquinone Oxidoreductase during Dark-Induced Starvation, 17(September), 2587–2600. doi:10.1105/tpc.105.035162.1
- Ishizaki, K., Schauer, N., Larson, T. R., Graham, I. a, Fernie, A. R., & Leaver, C. J. (2006). The mitochondrial electron transfer flavoprotein complex is essential for survival of *Arabidopsis* in extended darkness. *The Plant Journal : For Cell and Molecular Biology*, 47(5), 751–60. doi:10.1111/j.1365-313X.2006.02826.x
- Jakoby, M., Weisshaar, B., Dröge-Laser, W., Vicente-Carbajosa, J., Tiedemann, J., Kroj, T., & Parcy, F. (2002). bZIP transcription factors in *Arabidopsis*. *Trends in Plant Science*, 7(3), 106–11. Retrieved from <http://www.ncbi.nlm.nih.gov/pubmed/21279647>
- Kültz, D. (2005). Molecular and evolutionary basis of the cellular stress response. *Annual Review of Physiology*, 67(1), 225–57. doi:10.1146/annurev.physiol.67.040403.103635
- Lastdrager, J., Hanson, J., & Smeekens, S. (2014). Sugar signals and the control of plant growth and development. *Journal of Experimental Botany*, 1–9. doi:10.1093/jxb/ert474
- Ma, J., Hanssen, M., Lundgren, K., Hernández, L., Delatte, T., Ehlert, A., ... Hanson, J. (2011). The sucrose-regulated *Arabidopsis* transcription factor bZIP11 reprograms metabolism and regulates trehalose metabolism. *The New Phytologist*, 191(3), 733–745. doi:10.1111/j.1469-8137.2011.03735.x

- Rahmani, F., Hummel, M., Schuurmans, J., Wiese-Klinkenberg, A., Smeekens, S., & Hanson, J. (2009). Sucrose control of translation mediated by an upstream open reading frame-encoded peptide. *Plant Physiology*, *150*(3), 1356–67. doi:10.1104/pp.109.136036
- Stitt, M., & Zeeman, S. C. (2012). Starch turnover: pathways, regulation and role in growth. *Current Opinion in Plant Biology*, *15*(3), 282–92. doi:10.1016/j.pbi.2012.03.016
- Sulpice, R., Pyl, E.-T., Ishihara, H., Trenkamp, S., Steinfath, M., Witucka-Wall, H., ... Stitt, M. (2009). Starch as a major integrator in the regulation of plant growth. *Proceedings of the National Academy of Sciences of the United States of America*, *106*(25), 10348–53. doi:10.1073/pnas.0903478106
- Tomé, F., Nägele, T., Adamo, M., Garg, A., Marco-Llorca, C., Nukarinen, E., ... Gamm, M. (2014). The low energy signaling network. *Frontiers in Plant Science*, *5*(July), 353. doi:10.3389/fpls.2014.00353
- Weiste, C., & Dröge-Laser, W. (2014). The Arabidopsis transcription factor bZIP11 activates auxin-mediated transcription by recruiting the histone acetylation machinery. *Nature Communications*, *5*(May). doi:10.1038/ncomms4883
- Weltmeier, F., Rahmani, F., Ehlert, A., Dietrich, K., Schütze, K., Wang, X., ... Dröge-Laser, W. (2009). Expression patterns within the Arabidopsis C/S1 bZIP transcription factor network: availability of heterodimerization partners controls gene expression during stress response and development. *Plant Molecular Biology*, *69*(1-2), 107–19. doi:10.1007/s11103-008-9410-9

Chapter 3: SnRK1-triggered switch of bZIP63 dimerization mediates the low-energy response in plants

Andrea Mair¹, Lorenzo Pedrotti², Bernhard Würzinger¹, Dorothea Anrather³, Andrea Simeunovic¹, Thomas Nägele¹, Katrin Dietrich², Jesús Vicente Carbajosa⁴, Johannes Hanson^{5,6}, Elena Baena-González⁷, Christina Chaban⁸, Wolfram Weckwerth¹, Wolfgang Dröge-Laser², and Markus Teige^{1,9*}

Authors affiliation

¹ Department of Ecogenomics and Systems Biology, University of Vienna, Vienna, Austria

² Julius-von-Sachs-Institute, Pharmaceutical Biology, University of Würzburg, Würzburg, Germany

³ Mass Spectrometry Facility, Max F. Perutz Laboratories, University of Vienna, Vienna, Austria

⁴ Centro de Biotecnología y Genómica de Plantas, Universidad Politécnica de Madrid, Madrid, Spain

⁵ Department of Molecular Plant Physiology, Utrecht University, Utrecht, The Netherlands.

⁶ Department of Plant Physiology, Umea Plant Science Center, University of Umea, Umea, Sweden

⁷ Instituto Gulbenkian de Ciência, Oeiras, Portugal

⁸ Department of Plant Physiology, Center for Plant Molecular Biology, University of²⁹ Tübingen, Tübingen, Germany

⁹ Department of Applied Genetics and Cell Biology, University of Natural Resources and Life Sciences, Vienna, Austria

* Contact Information: markus.teige@univie.ac.at

ABSTRACT

Metabolic adjustment to changing growth conditions, particularly balancing of growth and defense responses, is crucial for all organisms to survive. The evolutionary conserved AMPK/Snf1/SnRK1 kinases are well-known metabolic master regulators in the low-energy response in animals, yeast and plants. They act at two different levels: by modulating the activity of key metabolic enzymes, and by massive transcriptional reprogramming. While the first part is well established, the latter function is only partially understood in animals and not at all in plants. Here we identified the Arabidopsis transcription factor bZIP63 as key regulator of the starvation response and direct target of the SnRK1 kinase. Phosphorylation of bZIP63 by SnRK1 changed its dimerization preference, thereby affecting target gene expression and ultimately primary metabolism. A *bzip63* knock-out mutant exhibited starvation-related phenotypes, which could be functionally complemented by wild type bZIP63, but not by a version harboring point mutations in the identified SnRK1 target sites.

INTRODUCTION

Flexibility in the regulation of gene expression is crucial for all organisms to adjust their metabolism to changing growth conditions. Particularly under stress, available energy resources need to be balanced between defense and growth. The SUCROSE NON-FERMENTING RELATED KINASE 1 (SnRK1) in plants and its orthologs, the sucrose-non-fermenting 1 (Snf1) kinase in yeast and the AMP-dependent protein kinase (AMPK) in mammals, are well-known and crucial master regulators of energy homeostasis. SnRK1 is involved in the regulation of plant metabolism, development, and stress response (Baena-Gonzalez and Sheen, 2008; Polge and Thomas, 2007), Snf1 is required for the switch from fermentative to oxidative metabolism in the absence of glucose (Hedbacker and Carlson, 2009), and AMPK regulates glucose, lipid, and protein metabolism, mitochondrial biogenesis, and feeding behavior in animals (Hardie et al., 2012). They are generally activated under energy starvation conditions and trigger metabolic reprogramming to slow down energy-consuming processes and turn on pathways for alternative energy production in order to survive the stress conditions (Hardie 2007, Tome et al., 2014). This happens, in two ways: by direct phosphorylation and modulation of the activity of key enzymes in nitrogen, carbon, or fatty acid metabolism, and by massive transcriptional reprogramming (Baena-Gonzalez and Sheen, 2008; McGee and Hargreaves, 2008; Polge and Thomas, 2007). Especially in plants, the latter aspect, the regulation of transcription, is still poorly understood. In *Arabidopsis* protoplasts, transient overexpression of AKIN10, a catalytic subunit of the SnRK1 complex, resulted in a transcriptional profile reminiscent of various starvation conditions and led to the identification of 1021 putative SnRK1 target genes (Baena-Gonzalez et al., 2007). However, the transcription factors mediating the transcriptional response of SnRK1 to energy starvation are still unknown. Based on reporter gene activation assays in protoplasts (Baena-Gonzalez et al., 2007) and modelling of microarray data (Usadel et al., 2008), some members of the C/S1 group of basic leucine zipper (bZIP) transcription factors (TFs) – foremost bZIP11 and bZIP1 from the S1 group - were speculated to be involved in this process. Yet, a direct regulation of these bZIPs by SnRK1 has never been shown.

bZIP proteins form a large and highly conserved group of eukaryotic TFs, which are characterized by a basic region for specific DNA binding and a leucine zipper for bZIP dimerization (Deppmann et al., 2006; Reinke et al., 2013). They are involved in a

multitude of cellular processes, including cell proliferation and differentiation, metabolism, stress response, and apoptosis (Jakoby et al., 2002; Mayr and Montminy, 2001; Motohashi et al., 2002; Rodrigues-Pousada et al., 2010; Tsukada et al., 2011). The diversity and flexibility of transcriptional regulation by bZIP TFs can at least partially be attributed to their potential to form variable dimer combinations, which bind to different consensus target sites (Deppmann et al., 2006; Tsukada et al., 2011). While the leucine zipper determines the possible dimer combinations (Deppmann et al., 2006; Reinke et al., 2013), the actual *in vivo* dimer composition is further influenced by factors such as protein availability, binding of regulatory proteins, or post-translational modifications (Kim et al., 2007; Lee et al., 2010; Schuetze et al., 2008). Since the initial discovery that the mammalian bZIP cAMP response element binding protein (CREB) is regulated by reversible phosphorylation, many bZIP TFs were reported to be phosphorylated (Holmberg et al., 2002; Schuetze et al., 2008; Tsukada et al., 2011). However, particularly in plants, the functional consequences of these phosphorylation events often remained unclear. For example, it has been known for several years that abscisic acid (ABA)-dependent phosphorylation of some ABA-responsive element binding proteins (AREBs) by SnRK2 kinases increases their transcriptional activity (Furihata et al., 2006), yet the underlying mechanism of this activation is still unknown. It is also surprising that, while many examples for phosphorylation-dependent regulation of bZIP activity, DNA-binding, subcellular localization, stability, and interaction with regulatory proteins are known (Schuetze et al., 2008; Tsukada et al., 2011), reports on the regulation of dimerization are scarce. So far, only three publications (Guo et al., 2010; Kim et al., 2007; Lee et al., 2010) showed compelling evidence for phosphorylation-dependent changes in bZIP dimerization in animals. Still, even in these cases it is often not entirely clear whether bZIP phosphorylation affects dimerization directly or indirectly by enhancing DNA binding.

bZIP63 is a member of the C-group of Arabidopsis bZIPs, which was proposed to play a role in energy metabolism, seed maturation, and germination under osmotic stress (Correa et al., 2008; Jakoby et al., 2002; Veerabagu et al., 2014). Its transcriptional profile indicates that bZIP63 could be involved in the (energy) starvation response, as transcription and mRNA stability are repressed by sugars and ABA and mRNA levels increase in the night and even more during extended night treatments (Kunz et al., 2014; Matioli et al., 2011). A small set of potential target genes for bZIP63 has been identified, including genes

involved in amino acid metabolism (*ASN1/DIN6* = ASPARAGINE SYNTHETASE 1, *ProDH* = PROLINE DEHYDROGENASE), energy starvation response (*DIN10* = RAFFINOSE SYNTHASE 6), and senescence (*SEN1* = SENESCENCE 1) (Baena-Gonzalez et al., 2007; Dietrich et al., 2011; Matiolli et al., 2011; Veerabagu et al., 2014). The C-group bZIPs form a dimerization network with the S1-group in plants, in which bZIP63 can interact with all members (Ehlert et al., 2006; Kang et al., 2010). Three of its dimerization partners from the S1-group – bZIP1, bZIP11, and bZIP53 – were shown to be important metabolic regulators, especially under energy starvation conditions, and to regulate the expression of *ASN1* and *ProDH* as well (Dietrich et al., 2011; Hanson et al., 2008; Ma et al., 2011).

Here we show that bZIP63 is an important metabolic regulator, especially under stress/starvation conditions, and that bZIP63 is phosphorylated at multiple sites in vivo in a sugar and energy-dependent manner. In an unbiased approach, we identified SnRK1 as one of the kinases responsible for bZIP63 phosphorylation and found that it targets three highly conserved serine residues in the N- and C-terminus of bZIP63. Moreover, we demonstrate that the phosphorylation of these sites is crucial for bZIP63's dimerization and activity in planta and propose a molecular model for a phosphorylation-triggered switch of bZIP63 dimerization partners, which ultimately regulates metabolic reprogramming.

RESULTS

bZIP63 controls dark-induced senescence and primary metabolism

To better understand the role of bZIP63 in the plant we first tested whether bZIP63 has a similar phenotype as its dimerization partners. Prolonged darkness was shown to induce increased chlorophyll loss in plants overexpressing bZIP1 (Dietrich et al., 2011). Therefore, we incubated a bZIP63 knock-out (ko), two independent overexpressor (ox) lines, and their respective wild types (wt) in the dark and determined the percentage of the green leaf area as a measure for chlorophyll content. While no differences were observed before dark treatment (Figure 1 – figure supplement 1 A-C), significant differences were visible after 9 days in darkness. Similar to the bZIP1 ox, the bZIP63 ox lines (ox#2 and ox#3) had a significantly higher percentage of yellow leaf area than the wt. In contrast, *bzip63* plants displayed a stay-green phenotype (Figure 1A and 1B; Figure 1 - figure supplement 1D).

The notion that several heterodimerization partners of bZIP63, including bZIP1 and bZIP11, are important metabolic regulators under starvation conditions (Dietrich et al., 2011; Ma et al., 2011) prompted us to do an unbiased metabolomics analysis of *bzip63* and *ox#3* plants and their respective wt lines. Leaves of five week-old plants were harvested after 6h of light and extended night and analyzed for changes in the primary carbon and nitrogen metabolism using gas chromatography coupled to mass spectrometry (Figure 1C; Figure 1 – figure supplement 2; Figure 1 - source data 1). Intriguingly, almost all amino acid levels were increased in the ko and decreased in the ox plants. This effect was even more pronounced after the extended night treatment. The biggest differences were observed for proline, glutamate, glutamine and asparagine. Most analyzed sugars were slightly increased in the ko in the light, but decreased in the extended night, while the ox showed a decrease in glucose, fructose, and raffinose and an increase in sucrose content under both conditions. TCA cycle intermediates were in general slightly increased in the ko. Taken together, these data show that misregulation of bZIP63 expression results in altered regulation of starvation-induced senescence and has a strong effect on primary metabolism.

bZIP63 is phosphorylated at multiple sites in an energy-dependent manner

Kirchler et al. (2010) showed that bZIP63 can be phosphorylated in vitro by crude Arabidopsis extracts. To test whether bZIP63 is also phosphorylated in vivo, we treated total leaf protein extracts of *ox#3* plants, expressing GFP-tagged bZIP63, with lambda protein phosphatase (λ PP) and separated treated and untreated extracts on 2D gels by isoelectric focusing (IEF) in the first, and SDS-PAGE in the second dimension (Figure 2A). λ PP treatment induced a clear shift of bZIP63 towards the basic region of the IEF strip, thus indicating dephosphorylation of the protein.

As bZIP63 expression is strongly regulated by the day/night cycle and by sugars (Kunz et al., 2014; Matioli et al., 2011), we investigated its phosphorylation status under these conditions, applying the Phos-tag technique to enhance phosphorylation-induced mobility shifts in 1D SDS-PAGE (Kinoshita et al., 2006). Comparison of leaf protein extracts harvested after 6h of light or extended night revealed a strongly reduced electrophoretic mobility of the majority of plant-expressed bZIP63-GFP as compared to the recombinantly expressed bZIP63-YFP (Figure 2B). In the light, two strong bands were visible, possibly reflecting the two spots on the 2D gel (Figure 2A). Under extended night conditions, an

additional band appeared, indicating increased phosphorylation of bZIP63. Moreover, in seedlings, which were grown in liquid culture, the extended night-triggered phosphorylation of bZIP63 could be abolished by the addition of 1% of sucrose (Figure 2B). In fact, phosphorylation was even lower than in the light. These data indicate that bZIP63 has a basal level of phosphorylation in the plant and gets hyper-phosphorylated under starvation conditions. In contrast, addition of external sugars leads to a reduced phosphorylation status of bZIP63.

In order to identify the *in vivo* phosphorylated residues, bZIP63-GFP was immune precipitated from total leaf extracts using bead-coupled anti-GFP antibodies, subjected to proteolytic digest and analyzed by liquid chromatography coupled to tandem mass spectrometry (LC-MS/MS) (Figure 2 – figure supplement 1A). To achieve maximum sequence coverage of the protein we combined proteolytic digests from four proteolytic enzymes (trypsin, chymotrypsin, LysC, and subtilisin). This approach resulted in a total sequence coverage of 93.6% and the identification of several phospho-peptides, indicating that bZIP63 is phosphorylated at up to seven serines (S29, S59, S102, S160, S261, S294, and S300) *in vivo* (Figure 2C; Figure 2 – figure supplement 1 B-C). Two of these sites – S29 and S300 – were also found in a recent phospho-proteomics study (Umezawa et al., 2013). Notably, only three of the seven sites – S29, S294, and S300 – were found by tryptic protein digest, underpinning the advantage of alternative proteolytic digests for phospho-peptide identification in targeted proteomics.

SnRK1, CDPKs and CKII are potential upstream kinases of bZIP63

To identify potential upstream kinases of bZIP63, we performed *in-gel* kinase assays with total plant protein extracts using recombinantly expressed bZIP63 as substrate. Three strong bands of about 40, 50, and 55kDa, respectively, were visible on the autoradiogram (Figure 3A), indicating that at least three kinases can phosphorylate bZIP63 *in vitro*. These bands were not visible on a gel without substrate, excluding the possibility that they originate from kinase auto-phosphorylation (Figure 3 – figure supplement 1). To reduce the sample complexity and to enrich low abundant bZIP63-binding proteins before kinase identification, we affinity purified plant protein extracts on immobilized bZIP63. The eluted fractions were tested in an *in-gel* kinase assay for kinase activity towards bZIP63 and loaded on an SDS-PAGE gel for kinase identification. Bands corresponding in molecular weight (MW) to the signal from the kinase assay were excised from the gel,

digested with trypsin and analyzed by LC-MS/MS (Figure 3B and C). In total, 27 protein kinases and kinase complex subunits were identified in three independent experiments (Figure 3 – figure supplement 2; Figure 3 – source data 1). From those, proteins which did not match the expected MW or for which it had been shown experimentally that they are not localized in the nucleus were excluded. Only proteins which were identified in more than one sample with at least one proteotypic peptide were considered to be high confidence candidates, resulting in six protein kinases and two regulatory subunits (Figure 3C; Figure 3 – figure supplement 2; Figure 3 – source data 1). We identified the two main catalytic subunits of SnRK1, AKIN10 and AKIN11, as well as the regulatory subunit SNF4. Several members of the calcium dependent protein kinase (CDPK) family were found, but only CPK3 was identified with high confidence. In addition, two catalytic (CKA1 and CKA2) and one regulatory subunit (CKB1) of casein kinase II (CKII) were found, as well as Casein kinase like 2 (CKL2). The SnRK1 kinases, CDPKs, and CKL2, correspond in MW to the two upper bands, while the lower band corresponds to the CKII kinase subunits. As SnRK1 was previously reported to enhance the activity of several C/S1 group bZIPs (Baena-Gonzalez et al., 2007) and was suggested to be activated under energy starvation conditions (Baena-Gonzalez and Sheen, 2008) – which could explain the observed hyper-phosphorylation of bZIP63 in extended night – we focused our further analysis on AKIN10 and AKIN11.

The SnRK1 kinase AKIN10 interacts with and phosphorylates bZIP63 in vivo

To confirm that AKIN10 and AKIN11 phosphorylate bZIP63, we first performed an in-gel kinase assay with protein extracts of wt and *akin10* seedlings in the presence of EGTA, to reduce the signal from CDPKs of the same MW (Figure 4A). In both root and leaf extracts of *akin10* one band at the expected MW of AKIN10 nearly disappeared. As AKIN11 has approximately the same MW as AKIN10, the remaining signal likely originates from AKIN11. In vitro kinase assays, with equal amounts of both kinases, showed that AKIN10 phosphorylates bZIP63 much stronger than AKIN11 (Figure 4B). Addition of the SnRK1 upstream kinase SnAK2 increased the activity of AKIN10 and AKIN11 about seven-fold, but had no effect on the ratio between the signal intensities (Figure 4 – figure supplement 1). In vivo interaction assays with the identified SnRK1 complex subunits supported the findings of the kinase assays. In both yeast 2-hybrid (Y2H) and bimolecular fluorescence complementation (BiFC) assays AKIN10 and the regulatory subunit SNF4 interacted

strongly with bZIP63, almost comparable to the signal from the bZIP63 homodimer, which was used as positive control (Walter et al., 2004). In contrast, AKIN11 and the two regulatory subunits AKIN^o 1 and AKIN^o 2 showed almost no interaction with bZIP63 (Figure 4C and D; Figure 4 – figure supplement 2). It appears therefore, that AKIN10 plays the major role in bZIP63 phosphorylation.

To verify that AKIN10 plays a role in the in vivo phosphorylation of bZIP63 we compared the phosphorylation state of bZIP63 in plants overexpressing bZIP63-GFP or -YFP in the wt and *akin10* background, respectively. As SnRK1 has been suggested to act as a major regulator in the energy deprivation response, we again compared leaf protein extracts after 6h light and extended night and found that the hyper-phosphorylated form of bZIP63, observed in the wt in extended night, was almost gone in the *akin10* background (Figure 4E). The same effect was observed in seedling cultures after 6h of extended night (Figure 4 – figure supplement 3), thus confirming that AKIN10 is the major kinase responsible for bZIP63 hyper-phosphorylation under starvation conditions.

AKIN10 phosphorylates three conserved and functionally important serine residues in bZIP63

Next, to elucidate which of the seven in vivo phosphorylation sites can be phosphorylated by AKIN10, we performed in vitro kinase assays using the wt version of bZIP63 and different serine to alanine (S/A) mutants as substrates (Figure 5A; Figure 5 – figure supplement 1 and 2). Differences in phosphorylation could be observed for proteins with mutations in S29, S294, and S300. In detail, the signal from S29A was strongly decreased in full length bZIP63 and completely gone in the N-terminal peptides that appeared as lower MW degradation products in these assays. The S300A mutation led to an even stronger decrease of the signal, comparable to the S294/300A double mutant. Even though the S294A single mutant showed a similar signal as the wt, all three serines had to be mutated to completely abolish phosphorylation, suggesting that all of them are in vitro targets for AKIN10, with S294 being the weakest. Interestingly, the S300D mutant displayed a stronger signal than the S300A mutant, implying that S300 needs to be phosphorylated first for S294 to become a target for AKIN10. Importantly, all three sites match the SnRK1 consensus sequence (Figure 5B).

A comparison of Arabidopsis bZIP63 with orthologs from eight other plant species, ranging from mosses to higher plants, showed that the three putative AKIN10 target sites

are highly conserved throughout evolution (Figure 5B; Figure 5 – figure supplement 3). As the origin of SnRK1 dates back even further, to the common ancestor of plants and animals (Bayer et al., 2014), it is likely that phosphorylation of bZIP63 by AKIN10 poses an ancient and important regulatory mechanism. We therefore set out to test the functional relevance of AKIN10-mediated phosphorylation of bZIP63. To this end, we tested the transcriptional activity of bZIP63 in protoplast-based promoter activation assays using the *ASN1* or *ProDH* promoter fused to the beta galactosidase (GUS) reporter (Figures 5C; Figure 5 – figure supplement 4). In both cases, co-transformation of wt bZIP63 and AKIN10 strongly induced reporter gene expression, while transformation of bZIP63 alone was not sufficient for significant induction. Transformation of AKIN10 alone also led to a weak induction of the reporters, which could be explained by the action of endogenous bZIPs. Mutation of S29 or all three AKIN10 target sites on bZIP63 to alanine reduced the reporter activation almost to background level. In contrast, mutation of the two C-terminal serines, S294 and S300, had only a weak negative effect on *ASN1* and no effect on *ProDH* activation. Taken together, our data suggest that that AKIN10 phosphorylates bZIP63 at up to three conserved sites, namely S29, S294, and S300 and phosphorylation by AKIN10, especially at S29, is crucial for bZIP63 TF activity.

The AKIN10 target sites play an important role for bZIP63 function in planta

To determine the impact of bZIP63 phosphorylation in planta, we transformed the *bzip63* mutant with genomic constructs of bZIP63 containing either the wt sequence (GY lines) or S/A mutation of S29, S294, and S300, respectively (GAY lines) with a C-terminal YFP tag (Figure 6A; Figure 6 – figure supplement 1 A-D). The phosphorylation status of the wt construct after 6h of light and extended night and in the presence or absence of sugar was similar to the one observed in *ox#3* plants (Figure 6B; Figure 6 – figure supplement 1E). Notably, hyper-phosphorylation of bZIP63 in the extended night was even stronger in the GY lines than in *ox#3*, probably due to lower bZIP63 expression. In contrast, the S/A construct showed only weak phosphorylation and no difference between all tested conditions. This indicates that S29, S294 and S300 are the major in vivo phosphorylation sites on bZIP63, which are also responsible for the observed condition-dependent shift in bZIP63 phosphorylation.

Next, we tested whether complementation of the observed *bzip63* phenotypes depends on the bZIP63 phosphorylation status, using two independent GY and GAY lines. The dark-

induced senescence phenotype of *bzip63* was complemented in the GY lines, but not in the GAY lines (Figure 6C and D; Figure 6 – figure supplement 2). After 9 days in darkness, the ko and GAY lines showed visibly less chlorosis and had a higher percentage of green leaf area as compared to the wt and GY lines. Metabolite profiling of leaves harvested after 6h of light also revealed marked differences between the GY and GAY lines (Figures 6E and F; Figure 6 – source data 1). The metabolite profile of the GAY lines was similar to that of *bzip63* plants. In contrast, in the GY lines the metabolic changes between mutant and wt were mostly weaker than in *bzip63* or even resembled those observed for *ox#3* (Figure 6E). In a principal component analysis the GAY lines grouped together with *bzip63*, while the GY lines were closer to the two wt lines and the *ox* (Figure 6F).

To test the effect of the S/A mutation on the expression of bZIP63 target genes, we performed RT-qPCR of *ASN1*, *DIN10*, and *ProDH* (Figure 6G) - three suggested AKIN10 target genes (Baena-Gonzalez et al., 2007). The expression of all three genes increased steadily during a 4h extended night treatment, but the increase was delayed in the *bzip63* mutant as compared to the wt. At the 4h time point we could observe a clear difference between wt and ko. We therefore chose this time point to quantify *ASN1*, *DIN10*, and *ProDH* transcripts in one GY and GAY line. As expected, the GY line had the same or even more transcript than the wt for all three genes, while the GAY line had significantly lower expression levels, similar to *bzip63*.

In summary, expression of wt bZIP63 but not of the S/A mutant - which cannot be phosphorylated by AKIN10 - in the *bzip63* background led to complementation of the *bzip63* phenotypes. Together, these experiments demonstrate that phosphorylation of bZIP63 at the AKIN10 target sites is essential for the function of bZIP63 in the plant.

AKIN10-mediated phosphorylation affects bZIP63 dimerization

Our findings show that bZIP63 phosphorylation, at residues distant from the central bZIP domain, strongly regulates its activity. As we suspected that this could be due to changes in dimerization preferences, we tested the effect of AKIN10-mediated phosphorylation on bZIP63 homo- and heterodimerization with bZIP1 and bZIP11. Both bZIP1 and bZIP11 are metabolic regulators and mediate transcription of *ASN1* and *ProDH* (Dietrich et al., 2011; Hanson et al., 2008). In protoplast two-hybrid (P2H) assays, without the addition of exogenous AKIN10, only bZIP1 showed a strong interaction with bZIP63 (Figure 7A; Figure 7 – figure supplement 1A). When AKIN10 was co-transformed with the bZIPs, the

dimerization potential increased for all three dimers, but to a strikingly different extent. The increase was strongest for the bZIP63-11 heterodimer, which showed a 62.7-fold induction, followed by a 5.2-fold induction for the bZIP63 homodimer, and a 1.9-fold induction for the bZIP63-1 heterodimer (Figure 7A). From that we concluded that AKIN10 is required for bZIP63-11 and bZIP63-63, but not bZIP63-1 dimer formation. We therefore tested the effect of S/A mutation of the AKIN10 target sites on bZIP63 homo- and heterodimerization with bZIP11 (Figure 7B; Figure 7 – figure supplement 1B). In both cases, the signal was reduced to about 30-40% of the signal obtained from dimerization with wt bZIP63 when S29 or all three serines were mutated to alanine. Mutation of one or two of the C-terminal sites decreased bZIP63 homodimerization weakly but had no visible effect on bZIP63-11 dimerization, indicating that these sites play, at most, a minor role in regulation of dimer formation.

To exclude the possibility that the observed effects on dimerization are due to phosphorylation of the heterodimerization partner rather than bZIP63 itself, we tested whether AKIN10 is able to phosphorylate any of the S1 group bZIPs. To increase the phosphorylation efficiency of AKIN10 we included SnAK2 in the reactions. In contrast to bZIP63, none of the S1 group bZIPs were phosphorylated by AKIN10 (Figure 7C; Figure 7 – figure supplement 2). Together, these data indicate that AKIN10-mediated phosphorylation of bZIP63 – especially at S29 – strongly enhances its ability to dimerize with bZIP11, and to a weaker extent with bZIP63.

DISCUSSION

bZIP63 is an important metabolic regulator in the starvation response

Here we show that bZIP63 plays an important role in the energy starvation response and metabolic regulation. This is in accordance with the sugar/energy-dependent expression of bZIP63 (Kunz et al., 2014; Matioli et al., 2011), as well as with the fact that several of its proposed target genes are involved in starvation response and metabolism (Matioli et al., 2011; Veerabagu et al., 2014). Furthermore, three members of the S1-group of plant bZIPs – heterodimerization partners of bZIP63 (Ehlert et al., 2006; Kang et al., 2010) – have also been linked to energy starvation response and metabolism. Inducible bZIP11 ox lines exhibit a severe dwarf phenotype (Hanson et al., 2008) and a metabolic profile resembling that of carbon starved plants (Ma et al., 2011), while overexpression of bZIP1 and bZIP53

results in enhanced dark-induced senescence and reduced levels of proline and branched-chain amino acids (Dietrich et al., 2011).

Similar to the bZIP1 ox, bZIP63 ox plants showed increased chlorosis after 9 days of darkness, while the bZIP63 ko displayed a clear stay-green phenotype under these conditions. In contrast, neither the single, nor the double ko of bZIP1 and 53 showed reduced dark-induced senescence (Dietrich et al., 2011). This suggests that other bZIPs can take over the function of bZIP1 - in starvation-induced leaf yellowing, while bZIP63 plays a more unique role. In line with this observation, the expression of the senescence marker gene *SEN1*, which is up-regulated in natural senescence as well as in dark-induced senescence (Chung et al., 1997), was found to be lower in a bZIP63 ko after 24h in darkness (Matiolli et al., 2011).

Looking at primary metabolism, we found that misregulation of bZIP63 expression has a strong effect, especially on amino acids and sugars, which was further enhanced under starvation conditions. In line with the finding that bZIP63 is a positive regulator of *ProDH* and *ASN1* (Matiolli et al., 2011; Veerabagu et al., 2014, Figures 5C and 6G) and the changes in proline levels in *bZIP63* mutants reported by Veerabagu et al. (2014), we measured strong differences in proline and asparagine levels in the bZIP63 ko and ox. Curiously, there was a general increase of all amino acids in the ko and a decrease in the ox. This cannot be explained by misregulation of individual amino acid metabolism genes alone, but rather points to the involvement of a more general regulatory mechanism, like altered carbon- or nitrogen assimilation or protein turnover.

bZIP63 function is regulated by SnRK1-dependent phosphorylation

We showed that bZIP63 is highly phosphorylated in Arabidopsis. By applying different proteolytic digests we were able to identify seven in vivo phosphorylated serine residues, distributed all over the protein. While exogenous sucrose decreased the global phosphorylation level of bZIP63, extended night treatment further increased its phosphorylation, supporting the idea that bZIP63 plays a role in energy signaling. Moreover, we found that the SnRK1 kinase AKIN10, which was proposed to be a central regulator of transcription in starvation response (Baena-Gonzalez and Sheen, 2008), is the major kinase responsible for the starvation-induced hyper-phosphorylation of bZIP63. Therefore, bZIP63 presents the first TF acting as direct target of SnRK1 in the transcriptional energy deprivation response. AKIN10 targets three highly conserved and

functionally important residues in the N- and C-terminus of bZIP63 - S29, S294, and S300, respectively. Reporter activation assays in protoplasts revealed that these sites are essential for AKIN10-dependent induction of *ASN1* and *ProDH* by bZIP63. Moreover, complementation of the metabolic and senescence phenotypes of the *bzip63* mutant with genomic bZIP63 constructs confirmed that the function of bZIP63 in planta depends on the SnRK1 target sites. Also the delay in extended night-triggered induction of *ASN1*, *DIN10*, and *ProDH* in *bzip63* plants was complemented with wt bZIP63, but not the S/A mutant. The relatively small difference in *ProDH* expression in plants, as compared to the protoplast assay, is probably due to redundancy within the C/S1 group bZIPs, as it was shown by Dietrich et al. (2011), that only ko of multiple members of the C/S1 group leads to a strong reduction in *ProDH* and *ASN1* expression.

Since the discovery that AKIN10 can activate several members of the C/S1 network (Baena-Gonzalez et al., 2007), it has been speculated (Baena-Gonzalez and Sheen, 2008; Usadel et al., 2008), but never shown experimentally, that they are downstream targets of SnRK1. Our data provide compelling evidence that bZIP63, but none of the S1 group bZIPs, is a bona fide in vivo target of SnRK1 in low-energy signaling.

Phosphorylation of bZIP63 alters its dimerization preferences

Differential dimerization is a well-known mechanism for changing the target recognition site, and thereby the target genes of bZIP TFs (Tsukada et al., 2011). For the S1-group bZIP1 it has been shown that dimerization with C-group bZIP10 or bZIP63 affects its in vitro binding to ACGT-based motifs differently (Kang et al., 2010). The notion that different C/S1 dimers have different target genes is further supported by a recent transcriptomics study in protoplasts. Overexpression of four C/S1 group bZIPs (bZIP1, bZIP10, bZIP11, and bZIP63), individually or in combination of two, revealed overlapping but distinct gene expression patterns (Ma, 2012). This means, that although they regulate a core set of common genes, such as *ASN1* and *ProDH* (Baena-Gonzalez et al., 2007; Dietrich et al., 2011; Ma et al., 2011), different dimers also have distinct functions, and switching of dimerization partners can have a considerable impact on gene expression.

Our data indicate that dimerization and activity of bZIP63 strongly depend on its phosphorylation status. Interaction of bZIP63 with bZIP11, and to a lesser extent with bZIP63, was boosted by AKIN10-mediated phosphorylation. In contrast, interaction with bZIP1 was largely independent of bZIP63 phosphorylation. Based on the data presented in

this study, we propose a simplified model for the regulation of bZIP63 dimerization by AKIN10 (Figure 7D). When bZIP63 is not phosphorylated, its capacity to bind bZIP11 or bZIP63 is low, favoring the formation of bZIP63-1 dimers. Activated AKIN10 - for example due to energy starvation - phosphorylates bZIP63, thereby promoting the formation of bZIP63-11 heterodimers and the induction of a different set of target genes, involved in the transcriptional reprogramming of metabolism. This is supported by transcriptomics experiments, which showed a large overlap between bZIP11 and AKIN10 target genes (Delatte et al., 2011). Moreover, enhanced dimerization with bZIP63 would explain why AKIN10 was found to activate bZIP11 in protoplast assays (Baena-Gonzalez et al., 2007), although it is not a direct target of AKIN10. However, it is clear that in the plant additional factors like bZIP expression, stability and interaction with other components add more complexity to the situation.

Surprisingly, to date only a small number of papers have reported an influence of phosphorylation on bZIP dimerization (Guo et al., 2010; Kim et al., 2007; Lee et al., 2010). Moreover, to our knowledge this is the first time that phosphorylation outside the bZIP domain was shown to affect dimerization with different partners in a distinct way. While there are numerous reports on phosphorylation-mediated changes in bZIP activity in animals, plants, and yeast, in many cases the underlying mechanism is still unknown. We therefore believe that this novel mechanism of phosphorylation-triggered switch of bZIP dimerization partners could play a substantial role in the regulation of bZIP TF activity in all higher organisms, and should be further addressed in future studies.

EXPERIMENTAL PROCEDURES

Plant lines

the *akin10* line are in the Col-0 background and express bZIP63.2-GFP or YFP under control of the 35S or UBI10 promoter, respectively. GY9, GY11, GAY4 and GAY14 express a genomic construct (wt or S29/294/300A) of bZIP63 under its endogenous promoter in the *bzip63* background in *Ws-2*.

The lines *ox#2* and *ox#3* are bZIP63 overexpressor lines in the Col-0 background, expressing bZIP63.2 with a C-terminal GFP tag under the control of the 35S promoter. Generation of these plant lines was previously described in Veerabgu et al., 2014. Overexpression was confirmed by qPCR of *bZIP63* mRNA and western blots with an antibody against GFP (Figure 6 – figure supplement 1 B-C).

The bZIP63 knock-out line (*bzip63*) in the *Ws-2* ecotype is a T-DNA insertion line. Pool number CSJ1 (NASC ID: N700001) from the Arabidopsis Knockout Facility (AKF) (Sussman et al., 2000) was screened for a T-DNA insertion in *bZIP63* and homozygous plants were selected using Kanamycin. Sequencing of the flanking regions revealed that the T-DNA is inserted in the first exon at position 76 (Figure 6 – figure supplement 1A). The knock-out was confirmed by qPCR of *bZIP63* mRNA (Figure 6 – figure supplement 1B). The same line was used by Veerabgu et al., 2014.

For the complementation lines (GY = wt, GAY = S29/294/300A), a genomic fragment containing *bZIP63* and 2kb of upstream sequence was obtained by PCR on Col-0 genomic DNA and ligated into pCRBlunt (Invitrogen, Austria). For the S/A construct, S29, S294, and S300 were mutated to alanine by mutagenesis PCR. The genomic fragments were then ligated into modified pBIN19, containing a BASTA resistance for plant selection and a C-terminal YFP tag, before transformation into *Agrobacterium tumefaciens* (GV3101). Homozygous *bzip63* plants were transformed with the floral dip method and selected for positive transformation events by spraying seedlings with 200mg/l BASTA solution (Bayer, Germany). Transgene expression was tested using qPCR, western blots with an antibody against GFP, and epifluorescence microscopy (Figure 6 – figure supplement 1 B-D).

For the line expressing bZIP63-GFP in *akin10* in the Col-0 background, *bZIP63.2* was amplified from Col-0 cDNA and ligated into modified pBIN19 containing the UBI10 promoter, a BASTA resistance for plant selection, and a C-terminal YFP tag. Homozygous *akin10* (GabiKat: GK 579E09) plants were transformed and selected like the GY and GAY lines.

Plant growth

Arabidopsis seeds were surface sterilized with chlorine gas before sowing on soil or growth medium and then vernalized at 4°C for two days. Plants were grown in a growth chamber in a 12h light/12h dark regime with day temperatures between 20 and 22°C and night temperatures between 18 and 20°C and a light intensity of 60 – 150 $\mu\text{mol}/\text{m}^2\text{s}$ unless specified otherwise. Plants grown under short or long day conditions were cultivated with 8h or 16h of light per day, respectively. The soil mixture consisted of 4 parts Huminsubstrat N3 (Neuhaus, Germany), 1 part perlite (Gramoflor, Germany), and the fertilizer Osmocote (Substral/Scotts, Germany) according to manufacturer's instructions.

For hydroponic cultures, plants were grown with their roots in light-tight box filled with liquid $\frac{1}{2}$ Hoagland medium (2mM $\text{Ca}(\text{NO}_3)_2$, 0.25mM K_3PO_4 , 3mM KNO_3 , 1mM MgSO_2 , 45 μM NaFeIII EDTA, 5 μM H_3BO_3 , 1 μM MnCl_2 , 0.15 μM ZnSO_4 , 0.1 μM CuSO_4 , 7nM MoO_3 , 4.5nM $\text{Co}(\text{NO}_3)$). Seedling cultures in liquid medium were grown in $\frac{1}{2}$ Gambourg (Duchefa, Harlem, The Netherlands) with or without 0.5% sucrose and the medium was exchanged after 7 days. Seedlings on plates were grown on $\frac{1}{2}$ MS (Duchefa, Harlem, The Netherlands) with 0.7g/l plant agar (Duchefa, Harlem, The Netherlands) and a pH of 5.8. The root cell suspension culture was grown in MS medium containing 30g/l sucrose and 2.5 μM 2,4D at 22°C in the dark under constant shaking. The medium was exchanged every seven days by transferring $\frac{1}{3}$ to $\frac{1}{2}$ of the culture to a fresh flask and addition of fresh medium.

Dark-induced senescence

4.5 week-old soil-grown plants were incubated in the dark - in a box with tubes allowing for gas exchange - for 9 days. Before and after incubation the true leaves of 4-8 representative plants were harvested, stuck on white paper with double sided tape, scanned with a flatbed scanner without color correction at a resolution of 600dpi, and saved as TIFF files. Images were then imported in ImageJ (FIJI) (Schindelin et al., 2012) and the total and green leaf area of each leaf were quantified using the built-in threshold and color threshold function, respectively. The green leaf area in % was then calculated by dividing the green area of a leaf or the whole plant by the respective total area.

See Figure 1 – source data 2 for the ImageJ macro for semi-automatic image processing. A color gradient indicating the color threshold and a scheme depicting the main steps in image processing can be found in Figure 1 – figure supplement 1B.

Metabolic profiling

Metabolites were extracted from leaves of 5 week-old plants, derivatized and measured as described in Naegele et al. (2014) with minor variations. Approximately 80mg frozen and ground plant material were extracted with 1ml -20°C cold MeOH:chloroform:H₂O (2.5:1:0.5) by mixing and incubation on ice. The supernatant after centrifugation was mixed with 400 – 500 μl H₂O and centrifuged. For the experiment shown in Figure 1 (1) the polar phase was split into 2 aliquots, spiked with 1 μg C13 labeled Sorbitol (Campro Scientific, Berlin, Germany) and dried. For the experiment shown in Figure 6 (6) the polar phase was not split and 2 μg of Sorbitol were added. For derivatization, metabolites were

first dissolved in 10 μ l (1) or 30 μ l (6) pyridine containing 40mg/ml methoxyamine hydrochloride by 90min incubation at 30°C. Then, 40 μ l (1) or 120 μ l (6) of N-methyl-N-trimethylsilyltrifluoroacetamid (MSTFA; Macherey-Nagel, Düren, germany), spiked with 60 μ l/ml of an Alkane Standard Mixture C₁₀-C₄₀ (Fluka, Vienna, Austria), were added and the samples were incubated for 30min at 37°C. GC-MS measurements were carried out on an Agilent 6890 gas chromatograph coupled to a LECO Pegasus 4D GCxGC-TOF mass spectrometer (LECO, USA). Injection volume was 1 μ l. In the GC step, the initial oven temperature was 70°C, which was held for 1min, followed by a 9°C/min temperature increase until the final temperature of 350°C was reached, which was held again for 8min. Metabolites were measured in splitless mode (1 and 6) and alternatively also in split mode with a split ratio of 5 (6). In the MS step the data acquisition rate was set to 20 spectra/sec, the detector voltage to 1550V and the mass range to 40-600 m/z. Raw data were processed with the LECO Chroma-TOF software (LECO, USA). Peak areas were normalized to the area of the internal standard and to the fresh weight before statistical analysis. Outliers, as determined by Grubb's test, were removed from the dataset. For Hierarchical clustering, log-2 transformed fold change values were imported into MeV (MultiExperimentViewer, version 4.9.0, Saeed et al., 2003) and clustering was done using the standard settings with gene tree optimization, Pearson correlation, and average linkage clustering. For the PCA plot, normalized data were imported into R (RStudio, version 0.98.507), missing values were replaced with the k nearest neighbor (knn) method using the "impute.knn()" function and data were Z-transformed. PCA analysis was done using the "prcomp()" function and scores for PC1 and PC2 were plotted against each other.

Electrophoresis and Western blotting

For 2D gels, proteins were extracted from 5-7 week-old soil-grown ox#3 plants which were grown in short day. 4ml of 1x lambda phosphatase (λ PP) buffer (NEB, Frankfurt am Main, Germany), including cOmplete protease inhibitor (Roche, Vienna, Austria), were added to 2ml frozen and ground plant material, followed by vortexing and centrifugation. 0, 30 or 50 μ g of λ PP were added to 1.5ml of the supernatant, followed by 15min incubation at 30°C. Proteins were extracted with phenol, precipitated with ammonium acetate and resuspended in 1x rehydration stock solution (7M urea, 2M thiourea, 2% (w/v) CHAPS, 2% IPG buffer (GE Healthcare, Vienna, Austria), 2.8mg/ml DTT, Bromphenol blue). Protein extracts were then applied to 7cm ImmobilineTM DryStrips (GE Healthcare,

Vienna, Austria) over night and separated by isoelectric focusing on an IPGphor (GE Healthcare, Vienna, Austria) according to the manufacturer's instructions. For second dimension separation, the strip was incubated in SDS equilibration buffer (6M urea, 75mM TrisCl, 29.3% glycerol, 2% SDS, Bromphenol blue, pH 8.8) with 10mg/ml DTT and then without DTT for 15min each, followed by standard SDS PAGE and western blotting.

Phos-tag gel electrophoresis was done according to the manufacturer's instructions. Proteins were separated on SDS PAGE gels containing 8% SDS, 25 μ M Phos-Tag (WAKO, Neuss, Germany) and 50 μ M MnCl₂ with an amperage of 15mA/gel for 1.25h. Before semi dry blotting, the gels were incubated in transfer buffer containing 1mM EDTA, followed by washing with transfer buffer without EDTA. Recombinantly expressed bZIP63-YFP was used as a size marker for the unphosphorylated fusion protein. The protein was expressed in *E. coli* (ER2566), transformed with a pTWIN plasmid (NEB, Frankfurt am Main, Germany) containing bZIP63-YFP, and purified according to the manufacturer's instructions. Total plant proteins were extracted with phenol. For light/extended night comparison, rosettes of 5 week old plants were collected after 6h of light or extended night. For +/- sucrose comparison, seedlings were first germinated and grown for one week in liquid ½ Gambourg containing 0.5% sucrose, followed by 1 week in medium without sucrose. For treatment, at the onset of light 1% suc was added to half of the cultures and all cultures were kept in the dark for 6 additional hours. For Phos-tag gels from kinase assays, the reactions were mixed with 2x laemmli buffer and loaded on the gel.

Western blotting was done by semi dry transfer onto a PVDF membrane, antibody incubation, and detection with an ECL kit following standard procedures. The following primary antibodies were used: Anti-GFP (Roche, Vienna, Austria; or ChromoTek, Munich, Germany), Anti-AKIN10 (Agrisera, Sweden), Anti-Flag (Sigma-Aldrich, Vienna, Austria), Anti-HA High Affinity (Roche, Vienna, Austria), Anti-HA (Santacruz, Heidelberg, Germany), Anti-GAL4 DNA BD (Sigma-Aldrich, Vienna, Austria), peptide antibodies against bZIP63: N-terminal peptide (EKVFSDEEISGNHHWSVNGM) or C-terminal peptide (SLEHLQKRIRSVGDQ). The following HRP-coupled secondary antibodies were used: Anti-mouse IgG, Anti-rabbit IgG, Anti-rat IgG (GE Healthcare, Vienna, Austria).

Immune precipitation of bZIP63-GFP

To identify *in vivo* phosphorylation sites on bZIP63, bZIP63-GFP was immune precipitated from ox#3 seedlings grown on ½ MS agar plates or leaves of mature soil-

grown *ox#3* plants, harvested at different time points in the light cycle and in extended night (see Figure S – figure supplement 1A for growth and harvesting conditions). In one experiment, leaves were infiltrated with H₂O containing 100µM of the proteasome inhibitor MG-132 (Calbiochem/Merck Millipore, Vienna, Austria) 6h before harvesting. Protein extracts were prepared by mixing frozen and ground plant material with an equal volume of cold extraction buffer (25mM TrisCl, 10mM MgCl₂, 15mM EDTA, 150mM NaCl, 1mM DTT, 1mM NaF, 0.5mM Na₃VO₄, 15mM β-glycerophosphate, 0.1% Tween20, cOmplete protease inhibitor, pH 7.5), followed by centrifugation. The supernatant was then incubated with protein A Sepharose CL-4B (GE Healthcare, Vienna, Austria), which had been pre-incubated for 2.5h in extraction buffer with Anti-GFP antibody (Roche, Vienna, Austria), or with GFP-Trap_A beads (ChromoTek, Munich, Germany) for 1h at 4°C. The beads were washed 2 – 3 times with extraction buffer and alternatively twice with wash buffer (50mM TrisCl, 250mM NaCl, 0.1% NP-40, 0.05% sodium deoxycholate, pH 7.5). Finally, the beads were resuspended in 1x laemmli buffer, boiled for 5min at 95°C, and centrifuged. The supernatant was separated by SDS PAGE and bands were excised for LC-MS/MS analysis.

Identification of proteins and in vivo phosphorylation sites by LC-MS/MS

For the identification of phosphorylation sites, bZIP63-GFP was immune precipitated from leaves of *ox#3* plants (see “Immune precipitation of bZIP63-GFP”). For the identification of kinases, root protein extracts were affinity purified with recombinant GST-bZIP63 (see Figure 3B for a scheme and the methods section “Kinase assays” for detailed description of the affinity purification).

Proteins were first separated by SDS PAGE. Bands of interest were then excised from Coomassie-stained gels and gel sections were chopped, washed with 50mM ammonium bicarbonate (ABC, pH 8.5), and dried with acetonitrile (ACN). Disulfide bonds were reduced by incubating in 200µl of 10mM DTT for 30min at 56°C. DTT was washed off and cysteines were alkylated by incubation with 100 µl of 54mM iodoacetamide for 20min at RT in the dark. Gel pieces were dried with ACN, then swollen in 10ng/µl trypsin (recombinant, proteomics grade, Roche, Vienna, Austria) in 50mM ABC and incubated over night at 37°C. For higher sequence coverage of bZIP63 alternative proteases were used: LysC (MS grade, WAKO, Neuss, Germany) at 37°C over night, subtilisin (Sigma-Aldrich, Vienna, Austria) at 37°C for 0.5 – 2h, chymotrypsin (sequencing grade, Roche,

Vienna, Austria) at 25°C for 4 hours. Digestion was stopped by adding formic acid to a final concentration of approximately 1% and peptides were extracted by sonication. Peptides were separated on an UltiMate 3000 HPLC system or on a U3000 nano HPLC (both Dionex, Thermo Fisher Scientific). Digests were loaded on a trapping column (PepMap C18, 5µm particle size, 300µm i.d. x 5mm, Thermo Fisher Scientific), equilibrated with 0.1% trifluoroacetic acid (TFA), and separated on an analytical column (PepMap C18, 3µm, 75µm i.d. x 150mm, Thermo Fisher Scientific) by applying a 60 minutes linear gradient from 2.5% up to 40% ACN with 0.1% formic acid, followed by a washing step with 80% ACN and 10% trifluoroethanol (TFE) on the U3000 HPLC. The UltiMate 3000 HPLC was directly coupled to a linear ion trap (LTQ, Thermo Fisher Scientific), which was operated in a data-dependent MS3 method for the phosphorylation analysis. One full scan (m/z: 450-1600) was followed by maximal 4 MS/MS scans. If in the MS/MS scan a fragment corresponding to a neutral loss from the precursor of 98, 49, or 32 Th was observed among the top 8 peaks, a MS3 scan was triggered. Fragmentation energy was set at 35%, Q-value at 0.25, and the activation time at 30ms. High resolution measurements were acquired on an LTQ-Orbitrap Velos mass spectrometer (Thermo Fisher Scientific), equipped with a nanoelectrospray ionization source (Proxeon, Thermo Fisher Scientific). The electrospray voltage was set to 1500V. The mass spectrometer was operated in the data-dependent mode: 1 full scan (m/z: 350-1800, resolution 60000) with lock mass enabled was followed by maximal 12 MS/MS scans. The lock mass was set at the signal of polydimethylcyclsiloxane at m/z 445.120025. Monoisotopic precursor selection was on, precursors with charge state 1 were excluded from fragmentation. The collision energy was set at 35%, Q-value at 0.25, and the activation time at 10ms. Fragmented ions were set onto an exclusion list for 60s. When ETD (electron transfer dissociation) was applied, the top 6 peaks from the full scan were fragmented with CID (collision-induced dissociation) and subsequently with ETD. For ETD, the energy parameters were as for the CID except the activation time was set to 80 or 120ms.

Data interpretation: Raw spectra for the kinase identification were interpreted by Mascot 2.2.04 (Matrix Science) using Mascot Daemon 2.2.2. Spectra were searched against the *Arabidopsis thaliana* entries in the nr-database with the following parameters: the peptide tolerance was set to 2Da, MS/MS tolerance was set to 0.8Da, carbamidomethylcysteine was set as a static modification, oxidation of Met as variable modification. Trypsin was

selected as the protease allowing two missed cleavages. Mascot score cut-off was set to 30, except for the low abundance sample 1, where the cut-off was set to 20. For the phosphorylation analysis of purified bZIP63, either Mascot or Sequest (Proteome Discoverer 1.2; Thermo Scientific) were used. The search was extended to the phosphorylation of Ser, Thr, and Tyr. High resolution data were searched with 3ppm precursor mass tolerance. Proteolytic specificity was defined according to the digest. Results were manually validated including comparison of the fragmentation pattern and the relative retention of the unphosphorylated counterpart. Site localization was checked by manual inspection at the spectrum level in the first place and was confirmed by the site-localization algorithm PhosphoRS (Taus et al., 2011).

Kinase assays

In vitro kinase assays were performed with GST-tagged recombinant proteins. The cDNA of *bZIP63.2*, *bZIP1*, *bZIP2*, *bZIP11*, *bZIP44.1*, *bZIP55*, *AKIN10.1/3*, and *AKIN11.1/2* was cloned into pGEX-4T, and *SnAK2* was cloned into pDEST15. An inactive version (K/M) of *AKIN10* and non-phosphorylatable (S/A) versions of *bZIP63* were created by mutagenesis PCR. The proteins were expressed in *E. coli* (ER2566 or BL21), purified using Glutathione Sepharose 4B (GE Healthcare, Vienna, Austria) according to the manufacturer's instructions, and stored at -80°C in GST elution buffer containing 10 – 25% glycerol.

Kinase assays were performed by incubating the kinase and substrate for 20 – 30min in kinase reaction buffer (20mM Hepes, 20mM MgCl₂, 100μM EGTA, 1mM DTT, 50μM ATP, pH 7.5) at room temperature. For radioactive assays, 1μCi γ-³²P-labeled ATP (NEN/PerkinElmer, Waltham, MA, USA) was added in each reaction. The reactions were then separated by SDS PAGE and exposure on a Storage Phosphor Screen (GE Healthcare, Vienna, Austria) or Phos-tag gel electrophoresis and Western blotting, respectively.

For in-gel kinase assays, bZIP63 with an N-terminal 6xHis tag was used as a substrate. The protein was expressed in *E. coli* (ER2566) and purified over a HiTrap column (GE Healthcare, Vienna, Austria) according to the manufacturer's instructions. Total plant proteins were extracted from roots of 8 week-old plants that were grown in hydroponic culture in short day and collected in the light phase, or from roots and leaves of 2 week-old seedlings grown in liquid culture in a 12hlight/12h dark cycle and collected after 4h of extended night. Extraction was done by mixing the frozen and ground plant material with an equal volume of cold protein extraction buffer (25mM TrisCl, 15mM EGTA, 10mM

MgCl₂, 75mM NaCl, 1mM NaF, 0.5mM NaVO₃, 15mM beta-glycerophosphate, 0.1% Tween20, 1mM DTT, cOmplete protease inhibitor, pH 7.5), followed by centrifugation. Protein amounts were determined by Bradford assay. For affinity purification of bZIP63-binding proteins, GST-tagged bZIP63 was expressed in *E. coli*, and the cell lysate of up to 1l culture in GST binding buffer (50mM TrisCl, 20mM MgSO₄, 2mM DTT, 5mM EDTA, 0.5% Tween20, pH 8) was loaded on an equilibrated GSTrap FF column (GE Healthcare, Vienna, Austria). The column was then washed with 5ml cold GST binding buffer and protein extraction buffer, respectively, and 2 – 5ml of total root protein extracts from hydroponic culture or white root cell suspension culture in cold protein extraction buffer were loaded. Subsequently, proteins were eluted from the column by repeated washing with 5ml cold protein extraction buffer with increasing salt concentrations, and concentrated with Amicon Ultra Centrifugal Filter Units (Millipore). 8 – 20µg total protein extracts and up to 40µg affinity purified proteins were loaded on standard SDS PAGE gels containing 1mg/ml substrate (6x His-bZIP63) in the separating gel and run at 4°C with 20mA per gel. The gel was then incubated three times for 20min, respectively, at room temperature in each of the following buffers: wash buffer I (50mM TrisCl, 20% isopropanol, pH 8), wash buffer II (50mM TrisCl, 1mM DTT, pH 8), and denaturation buffer (50mM TrisCl, 1mM DTT, 6M guanidinium HCl, pH 8). Subsequently, the gel was incubated in renaturation buffer (50mM TrisCl, 0.05% Tween 20, pH 8) at 4°C for 12 – 18h. In this period, the buffer was exchanged 10 times after at least 30min. After renaturation, the gel was incubated two times for 30min, respectively, in kinase buffer (20mM HEPES, 20mM MgCl₂, 50µM CaCl₂ or 500µM EGTA, 1mM DTT, 0.05% Tween 20, pH 7.5), followed by 30min incubation in kinase reaction solution (kinase buffer containing 50µM ATP and 100µCi γ -³²P-labeled ATP). Finally, the gel was washed two times for 15min, respectively, in 5% TCA and several times in 5% TCA containing 1% sodium pyrophosphate, until the wash solution was only weakly radioactive. The dried gels were exposed on a Storage Phosphor Screen and the signal was recorded on a Typhoon 8600 (GE Healthcare, Vienna, Austria).

Y2H assay

AKIN10.1/3, *AKIN11.1/2*, *SNF4*, and *bZIP63.2* were cloned into pBTM117 and *bZIP63.2* was cloned into pACTIIJ to generate N-terminal fusions with the LexA-BD and the GAL4-AD, respectively. The yeast strain L40 (*MAT α his Δ 200 trp1-900 leu2-3.112 ade2 LYS2::*

(*lexA op*)₄HIS3 URA3::(*lexA op*)₈lacZ Gal4 gal80) was transformed with empty pACTIIJ or *bZIP63.2*-containing pACTIIJ in combination with different pBTM117 vectors. Freshly grown L40 was mixed gently with 1ml transformation mix (800µl 50% PEG 3600, 100µl 2M LiAc, 100µl 1M DTT, 10µl bacterial RNA (10µg/µl)), to get a cloudy suspension. 2.5µg of each plasmid were added to 125µl transformation mix, followed by 20min incubation at 30°C and 44°C, respectively, addition of 1ml H₂O, and 1min centrifugation at 3500g. The cells were resuspended in a small volume and plated on SD medium without Leu and Trp to select for successful transformation. Single colonies were inoculated in SD medium without Leu and Trp and proteins were extracted from 2ml of an over-night culture. The yeast cells were resuspended in 200µl enzyme lysis buffer (25mM TrisCl, 20mM NaCl, 8mM MgCl₂, 5mM DTT, 0.1% NP-40, pH 7.5), 200µl glass beads (0.4 – 0.6mm diameter) were added, the cells were frozen in N₂, thawed, and broken by vigorous shaking on a Vibrax at 4°C for 20min. The supernatant after 10min centrifugation was transferred to a fresh tube and kept on ice. The protein concentration of the extract was determined by Bradford assay. The GUS activity was determined by mixing 50µl of the extract with 650µl Z-buffer (60mM Na₂HPO₄, 40mM NaH₂PO₄, 10mM KCl, 10mM MgSO₄, 0.25% beta mercaptoethanol) and 100µl ONPG (4mg/ml), and incubating for up to 10min at room temperature. The reaction was stopped by adding 400µl 1M Na₂CO₃ and the extinction at 420nm was measured on a photometer. The GUS activity in U/mg protein was calculated as follows: (A₄₂₀ x 24 x 1000)/(45 x incubation time [min] x protein concentration [mg/ml])

Bimolecular fluorescence complementation (BiFC)

For BiFC interaction studies in *Nicotiana tabacum*, *bZIP63.2*, *AKIN10.1/3*, *AKIN11.1/2* and *SNF4* were cloned into modified pBIN19 vectors, containing either the N- or C-terminal moieties of the split CFP system as N-terminal fusions as described in Waadt et al., 2008 (see Figure 4D for scheme). *Agrobacterium tumefaciens* (AGL1) was transformed with the resulting plasmids by electroporation and further used for transient transformation of tobacco leaf epidermis. For transformation, 5ml agrobacterium overnight cultures were filled to 50ml with fresh LB medium containing 50µg/ml Kanamycin and 10µg/ml Gentamicin and grown for 4h at 30°C. The cells were pelleted by centrifugation at 3500g, resuspended in LB containing 150µM acetosyringone, and grown for another 2h. The cultures were then pelleted again and resuspended in 5% sucrose solution to reach a final

OD600 of 2. For co-infiltration, equal volumes of agrobacteria suspensions, containing the respective constructs, were mixed and infiltrated into the leaves of 5 week-old plants. 48h after infiltration equally sized leaf sections were analyzed for their CFP fluorescence signal with an LSM510 confocal laser scanning microscope (Zeiss) and the corresponding ZEN software (Zeiss). The same settings were used for each construct to allow comparison of the signal intensities. To verify that the fusion proteins were expressed and to determine the relative amount of each interaction partner, proteins were extracted from the leaf sections used for microscopy and subjected to Western blot analysis with antibodies against the Flag (N-terminal CFP moiety) and HA (C-terminal CFP moiety) epitopes.

Protoplast transformation for P2H and promoter activation assays

Protoplast were obtained from 3 week-old soil-grown wt *Arabidopsis* plants and transformed according to the guide method (Yoo et al., 2007) with small modifications. Leaves were harvested 1h after onset of the light phase, cut into tiny stripes, and digested for 30min under vacuum and 3h at atmospheric pressure, respectively, with enzyme solution (1.25% (w/v) Cellulase R-10, 0.3% Macerozyme R-10, 400mM mannitol, 20mM KCl, 10mM CaCl₂, 20mM MES, pH 5.7). The protoplast suspension was filtered on a metal net to remove leaf debris and washed twice with 10ml of W5 solution (2mM MES, 154mM NaCl, 125mM CaCl₂, 5mM KCl, pH 5.7). Protoplasts were resuspended in 10ml of W5, incubated on ice for at least 1h and subsequently resuspended to a final concentration of 1 x 10⁵ cells/ml in MMg buffer (4mM MES, 400mM mannitol, 15mM MgCl₂, pH 5.7). Protoplasts were then co-transformed with 10µg each of up to three effector plasmids, 7µg of a reporter plasmid, and 3µg of a transfection control reporter plasmid. For P2H assays, the effector plasmids were pHBTL containing *bZIP63.2*, *bZIP1*, or *bZIP11* with an N-terminal GAL4-AD or GAL4-BD fusion (described in detail in Ehlert et al., 2006) and alternatively pHBTL containing *AKIN10.1/3*. The reporter plasmid contained either *GAL-UAS₄:LUC* (luciferase) or *GAL-UAS₄:GUS* (beta galactosidase) (Ehlert et al., 2006). For normalization of the LUC or GUS signals, a transfection control plasmid containing *35S:REN* (Renilla luciferase, Wehner et al., 2011) or *35S:NAN* (Kirby and Kavanagh, 2002), respectively, was used. For promoter activation assays, effector plasmids were pHBTL containing HA-tagged *bZIP63.2* or *AKIN10.1/3*. pBT10 containing *proASN1:GUS* or *proProDH:GUS* (Dietrich et al., 2011) was used as a reporter plasmid, and a plasmid containing *35S:NAN* was used as a transfection control. For transformation,

200µl of the protoplast suspension were gently mixed with the DNA and 220µl of PEG (40% PEG 4000, 200mM mannitol, 100mM CaCl₂) were added, followed by gentle mixing, and 10min incubation at room temperature. The protoplasts were then washed by addition of 800µl W5 and 1min centrifugation at 300g. The supernatant was removed and the protoplasts were incubated for 16h in 200µl of WI solution (4mM MES, 500mM mannitol, 20mM KCl, pH 5.7) in the growth chamber in order to not affect their diurnal circle. GUS and NAN enzyme assays were performed according to Kirby and Kavanagh (2002). LUC and REN activity was measured as described in Wehner et al. (2011). The relative activity of GUS and LUC was calculated as GUS/NAN and LUC/REN. The expression of the effector constructs was confirmed by Western blot analysis.

Sequence alignment of bZIP63 homologues

Homologues of bZIP63 in 8 plant species were identified by blasting the protein sequence of bZIP63.2 on the Phytozome webpage (<http://phytozome.net>). The protein sequences were aligned with ClustalΩ (<http://www.ebi.ac.uk/Tools/msa/clustalo/>) using the default settings and the clustal output file was imported into GeneDoc (<http://www.psc.edu/biomed/genedoc>) for visualization and minor adjustments of the alignment. The identity matrix for the alignment was calculated using the PID3 method in the SIAS webmask (<http://imed.med.ucm.es/Tools/sias.html>).

Gene identifiers of the *bZIP63* homologues (numbers are the Phytozome10 references): *Medicago truncatula* (Medtr7g115120), *Glycine max* (Glyma.10G162100), *Populus trichocarpa* (Potri.013G040700), *Vitis vinifera* (GSVIVG0102179000), *Zea mays* (GRMZM2G007063), *Oryza sativa* (LOC_Os03g58250), *Selaginella moellendorffii* (270282), *Physcomitrella patens* (Phpat.009G02690)

RT-qPCR

RNA was extracted with phenol from total rosettes of 4.5 week-old soil-grown plants at the indicated time points. 500µl RNA extraction buffer (1% SDS, 10mM EDTA, 200mM NaAc, pH 5.2) and 500µl acidic phenol (pH 4, Carl Roth, Karlsruhe, Germany) were added to 100mg frozen and ground plant material, followed by 1min vortexing and 10min centrifugation. The aqueous phase was extracted twice with an equal volume of PCI (Phenol:Chloroform:Isoamylalcohol (25:24:21), Carl Roth, Karlsruhe, Germany) by vortexing for 30sec and 2min centrifugation, and twice with chloroform. Then, the RNA was precipitated by adding 1/3 volume 10M LiCl and incubating at 4°C for at least 2h,

followed by 15min centrifugation at 4°C. The pellet was washed once with 2.5M LiCl and then with 70% EtOH, dried and resuspended in 50µl RNase free H₂O. 6.5µg RNA were treated with 2u of RQ1 DNase (Promega, Mannheim, germany), according to the manufacturer's instructions and precipitated again for at least 2h with 1/3 volume of 10M LiCl to remove the DNase from the solution. The solution was then centrifuged for 15min, washed once with 70% EtOH, dried and resuspended in RNase free H₂O. 1.5µg RNA were reverse transcribed using M-MLV RT [H-] Point Mutant (Promega, Mannheim, germany) according to the manufacturer's instructions and diluted 1:4 with RNase free H₂O. 2µl of cDNA (15ng/µl) or H₂O (for the no template control) were added to 18µl of a PCR reaction mix containing 0.25u DreamTaq polymerase (Thermo Scientific, Vienna, Austria), 1x Dream Taq buffer, additional 3mM MgCl₂, 100µM dNTPs, 400nM of each primer, and 0.4x SYBR Green I nucleic acid gel stain (Sigma-Aldrich, Vienna, Austria). The qPCR was performed on a Mastercycler ep realplex2 (Eppendorf) in white 96-well twin.tec real-time PCR plates (Eppendorf, Vienna, Austria) with the following program: 1 cycle with 3min at 95°C, followed by 40 cycles with 20sec at 95°C, 20sec at 59/60°C, and 12sec at 72°C. A 20min melting curve was added in the end. For data evaluation, raw data were imported into LinRegPCR (version 2014.02, Ramakers et al., 2003), where the PCR efficiency was checked and the N0 (starting concentration of cDNA) was calculated with a common baseline setting for each primer pair. Samples excluded by LinRegPCR and samples for which the dCq between the two technical replicates was bigger than 0.5 were excluded from the calculations. The mean N0 of the technical replicates was calculated for each sample and primer pair. The resulting mean N0 of the test genes was then normalized by dividing by the mean N0 of the reference genes. For qPCR of *ASN1*, *DIN10*, and *ProDH*, *TBP2* (Tata binding protein 2) was used as a reference gene. For pPCR of *bZIP63*, the geometric mean of the values for *TBP2* and *MHF15* (Thioredoxin superfamily protein) were used. The normalized N0 values were then used to calculate the mean and SD. Outliers were determined with the Grubb's test and removed.

Statistical tests

Statistical tests were performed in excel or R. Equality of variances was tested with Levene's test. This was followed by unpaired t-tests or multivariate statistics. In case of equal variance ANOVA followed by Bonferroni or TukeyHSD corrected pairwise comparison was chosen. In case of unequal variance Welch corrected ANOVA was applied,

followed by Games Howell test of all samples or pairwise comparison of samples with equal variance.

Gene identifiers of *Arabidopsis thaliana* genes

bZIP63 (At5g28770), *bZIP1* (At5g49450), *bZIP11* (At4g34590), *bZIP2* (At2g18160), *bZIP44* (At1g75390), *bZIP53* (At3g62420), *AKIN10/SnRK1.1* (At3g01090), *AKIN11/SnRK1.2* (At3g29160), *AKIN β 1* (At5g21170), *AKIN β 2* (At4g16360), *SNF4/AKIN β γ* (At1g09020), *SnAK2/GRIK1* (At3g45240), *ASN1/DIN6* (At3g47340), *DIN10* (At5g20250), *ProDH/ERD5* (At3g30775), *TBP2* (At1g55520), *MHF15* (At5g06430).

Primer table

Gene	forward primer	reverse primer
Primers for cloning		
genomic	GGTACCAAACTATAAATTTCT	TTGCGGCCGCCCTGATCCCCA
<i>bZIP63</i>	TGTAGGACAGTG	ACGCTTCGAATACG
<i>bZIP63.2</i>	AACCATGGAAAAGTTTTCTC	TTGCGGCCGCCCTGATCCCCA
	CGACGAAGAAATCTCC	ACGCTTCGAATACG
<i>AKIN10.1+3</i>	GGGCCCATGGATGGATCAGGC	GCGGCCGCAGAGGACTCGGA
	ACAGGCAGTA	GCTGAGCAA
<i>AKIN11.1+2</i>	GGGCCCATGGATCATTATCAA	GCGGCCGCAGATCACACGAA
	ATAG	GCTCTGTAA
<i>SNF4</i>	GGGCCCATGTTTGGTTCTACAT	GCGGCCGCAAAGACCGAGCA
	TGGA	GGAATTGGAA
<i>AKINβ1.1</i>	GGGCCCATGGGAAATGCGAAC	GCGGCCGCACCGTGTGAGCG
	GGCAA	GTTTGTAG
<i>AKINβ2.1+2</i>	GGGCCCATGTCTGCTGCTTCT	GCGGCCGCACCTCTGCAGGGA
	GATGGT	TTTGTAG
<i>bZIP1</i>	CGATGGGCCCCCATGGCAAACG	CGATGCGGCCGCTGTCTTAAA
	CAGAGAAG	GGACG
<i>bZIP2</i>	AAAACCATGGCGTCATCTAGC	TGCGGCCGCTATACATATTGAT
	AGCAC	ATCATTAG
<i>bZIP11</i>	TAGGGCCCATGGAATCGTCGT	TGGCGGCCGCAATACATTAAA
	CGTCGGGAA	GCATCAGAAG
<i>bZIP44.1</i>	CAGGGCCCATGAATAATAAAA	CTGCGGCCGCAACAGTTGAA
	CTG	AACATC
<i>bZIP53</i>	AAAACCATGGGGTCGTTGCAA	TGCGGCCGCTGCAATCAAACA
	ATGCAAAC	TATCAGCAG
Mutagenesis		

<i>bZIP63S29A</i>	CGTCGTTGAATCGCTCGGCCG CCGAATGGGCATTCAATC	ACGTCATTCCATTAACCGACC AGTG
<i>bZIP63S59A</i>	GTGTGGTGTTCCTCGTCTCCGCT CCTCCTAATGTTCTG	CACACGCCGTCGTAGATTCTC CGTCGTC
<i>bZIP63S102A</i>	GATACTTCTGGTAGAGCTGAC AATGGTGGAGC	GTATCCTGAGGTTTGATGAAA GTTC
<i>bZIP63S160A</i>	CTGATTCTCTATTAGCTAGCAT CCTTTTAACG	ATCAGCTAGACGGTCCAGAAG AAG
<i>bZIP63S261A</i>	CAGAGACATCAAATGCTCCAG ACACTACAAG	CTTGATAGTGTCTGGAGCATTT GATGTCTCTG
<i>bZIP63S294A</i>	GAACAGAACAGCTGCCATGCG TAGAGTTGAG	TGTTTCATCTTGACCCTATCAA GGC
<i>bZIP63S294/30 0A</i>	GAACAGAACAGCTGCCATGCG TAGAGTTGAGGCCTTGGAACA TCTGCAG	TGTTTCATCTTGACCCTATCAA GGC
<i>AKIN10K48M</i>	GGTTGCTATCATGATCCTCAAT CGTCG	GCAACCTTATGTCCTGTCAAT GC
qPCR		
<i>bZIP63</i>	GAAGAAATCTCCGGTAACCAT CAC	GATTCTCCGTCGTCTGCAGC
<i>ASN1</i>	GTCGCAAGATCAAGGCTC	TGAAGTCTTTGTCAAGGAAAG G
<i>DIN10</i>	GCTTGATTGCTGATGGA	ATCTTTAGCAAGCTGACACC
<i>ProDH</i>	CGCCAGTCCACGACACAATTC A	CGAATCAGCGTTATGTGTTGC G
<i>TBP2</i>	TGCAAGAAAGTATGCTCGG	ACATGAGCCTACAATGTTCTG
<i>MHF15</i>	GTTTCCTGAGCTTCTCCAC	TGGTCGCTTCATCTTGAG

AUTHOR CONTRIBUTION

AM, LP, BW, DA, and AS performed experimental research and data analysis with substantial input from TN, JVC, JH, EBG, CC, and WW. AM, LP, BW, WDL and MT designed the experiments. AM and MT wrote the manuscript.

ACKNOWLEDGMENT

We thank Lena Fragner (University of Vienna) for help with the metabolomics measurements and Klaus Harter (University of Tübingen) and Sjef Smeekens (Utrecht University) for critical comments on the manuscript. This work was funded by the FP7

Marie Curie ITN MERIT (GA 264474) (LP, AS, TN), the Austrian Science Fund (FWF) projects AP19825 (AM, BW, MT) and AP23435 (AM, MT), the Deutsche Forschungsgemeinschaft (DFG) project HA2146/8-2 (CC)

List of supporting material

Figure 1 – figure supplement 1. Phenotypes of *bZIP63* mutants in dark-induced senescence

Figure 1 – figure supplement 2. Metabolic changes in *bZIP63* ko and ox plants

Figure 1 – source data 1. Excel table of relative metabolite levels in *bZIP63* mutants and p-values from T-tests

Figure 1 – source data 2. ImageJ macro for determination of leaf area and green leaf area

Figure 2 – figure supplement 1. Overview over identified phospho-peptides of *bZIP63*

Figure 3 – figure supplement 1. Auto-phosphorylation from the protein extracts is negligible in in-gel kinase assays

Figure 3 – figure supplement 2. Overview over all kinases identified by LC-MS/MS after affinity purification with *bZIP63*

Figure 3 – source data 1. Excel table containing a detailed overview over all identified kinases and analyzed samples as well as all peptides found for the kinase subunit

Figure 4 – figure supplement 1. SnAK2 increases the kinase activity of AKIN10 and AKIN11 but does not phosphorylate *bZIP63*

Figure 4 – figure supplement 2. AKIN β 1 and AKIN β 2 don not interact with *bZIP63*

Figure 4 – figure supplement 3. Sugar-dependent in vivo phosphorylation of *bZIP63* in seedlings

Figure 5 – figure supplement 1. AKIN10 phosphorylates *bZIP63* but not GST

Figure 5 – figure supplement 2. AKIN10 phosphorylates S29, S294, and S300 on *bZIP63*

Figure 5 – figure supplement 3. The AKIN10 target sites and S160 in the *bZIP* domain hare highly conserved

Figure 5 – figure supplement 4. Expression of *bZIP63* and AKIN10 in the promoter activation assays

Figure 5 – source data 1. Sequences of the *bZIP63* homologues

Figure 6 – figure supplement 1. Characterization of the *bzip63* complementation lines

Figure 6 – figure supplement 2. Complementation of the dark-induced senescence phenotype of *bzip63*

Figure 6 – source data 1. Excel table containing the relative metabolite levels of the complementation lines and the PCA loadings

Figure 7 – figure supplement 1. Protoplast 2-hybrid (P2H) controls

Figure 7 – figure supplement 2. SnAK2 does not phosphorylate bZIP63 or the S1 class bZIPs

References

Baena-Gonzalez E, Rolland F, Thevelein JM, Sheen J. 2007. A central integrator of transcription networks in plant stress and energy signalling. *Nature* **448**: 938-42. doi: 10.1038/nature06069

Baena-Gonzalez E, Sheen J. 2008. Convergent energy and stress signaling. *Trends in Plant Science* **13**: 474-482. doi: 10.1016/j.tibs.2008.02.002

Bayer RG, Kostler T, Jain A, Stael S, Ebersberger I, Teige M. 2014. Higher plant proteins of cyanobacterial origin - are they or are they not preferentially targeted to chloroplasts? *Molecular plant*. pii: ssu095. doi: 10.1093/mp/ssu095

Chung B-C, Lee SY, Oh SA, Rhew TH, Nam HG, Lee C-H. 1997. The promoter activity of *sen 1*, a senescence-associated gene of Arabidopsis, is repressed by sugars. *Journal of Plant Physiology* **151**: 339-45. doi:10.1016/S0176-1617(97)80262-3

Correa LG, Riano-Pachon DM, Schrago CG, dos Santos RV, Mueller-Roeber B, Vincentz M. 2008. The role of bZIP transcription factors in green plant evolution: adaptive features emerging from four founder genes. *PloS One* **3**: e2944. doi: 10.1371/journal.pone.0002944

Delatte TL, Sedijani P, Kondou Y, Matsui M, de Jong GJ, Somsen GW, Wiese-Klinkenberg A, Primavesi LF, Paul MJ, Schluepmann H. 2011. Growth arrest by trehalose-6-phosphate: an astonishing case of primary metabolite control over growth by way of the SnRK1 signaling pathway. *Plant Physiology* **157**: 160-74. doi: 10.1104/pp.111.180422

Deppmann CD, Alvania RS, Taparowsky EJ. 2006. Cross-species annotation of basic leucine zipper factor interactions: Insight into the evolution of closed interaction networks. *Molecular Biology and Evolution* **23**: 1480-92. doi: 10.1093/molbev/msl022

Dietrich K, Weltmeier F, Ehlert A, Weiste C, Stahl M, Harter K, Droege-Laser W. 2011. Heterodimers of the Arabidopsis transcription factors bZIP1 and bZIP53 reprogram amino acid metabolism during low energy stress. *The Plant Cell* **23**: 381-95. doi: 10.1105/tpc.110.075390

Ehlert A, Weltmeier F, Wang X, Mayer CS, Smeekens S, Vicente-Carbajosa J, Droege-Laser W. 2006. Two-hybrid protein-protein interaction analysis in Arabidopsis protoplasts: establishment of a heterodimerization map of group C and group S bZIP transcription factors. *The Plant Journal* **46**: 890-900. doi: 10.1111/j.1365-313X.2006.02731.x

Furihata T, Maruyama K, Fujita Y, Umezawa T, Yoshida R, Shinozaki K, Yamaguchi-Shinozaki K. 2006. Abscisic acid-dependent multisite phosphorylation regulates the activity of a transcription activator AREB1. *Proceedings of the National Academy of Sciences USA* **103**: 1988-93. doi: 10.1073/pnas.0505667103

Guo S, Vanderford NL, Stein R. 2010. Phosphorylation within the MafA N terminus regulates C-terminal dimerization and DNA binding. *The Journal of Biological Chemistry* **285**: 12655-61. doi: 10.1074/jbc.M110.105759

Hanson J, Hanssen M, Wiese A, Hendriks MM, Smeekens S. 2008. The sucrose regulated transcription factor bZIP11 affects amino acid metabolism by regulating the expression of ASPARAGINE SYNTHETASE1 and PROLINE DEHYDROGENASE2. *The Plant Journal* **53**: 935-49. doi: 10.1111/j.1365-313X.2007.03385.x

Hardie DG. 2007. AMP-activated/SNF1 protein kinases: conserved guardians of cellular energy. *Nature reviews Molecular Cell Biology* **8**: 774-85. doi: 10.1038/nrm2249

Hardie DG, Ross FA, Hawley SA. 2012. AMPK: a nutrient and energy sensor that maintains energy homeostasis. *Nature reviews Molecular Cell Biology* **13**: 251-62. doi: 10.1038/nrm3311

Hedbacker K, Carlson M. 2008. SNF1/AMPK pathways in yeast. *Frontiers in Bioscience* **13**: 2408-20

- Holmberg CI, Tran SE, Eriksson JE, Sistonen L. 2002. Multisite phosphorylation provides sophisticated regulation of transcription factors. *Trends in Biochemical Sciences* **27**: 619-27. doi: 10.1016/S0968-0004(02)02207-7
- Huang J Z, Huber S C. 2001. Phosphorylation of synthetic peptides by a CDPK and plant SNF1-related protein kinase. Influence of proline and basic amino acid residues at selected positions. *Plant and Cell Physiology*. **42**: 1079-1087. doi: 10.1093/pcp/pce137
- Jakoby M, Weisshaar B, Droege-Laser W, Vicente-Carbajosa J, Tiedemann J, Kroj T, Parcy F. 2002. bZIP transcription factors in Arabidopsis. *Trends in Plant Science* **7**: 106-11. doi: 10.1016/S1360-1385(01)02223-3
- Kang SG, Price J, Lin PC, Hong JC, Jang JC. 2010. The arabidopsis bZIP1 transcription factor is involved in sugar signaling, protein networking, and DNA binding. *Molecular Plant* **3**: 361-73. doi: 10.1093/mp/ssp115
- Kim JW, Tang QQ, Li X, Lane MD. 2007. Effect of phosphorylation and S-S bond-induced dimerization on DNA binding and transcriptional activation by C/EBPbeta. *Proceedings of the National Academy of Sciences USA* **104**: 1800-4. doi: 10.1073/pnas.0611137104
- Kirby J, Kavanagh TA. 2002. NAN fusions: a synthetic sialidase reporter gene as a sensitive and versatile partner for GUS. *The Plant Journal* **32**: 391-400. doi: 10.1046/j.1365-313X.2002.01422.x
- Kinoshita E, Kinoshita-Kikuta E, Takiyama K, Koike T. 2006. Phosphate-binding tag, a new tool to visualize phosphorylated proteins. *Mol Cell Proteomics* **5**: 749-57. doi: 10.1074/mcp.T500024-MCP200
- Kirchler T, Briesemeister S, Singer M, Schutze K, Keinath M, Kohlbacher O, Vicente-Carbajosa J, Teige M, Harter K, Chaban C. 2010. The role of phosphorylatable serine residues in the DNA-binding domain of Arabidopsis bZIP transcription factors. *European Journal of Cell Biology* **89**: 175-83. doi: 10.1016/j.ejcb.2009.11.023
- Kunz S, Pesquet E, Kleczkowski LA. 2014. Functional dissection of sugar signals affecting gene expression in Arabidopsis thaliana. *PloS One* **9**: e100312. doi: 10.1371/journal.pone.0100312

Lee S, Shuman JD, Guszczynski T, Sakchaisri K, Sebastian T, Copeland TD, Miller M, Cohen MS, Taunton J, Smart RC, Xiao Z, Yu LR, Veenstra TD, Johnson PF. 2010. RSK-mediated phosphorylation in the C/EBP leucine zipper regulates DNA binding, dimerization, and growth arrest activity. *Molecular and Cellular Biology* **30**: 2621-35. doi: 10.1128/MCB.00782-09

Ma J. 2012. Reprogramming of metabolism by the *Arabidopsis thaliana* bZIP11 transcription factor. PhD thesis, Utrecht University.

Ma J, Hanssen M, Lundgren K, Hernandez L, Delatte T, Ehlert A, Liu CM, Schlupe H, Droege-Laser W, Moritz T, Smeekens S, Hanson J. 2011. The sucrose-regulated *Arabidopsis* transcription factor bZIP11 reprograms metabolism and regulates trehalose metabolism. *The New Phytologist* **191**: 733-45. doi: 10.1111/j.1469-8137.2011.03735.x

Matiolli CC, Tomaz JP, Duarte GT, Prado FM, Del Bem LE, Silveira AB, Gauer L, Correa LG, Drumond RD, Viana AJ, Di Mascio P, Meyer C, Vincenz M. 2011. The *Arabidopsis* bZIP gene *AtbZIP63* is a sensitive integrator of transient abscisic acid and glucose signals. *Plant Physiology* **157**: 692-705. doi: 10.1104/pp.111.181743

Mayr B, Montminy M. 2001. Transcriptional regulation by the phosphorylation-dependent factor CREB. *Nature reviews Molecular Cell Biology* **2**: 599-609. doi: 10.1038/35085068

McGee SL, Hargreaves M. 2008. AMPK and transcriptional regulation. *Frontiers in Bioscience* **13**: 3022-33. doi: 10.2741/2907

Motohashi H, O'Connor T, Katsuoka F, Engel JD, Yamamoto M. 2002. Integration and diversity of the regulatory network composed of Maf and CNC families of transcription factors. *Gene* **294**: 1-12. doi: 10.1016/S0378-1119(02)00788-6

Naegele T, Mair A, Sun X, Fagner L, Teige M, Weckwerth W. 2014. Solving the differential biochemical Jacobian from metabolomics covariance data. *PLoS One* **9**: e92299. doi: 10.1371/journal.pone.0092299

Polge C, Thomas M. 2007. SNF1/AMPK/SnRK1 kinases, global regulators at the heart of energy control? *Trends in Plant Science* **12**: 20-8. doi: 10.1016/j.tplants.2006.11.005

Reinke AW, Baek J, Ashenberg O, Keating AE. 2013. Networks of bZIP protein-protein interactions diversified over a billion years of evolution. *Science* **340**: 730-4. doi: 10.1126/science.1233465

Rodrigues-Pousada C, Menezes RA, Pimentel C. 2010. The Yap family and its role in stress response. *Yeast* **27**: 245-58. doi: 10.1002/yea.1752

Ramakers C, Ruijter JM, Deprez RH, Moorman AF. 2003. Assumption-free analysis of quantitative real-time polymerase chain reaction (PCR) data. *Neuroscience letters* **339**: 62-6. doi: 10.1016/S0304-3940(02)01423-4

Saeed AI, Sharov V, White J, Li J, Liang W, Bhagabati N, Braisted J, Klapa M, Currier T, Thiagarajan M, *et al.* 2003. TM4: a free, open-source system for microarray data management and analysis. *BioTechniques* **34**: 374-8.

Schindelin J, Arganda-Carreras I, Frise E, Kaynig V, Longair M, Pietzsch T, Preibisch S, Rueden C, Saalfeld S, Schmid B, *et al.* 2012. Fiji: an open-source platform for biological-image analysis. *Nature Methods* **9**: 676-82. doi: 10.1038/nmeth.2019

Schuetze K, Harter K, Chaban C. 2008. Post-translational regulation of plant bZIP factors. *Trends in Plant Science* **13**: 247-55. doi: 10.1016/j.tplants.2008.03.002

Sussman MR, Amasino RM, Young JC, Krysan PJ, Austin-Phillips S. 2000. The Arabidopsis knockout facility at the University of Wisconsin-Madison. *Plant Physiology* **124**: 1465-7. doi: 10.1104/pp.124.4.1465

Taus T, Kocher T, Pichler P, Paschke C, Schmidt A, Henrich C, Mechtler K. 2011. Universal and confident phosphorylation site localization using phosphoRS. *Journal of Proteome Research* **10**: 5354-62. doi: 10.1021/pr200611n

Tome F, Naegele T, Adamo M, Garg A, Marco-Llorca C, Nukarinen E, Pedrotti L, Peviani A, Simeunovic A, Tatkiewicz A, Tomar M, Gamm M. 2014. The low energy signaling network. *Frontiers in plant science* **5**: 353. doi: 10.3389/fpls.2014.00353

Tsukada J, Yoshida Y, Kominato Y, Auron PE. 2011. The CCAAT/enhancer (C/EBP) family of basic-leucine zipper (bZIP) transcription factors is a multifaceted highly-regulated system for gene regulation. *Cytokine* **54**: 6-19. doi: 10.1016/j.cyto.2010.12.019

Umezawa T, Sugiyama N, Takahashi F, Anderson JC, Ishihama Y, Peck SC, Shinozaki K. 2013. Genetics and phosphoproteomics reveal a protein phosphorylation network in the abscisic acid signaling pathway in *Arabidopsis thaliana*. *Science Signaling* **6**: rs8. doi: 10.1126/scisignal.2003509

Usadel B, Blasing OE, Gibon Y, Retzlaff K, Hohne M, Gunther M, Stitt M. 2008. Global transcript levels respond to small changes of the carbon status during progressive exhaustion of carbohydrates in *Arabidopsis* rosettes. *Plant Physiology* **146**: 1834-61. doi: 10.1104/pp.107.115592

Veerabagu M, Kirchler T, Elgass K, Stadelhofer B, Stahl M, Harter K, Mira-Rodado V, Chaban C. 2014. The Interaction of the *Arabidopsis* Response Regulator ARR18 with bZIP63 Mediates the Regulation of PROLINE DEHYDROGENASE Expression. *Molecular Plant* **7**: 1560-77. doi: 10.1093/mp/ssu074

Waadt R, Schmidt LK, Lohse M, Hashimoto K, Bock R, Kudla J. 2008. Multicolor bimolecular fluorescence complementation reveals simultaneous formation of alternative CBL/CIPK complexes in planta. *The Plant Journal* **56**: 505-16. doi: 10.1111/j.1365-313X.2008.03612.x

Walter M, Chaban C, Schutze K, Batistic O, Weckermann K, Nake C, Blazevic D, Grefen C, Schumacher K, Oecking C, Harter K, Kudla J. 2004. Visualization of protein interactions in living plant cells using bimolecular fluorescence complementation. *The Plant Journal* **40**: 428-38. doi: 10.1111/j.1365-313X.2004.02219.x

Wehner N, Hartmann L, Ehlert A, Bottner S, Onate-Sanchez L, Droege-Laser W. 2011. High-throughput protoplast transactivation (PTA) system for the analysis of *Arabidopsis* transcription factor function. *The Plant Journal* **68**: 560-9. doi: 10.1111/j.1365-313X.2011.04704.x

Yoo SD, Cho YH, Sheen J. 2007. Arabidopsis mesophyll protoplasts: a versatile cell system for transient gene expression analysis. *Nature Protocols* **2**: 1565-72. doi: 10.1038/nprot.2007.199

FIGURES, SUPPLEMENTAL FIGURES AND TABLES

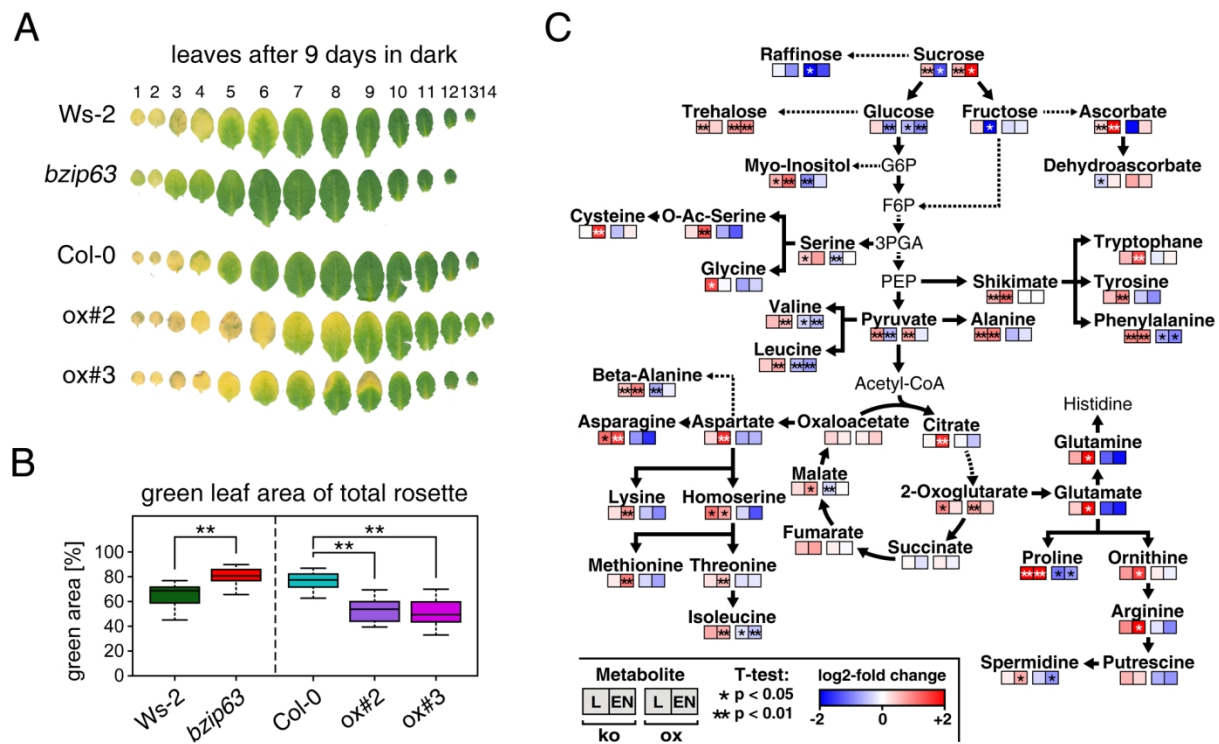


Figure 1. *bZIP63* mutants have a phenotype in dark-induced senescence and primary metabolism

(A) and (B) Dark-induced senescence phenotype of 4.5 week-old soil grown plants. Comparison of a *bzip63* line in the Wassilewskya (*Ws-2*) and two *bZIP63* ox lines in the Columbia (*Col-0*) background after 9 days in darkness. (A) Representative leaf series. (B) Box-and-whiskers plot of the total green leaf area of 8 biological replicates as determined with ImageJ. See Figure 1 – figure supplement 1 for controls and green area of individual leaves.

(C) Metabolic phenotype of 5 week-old soil grown plants after 6h light (L) and extended night (EN). Log-2 fold changes of metabolite levels in ko and ox compared to their respective wt, displayed on a simplified map of the central primary metabolism. Values are means of 5 biological replicates. For more details including mean values and SD see Figure 1 – figure supplement 2 and Figure 1 – source data 1.

P-values from T-tests between mutants and wt < 0.05 and < 0.01 are indicated by * and **, respectively.

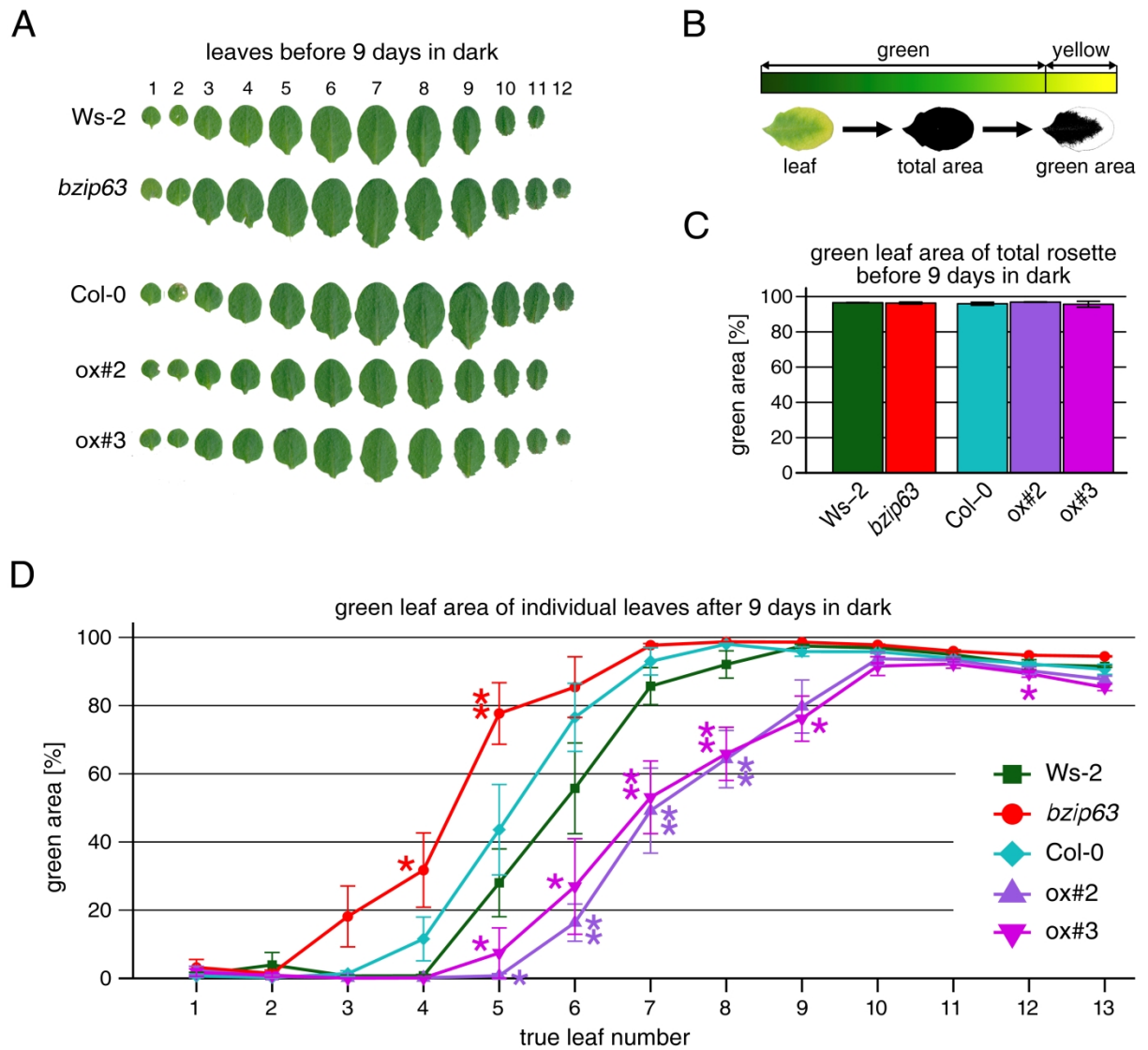


Figure 1 – figure supplement 1. Phenotypes of *bZIP63* mutants in dark-induced senescence

Dark-induced senescence phenotype of 4.5 week-old soil-grown plants Comparison of a *bzip63* line in the Wassilewskya (*Ws-2*) and two *bZIP63* ox lines in the Columbia (*Col-0*) background. **(A)** Representative leaf series of plants before dark treatment. **(B)** Scheme of the image processing with ImageJ. The color threshold and an exemplary leaf are shown. **(C)** Barplot of the total green leaf area of the rosette before darkness. Values are the mean \pm SD of 4 biological replicates. **(D)** Dotplot of the green leaf area of individual leaves after 9 days in darkness. P-values from T-tests between mutants and wt < 0.05 and < 0.01 are indicated by * and **, respectively.

		log2-fold changes to wt					
		-2		0		+2	
		<i>bzip63</i>		<i>ox#3</i>			
Metabolites		6h L	6h EN	6h L	6h EN		
amino acids	Serine	0,42*	0,75	-0,40**	0,02		
	O-Acetyl-Serine	0,25	1,30**	-0,64	-1,29		
	Cysteine	0,04	1,64**	-0,50	0,16		
	Glycine	1,47*	-0,05	-0,71	-0,36		
	Shikimate	0,60**	1,09**	-0,02	0,02		
	Tryptophane	0,55	1,43**	-0,15	0,11		
	Tyrosine	0,50	0,91**	-0,42	-0,88		
	Phenylalanine	0,91**	0,92**	-0,68*	-0,97*		
	Alanine	0,88**	1,03**	-0,55	-0,24		
	Valine	0,55	0,52**	-0,35*	-0,52**		
	Leucine	0,43	0,65**	-0,54**	-0,77**		
	Glutamate	0,41	2,24*	-1,44	-1,80		
	Glutamine	0,66	2,10*	-1,25	-1,90		
	Proline	2,18**	3,04**	-1,08*	-0,81*		
	Ornithine	0,79	1,54*	0,14	-0,13		
	Arginine	0,92	2,12*	-0,21	-0,95		
	Aspartate	0,31	1,67**	-0,65	-0,59		
	Asparagine	1,15*	1,51**	-0,83	-1,64		
	Lysine	0,27	0,83**	-0,44	-0,92		
	Beta alanine	0,50**	0,96**	-0,64**	-0,14		
Homoserine	1,11*	0,75*	-0,31	-1,36			
Methionine	0,19	1,03**	-0,30	-0,70			
Threonine	0,23	0,51**	-0,23	-0,18			
Isoleucine	0,65	0,63**	-0,22*	-0,46**			
TCA cycle	Pyruvate	0,80**	-0,57**	0,71**	-0,16		
	Citric acid	0,07	1,62**	-0,07	-0,47		
	2-Oxoglutarate	0,91*	0,26	0,76**	0,37		
	Succinate	0,07	-0,23	0,13	-0,11		
	Fumarate	0,48	0,74	0,13	-0,05		
	Malate	0,28	0,75*	-0,31**	0,04		
	Oxaloacetate	0,34	0,15	0,14	0,40		
sugars	Sucrose	0,55**	-1,39*	0,62**	2,89*		
	Glucose	0,30	-0,84**	-0,55*	-0,89**		
	Fructose	0,29	2,89*	-0,27	-0,17		
	Trehalose	0,56**	0,38	0,80**	0,92**		
	Myo-Inositol	0,62*	1,14**	-0,89**	-0,29		
	Raffinose	-0,12	-0,85	-3,12*	-1,43		
other	Putrescine	0,60	0,33	-0,63	-0,83		
	Spermidine	0,15	0,65*	-0,35	-0,85*		
	Ascorbate	0,35**	2,01**	-1,94	0,32		
	Dehydroascorbate	-0,34*	0,16	0,69	0,36		

Figure 1 – figure supplement 2. Metabolic changes in bZIP63 ko and ox plants

Table of the metabolite levels of *bzip63* and *ox#3* compared to their respective wt shown in Figure 1C. Values are the log-2 transformed means of 5 biological replicates. P-values from T-tests between mutant and wt (done on untransformed data) < 0.05 and < 0.01 are indicated by * and **, respectively. The color gradient indicates increased (red) or decreased (blue) metabolite levels in the mutant. For relative changes between mutant and wt including the SD and p-values from T-tests see Figure 1 – source data 1.

Figure 1 - source data 1.xlsx - Microsoft Excel

Means (n=5) and standard deviations of metabolites measured in wild-type and bZIP63 mutant lines normalized to the corresponding wild-type. p-values are from 2-tailed t-test assuming unequal variance

Metabolites	6h light				6h extended night				12h light				12h extended night							
	mean	SD	mean	SD	mean	SD	mean	SD	mean	SD	mean	SD	mean	SD	mean	SD				
Sucrose	1.00	0.17	1.33	0.20	0.0225	1.00	0.00	0.76	0.07	0.0074	1.00	0.21	1.68	0.23	0.0071	1.00	0.22	1.02	0.23	0.0025
Glucose	1.00	0.12	1.39	0.31	0.3625	1.00	0.52	0.64	0.42	0.2627	1.00	0.22	2.47	0.31	0.0001	1.00	0.44	0.41	0.25	0.0073
Fructose	1.00	0.41	1.03	0.44	0.3231	1.00	0.35	0.71	0.47	0.3032	1.00	0.65	3.11	0.68	0.0032	1.00	0.49	1.12	0.57	0.0061
Galactose	1.00	0.08	2.27	1.85	0.0263	1.00	0.44	0.61	0.30	0.1843	1.00	0.16	0.97	0.61	0.0777	1.00	0.20	0.78	0.44	0.2020
Mannose	1.00	0.16	1.52	0.25	0.0075	1.00	0.63	0.98	0.68	0.6807	1.00	0.37	2.13	0.15	0.0071	1.00	0.07	1.02	0.87	0.8801
Tyrosine	1.00	0.25	1.47	0.57	0.0565	1.00	0.11	0.90	0.69	0.1400	1.00	0.45	2.83	0.61	0.0026	1.00	0.18	1.09	0.69	0.5221
Threonine	1.00	0.12	1.41	0.50	0.1430	1.00	0.33	0.75	0.50	0.2784	1.00	0.32	1.88	0.22	0.0013	1.00	0.27	0.54	0.29	0.0023
Phenylalanine	1.00	0.19	1.68	0.44	0.0061	1.00	0.25	0.62	0.19	0.0102	1.00	0.24	1.69	0.19	0.0002	1.00	0.22	0.51	0.18	0.0442
Alanine	1.00	0.20	1.03	0.41	0.0066	1.00	0.35	0.68	0.35	0.1074	1.00	0.19	2.04	0.20	0.0000	1.00	0.51	0.95	0.25	0.0130
Valine	1.00	0.10	1.46	0.42	0.0700	1.00	0.12	0.78	0.12	0.0278	1.00	0.16	1.43	0.09	0.0071	1.00	0.14	0.70	0.17	0.0005
Leucine	1.00	0.17	1.35	0.33	0.0796	1.00	0.33	0.69	0.36	0.0765	1.00	0.20	1.07	0.12	0.0025	1.00	0.08	0.59	0.35	0.0021
Glutamine	1.00	0.23	1.53	0.43	0.1938	1.00	0.25	0.37	0.15	0.1314	1.00	0.89	4.72	2.30	0.0429	1.00	0.84	0.29	0.06	0.1443
Glutamate	1.00	0.42	1.98	0.31	0.0502	1.00	0.44	0.42	0.32	0.1523	1.00	0.52	2.49	1.21	0.0020	1.00	0.60	0.27	0.10	0.0088
Proline	1.00	0.71	4.52	0.46	0.0001	1.00	0.37	0.47	0.33	0.0423	1.00	0.57	2.21	2.21	0.0016	1.00	0.18	0.57	0.26	0.0247
Asparagine	1.00	0.76	1.73	0.91	0.2048	1.00	0.71	1.10	1.14	0.0601	1.00	0.52	2.89	1.21	0.0020	1.00	0.70	0.91	0.26	0.0038
Arginine	1.00	0.67	1.89	1.06	0.1647	1.00	0.67	0.86	0.79	0.1744	1.00	0.56	4.35	2.68	0.0470	1.00	0.77	0.52	0.25	0.2881
Asparagine	1.00	0.52	1.24	0.44	0.2086	1.00	0.26	0.54	0.37	0.1608	1.00	0.22	3.19	0.46	0.0001	1.00	0.29	0.98	0.37	0.1812
Lysine	1.00	0.15	2.31	0.74	0.0033	1.00	0.67	0.56	0.47	0.2885	1.00	0.42	2.84	0.84	0.0049	1.00	0.49	0.32	0.12	0.0773
Urea	1.00	0.18	1.20	0.20	0.2727	1.00	0.37	0.73	0.38	0.2867	1.00	0.36	1.77	0.21	0.0053	1.00	0.27	0.53	0.20	0.0622
Glutamate	1.00	0.12	1.42	0.21	0.0078	1.00	0.15	0.64	0.17	0.0090	1.00	0.06	1.95	0.20	0.0002	1.00	0.02	0.31	0.22	0.0439
Homoserine	1.00	0.16	2.16	0.60	0.0095	1.00	0.47	0.80	0.64	0.0584	1.00	0.38	1.69	0.31	0.0043	1.00	0.60	0.39	0.13	0.1412
Methionine	1.00	0.25	1.34	0.26	0.4236	1.00	0.30	0.91	0.35	0.4026	1.00	0.40	2.04	0.30	0.0021	1.00	0.26	0.61	0.33	0.0778
Threonine	1.00	0.09	1.17	0.23	0.3775	1.00	0.62	0.86	0.22	0.1260	1.00	0.09	1.42	0.13	0.0009	1.00	0.16	0.88	0.25	0.2841
Isoleucine	1.00	0.08	1.68	0.57	0.0646	1.00	0.18	0.36	0.08	0.0460	1.00	0.18	1.95	0.12	0.0010	1.00	0.08	0.12	0.11	0.0818
Propanoate	1.00	0.17	1.74	0.11	0.0001	1.00	0.15	1.64	0.25	0.0021	1.00	0.13	0.67	0.07	0.0023	1.00	0.19	0.30	0.15	0.1447
Citric acid	1.00	0.23	1.05	0.44	0.0453	1.00	0.26	0.95	0.35	0.0164	1.00	0.21	3.08	0.36	0.0000	1.00	0.49	0.12	0.20	0.0066
L-Aspartate	1.00	0.28	1.68	0.63	0.0009	1.00	0.19	1.59	0.32	0.0051	1.00	0.28	1.20	0.29	0.0064	1.00	0.23	1.29	0.37	0.0020
Succinate	1.00	0.33	1.05	0.12	0.7775	1.00	0.14	1.18	0.30	0.0104	1.00	0.21	0.65	0.13	0.2296	1.00	0.20	0.59	0.26	0.0367
Fumarate	1.00	0.42	1.40	0.14	0.1011	1.00	0.17	1.09	0.13	0.3821	1.00	0.46	1.67	0.61	0.0862	1.00	0.31	0.36	0.38	0.1766
Malate	1.00	0.44	1.21	0.13	0.3461	1.00	0.31	0.80	0.03	0.0095	1.00	0.47	1.98	0.32	0.0299	1.00	0.25	1.03	0.45	0.0814
Diacylglycerol	1.00	0.16	1.26	0.24	0.1222	1.00	0.54	1.10	0.44	0.1644	1.00	0.21	1.11	0.31	0.0339	1.00	0.19	1.32	0.45	0.1214
Succose	1.00	0.18	1.46	0.19	0.0043	1.00	0.14	1.54	0.14	0.0094	1.00	0.33	0.39	0.08	0.0118	1.00	0.06	7.42	4.17	0.0085
Glucose	1.00	0.34	1.23	0.23	0.2008	1.00	0.17	0.65	0.30	0.0299	1.00	0.13	0.56	0.17	0.0019	1.00	0.24	0.64	0.09	0.0049
Fructose	1.00	0.43	1.22	0.42	0.4521	1.00	0.20	0.93	0.38	0.1977	1.00	0.64	0.10	0.05	0.0394	1.00	0.42	0.89	0.47	0.0623
Galactose	1.00	0.18	1.46	0.31	0.0067	1.00	0.15	1.74	0.18	0.0001	1.00	0.42	1.80	0.15	0.0044	1.00	0.26	1.69	0.38	0.0102
Mannitol	1.00	0.21	1.54	0.22	0.0052	1.00	0.06	0.54	0.03	0.0000	1.00	0.19	2.20	0.21	0.0000	1.00	0.16	0.52	0.12	0.1867
Raffinose	1.00	0.67	0.62	0.50	0.9414	1.00	0.44	0.17	0.03	0.0001	1.00	0.25	0.95	0.56	0.1610	1.00	0.75	0.37	0.12	0.2660
Putrescine	1.00	0.26	1.52	0.54	0.1035	1.00	0.63	0.65	0.50	0.0539	1.00	0.30	1.25	0.28	0.2843	1.00	0.46	0.56	0.11	0.2299
Spermidine	1.00	0.20	1.31	0.44	0.0406	1.00	0.11	0.79	0.29	0.0070	1.00	0.17	1.57	0.16	0.0330	1.00	0.02	0.96	0.27	0.0222
Acetate	1.00	0.09	1.27	0.02	0.0000	1.00	0.64	0.26	0.18	0.1021	1.00	0.96	4.04	1.00	0.0001	1.00	0.54	1.34	0.43	0.1256
Dehydroascorbate	1.00	0.06	0.79	0.16	0.0455	1.00	0.25	1.61	0.51	0.0556	1.00	0.19	1.12	0.36	0.0008	1.00	0.19	1.09	0.43	0.3373

Screenshot of the excel file.

Figure 1 – source data 1. Excel table of relative metabolite levels in *bZIP63* mutants and p-values from T-tests

Table of relative metabolite levels in Ws-2, *bzip63*, Col-0 and *ox#3* after 6h in light or extended night, which were used to calculate the log2-fold changes shown in Figures 1C and see Figure 1 – figure supplement 2. Mean values and SD of 5 biological replicates are given as fold changes to the corresponding wt. P-values from T-tests between wt and mutant are listed.

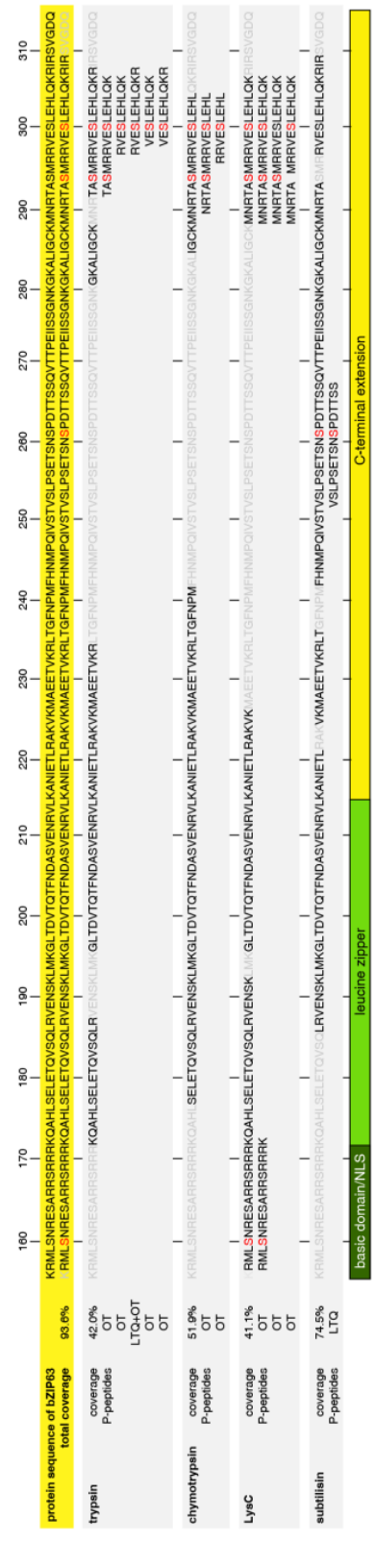
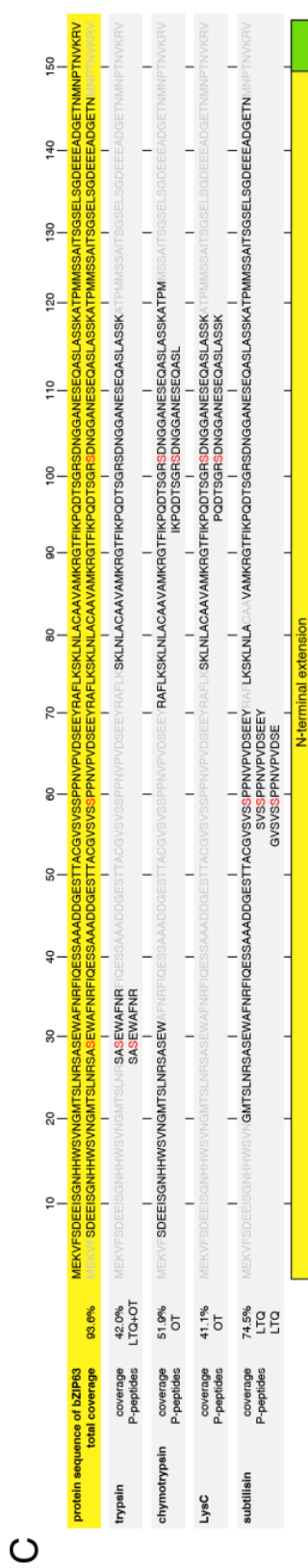
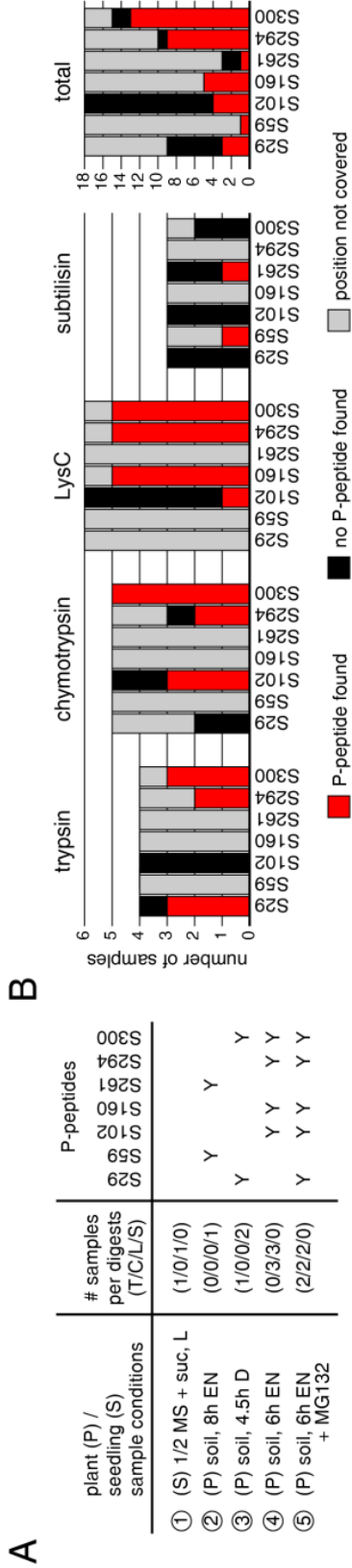


Figure 2 – figure supplement 1. Overview over identified phospho-peptides of bZIP63

(A) Sample overview, summarizing for each of the five independent experiments: plant material, growth conditions, the number of samples digested with each proteolytic enzyme, and the identified phospho-sites (Y). Experiments 1 to 3 were measured with a linear ion trap quadrupole (LTQ), experiments 4 and 5 with an LTQ-Oribtrap (OT).

(B) Phospho-peptide identification frequencies for the proteolytic enzymes. The barplot shows, for each proteolytic enzyme, the number of samples in which an *in vivo* phosphorylation-site was covered (black or red) or not covered (grey), and how often a phospho-peptide was identified (red).

(C) Graph showing the total protein coverage from all experiments, as well as the protein coverage that was achieved with each of the four proteolytic enzymes in % and as a sequence. Parts of the sequence that were covered and not covered are shown in black and light grey, respectively. Identified phospho-serines are red. Below the coverage, all identified phospho-peptides are listed and the instrument used for identification is specified (LTQ or OT). The numbers on top indicate the position in the protein sequence. The scheme below indicates the position of the conserved bZIP domain (green), including the basic domain (dark green), and the N- and C-terminal extensions (yellow).

L, light; EN, extended night; D, dark; suc, sucrose; T, trypsin; C, chymotrypsin; L, LysC; S, subtilisin; NLS, nuclear localization signal

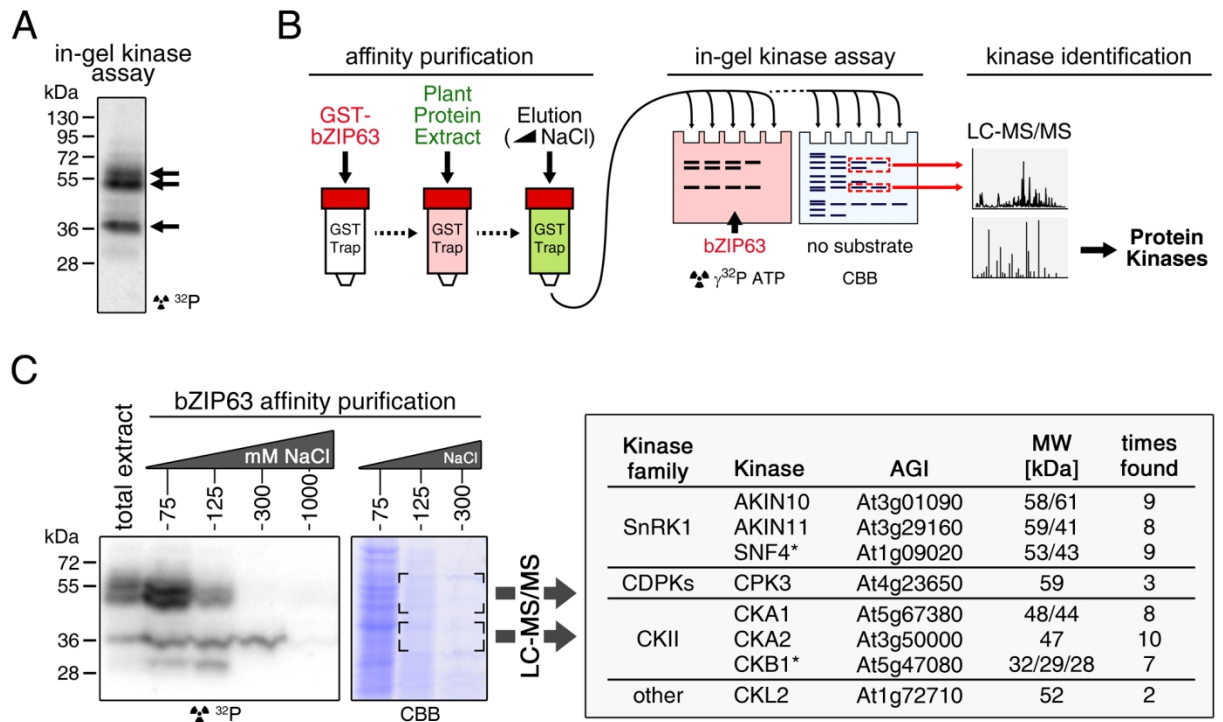


Figure 3. Several different kinases can phosphorylate bZIP63

(A) In-gel kinase assay with a wild type plant protein extract and bZIP63 as substrate. Arrows indicate the positions of potential bZIP63 kinases.

(B) Scheme of the kinase identification process.

(C) In-gel kinase assay with samples from affinity purification with bZIP63 and bZIP63 as a substrate (left) and a list of catalytic and regulatory (*) kinase subunits identified with high confidence (right). The list also contains the gene identifier (AGI), molecular weight (MW), and number of samples in which the protein was found. For controls and a list of all identified kinases and kinase peptides see Figure 3 – figure supplement 1 – 2 and Figure 3 – source data 1.

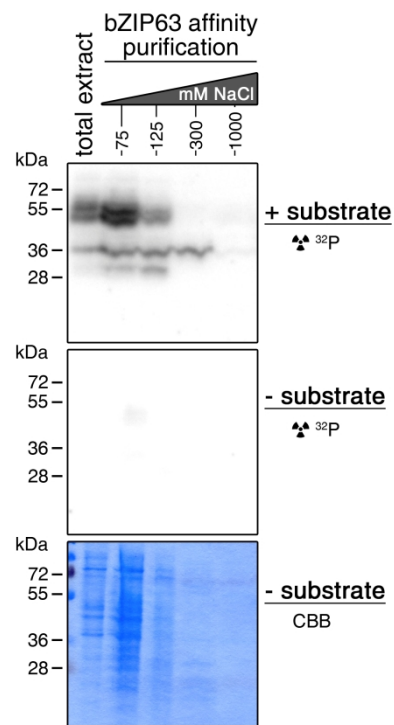


Figure 3 – figure supplement 1. Auto-phosphorylation from the protein extracts is negligible in in-gel kinase assays

In-gel kinase assay with samples from affinity purification with bZIP63. Comparison of a gel with bZIP63 as a substrate (top, see also Figure 3C) and a gel without substrate (middle). A coomassie brilliant blue (CBB) stained gel is shown at the bottom.

Kinase family	found in		Kinase subunit				
	IP-MS/MS		Protein name	AGI	MW (all s.f.)	Subcellular localization** shown by GFP fusion [Ref]	
	Yes/No	# of finds					
SnRK1	Yes	9	AKIN10 / SnRK1.1	SNF1 Kinase homolog 10, SNF1-related protein kinase 1.1	At3g01090	58/61/58	N[1,2], C[1,2,3], CP[3]
	Yes	7/8*	AKIN11 / SnRK1.2	SNF1 Kinase homolog 11, SNF1-related protein kinase 1.2	At3g29160	59/59/41	N[1,2], C[1,2,3], CP[3]
	Yes	0/1*	AKIN12 / SnRK1.3	SNF1 Kinase homolog 12, SNF1-related protein kinase 1.3	At5g39440	57	?
	No		AKINb1	SnRK1 kinase regulatory subunit beta-1	At5g21170	31/35	PM[4], N[4]
	Yes	1	AKINb2	SnRK1 kinase regulatory subunit beta-2	At4g16360	29/29/29	PM[4], C[4,5], N[5]
	No		AKINb3	SnRK1 kinase regulatory subunit beta-3	At2g28060	13	N[5], C[5]
	Yes	9	SNF4	Sucrose Nonfermenting 4	At1g09020	53/43	N[2,5], C[2,5]
CDPKs	Yes	3	CPK3 / CDPK6	Calcium-dependent protein kinase 3	At4g23650	59	C[6,7,8], N[6,7,8], PM[7], VM[7]
	Yes	1	CPK5	Calcium-dependent protein kinase 5	At4g35310	63	C[9], N[9]
	Yes?	0/2*	CPK4	Calcium-dependent protein kinase 4	At4g09570	56	C[6,9,10], N[9,10]
	Yes?	0/2*	CPK11 / CDPK2	Calcium-dependent protein kinase 11	At1g35670	56	C[9,10,11], N[9,10,11]
	Yes	1	CPK9	Calcium-dependent protein kinase 9	At3g20410	60	PM[6,12,13,14]
CKII	Yes	7/8*	CKA1	Casein Kinase II alpha chain 1	At5g67380	48/44	N[15]
	Yes	9/10*	CKA2	Casein Kinase II alpha chain 2	At3g50000	47	N[15]
	No		CKA3	Casein Kinase II alpha chain 3	At2g23080	39/36	N[15]
	Yes	7	CKAcp	Casein Kinase II chloroplastic alpha chain	At2g23070	50	<u>CP[1,15]</u>
	Yes	7	CKB1	Casein Kinase II beta chain 1	At5g47080	32/29/28/32	N[15,16], C[15,16?]
	No		CKB2	Casein Kinase II beta chain 2	At4g17640	32/31	N[15,16]
	No		CKB3	Casein Kinase II beta chain 3	At3g60250	31/31	N[15], C[15]
No		CKB4	Casein Kinase II beta chain 4	At2g44680	32/32	C[15,17], N[17]	
other	Yes	2	CKL2	Casein kinase I-like protein 2	At1g72710	52	N[18], C[18]
	Yes	1	MPK16	Mitogen-activated protein kinase 16	At5g19010	56	?
	Yes?	0/1*	CDK2	Cyclin-dependent kinase C2	At5g64960	57/51	N[19,20]
	Yes?	0/1*	CDKC1	Cyclin-dependent kinase C1	At5g10270	57	N[21]
	Yes	1	CRK9, EP1	Cysteine-Rich RLK (Receptor-Like Protein Kinase) 9	At4g23170	30	?

* including samples without proteotypic peptide for this kinase subunit

** N (nucleus), C (cytoplasm), CP (chloroplast), PM (plasma membrane), VM (vacuolar membrane)

Figure 3 – figure supplement 2. Overview over all kinases identified by LC-MS/MS after affinity purification with bZIP63

Table of all kinase complex subunits identified. For SnRK1 and CKII, the remaining, but not identified kinase subunits, are also included. Kinase subunits which were identified with proteotypic peptides in more than one sample, have approximately the expected size, and don't have a contradicting subcellular localization were considered high confidence candidates and are shown in black. Low confidence kinases subunits and kinases subunits not found are shown in grey and reasons for exclusion from the high confidence list are underlined. References for the subcellular localization: [1] Bayer et al., 2012; [2] Bitrian et al., 2011; [3] Fragoso et al., 2009; [4] Pierre et al., 2007; [5] Gissot et al., 2006; [6] Dammann et al., 2003; [7] Mehlmer et al., 2010; [8] Berendzen et al., 2012; [9] Boudsocq et al., 2010; [10] Zhu et al., 2007; [11] Rodriguez Milla et al., 2006; [12] Benetka et al., 2008; [13] Dong et al., 2008; [14] Padmanaban et al., 2007; [15] Salinas et al., 2006; [16] Park et al., 2008; [17] Perales et al., 2006; [18] Lee et al., 2005; [19] Koroleva et al., 2005; [20] Kitsios et al., 2008; [21] Boruc et al., 2010

IP-MS/MS, immune precipitation followed by tandem mass spectrometry; # of finds, number of samples in which the protein was found; AGI, gene identifier; s.f., splicing forms

REFERENCES for Figure 3 – figure supplement 2

Bayer RG, Stael S, Rocha AG, Mair A, Vothknecht UC, Teige M. 2012. Chloroplast-localized protein kinases: a step forward towards a complete inventory. *Journal of Experimental Botany* **63**: 1713-23. doi: 10.1093/jxb/err377

Benetka W, Mehlmer N, Maurer-Stroh S, Sammer M, Koranda M, Neumuller R, Betschinger J, Knoblich JA, Teige M, Eisenhaber F. 2008. Experimental testing of predicted myristoylation targets involved in asymmetric cell division and calcium-dependent signalling. *Cell Cycle* **7**: 3709-19. doi: 10.4161/cc.7.23.7176

Berendzen KW, Bohmer M, Wallmeroth N, Peter S, Vesic M, Zhou Y, Tiesler FK, Schleifenbaum F, Harter K. 2012. Screening for in planta protein-protein interactions combining bimolecular fluorescence complementation with flow cytometry. *Plant Methods* **8**: 25. doi: 10.1186/1746-4811-8-25

Bitrian M, Roodbarkelari F, Horvath M, Koncz C. 2011. BAC-recombineering for studying plant gene regulation: developmental control and cellular localization of SnRK1 kinase subunits. *The Plant Journal* **65**: 829-42. doi: 10.1111/j.1365-313X.2010.04462.x

Boruc J, Mylle E, Duda M, De Clercq R, Rombauts S, Geelen D, Hilson P, Inze D, Van Damme D, Russinova E. 2010. Systematic localization of the Arabidopsis core cell cycle proteins reveals novel cell division complexes. *Plant Physiology* **152**: 553-65. doi: 10.1104/pp.109.148643

Boudsocq M, Willmann MR, McCormack M, Lee H, Shan L, He P, Bush J, Cheng SH, Sheen J. 2010. Differential innate immune signalling via Ca(2+) sensor protein kinases. *Nature* **464**: 418-22. doi: 10.1038/nature08794

Dammann C, Ichida A, Hong B, Romanowsky SM, Hrabak EM, Harmon AC, Pickard BG, Harper JF. 2003. Subcellular targeting of nine calcium-dependent protein kinase isoforms from Arabidopsis. *Plant Physiology* **132**: 1840-48. doi: 10.1104/pp.103.020008

- Dong CH, Rivarola M, Resnick JS, Maggin BD, Chang C. 2008. Subcellular co-localization of Arabidopsis RTE1 and ETR1 supports a regulatory role for RTE1 in ETR1 ethylene signaling. *The Plant Journal* **53**: 275-86. doi: 10.1111/j.1365-313X.2007.03339.x
- Fragoso S, Espindola L, Paez-Valencia J, Gamboa A, Camacho Y, Martinez-Barajas E, Coello P. 2009. SnRK1 isoforms AKIN10 and AKIN11 are differentially regulated in Arabidopsis plants under phosphate starvation. *Plant Physiology* **149**: 1906-16. doi: 10.1104/pp.108.133298
- Gissot L, Polge C, Jossier M, Girin T, Bouly JP, Kreis M, Thomas M. 2006. AKINbetagamma contributes to SnRK1 heterotrimeric complexes and interacts with two proteins implicated in plant pathogen resistance through its KIS/GBD sequence. *Plant Physiology* **142**: 931-44. doi: 10.1104/pp.106.087718
- Kitsios G, Alexiou KG, Bush M, Shaw P, Doonan JH. 2008. A cyclin-dependent protein kinase, CDKC2, colocalizes with and modulates the distribution of spliceosomal components in Arabidopsis. *The Plant Journal* **54**: 220-35. doi: 10.1111/j.1365-313X.2008.03414.x
- Koroleva OA, Tomlinson ML, Leader D, Shaw P, Doonan JH. 2005. High-throughput protein localization in Arabidopsis using Agrobacterium-mediated transient expression of GFP-ORF fusions. *The Plant Journal* **41**: 162-74. doi: 10.1111/j.1365-313X.2004.02281.x
- Lee JY, Taoka K, Yoo BC, Ben-Nissan G, Kim DJ, Lucas WJ. 2005. Plasmodesmal-associated protein kinase in tobacco and Arabidopsis recognizes a subset of non-cell-autonomous proteins. *The Plant Cell* **17**: 2817-31. doi: 10.1105/tpc.105.034330
- Mehlmer N, Wurzinger B, Stael S, Hofmann-Rodrigues D, Csaszar E, Pfister B, Bayer R, Teige M. 2010. The Ca(2+) -dependent protein kinase CPK3 is required for MAPK-independent salt-stress acclimation in Arabidopsis. *The Plant Journal* **63**: 484-98. doi: 10.1111/j.1365-313X.2010.04257.x
- Padmanaban S, Chanroj S, Kwak JM, Li X, Ward JM, Sze H. 2007. Participation of endomembrane cation/H⁺ exchanger AtCHX20 in osmoregulation of guard cells. *Plant Physiology* **144**: 82-93. doi: 10.1104/pp.106.092155

- Park HJ, Ding L, Dai M, Lin R, Wang H. 2008. Multisite phosphorylation of Arabidopsis HFR1 by casein kinase II and a plausible role in regulating its degradation rate. *The Journal of biological chemistry* **283**: 23264-73. doi: 10.1074/jbc.M801720200
- Perales M, Portoles S, Mas P. 2006. The proteasome-dependent degradation of CKB4 is regulated by the Arabidopsis biological clock. *The Plant Journal* **46**: 849-60. doi: 10.1111/j.1365-313X.2006.02744.x
- Pierre M, Traverso JA, Boisson B, Domenichini S, Bouchez D, Giglione C, Meinel T. 2007. N-myristoylation regulates the SnRK1 pathway in Arabidopsis. *The Plant Cell* **19**: 2804-21. doi: 10.1105/tpc.107.051870
- Rodriguez Milla MA, Uno Y, Chang IF, Townsend J, Maher EA, Quilici D, Cushman JC. 2006. A novel yeast two-hybrid approach to identify CDPK substrates: characterization of the interaction between AtCPK11 and AtDi19, a nuclear zinc finger protein. *FEBS Letters* **580**: 904-11. doi: 10.1016/j.febslet.2006.01.013
- Salinas P, Fuentes D, Vidal E, Jordana X, Echeverria M, Holuigue L. 2006. An extensive survey of CK2 alpha and beta subunits in Arabidopsis: multiple isoforms exhibit differential subcellular localization. *Plant Cell Physiology* **47**: 1295-1308. doi: 10.1093/pcp/pcj100
- Zhu SY, Yu XC, Wang XJ, Zhao R, Li Y, Fan RC, Shang Y, Du SY, Wang XF, Wu FQ, Xu YH, Zhang XY, Zhang DP. 2007. Two calcium-dependent protein kinases, CPK4 and CPK11, regulate abscisic acid signal transduction in Arabidopsis. *The Plant Cell* **19**: 3019-36. doi: 10.1105/tpc.107.050666

The figure displays two screenshots of an Excel spreadsheet. The top screenshot, titled 'Table S3.xlsx - Microsoft Excel', shows a 'kinase overview' table. The columns include kinase names (e.g., AKIN10, AKIN11, AKIN12), sample identifiers (e.g., K12, K13, K14), and various counts for peptides and proteotypic peptides. The bottom screenshot shows a detailed 'peptides' table with columns for 'data range', 'peptides', and 'proteotypic?'. It lists numerous peptide sequences (e.g., K.YLLDQRY, K.IAEHALTKR.V) and indicates whether each is proteotypic (Y) or not (N). The table is organized into sections for different kinase subunits (AKIN10, AKIN11, AKIN12).

Figure 3 – source data 1. Excel table containing a detailed overview over all identified kinases and analyzed samples as well as all peptides found for the kinase subunit. The tab “kinase overview” contains a table showing in which samples each kinase subunit was identified, including the number of peptides, proteotypic peptides, MASCOT (Matrix Science) score, and expected molecular weight. The other tabs list all peptides found for the kinase subunits in each sample and state whether the peptide is proteotypic (Y) or not.

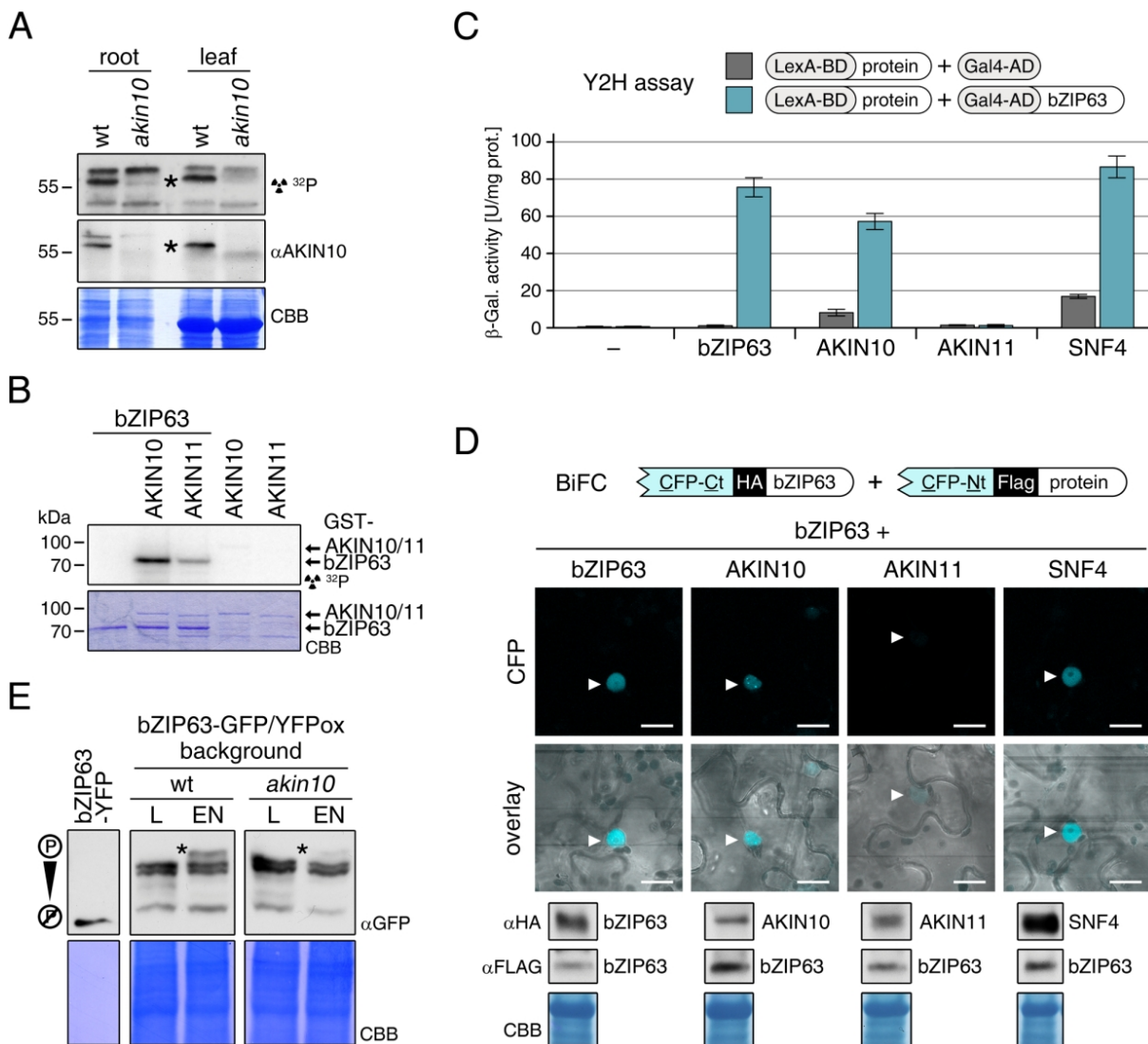


Figure 4. The SnRK1 kinase AKIN10 phosphorylates bZIP63 and interacts with bZIP63 in vivo

(A) In-gel kinase assay with protein extracts from wt and *akin10* plants and bZIP63 as a substrate (top), western blot against AKIN10 (α AKIN10, middle), and coomassie brilliant blue stain (CBB, bottom). Asterisks mark the position of AKIN10.

(B) In vitro kinase assay with recombinant AKIN10/AKIN11 and bZIP63 as a substrate. See also Figure 4 – figure supplement 1 for kinase assays including the SnRK1 upstream kinase SnAK2.

(C) and **(D)** Interaction of SnRK1 subunits with bZIP63. Homodimerization of bZIP63 was used as a positive control. **(C)** Yeast 2-hybrid (Y2H) assay with auto-activation in grey and interaction with bZIP63 in blue. Bars represent means \pm SD of 8 biological replicates. For Y2H with SnK1 β 1 and β 2 see Figure 4 – figure supplement 2. **(D)** Laser scanning microscopy images of bimolecular fluorescence complementation (BiFC) in transiently transformed *N. tabacum* leaves (top). Arrowheads indicate the position of the nucleus. Size bar = 20 μ m. Expression of the fusion proteins was verified by western blots (α HA, α Flag, bottom).

(E) Phos-tag gel western blots showing the in vivo phosphorylation state of bZIP63 after 6h light (L) or extended night (EN) in 5 week-old plants expressing bZIP63-GFP/YFP in the wt and *akin10* background. Recombinant bZIP63-YFP was used as an unphosphorylated control. Asterisks mark hyper-phosphorylated bZIP63. See Figure 4 – figure supplement 3 for phosphorylation in seedlings.

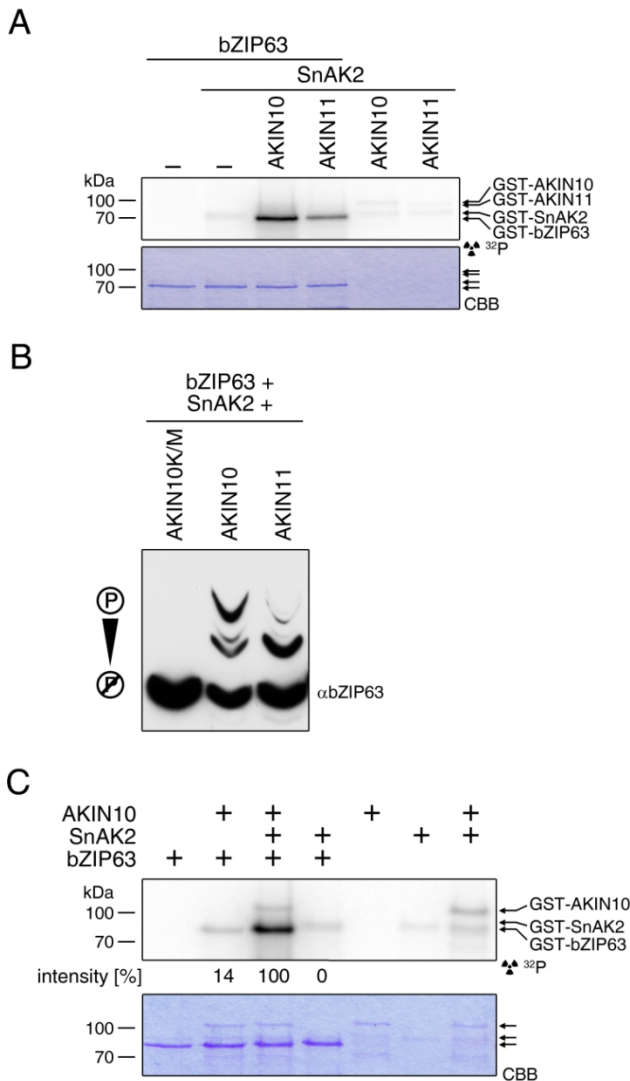


Figure 4 – figure supplement 1. SnAK2 increases the kinase activity of AKIN10 and AKIN11 but does not phosphorylate bZIP63

(A) In vitro kinase assay with recombinant AKIN10 or AKIN11 and bZIP63 as a substrate in the presence of SnAK2. (B) Phos-tag gel western blot of an in vitro kinase assay with inactive AKIN10 (AKIN10 K/M), active AKIN10, or AKIN11 and bZIP63 as a substrate in the presence of SnAK2. An antibody recognizing the C-terminus of bZIP63 (α bZIP63) was used (see Figure 5 - figure supplement 1). (C) In vitro kinase assay with AKIN10 and/or SnAK2 and bZIP63 as a substrate showing the activity of AKIN10 in the presence or absence of SnAK2. The signal intensity from the bZIP63 phosphorylation is given in % of the strongest signal.

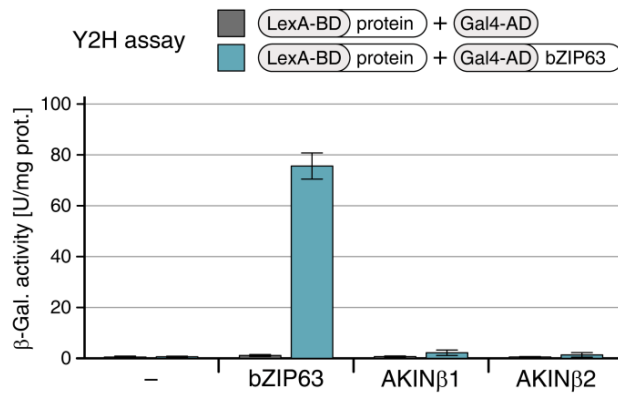


Figure 4 – figure supplement 2. AKINβ1 and AKINβ2 do not interact with bZIP63

Yeast 2-hybrid (Y2H) assay showing of AKINβ1 and AKINβ2 with bZIP63. Homodimerization of bZIP63 was used as a positive control. Autoactivation of BD-fusion proteins is shown in grey, interaction with bZIP63 in blue. Bars represent means \pm SD of 8 biological replicates.

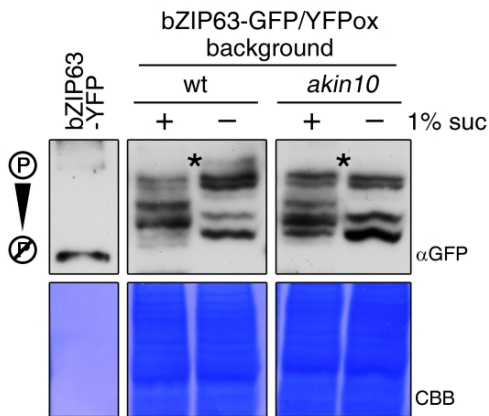


Figure 4 – figure supplement 3. Sugar-dependent in vivo phosphorylation of bZIP63 in seedlings

Phos-tag gel western (α GFP) blots showing the in vivo phosphorylation state of bZIP63 in plants expressing bZIP63-GFP/YFP in the wt or *akin10* background. Proteins were extracted from seedling cultures after 6h extended night in the presence (+) or absence (–) of 1% sucrose. Recombinant bZIP63-YFP was used as an unphosphorylated control. Asterisks mark the hyper-phosphorylated form of bZIP63.

CBB, Coomassie brilliant blue

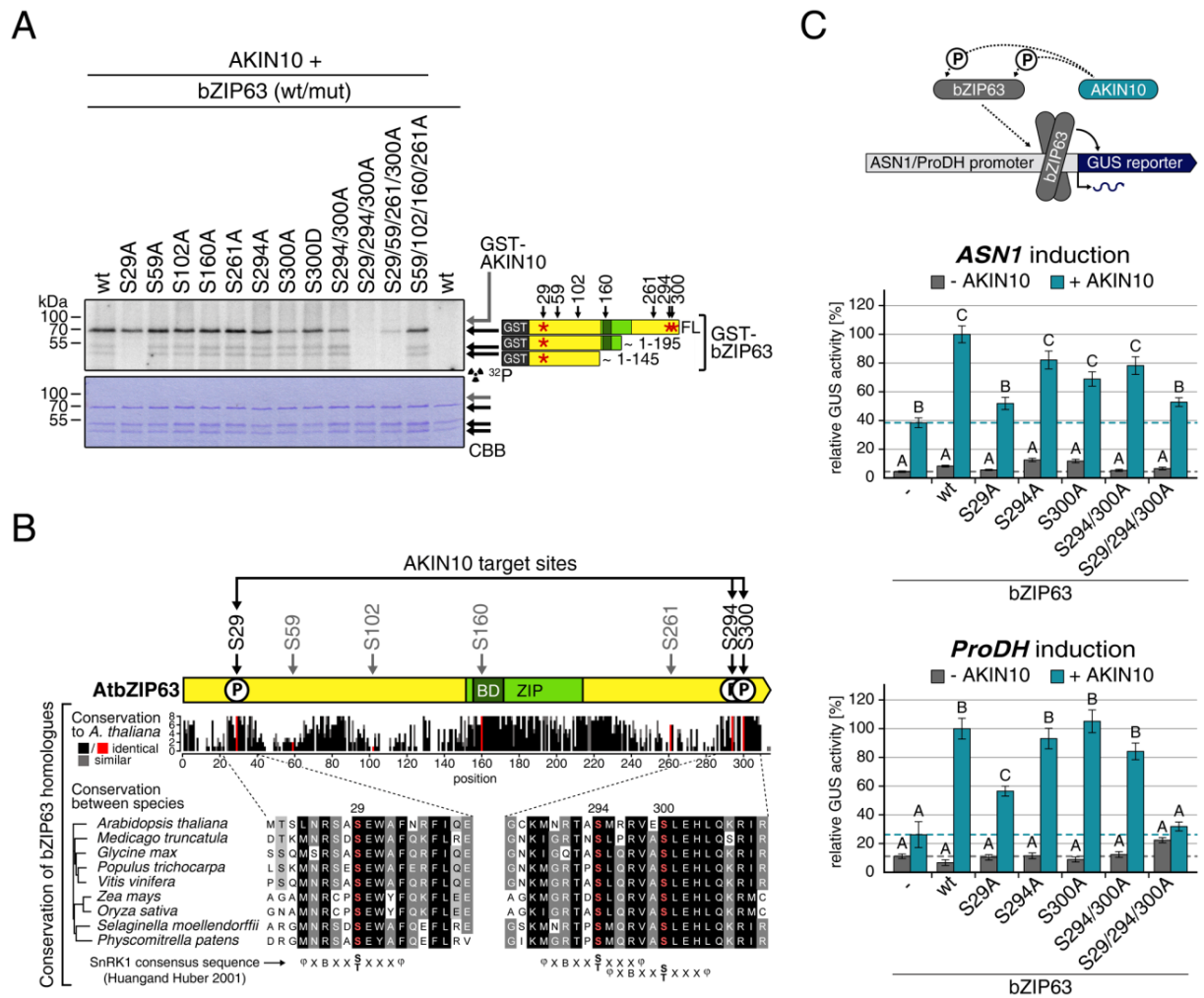


Figure 5. AKIN10 targets three highly conserved and functionally important serine residues in bZIP63

(A) In vitro kinase assay of wt and S/A mutants of GST-tagged bZIP63 with AKIN10. Positions of full length (FL) and N-terminal fragments of bZIP63 are marked by black arrows. The scheme on the right shows the position of the in vivo phosphorylation sites and the in vitro target sites of AKIN10 (red asterisk) on bZIP63. See Figure 5 – figure supplement 1 and 2 for controls and Phos-tag gel of kinase assays, respectively.

(B) Sequence conservation of bZIP63. Sequences of bZIP63 homologues from 8 species were aligned with ClustalΩ. The scheme on top indicates the positions of the in vivo phosphorylation and AKIN10 target sites on bZIP63. The histogram below shows the sequence identity (red/black) and similarity (grey) to *A. thaliana* bZIP63. Red bars represent the in vivo phosphorylation sites. Below, the alignment of the sequence surrounding the AKIN10 target sites and the SnRK1 consensus motif are shown. The

grey/black shading indicates the degree of conservation, phosphorylation sites are in red. For alignment of non-AKIN10 target sites and full sequence alignment see Figure 5 – figure supplement 3, for sequences in fasta format see Figure 5 – source data 1.

(C) Promoter activation assays in protoplasts with an ASN1/ProDH promoter-driven GUS reporter. Activation by bZIP63 wt and S/A mutants without (grey) or with (blue) co-transformation of AKIN10 is shown. Bars are means \pm SD of 4 biological replicates, given in % of the activity of wt bZIP63 with AKIN10. Horizontal dashed lines indicate the signal in the control without bZIP63. Letters indicate significant differences as determined by ANOVA and pairwise T-testing ($P < 0.05$). See Figure 5 – figure supplement 4 for a western blot control.

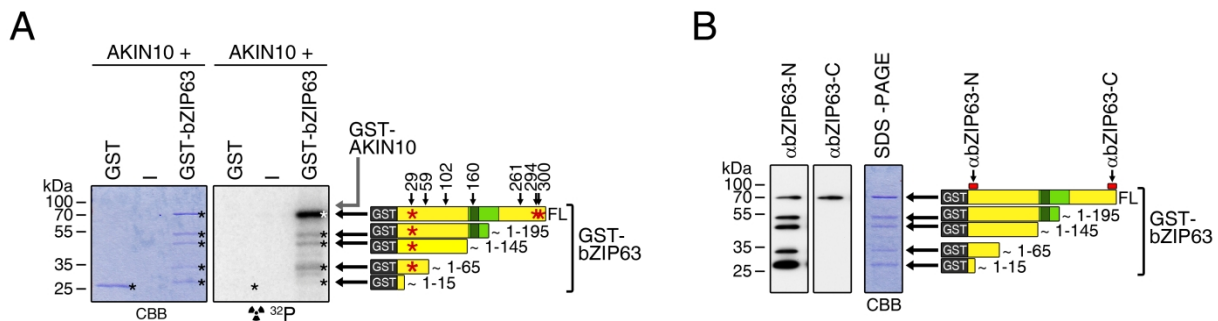


Figure 5 – figure supplement 1. AKIN10 phosphorylates bZIP63 but not GST

(A) In vitro kinase assay with recombinant AKIN10 and GST-tagged bZIP63 or GST as a substrate. Positions of full length (FL) and N-terminal fragments of bZIP63 are marked by black arrows. The scheme on the right shows the position of the in vivo phosphorylation sites and the in vitro target sites of AKIN10 (red asterisk) in GST-bZIP63, as well as the approximate length of the N-terminal fragments.

(B) Western blot (α bZIP63-N and -C) of GST-tagged bZIP63, used as substrate for the kinase assays. The scheme on the right indicates the binding sites of the two antibodies on bZIP63 and the approximate length of the detected fragments.

CBB, Coomassie brilliant blue

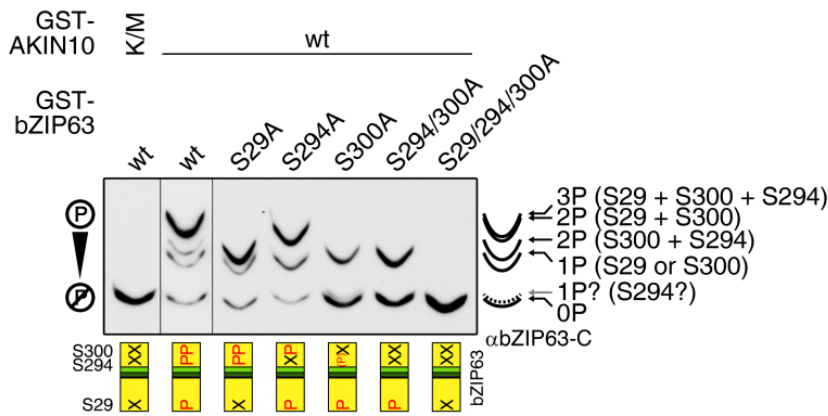


Figure 5 – figure supplement 2. AKIN10 phosphorylates S29, S294, and S300 on bZIP63

Phos-tag gel western blot (α bZIP63-C) of an in vitro kinase assay with active (wt) and inactive (K/M) AKIN10 and wt and S/A mutants of GST-tagged bZIP63 as substrate. The scheme on the bottom shows which of the three AKIN10 target sites can be phosphorylated (P) or are mutated (X). The scheme on the right indicates the likely phosphorylated sites for each band.

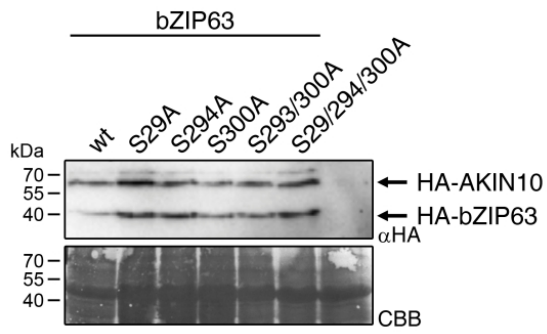


Figure 5 – figure supplement 4. Expression of bZIP63 and AKIN10 in the promoter activation assays

Exemplary western blot (α HA) of protoplasts co-transformed with *AKIN10* and wt or S/A mutants of *bZIP63*.

CBB, Coomassie brilliant blue

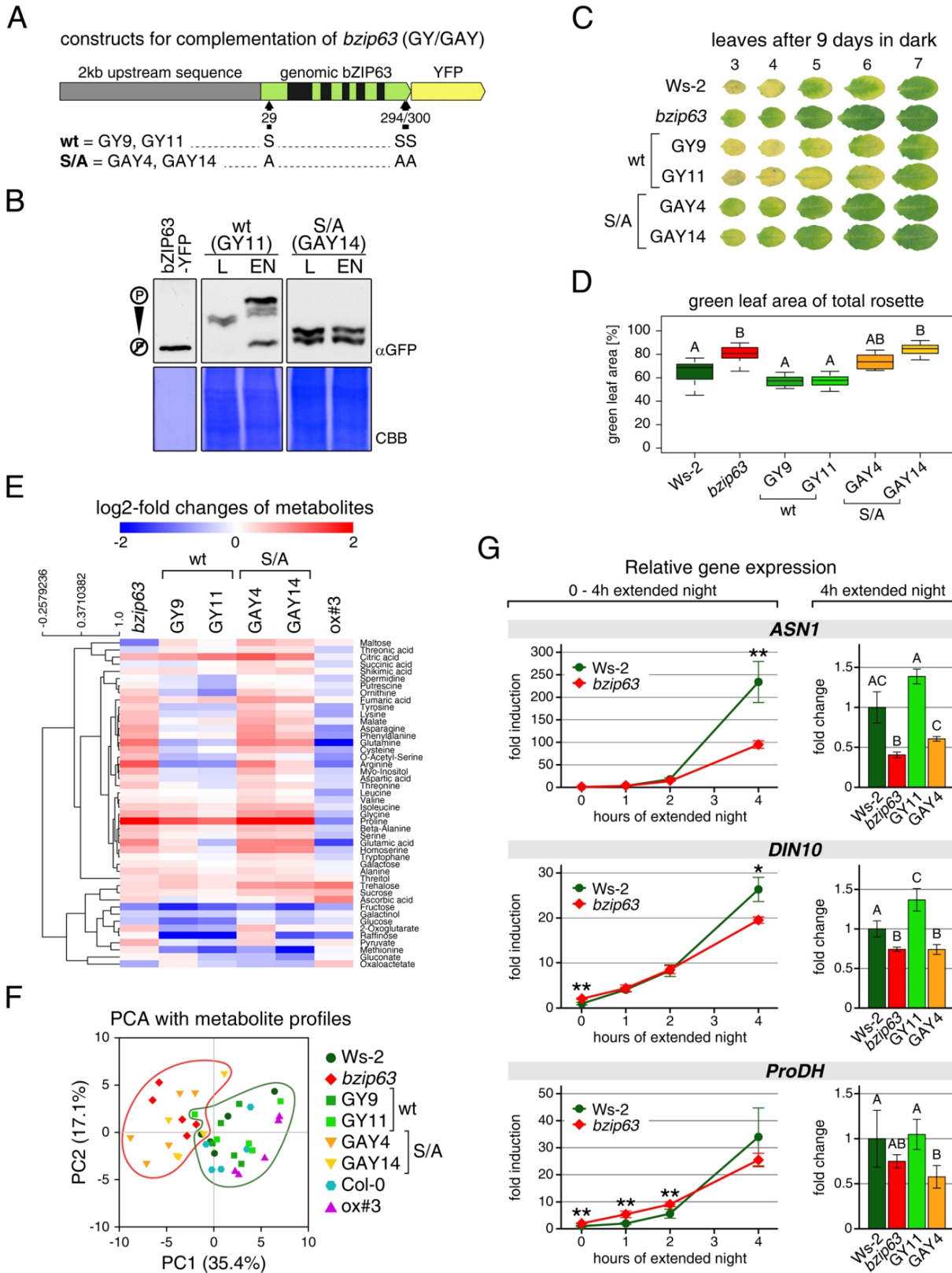


Figure 6. The *bzip63* phenotype can be complemented by wt bZIP63, but not by bZIP63 harboring S/A mutations of the AKIN10 target sites

(A) Genomic complementation constructs. Exons are green, introns black. See Figure 6 – figure supplement 1 for characterization of the complementation lines.

(B) Phos-tag gel western blots (α GFP) showing the in vivo phosphorylation state of bZIP63 in the complementation lines after 6h light (L) or extended night (EN) in 5 week-old soil-grown plants. Recombinant bZIP63-YFP was used as an unphosphorylated control.

(C) and **(D)** Dark-induced senescence phenotype of 4.5 week-old soil-grown plants after 9 days in darkness. **(C)** Leaves 3 – 7 of one representative plant per line. **(D)** Box-and-whiskers plot of the total green leaf area of 8 biological replicates. Letters indicate significant differences as determined by ANOVA and pairwise T-testing ($P < 0.05$). See Figure 6 – figure supplement 2 for untreated plants and green leaf area of individual leaves.

(E) and **(F)** Metabolite profile. **(E)** Hierarchical clustering of log-2 fold changes of metabolite concentrations compared to wt. Values are means of 5 biological replicates. **(F)** Principal component analysis (PCA). PC1 is plotted against PC2. The proportion of variance in % is indicated. The red line surrounds *bzip63* and GAY samples, the green line wt, GY, and ox#3 samples. For relative metabolite concentrations and PCA loading see Figure 6 – source data 1.

(G) Relative expression of potential bZIP63 target genes in 5 week-old plants during early extended night as determined by RT-qPCR. Values are means \pm SD of 4 biological replicates and are given as fold change compared to *Ws-2* at 0h (left) or 4h (right). P-values from T-tests < 0.05 and < 0.01 are indicated by * and **, respectively. Letters indicate significant differences as determined by ANOVA and pairwise T-testing ($P < 0.05$). CBB, coomassie brilliant blue

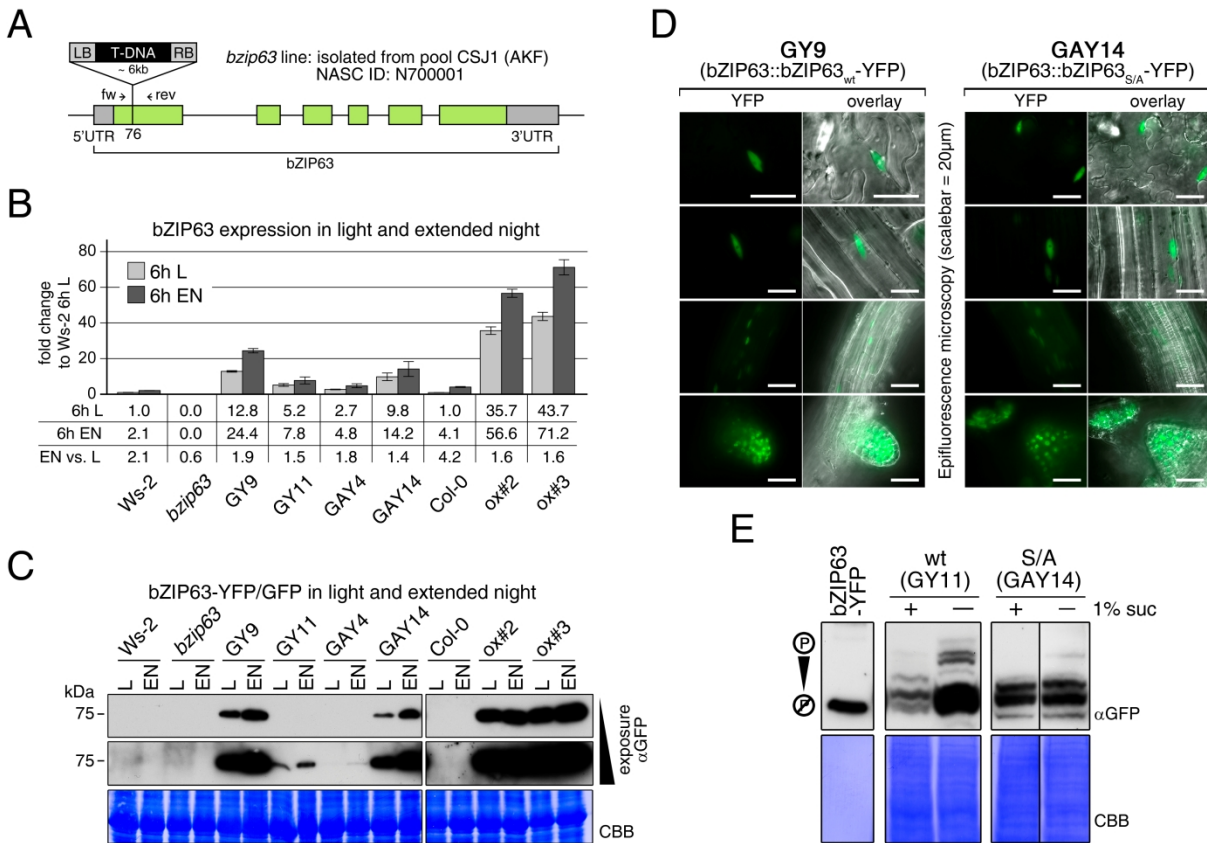


Figure 6 – figure supplement 1. Characterization of the *bzip63* complementation lines

(A) Scheme indicating the position of the T-DNA insertion in the *bzip63* line. The positions of the RT-qPCR primers used for (B) are shown.

(B) to (D) Expression of bZIP63 in different plant lines. (B) RT-qPCR of *bZIP63* in 5 week-old plants after 6h of light (L) or extended night (EN). Bars represent means \pm SD of 5 biological replicates and are given as fold change to Ws-2 in L. The table below gives numerical values of the fold changes and the ratio between EN and L. The 6h L samples were also used for the metabolic profiling shown in Figures 6E and F and Figure 6 – source data 1. (C) Western blot (α GFP) detecting GFP/YFP-tagged bZIP63 in transgenic plant lines after 6h of L and EN. (D) Epifluorescence microscopy images of soil-grown seedlings of the GY9 and GAY14 lines showing expression of bZIP63-YFP. From top to bottom: leaf epidermis, leaf veins, roots, lateral root tips. Scale bar is 20µm.

(E) Phos-tag gel western blots (GFP) showing the *in vivo* phosphorylation state of bZIP63 in the complementation lines. Proteins were extracted from seedling cultures after 6h extended night in the presence (+) or absence (-) of 1% sucrose. Recombinant bZIP63-YFP was used as an unphosphorylated control.

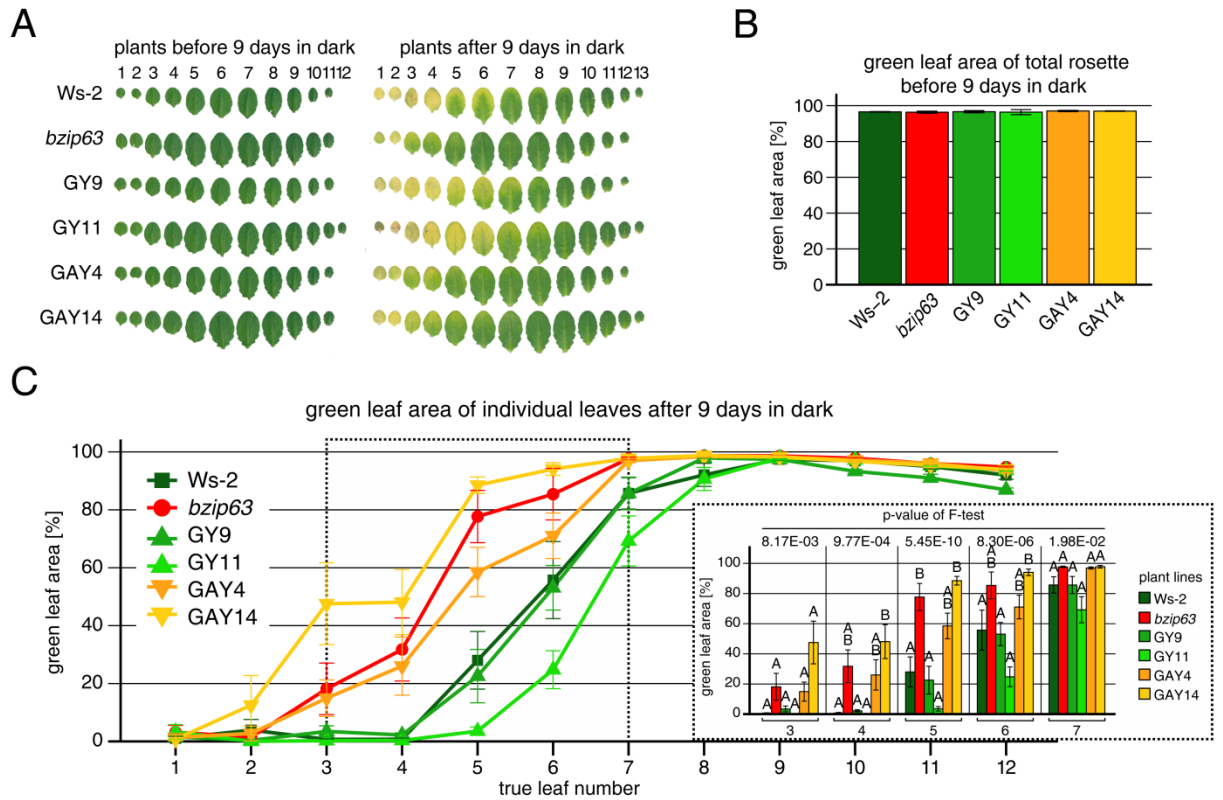


Figure 6 – figure supplement 2. Complementations of the dark-induced senescence phenotype of *bzip63*

(A) Representative leaf series of 4.5 week-old plants before and after 9 days in darkness.

(B) Barplot of the total green leaf area of the rosette before darkness. Values are the mean \pm SD of 4 biological replicates.

(C) Dotplot of the green leaf area of individual leaves after 9 days in darkness. Values are the mean \pm SD of 8 biological replicates. The insertion at the right side shows the values from leaves 3 – 7 as a barplot (framed by dotted line). Letters indicate significant differences as determined by ANOVA and pairwise T-testing ($P < 0.05$). The p-values of the F-test for each leaf are given.

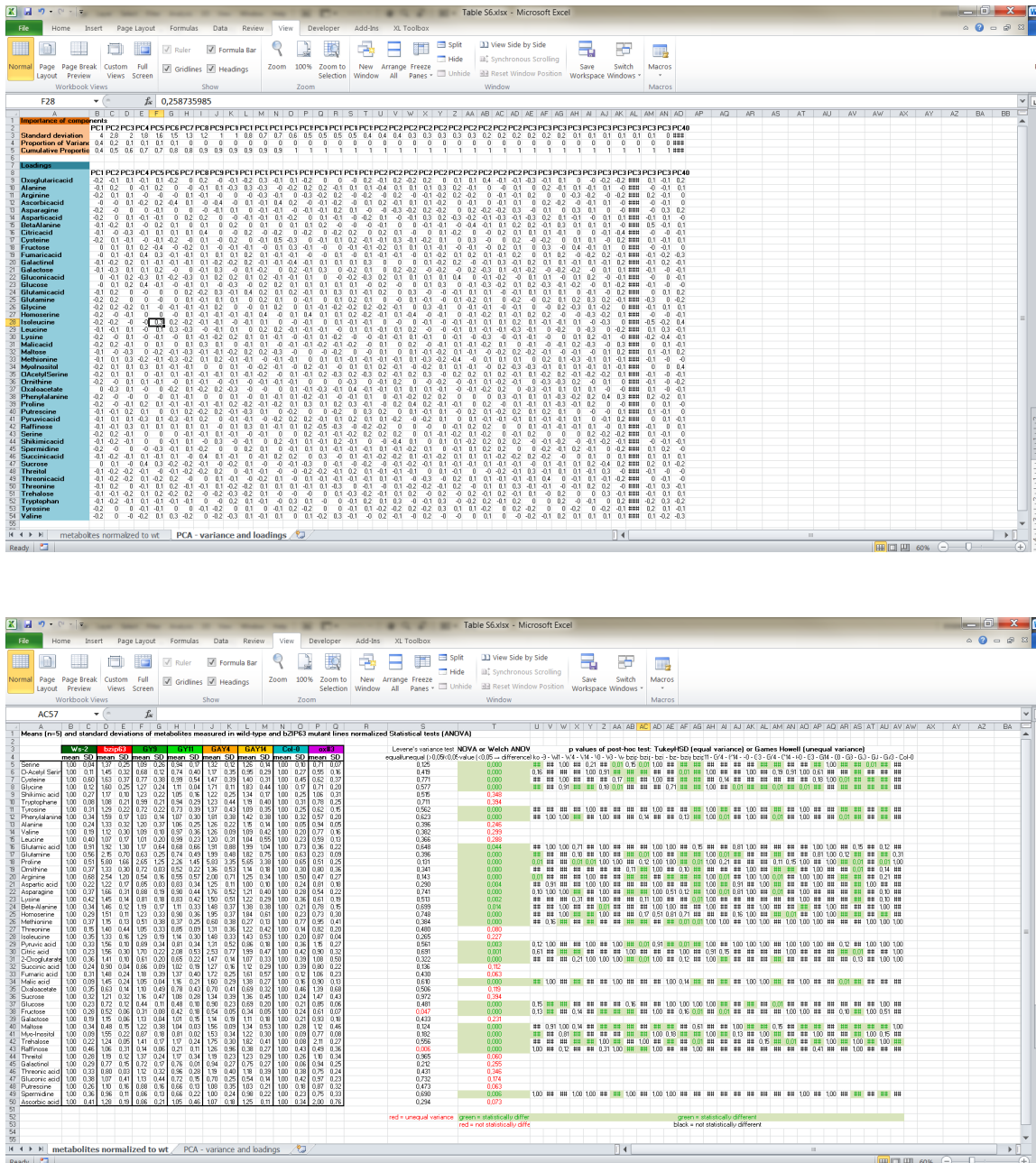


Figure 6 – source data 1. Excel table containing the relative metabolite levels of the complementation lines and the PCA loadings

The tab “metabolites normalized to wt” contains the relative metabolite levels, which were used to calculate the fold changes shown in Figure 6E, as well as P-values from statistical tests. Values are the mean \pm SD of 5 biological replicates given as fold change to the corresponding wt. The tab “PCA - variance and loadings” contains the SD, proportion of variance, and loadings of all principal components from the PCA analysis shown in Figure 6F.

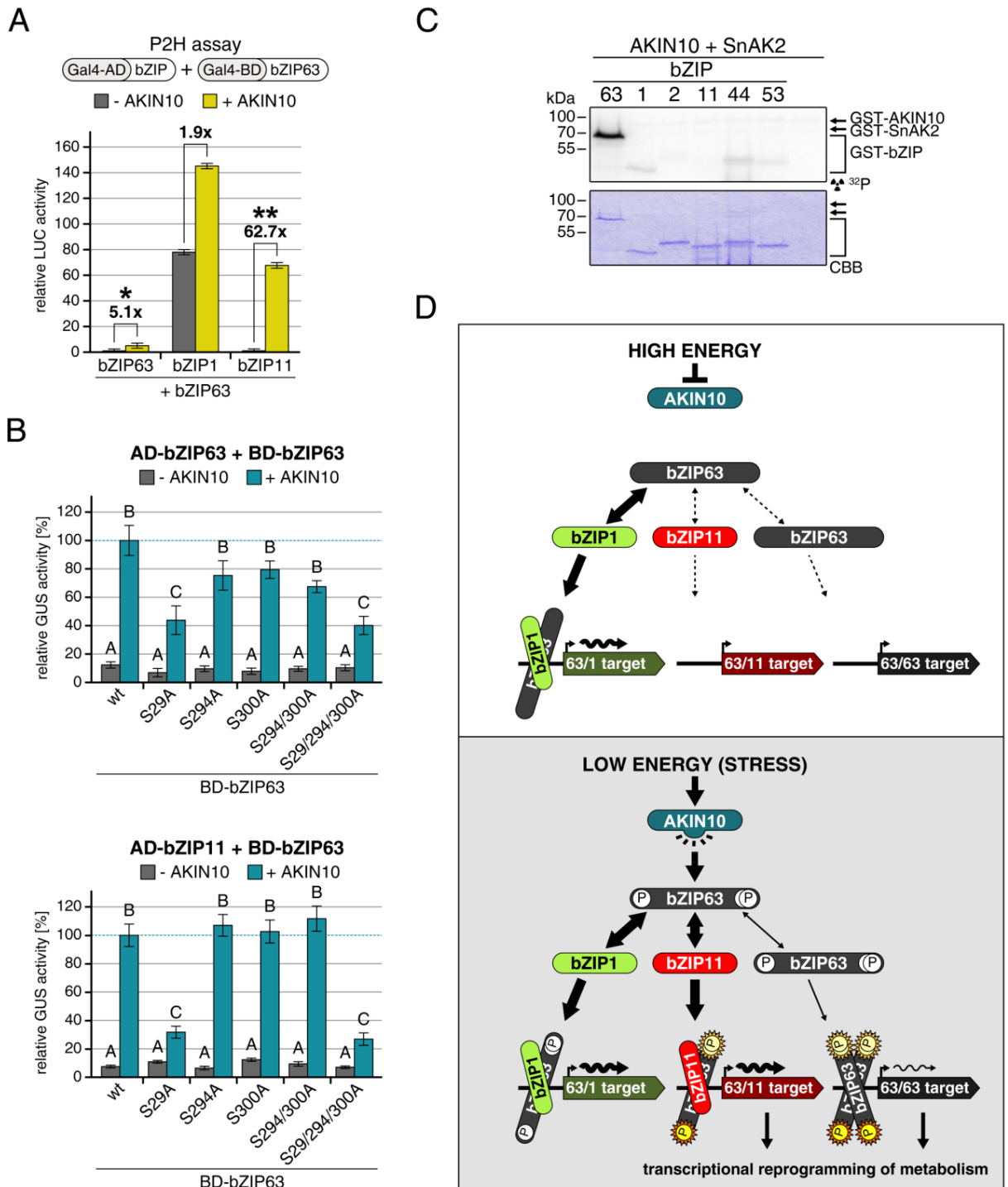


Figure 7. AKIN10-mediated phosphorylation of bZIP63 affects its dimerization with other bZIPs differentially

(A) and (B) Protoplast 2-hybrid (P2H) assays. Bars represent means \pm SD of 4 biological replicates. (A) Interaction of bZIP63 with bZIP63, 1, and 11 without (grey) or with (yellow) co-transformation of AKIN10. Values are normalized to bZIP63-bZIP63

interaction without AKIN10. Numbers above the bars indicate fold induction. P-values from T-tests < 0.05 and < 0.01 are indicated by * and **, respectively.

(B) Interaction of bZIP63 (top) or bZIP11 (bottom) with wt and S/A mutants of bZIP63 without (grey) or with (yellow) co-transformation of AKIN10. Values are given in % of the signal with wt bZIP63 and AKIN10. Letters indicate significant differences as determined by ANOVA and pairwise T-testing ($P < 0.05$). For controls see Figure 7 – figure supplement 1.

(C) In vitro kinase assay of bZIP63, 1, 2, 11, 44, and 53 with AKIN10 and the SnRK1 upstream kinase SnAK2. For a kinase assay with the bZIPs and SnAK2 see Figure 7 – figure supplement 2.

(D) Simplified model of the regulation of bZIP63 activity by AKIN10.

CBB, coomassie brilliant blue

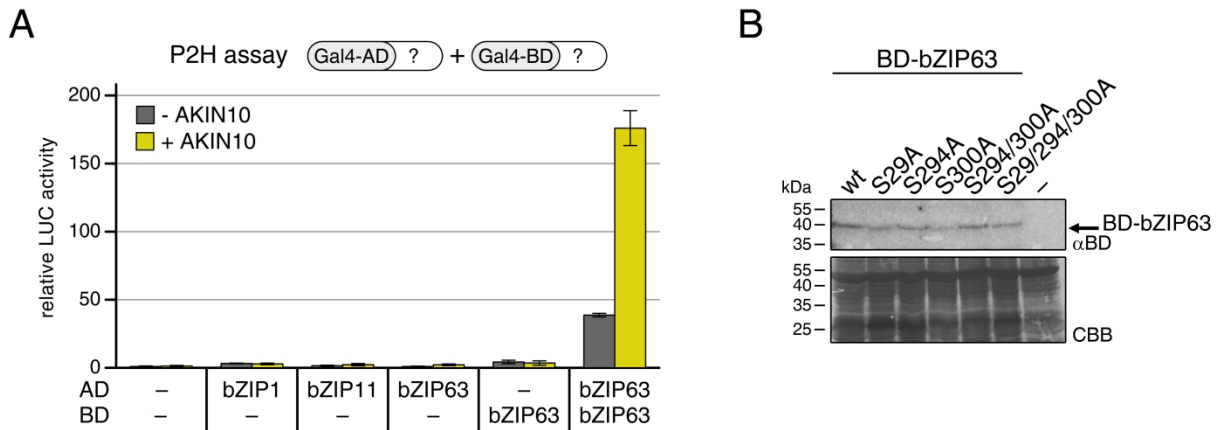


Figure 7 – figure supplement 1. Protoplast 2-hybrid (P2H) controls

(A) Barplot showing the lack of autoactivation of the constructs used for the P2H in Figure 7A. Homodimerization of bZIP63 was used as a positive control. **(B)** Exemplary western blot (α BD) showing the expression of BD (DNA binding domain)-bZIP63 in the P2H assays in Figure 7B.

CBB, Coomassie brilliant blue

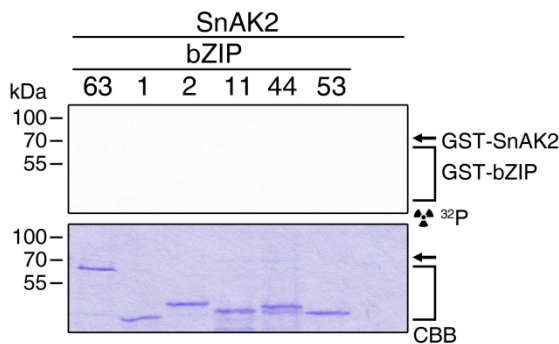


Figure 7 – figure supplement 2. SnAK2 does not phosphorylate bZIP63 or the S1 class bZIPs

In vitro kinase assay of bZIP63, 1, 2, 11, 44, and 53 with SnAK2.

Chapter 4: Stress-triggered reprogramming of mitochondrial metabolism via SnRK1-bZIP complex.

Lorenzo Pedrotti¹, Christoph Weiste¹, Thomas Nägele², Elmar Wolf³, Francesca Lorenzin³, Katrin Dietrich¹, Andrea Mair², Markus Teige², Wolfram Weckwerth², Elena Báena-Gonzalez⁴, and Wolfgang Dröge-Laser¹

Authors affiliation.

¹Department of Pharmaceutical Biology, Julius-von-Sachs-Institut, Julius-Maximilians-Universität Würzburg, Würzburg, 97082, Germany;

²Department of Ecogenomics and Systems Biology, University of Vienna, Vienna, 1090, Austria;

³Department of Biochemistry and Molecular Biology, Theodor Boveri Institut, Biocenter, Julius-Maximilians-Universität Würzburg, Würzburg, 97074, Germany;

⁴Instituto Gulbenkian de Ciência, Oeiras, 2780-156, Portugal

*Contact information: wolfgang.droege-laser@uni-wuerzburg.de

ABSTRACT

Sustaining energy homeostasis is of pivotal importance for all living organisms. Evolutionary conserved kinases related to yeast Snf1 and mammalian AMPK control metabolic adaptation to low energy stress. Transcriptome studies reveal that *Arabidopsis* Snf1-RELATED KINASE1 (SnRK1) controls thousands of starvation-related genes and that a subset is executed by downstream group-S1 basic leucine Zipper (bZIP) transcription factors. S1-bZIPs control amino acid catabolism, functioning as an essential alternative respiratory pathway to support mitochondrial electron transport upon starvation. Prototypic studies on *ETFQO*, a central target gene in this process gained insight into the mechanistic link between SnRK1 activity and transcription: SnRK1-mediated phosphorylation of group C-bZIPs initiates bZIP-heterodimerisation by forming a ternary SnRK1-C/S1-bZIP complex which directly binds the *ETFQO* promoter. Subsequently, complex-mediated recruitment of the histone acetylation machinery facilitates transcription. Taken together, this work reveals a molecular mechanism by which energy deprivation in plants is transduced to reprogram expression and ultimately drives metabolic adaptation.

INTRODUCTION

Mitochondrial respiration provides most of the cellular energy to eukaryotic organisms. For this process, sugars are the predominant substrates that are therefore stored to ensure constant energy supply. In photosynthetic organisms like plants, this storage function is carried out by starch, providing resources during the night (for review see Stitt and Zeeman, 2012). Under stress conditions, organisms exhibit a strong increased energy demand to enable adaptive responses. The cell could therefore face a situation of energy deprivation (for review see Baena-González 2010; Tome et al., 2014). Hence, it is of critical importance to precisely match the cellular energy supply and demand. Recent studies propose a relationship between energy availability and stress tolerance, survival, cell growth and longevity. In line with these findings, energy-deficiency signaling in plants is proposed to trigger convergent responses independently of the origin of its causes (Baena-González and Sheen, 2008; Tome et al., 2014; Yao et al., 2015)

The plant central regulatory kinase SnRK1 (Snf1-RELATED KINASE1), and its homologs AMPK (AMP-ACTIVATED PROTEIN KINASE) in mammals and Snf1 (SUCROSE-NON-FERMENTING1) in yeast have emerged to link growth and development to nutrients and energy availability (Hardie, 2007, 2015; Polge and Thomas, 2007; Robaglia et al., 2012; Sheen, 2008; Tome et al., 2014). Although the sensing of metabolic signals by SnRK1 is not well-understood (Crozet et al., 2014), this kinase is proposed to support cellular function during stress such as oxygen-limitation upon flooding, as well as aspects of plant developing such as vegetative-to-reproductive phase transitions (Baena-Gonzalez et al., 2007; Tsai and Gazzarrini, 2012). The principal processes activated by SnRK1-homologs are major catabolic pathways related to carbohydrate and amino acids (aa) metabolism, or autophagy. Opposite, a large set of energy-consuming processes are repressed, such as ribosome biogenesis and protein translation (Baena-Gonzalez et al., 2007; Hardie, 2015). Supporting the major function in energy homeostasis, SnRK1 regulated genes were found to be positively correlated with stress and starvation genes or negatively correlated with genes activated by sucrose or glucose (Baena-González and Sheen, 2008).

Functional SnRK1/AMPK/Snf1 consist of three evolutionary conserved subunits (Polge and Thomas, 2007). In *Arabidopsis thaliana*, the catalytic α -subunit is encoded by a small gene family of three members, namely SnRK1.1 (AKIN10), SnRK1.2 (AKIN11), and

SnRK1.3 (AKIN13). Whereas the latter is hardly expressed, the others possess partially redundant function, although they differ considerably in their expression profiles (Baena-Gonzalez et al., 2007; Williams et al., 2014). A stable double mutant in SnRK1.1 and SnRK1.2 appears to be lethal (Baena-Gonzalez et al., 2007).

SnRK1 controls energy metabolism through direct regulation of enzymes, transcription factors (TFs) and miRNAs (Confraria et al., 2013; Hardie, 2015; Sheen, 2014). Although several plant TF targets of SnRK1 have been proposed, detailed regulatory mechanisms remain elusive. Basic leucine Zipper (bZIP) TFs of the group S1 (bZIP1, bZIP2, bZIP11, bZIP44, and bZIP53; Jakoby et al., 2002) are likely targets of SnRK1s (Baena-Gonzalez et al., 2007; Ma et al., 2011). Indeed, S1-bZIPs have been shown to play an important role in transcriptional reprogramming of sugar and nitrogen metabolism in response to stress, growth and hormonal control as well as development aspects such as seed maturation (Alonso et al., 2009; Baena-Gonzalez et al., 2007; Dietrich et al., 2011; Hanson et al., 2008; Kang et al., 2010; Ma et al., 2011; Obertello et al., 2010; Para et al., 2014; Weiste and Dröge-Laser, 2014). (bZIP1, bZIP2, bZIP11, bZIP44, and bZIP53). Moreover, important dark-induced (DIN) genes, such as *ASPARAGIN SYNTHETASE*, (*ASN1*, *DIN6*) have been demonstrated to be directly regulated by S1-bZIPs via G-box *cis*-elements (Baena-Gonzalez et al., 2007; Dietrich et al., 2011; Ma et al., 2011). Finally, these TFs are controlled transcriptionally and post-transcriptionally by sugar, proposing that their regulation is highly correlated with the energy status of the cell (Dietrich et al., 2011; Kang et al., 2010; Weltmeier et al., 2009; Wiese et al., 2004).

S1-bZIPs preferentially form heterodimers with group C bZIPs (C-bZIPs: bZIP9, bZIP10, bZIP25, and bZIP63) (Ehlert et al., 2006; Weltmeier et al., 2006). In particular, bZIP63 has been implicated in controlling gene expression in response to starvation (Dietrich et al., 2011; Kang et al., 2010; Kunz et al., 2014; Matioli et al., 2011). Recently, bZIP63 was identified as the first *in vivo* TF target of SnRK1, leading to specific phosphorylation of three bZIP63 Ser-residues (Mair et al. Chapter 3). Strikingly, this bZIP63 phosphorylation enhances formation of C/S1 heterodimers, disclosing an important regulatory mechanism in gene expression. Taken together, these findings support a cooperative function of the C/S1 bZIP network in plant low energy management.

In this study we devised a combinatorial strategy of chemical, genetics, genomics, and cell-based analyses to dissect the SnRK1-C/S1-signaling network in response to extended

darkness, which is mimicking low energy stress in plants. We clearly show a significant overlap between the genome-wide transcriptional responses exerted by SnRK1 and S1-bZIPs supporting the view, that S1-bZIPs act downstream of SnRK1. Strikingly, both regulators control the expression of genes involved in an alternative respiratory pathways feeding electrons into the mitochondrial electron transport chain to support respiration under carbohydrate limiting conditions. Stress-triggered adjustment of energy homeostasis by inducing alternative respiratory pathways was determined as a key process to assure survival under stress. Making use of *ELECTRON-TRANSFER FLAVOPROTEIN: UBIQUINONE OXIDOREDUCTASE (ETFQO)*, an essential target gene in this process, we discovered that SnRK1 and C/S1 heterodimers form a ternary complex that binds directly to the *ETFQO* promoter and is responsible for subsequent histone acetylation and transcriptional activation. Taken together, the data presented here provide a mechanistic model linking SnRK1 mediated low energy signaling to gene regulation and cellular adaptation.

RESULTS

SnRK1 and S1-bZIPs control shared and distinct sets of genes in response to extended darkness

Previous work suggested S1-bZIPs as mediator of the transcriptional response driven by SnRK1 upon energy deprivation (Baena-Gonzalez et al., 2007). To investigate the SnRK1/S1-bZIP signaling network, we performed genome-wide expression profiling of wild-type (WT), *snrk1.1/1.2* and *bzipS1* mutant. Due to their proposed function in low energy signaling, starvation conditions were mimicked by 6 h of extended darkness (Usadel et al., 2008).

As constitutive *snrk1.1/1.2* double mutants are lethal (Baena-Gonzalez et al., 2007), we generated a *snrk1.1* mutant transformed with a β -estradiol (Est) inducible artificial-micro (ami)RNA, which specifically targets *snrk1.2*. S1-bZIPs have been characterized to support partially redundant functions (Alonso et al., 2009; Dietrich et al., 2011; Weltmeier et al., 2009). Hence, a multiple loss-of-function approach is required, which is targeting all five members of this sub-group. Accordingly, *bzipS1* was obtained by transforming a *bzip1/bzip53* T-DNA insertion mutant with an Est-inducible *amibZIP2/11/44* construct (Weiste and Dröge-Laser, 2014). Molecular characterization of these plant lines is provided in Figure S1A-E.

In comparison to WT, RNA sequencing (RNAseq) experiments performed with *snrk1.1/1.2* plants showed a strong impairment in transcriptional responses to extended darkness. Applying a filters (p.adjust < 0.01; log (fold change) logFC > 2), overall 2717 or 747 genes were differentially up- and down-regulated, respectively (Figure 1C, D, and Table S1). Processes controlled by SnRK1.1 and SnRK1.2 (Figure S1F-H) were similar to those previously identified by overexpression of SnRK1.1 in *Arabidopsis* protoplasts (Baena-González et al., 2007) . E.g. the *snrk1.1/1.2* mutant was unable, neither to induce the catabolic pathways providing alternative sources of energy, nor to repress highly energy demanding anabolic processes, such as ribonucleoprotein complex biogenesis (Figure S1F and Table S1).

The impact of S1-bZIPs on gene expression in response to extended darkness was of smaller entities. In particular, 92% of the differentially expressed genes (DEG) showed only minor changes between $\log_{2}FC \geq 2$ (Figure 1B). This finding may be explained due to the residual presence of bZIP2, bZIP11, and bZIP44 in the *bzipS1* plants, as the use of Est inducible amiRNA leads only to a reduction in bZIP expression (Figure S1B). Hence for the subsequent analyses, we did not apply any filter based on FC magnitude. . In comparison to WT, overall 307 genes were up- and 195 down-regulated in the in the *bzipS1* mutant (Figure 1C and D, Table S1).

Among the DEGs, 293 were regulated by both SnRK1s and S1-bZIPs. Despite the massive transcriptional reprogramming driven by SnRK1.1/1.2, 209 genes (67 down- and 142 up-regulated) were specifically de-regulated only in the *bzipS1* mutant, indicating that not only SnRK1 signaling is converging on S1-bZIPs. Compared to publicly available microarray data from WT plants exposed to extended darkness, the majority of genes de-regulated in both *snrk1.1/1.2* and *bzipS1* exhibited oppositional expression characteristics (Figure S1G-H). Precisely, 86% of genes induced by extended dark treatment in WT plants were down-regulated in *snrk1.1/1.2* and *bzipS1* mutant . GO (Gene ontology) annotation of biological processes of shared DEGs showed an enrichment in anabolic processes with respect to up-regulated genes and an over-representation of catabolic processes for down-regulated genes (Figure 1E-1F and S1F).

Metabolic studies on *snrk1.1/1.2* and *bzipS1* mutants revealed shared alterations in primary metabolism

In line with the transcriptome studies, metabolic analyses revealed that SnRK1 and S1-

bZIPs support adaptation processes towards energy deprivation. Primary leaf metabolites of WT, *snrk1.1/1.2* and *bzipS1* mutants displayed significant changes in sugar metabolism, Tricarboxylic Acid (TCA) cycle intermediates, aa and polyamines (Figure. 1 G-H, and Table S1). In comparison to WT, levels of sucrose and citrate were found to be reduced more than 2-fold in the *snrk1.1/1.2* mutant. Simultaneously, levels of other TCA cycle intermediates as well as TCA cycle related aa increased significantly. A strong overlap in metabolic changes between both mutants was found for the pools of myo-inositol and leucine.

Comparing metabolite levels of *bzipS1* to the WT, the observed changes were found to be similar to those of the *snrk1.1/1.2* plants: disaccharide levels decreased, while monosaccharides, myo-inositol and leucine increased. Nevertheless, there were almost no changes observed in TCA cycle intermediates in *bzipS1* plants. Taken together, both transcriptome and metabolome data support the view, that S1-bZIPs may execute a well-defined subset of the SnRK1 responses.

Expression of genes involved in leucine degradation are tightly regulated by SnRK1 and S1-bZIPs

As aa metabolism serves as an alternative energy resource upon starvation (for review see Araújo et al., 2011), the GO category “amino acid metabolic process” was of particular interest to us. RT-qPCR (Real-Time-quantitative-PCR) analysis revealed that the expression of several genes involved in the degradation of branched chain aa (BCAA) depends on both SnRK1 and S1-bZIPs (Figure 2A). Within 6h of exposition to extended dark, transcription of *BRANCHED CHAIN TRANSAMINASE2 (BCAT2)*, *ELECTRON-TRANSFER FLAVOPROTEIN:UBIQUINONE OXIDOREDUCTASE (ETFQO)*, *METHYLCROTONYL COA CARBOXYLASE (MCCA and MCCB)* was strongly induced in WT plants, whereas their expression was significantly reduced in *snrk1.1/1.2* and *bzipS1* mutants (Figure 2B-E). Among the enzymes involved in leucine degradation, ETFQO is of particular importance for the overall metabolic regulation as it encodes for an unique protein, feeding electrons into the mitochondrial electron transport chain. Making use of alternative substrates other than glucose, this essential pathway is supporting respiration under low energy stress, both in plants as in mammals (Araújo et al., 2010, 2011; Ishizaki et al., 2005, 2006; Watmough and Frerman, 2010).

SnRK1 and S1-bZIPs regulate mitochondrial metabolism via the electron transfer

protein ETFQO

To study the functional connection between SnRK1, S1-bZIPs and energy metabolism, we focused on the *ETFQO* gene. Indeed, *etfqo* mutants have already been described to be impaired in an adequate response to extended dark treatment and display an early senescence phenotype as demonstrated in Figure 3 (Ishizaki et al., 2005).

To quantify plant survival under low energy stress, chlorophyll content was used as an easy-to-measure marker (Baena-Gonzalez et al., 2007; Ishizaki et al., 2005). In our growth condition, no visible difference could be observed between *snrk1*, *bzipS1* and *etfqo* mutants when compared to WT plants (Figure 3A). However, exposition of *snrk1*, *bzipS1* and *etfqo* plants to 6 days of extended dark, resulted in significant reduction of chlorophyll in all plant lines tested (Figure 3B). Nevertheless, WT plants could cope better with extended dark treatment. Application of 2% glucose reverted the loss of chlorophyll content in all tested genotypes exposed to extended dark, indicating that glucose was used as primary carbon source and can be supplemented by addition to the growth medium. To connect the mutant phenotypes with a non-functional mitochondrial electron transport chain, we applied the inhibitor Antimycin-A (AMA) (Figure 3C). AMA treatment together with extended darkness results in a lower chlorophyll content as in light-grown plants. External application of glucose reverted this loss of chlorophyll content, even though mitochondrial electron transport chain was non-functional. Presumably, the fermentation pathway provides alternative sources of energy to support plant metabolism. Interestingly, when we used the ALCOHOL DEHYDROGENASE (ADH) inhibitor 4-methylpyrazole (4-MP) to block fermentation, we observed that external glucose, which prevented chlorophyll degradation in WT plants does not result in enhanced chlorophyll levels in *snrk1*, *bzipS1* and *etfqo* mutants (Figure 3D). Based on this evidence we assumed that the *snrk1*, *bzipS1* and *etfqo* mutants do not rely on a functional mitochondrial electron transport chain and that the external glucose has been assimilated via the fermentation pathway. Consequently, treatment of WT plants with AMA and 4-MP under extended dark conditions, indeed, resulted in low chlorophyll content, similarly to *snrk1*, *bzipS1* and *etfqo* mutants (Figure 3E). Taken together, these data support the view that SnRK1 and S1-bZIPs control the essential ETFQO-dependent pathway to exploit alternative resources under energy limiting conditions.

The *ETFQO* promoter is directly regulated by S1- and C-bZIPs

Based on the transcriptome analysis the *ETFQO* gene is perfectly suited to study the mechanistic connection between SnRK1, S1-bZIPs, and mitochondrial-dependent energy metabolism. The expression of *ETFQO* was only slightly altered in single or double S1-bZIPs mutants, although strongly impaired in the *bzipS1* background (Figure S2A). Presumably, this finding is attributed to functional redundancy between S1- and C-bZIPs, as it has already been described for other target genes. Protoplast transactivation assays using an *ETFQO* promoter-driven GUS reporter ($\text{Pro}_{\text{ETFQO}}:\text{GUS}$), demonstrate that in fact overexpression of any of the five S1-bZIPs activates the reporter expression, however with varying intensities (Figure 4A). Interestingly also *SnRK1.1* co-expression induces the *ETFQO* promoter and boosts the activation potential, in particular of bZIP1, bZIP2, and bZIP44. These results are in line with the observation that overexpression of SnRK1.1 in protoplasts is sufficient to mimic energy- deprived conditions (Baena-Gonzalez et al., 2007). Similar results have been confirmed by RT-qPCR (Figure S2B). Again, bZIP1, -2 and -44 show a stronger activation of *ETFQO* expression than bZIP11 or -53. As S1-bZIPs form heterodimers with C-bZIPs (Ehlert et al., 2006), we also tested their ability to regulate *ETFQO* expression. Indeed, bZIP9, -10 and bZIP63 are able to induce the activation of $\text{Pro}_{\text{ETFQO}}:\text{GUS}$ in a SnRK1.1-dependent manner (Figure 4B). Moreover, protoplast-2-hybrid (P2H) assays confirm, that heterodimerisation between bZIP2 and bZIP9, bZIP25, as well as bZIP63 are enhanced by co-expression of SnRK1.1 (Figure S3C).

C/S1-bZIPs preferentially bind to G-boxes (GACGTC) and ACGT-core sequences (Kang et al., 2010; Kirchler et al., 2010). Analysis of the *ETFQO* promoter revealed the presence of a G-box like motif at – 125 bp (G1), a G-box-core motif at – 450 bp (G2) and two other G-box motives adjacent to each other around - 900 bp (G3 and G4) relative to the translational start site (Figure 4C). Chromatin immuno-precipitation coupled to PCR (ChIP_{PCR}) demonstrates that bZIP1, bZIP2, and bZIP44 directly bind to the *ETFQO* promoter (Figure S3D) and that their recruitment is enhanced by co-expression of SnRK1.1. bZIP53 and bZIP11 bind the same sites, although with minor affinity. As TFs, when overexpressed tend to bind to less specific binding sites (Walz et al., 2014), this could explain why all five S1-bZIPs bound to the *ETFQO* promoter in our experiments. Despite the ability of all S1-bZIPs to activate the expression of *ETFQO*, bZIP2 alone and in co-operation with SnRK1.1 shows the strongest activation potential. Hence, promoter

scanning ChIP experiments were performed to fine-map bZIP2 binding to the *ETFQO* promoter. This analysis confirms binding of bZIP2 to the promoter, precisely at the G1 and G3-4 sites (Figure 4D). In fact, the integrity of these binding motives was necessary for the activation of the Pro_{*ETFQO*}:GUS reporter (Figure 4F). Moreover, bZIP63 has also been observed to occupy the *ETFQO* promoter at the same sides as bZIP2 (Figure 4E). These findings are supported by a mutational approach targeting the G-boxes in the *ETFQO* promoter. Indeed, the integrity of the G1, G3 and G4 binding motives was necessary for the activation of the Pro_{*ETFQO*}:GUS reporter by both, bZIP2 and SnRK1 (Figure 4F). As the dimerization between bZIP2 and bZIP63 is induced by co-expression of SnRK1.1 (Figure S3D) and as they occupy the same sites on the *ETFQO* promoter, we conclude that these bZIPs probably bind as heterodimers at the respective sites. Nevertheless, we cannot exclude a more complex dimer occupancy pattern on the three *ETFQO* promoter binding sites.

SnRK1.1, bZIP2, and bZIP63 form a ternary complex which mediates SnRK1.1 recruitment to the *ETFQO* promoter

Although S1-bZIPs were found to be essential for the SnRK1 dependent expression of *ETFQO*, they are not directly phosphorylated by SnRK1.1 (Mair et al., Chapter 3). Using a P2H approach, we demonstrate that interaction of bZIP2 and bZIP63 is promoted when SnRK1.1 is co-expressed (Figure 5A). Moreover, the interaction between bZIP63 and SnRK1.1 is also stronger in the presence of bZIP2. Surprisingly, we observed an interaction between bZIP2 and SnRK1.1 however, only when bZIP63 was co-expressed. Most-likely, this protein interaction is mediated by bZIP63 forming a ternary complex. It has recently been reported, that bZIP63 is directly phosphorylated by SnRK1.1 (Mair et al., Chapter 3). Indeed, dimerization between bZIP63 and bZIP2 is abolished when a mutated version of bZIP63 (*bZIP63ala*) is assayed in a P2H approach (Figure 5B). This bZIP63 mutant harbors Ser to Ala exchanges in those aa (S29/S294/S300) which have been identified as SnRK1.1-specific *in vivo* phosphorylation sites. .

Similarly to the already described dimer between bZIP63 and bZIP11 (Mair et al., *in preparation*), also the dimerization between bZIP63 and bZIP2 depended on the SnRK1.1 phosphorylation of bZIP63, as their interaction was abolished when a mutated version of bZIP63 (*bZIP63ala*: Ser-Ala exchange of SnRK1.1 specific phosphorylation sites, Mair et al.) was used (Figure 5B). Moreover, ChIP_{PCR} experiments demonstrate, that the integrity

of the SnRK1.1 phosphorylation sites within the bZIP63 protein is indispensable for its recruitment to the *ETFQO* promoter (Figure 5C). Taken together, it is tempting to speculate that formation of a stable ternary complex between SnRK1, bZIP63, and bZIP2 assists in recruiting SnRK1 to the chromatin.

SnRK1 is recruited to the chromatin and required for histone acetylation of the *ETFQO* promoter

Nuclear localization of SnRK1s has been demonstrated *in planta* (Bitrián et al., 2011). Remarkably, ChIP_{PCR} analyses demonstrate that SnRK1.1 is associated with the *ETFQO* promoter (Figure 6A). Strikingly, SnRK1.1 recruitment increases within 6 h of extended dark treatment, supporting the assumption that SnRK1.1 is recruited to the chromatin in response to low energy stress. S1-bZIPs and bZIP63 are crucial for SnRK1.1 recruitment to the *ETFQO* promoter as its binding was strongly impaired in the *bzipS1* and *bzip63* mutant background (Figure 6A, B). Moreover, we could demonstrate that a fully functional bZIP63 was indispensable for SnRK1.1 recruitment, as SnRK1.1 did not bind to the *ETFQO* promoter when a *bzip63* mutant line was applied, which has been complemented with a genomic Pro_{bZIP63}:*bZIP63*:*GFP* construct harboring Ala exchange mutations in the SnRK1 phosphorylation sites (*bZIP63ala*) (Figure 6B).

In yeast, the SnRK1 homolog Snf1 is also bound to promoters and regulates chromatin structure via histone acetyltransferases (HAT), which modify histones due to acetylation (Abate et al., 2012; Lo et al., 2001). Acetylation of histone 3 lysine 14 (H3K14) is a general mark, associated with an euchromatic state and high level of transcription (Lee and Workman, 2007). We recently demonstrated that bZIP2 (as well as bZIP11 and bZIP44) form a complex with the ADA2b adapter, necessary to recruit GCN5 related HATs (Weiste and Dröge-Laser, 2014). In WT plants, we found an increased level of H3K14 acetylation of the *ETFQO* promoter within 6 h of extended dark treatment which was abolished both in *snrk1.1/1.2* and *bzipS1* mutants (Figure 6C). These findings propose a mechanistic model that recruitment of a ternary SnRK1/bZIP complex is required for opening up the chromatin and to initiate transcription of the *ETFQO* gene.

DISCUSSION

In this work we unravel the molecular mechanisms by which energy deprivation is transduced to reprogram gene expression and to support plant survival. The findings are summarized in a model provided in Figure 7.

Acting as downstream transcription factors, S1-bZIPs execute a subset of the SnRK1 responses

We could demonstrate the importance of SnRK1 as a central regulator of transcriptional networks in stress and energy signaling. . In comparison to previous studies (Baena-Gonzalez et al., 2007), this transcriptome approach provides several advantages as (i) whole-plants instead of protoplast cultures, (ii) inducible loss-of-function instead of gain-of-function approaches and (iii) energy deprived situations were studied. In general, SnRK1s are activating catabolic processes and inactivating energy-consuming anabolic processes. Importantly, these functions proposed for plant SnRK1, largely match those described for orthologous kinases in other species, indicating evolutionary conservation of these crucial metabolic regulators (Baena-González and Sheen, 2008; Hardie, 2007).

Interestingly, downstream TF targets of Snf1 in yeast or AMPK in mammals appear not to be evolutionary conserved in plants. Although several downstream TFs have been proposed, unambiguous proof is still missing (Kleinow et al., 2009; Lin et al., 2014; O'Brien et al., 2015; Tsai and Gazzarrini, 2012). According to previous publications, C/S1-bZIPs have a strong impact on the expression of genes involved in the primary metabolism and starvation responses, such as *ASN1* (Baena-Gonzalez et al., 2007; Dietrich et al., 2011). Moreover, the substantial overlap of S1-bZIP and SnRK1-regulated genes, observed in our transcriptome analyses strongly support a function of S1-bZIPs downstream of SnRK1. Nevertheless, as only a subset of SnRK1-regulated genes are controlled by S1-bZIPs further TFs have to be postulated to execute SnRK1 responses. Despite the huge transcriptional reprogramming initiated by SnRK1 upon extended darkness, we could also identify genes regulated by S1-bZIPs, not overlapping with those of SnRK1. The C/S1-network could, hence serve as an important hub, where different input signals are converging to reprogram the plant transcriptome. In line with this assumption, the C/S1-network has been shown to be involved in a large variety of biological functions such as biotic and abiotic stresses, nutritional response, seed development or auxin signaling (Alonso et al., 2009; Baena-Gonzalez et al., 2007; Dietrich et al., 2011; Hanson et al., 2008; Kang et al., 2010; Ma et al., 2011; Obertello et al., 2010; Para et al., 2014; Weiste and Dröge-Laser, 2014).

By recruiting SnRK1 to target promoters, bZIP heterodimers link starvation signaling to transcriptional reprogramming

Although none of the S1-bZIPs were found to be directly phosphorylated by the SnRK1 kinase, we recently could demonstrate that the group C bZIP63 is phosphorylated by SnRK1 and hence, due to heterodimerisation provides an ideal partner to functionally link S1-bZIPs and SnRK1. Indeed, our present data suggest the formation of a ternary complex between SnRK1, bZIP2, and bZIP63, which depends on the integrity of the SnRK1-specific phosphorylation sites, which have been determined in bZIP63. We propose that SnRK1 activation leads to phosphorylation-driven complex formation, which in turn is recruited to target promoters such as *ETFQO* (Figure 7). Here, we define *ETFQO* as a direct C/S1-bZIP target, encoding an electron transfer protein supporting alternative mitochondrial electron transport upon energy stress. ChIP studies support that SnRK1 recruitment to the chromatin depends on both C- and S1-bZIP partners and the integrity of bZIP63 phosphorylation sites. Indeed preferential C/S1-heterodimerisation and its synergistic impact on gene regulation has been previously demonstrated (Alonso et al., 2009; Ehlert et al., 2006; Weltmeier et al., 2006). Hence, it is tempting to propose that further ternary SnRK1-C/S1-bZIP complexes may exist. However, whether they perform specific or redundant functions need to be elucidated. As bZIPs of the C/S1 network are characterized by a plethora of transcriptional and post-transcriptional regulatory mechanisms, bZIP dimerization has been proposed to function as a signaling hub to integrate inputs on environmental and cellular energy conditions into transcriptional patterns (Mair et al., Chapter 3; Weltmeier et al., 2006).

Recently, we have shown that the N-terminus of bZIP2 (as well as bZIP11 and bZIP44) interact with the adaptor protein Ada2b, which is part of a multi-protein HAT complex related to yeast SAGA (Rodriguez-Navarro, 2009; Vlachonasios et al., 2003; Weiste and Dröge-Laser, 2014). These findings are in line with starvation induced histone acetylation of the *ETFQO* promoter, which depends on the presence of SnRK1 and S1-bZIPs. Besides controlling bZIP heterodimerisation, SnRK1 may hence have a distinct second function in chromatin remodeling. It has to be noted that in yeast, the Snf1 kinase is also recruited to the chromatin to phosphorylate histones (H3S10) (Abate et al., 2012; Lo et al., 2001). This modification is recognized by HAT complexes that facilitate histone acetylation as a secondary chromatin mark. Thus, SnRK1s may contribute to modifications of the chromatin status by non-exclusive mechanisms. Taken together, SnRK1 appear to function as a moonlighting protein, performing both as a kinase and a scaffolding protein to link

low-energy-signaling to gene expression (Copley, 2012).

SnRK1-C/S1-bZIP-ETFQO signaling controls mitochondrial energy metabolism upon low energy stress

According to the proposed function in optimizing energy usage in situations of limited energy availability, *snrk1.1/1.2* and *bzipS1* mutants show an altered regulation of several energy-consuming or energy preserving processes. Comprehensive metabolic, pharmacological and genetic analyses disclosed a previously unexpected SnRK1-C/S1-bZIP dependent regulation of *ETFQO* expression. Reduced expression of *ETFQO* specifically affects mitochondrial electron transport as it leads to the inability of the plant to exploit fatty acids, choline or aa as an alternative source of energy, with the consequent inability to survive extended dark treatment (Engqvist et al., 2011; Hörtensteiner and Kräutler, 2011; Ishizaki et al., 2005, 2006). Indeed, mutants in all components of the pathway (*snrk1.1/1.2*, *bzipS1*, *etfqa*) displayed highly similar responses to pharmacologically administered blocks in central metabolic activities as well as impaired survival under stress. As *ETFQO* related proteins are well-conserved from plants to mammals and humans, the mechanism presented here is of broader interest. Several diseases, such as obesity and certain kinds of cancer, are related to dysfunctional *ETFQO* and mitochondrial metabolism (for review see Watmough and Freyman, 20). Further studies are needed to address an evolutionary conserved regulation of mitochondrial metabolism by SnRK1 and its homologs.

EXPERIMENTAL PROCEDURES

Plant material

Arabidopsis thaliana ecotype Col-0 was used as WT. To generate the *snrk1.1/1.2* mutant, an amiRNA targeting *snrk1.2* transcripts was transformed into the *snrk1.1* mutant via *Agrobacterium*-mediated floral-dip transformation (Weigel and Glazebrook, 2002). Similarly, *bzip1/bzip53* double mutant (Salk 059343; 069883; Dietrich et al., 2011) were transformed with an amiRNA construct targeting *bZIP2/11/44* (Weiste and Dröge-Laser, 2014). Furthermore, *etfqa* (Ishizaki et al., 2005), single and multiple *bzip* mutants (Alonso et al., 2009; Dietrich et al., 2011) and *bzip63* complemented lines (Mair et al., Chapter 3) were used.

Plant growth conditions

If not indicated otherwise, all plants were grown in a plant growth incubator (BINDER,

Tuttlingen, Germany) in a 12 h light/12 h dark photoperiod, at 22°C/20°C and a humidity of 60%. For sterile culture, plants were grown on MS-agar medium (MS: M0222, Duchefa-Biochemie, Germany; agar: P1003, Duchefa-Biochemie, Germany) for 4 weeks.

Extended dark treatment was obtained by prolonging the dark period into the subsequent light phase for 6 h. During these 6 h temperature was kept at 22°C.

Induction of amiRNA expression was performed by supplementing Est to MS-agar medium after sterilization (T<40°C) to a final concentration of 10 µM. In case of the *bzipS1* and *snrk1.1/1.2* mutants, Est treatment was perpetuated for 1 or 6 days, respectively.

For pharmaceutical studies, sterile grown plants were treated with Antimycin-A (20 µM) (A8674, Sigma-Aldrich, Germany) or 4-methylpyrazole hydrochloride (2 mM) (M1387, Sigma-Aldrich, Germany).

Vector construction

Target specific amiRNA sequences were generated using the online amiRNA design tool WMD3 (<http://wmd3.weigelworld.org>) and inserted in the GATEWAY[®] compatible binary vector pMDC7 (Zuo et al., 2000). The group S1 and C bZIP effector plasmids used for ChIP and transactivation assays were previously described by Ehlert et al. (2006). SnRK1.1 cDNA was PCR-amplified using GATEWAY[®] compatible primers, inserted in the pDONR201 entry vector and subsequently transferred into expression vectors (Ehlert et al., 2006). A 1000 bp *ETFQO* promoter was PCR amplified from WT genomic DNA, using sequence specific primers attaching *XhoI* or *NcoI* restriction sites. The promoter sequence was inserted in the pBT10:GUS reporter construct (B. Weisshaar, Bielefeld, Germany). To generate mutations in the G-box elements, the Quick change site-directed mutagenesis kit (Stratagene, La Jolla, USA) was used following the manufacturers manual. Mutagenic primers were designed online at: <http://www.genomics.agilent.com/primerDesign>. All primers are listed in Table S1

Statistics

Statistical tests were all performed using R.

Supplemental Data

The following materials are available in the online version of this article.

Supplemental Table 1. Report of the RNAseq analysis.

Supplemental Figure 1. Characterization of *snrk1.1/1.2* and *bzipS1* mutant lines

Supplemental Figure 2. SnRK1 and S1-bZIPs reprograms the primary metabolism.

Supplemental Figure 3. Regulation of the expression of *ETFQO* by C- and S1-bZIPs

AUTHOR CONTRIBUTIONS

L.P. performed most of the experiments. C.W. performed the Pro_{ETFQO}:GUS activation assays. K.D. designed the amiRNA construct for SnRK1.2 and generated the *snrk1.1/1.2* plant line. RNAsequencing experiments have been performed in the lab of M.E. under the supervision of E.W. F.L. prepared the RNA library for RNA seq. T.N. and W.W. performed the metabolic measurements and their analysis. A.M. and M.T. provided unpublished plant lines and vector constructs. E.B-G. Actively supported the conceptual work. L.P., C.W and W.D-L. designed the research and wrote the manuscript.

ACKNOWLEDGMENT

We are grateful to Jasmin Göttler for valuable technical assistance and to for proof reading. We thank Drs. N.H. Chua (New York, US), B. Weishaar (Bielefeld, Germany) and K. Ishizaki (Kuda University, Japan) for sharing seeds and vector constructs. The research was supported by FP7 Marie Curie ITN (GA 264474).

REFERENCES

- Abate, G., Bastonini, E., Braun, K. a, Verdone, L., Young, E.T., and Caserta, M. (2012). Snf1/AMPK regulates Gcn5 occupancy, H3 acetylation and chromatin remodelling at *S. cerevisiae* ADY2 promoter. *Biochim. Biophys. Acta* 1819, 419–427.
- Alonso, R., Onate-Sanchez, L., Weltmeier, F., Ehlert, A., Diaz, I., Dietrich, K., Vicente-Carbajosa, J., and Dröge-Laser, W. (2009). A pivotal role of the basic leucine zipper transcription factor bZIP53 in the regulation of Arabidopsis seed maturation gene expression based on heterodimerization and protein complex formation. *Plant Cell* 21, 1747–1761.
- Araújo, W.L., Ishizaki, K., Nunes-Nesi, A., Larson, T.R., Tohge, T., Krahnert, I., Witt, S., Obata, T., Schauer, N., Graham, I. a, et al. (2010). Identification of the 2-hydroxyglutarate and isovaleryl-CoA dehydrogenases as alternative electron donors linking lysine catabolism to the electron transport chain of Arabidopsis mitochondria. *Plant Cell* 22, 1549–1563.
- Araújo, W.L., Tohge, T., Ishizaki, K., Leaver, C.J., and Fernie, A.R. (2011). Protein degradation - an alternative respiratory substrate for stressed plants. *Trends Plant Sci.* 16, 489–498.
- Baena-Gonzalez, E., Rolland, F., Thevelein, J.M., and Sheen, J. (2007). A central integrator of transcription networks in plant stress and energy signalling. *Nature* 448, 938–942.
- Baena-González, E., and Sheen, J. (2008). Convergent energy and stress signaling. *Trends Plant Sci.* 13, 474–482.
- Binder, S. (2010). Branched-Chain Amino Acid Metabolism in Arabidopsis thaliana. *Arabidopsis Book* 8, e0137.
- Bitrián, M., Roodbarkelari, F., Horváth, M., Koncz, C., Bitrian, M., Roodbarkelari, F., Horvath, M., and Koncz, C. (2011). BAC-recombineering for studying plant gene regulation: developmental control and cellular localization of SnRK1 kinase subunits. *Plant J* 65, 829–842.
- Confraria, A., Martinho, C., Elias, A., Rubio-Somoza, I., and Baena-González, E. (2013). miRNAs mediate SnRK1-dependent energy signaling in Arabidopsis. *Front. Plant Sci.* 4, 197.
- Copley, S.D. (2012). Moonlighting is mainstream: Paradigm adjustment required. *BioEssays* 34, 578–588.

- Crozet, P., Margalha, L., Confraria, A., Rodrigues, A., Martinho, C., Adamo, M., Elias, C. a., and Baena-González, E. (2014). Mechanisms of regulation of SNF1/AMPK/SnRK1 protein kinases. *Front. Plant Sci.* 5, 1–17.
- Dietrich, K., Weltmeier, F., Ehlert, A., Weiste, C., Stahl, M., Harter, K., and Dröge-Laser, W. (2011). Heterodimers of the Arabidopsis transcription factors bZIP1 and bZIP53 reprogram amino acid metabolism during low energy stress. *Plant Cell* 23, 381–395.
- Ehlert, A., Weltmeier, F., Wang, X., Mayer, C.S., Smeeckens, S., Vicente-Carbajosa, J., and Dröge-Laser, W. (2006). Two-hybrid protein-protein interaction analysis in Arabidopsis protoplasts: establishment of a heterodimerization map of group C and group S bZIP transcription factors. *Plant J* 46, 890–900.
- Engqvist, M.K.M., Kuhn, A., Wienstroer, J., Weber, K., Jansen, E.E.W., Jakobs, C., Weber, A.P.M., and Maurino, V.G. (2011). Plant D-2-hydroxyglutarate dehydrogenase participates in the catabolism of lysine especially during senescence. *J. Biol. Chem.* 286, 11382–11390.
- Hanson, J., Hanssen, M., Wiese, A., Hendriks, M.M.W.B., and Smeeckens, S. (2008). The sucrose regulated transcription factor bZIP11 affects amino acid metabolism by regulating the expression of ASPARAGINE SYNTHETASE1 and PROLINE DEHYDROGENASE2. *Plant J* 53, 935–949.
- Hardie, D.G. (2007). AMP-activated/SNF1 protein kinases: conserved guardians of cellular energy. *Nat. Rev. Mol. Cell Biol.* 8, 774–785.
- Hardie, D.G. (2015). AMPK: positive and negative regulation, and its role in whole-body energy homeostasis. *Curr. Opin. Cell Biol.* 33, 1–7.
- Hörtensteiner, S., and Kräutler, B. (2011). Chlorophyll breakdown in higher plants. *Biochim. Biophys. Acta - Bioenerg.* 1807, 977–988.
- Ishizaki, K., Larson, T.R., Schauer, N., Fernie, A.R., Graham, I.A., and Leaver, C.J. (2005). The critical role of Arabidopsis electron-transfer flavoprotein:ubiquinone oxidoreductase during dark-induced starvation. *Plant Cell* 17, 2587–2600.
- Ishizaki, K., Schauer, N., Larson, T.R., Graham, I. a, Fernie, A.R., and Leaver, C.J. (2006). The mitochondrial electron transfer flavoprotein complex is essential for survival of Arabidopsis in extended darkness. *Plant J.* 47, 751–760.
- Jakoby, M., Weisshaar, B., Droge-Laser, W., Vicente-Carbajosa, J., Tiedemann, J., Kroj, T., and Parcy, F. (2002). bZIP transcription factors in Arabidopsis. *Trends Plant Sci* 7, 106–111.

- Kang, S.G., Price, J., Lin, P.-C.C., Hong, J.C., and Jang, J.-C.C. (2010). The arabidopsis bZIP1 transcription factor is involved in sugar signaling, protein networking, and DNA binding. *Mol. Plant* 3, 361–373.
- Kirchler, T., Briesemeister, S., Singer, M., Schütze, K., Keinath, M., Kohlbacher, O., Vicente-Carbajosa, J., Teige, M., Harter, K., and Chaban, C. (2010). The role of phosphorylatable serine residues in the DNA-binding domain of Arabidopsis bZIP transcription factors. *Eur. J. Cell Biol.* 89, 175–183.
- Kleinow, T., Himbert, S., Krenz, B., Jeske, H., and Koncz, C. (2009). NAC domain transcription factor ATAF1 interacts with SNF1-related kinases and silencing of its subfamily causes severe developmental defects in Arabidopsis. *Plant Sci.* 177, 360–370.
- Kunz, S., Pesquet, E., and Kleczkowski, L. a (2014). Functional dissection of sugar signals affecting gene expression in Arabidopsis thaliana. *PLoS One* 9, e100312.
- Lee, K.K., and Workman, J.L. (2007). Histone acetyltransferase complexes: one size doesn't fit all. *Nat Rev Mol Cell Biol* 8, 284–295.
- Lin, C.-R., Lee, K.-W., Chen, C.-Y., Hong, Y.-F., Chen, J.-L., Lu, C. -a., Chen, K.-T., Ho, T.-H.D., and Yu, S.-M. (2014). SnRK1A-Interacting Negative Regulators Modulate the Nutrient Starvation Signaling Sensor SnRK1 in Source-Sink Communication in Cereal Seedlings under Abiotic Stress. *Plant Cell*.
- Lo, W.S., Duggan, L., Emre, N.C., Belotserkovskya, R., Lane, W.S., Shiekhattar, R., and Berger, S.L. (2001). Snf1--a histone kinase that works in concert with the histone acetyltransferase Gcn5 to regulate transcription. *Science* 293, 1142–1146.
- Ma, J., Hanssen, M., Lundgren, K., Hernández, L., Delatte, T., Ehlert, A., Liu, C.-M., Schluepmann, H., Dröge-Laser, W., Moritz, T., et al. (2011). The sucrose-regulated Arabidopsis transcription factor bZIP11 reprograms metabolism and regulates trehalose metabolism. *New Phytol.* 191, 733–745.
- Matiolli, C.C., Tomaz, J.P., Duarte, G.T., Prado, F.M., Del Bem, L.E.V., Silveira, A.B., Gauer, L., Corrêa, L.G.G., Drumond, R.D., Viana, A.J.C., et al. (2011). The Arabidopsis bZIP gene AtbZIP63 is a sensitive integrator of transient abscisic acid and glucose signals. *Plant Physiol.* 157, 692–705.
- O'Brien, M., Kaplan-Levy, R.N., Quon, T., Sappl, P.G., and Smyth, D.R. (2015). PETAL LOSS, a trihelix transcription factor that represses growth in Arabidopsis thaliana, binds the energy-sensing SnRK1 kinase AKIN10. *J. Exp. Bot.* 1–11.

- Obertello, M., Krouk, G., Katari, M.S., Runko, S.J., and Coruzzi, G.M. (2010). Modeling the global effect of the basic-leucine zipper transcription factor 1 (bZIP1) on nitrogen and light regulation in Arabidopsis. *BMC Syst Biol* 4, 111.
- Para, A., Li, Y., Marshall-Colón, A., Varala, K., Francoeur, N.J., Moran, T.M., Edwards, M.B., Hackley, C., Bargmann, B.O.R., Birnbaum, K.D., et al. (2014). Hit-and-run transcriptional control by bZIP1 mediates rapid nutrient signaling in Arabidopsis. *Proc. Natl. Acad. Sci. U. S. A.* 111.
- Polge, C., and Thomas, M. (2007). SNF1/AMPK/SnRK1 kinases, global regulators at the heart of energy control? *Trends Plant Sci.* 12, 20–28.
- Robaglia, C., Thomas, M., and Meyer, C. (2012). Sensing nutrient and energy status by SnRK1 and TOR kinases. *Curr Opin Plant Biol* 15, 301–307.
- Rodriguez-Navarro, S. (2009). Insights into SAGA function during gene expression. *EMBO Rep* 10, 843–850.
- Sheen, J. (2014). Master regulators in plant glucose signaling networks. *J. Plant Biol.* 57, 67–79.
- Stitt, M., and Zeeman, S.C. (2012). Starch turnover: Pathways, regulation and role in growth. *Curr. Opin. Plant Biol.* 15, 282–292.
- Tome, F., Nägele, T., Adamo, M., Garg, A., Marco-Illorca, C., Nukarinen, E., Pedrotti, L., Peviani, A., Simeunovic, A., Tatkiewicz, A., et al. (2014). The low energy signaling network. *Front. Plant Sci.* 5, 1–12.
- Tsai, A.Y.-L., and Gazzarrini, S. (2012). AKIN10 and FUSCA3 interact to control lateral organ development and phase transitions in Arabidopsis. *Plant J.* 69, 809–821.
- Usadel, B., Blasing, O.E., Gibon, Y., Retzlaff, K., Hohne, M., Gunther, M., and Stitt, M. (2008). Global transcript levels respond to small changes of the carbon status during progressive exhaustion of carbohydrates in Arabidopsis rosettes. *Plant Physiol.* 146, 1834–1861.
- Vlachonasios, K.E., Thomashow, M.F., and Triezenberg, S.J. (2003). Disruption mutations of ADA2b and GCN5 transcriptional adaptor genes dramatically affect Arabidopsis growth, development, and gene expression. *Plant Cell* 15, 626–638.
- Watmough, N.J., and Frerman, F.E. (2010). The electron transfer flavoprotein: ubiquinone oxidoreductases. *Biochim. Biophys. Acta* 1797, 1910–1916.
- Weigel, R., and Glazebrook, J. (2002). *Arabidopsis: A Laboratory Manual* (New York:

Cold Spring Harbour Laboratory Press).

Weiste, C., and Dröge-Laser, W. (2014). The Arabidopsis transcription factor bZIP11 activates auxin-mediated transcription by recruiting the histone acetylation machinery. *Nat. Commun.* 5, 3883.

Weltmeier, F., Ehlert, A., Mayer, C.S., Dietrich, K., Wang, X., Schutze, K., Alonso, R., Harter, K., Vicente-Carbajosa, J., and Droge-Laser, W. (2006). Combinatorial control of Arabidopsis proline dehydrogenase transcription by specific heterodimerisation of bZIP transcription factors. *EMBO J* 25, 3133–3143.

Weltmeier, F., Rahmani, F., Ehlert, A., Dietrich, K., Schutze, K., Wang, X., Chaban, C., Hanson, J., Teige, M., Harter, K., et al. (2009). Expression patterns within the Arabidopsis C/S1 bZIP transcription factor network: availability of heterodimerization partners controls gene expression during stress response and development. *Plant Mol Biol* 69, 107–119.

Wiese, A., Elzinga, N., Wobbes, B., and Smekens, S. (2004). A conserved upstream open reading frame mediates sucrose-induced repression of translation. *Plant Cell* 16, 1717–1729.

Williams, S.P., Rangarajan, P., Donahue, J.L., Hess, J.E., and Gillaspay, G.E. (2014). Regulation of Sucrose non-Fermenting Related Kinase 1 genes in Arabidopsis thaliana. *Front. Plant Sci.* 5, 1–13.

Yao, Y., Tsuchiyama, S., Yang, C., Bulteau, A.L., He, C., Robison, B., Tsuchiya, M., Miller, D., Briones, V., Tar, K., et al. (2015). Proteasomes, Sir2, and Hxk2 Form an Interconnected Aging Network That Impinges on the AMPK/Snf1-Regulated Transcriptional Repressor Mig1. *PLOS Genet.* 11, e1004968.

Zuo, J., Niu, Q.W., and Chua, N.H. (2000). Technical advance: An estrogen receptor-based transactivator XVE mediates highly inducible gene expression in transgenic plants. *Plant J* 24, 265–273.

FIGURES

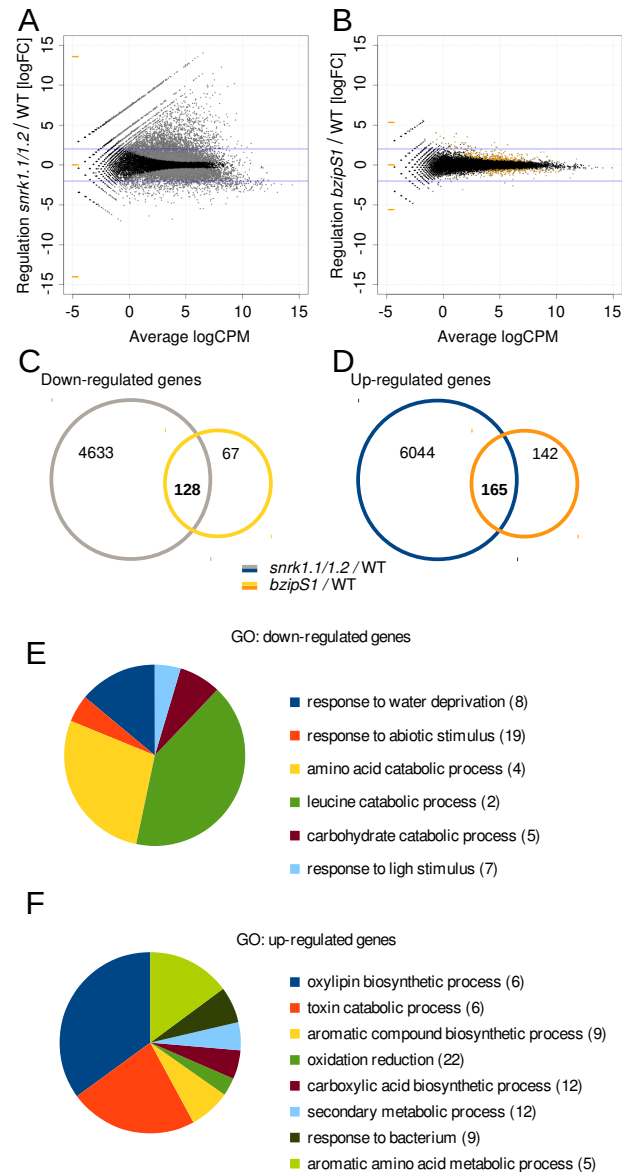


Figure 1. SnRK1 and S1-bZIPs control shared and distinct sets of genes and support overlapping changes in primary metabolism in response to extended darkness

(A, B) RNAseq of 4-week-old *snrk1.1/1.2* (A) and *bzipS1* (B) plants in comparison to WT. Smear plots of DEGs, 6h after extended darkness. Grey and yellow dots represent genes with significantly differential expression with P_{adj} (“BH correction”) < 0.01 . Blue lines are at $\log_{2}FC = 2$. Average logCPM:

(C, D) Venn-diagram displaying the number of down- and up-regulated genes in

snrk1.1/1.2 (grey and blue) and *bzipS1* (yellow and orange). The respective overlap provides the number of DEGs shared by both mutants.

(E, F) GO enrichment of shared DEGs in *snrk1.1/1.2* and *bzipS1*. Pie-charts represent the fold enrichment of down- (E) and up-regulated (F) categories. All the presented categories had a benjamini value < 0.05; number of genes in each category are given in brackets. For detailed analyses see Table S1.

(G, H) Changes in primary metabolites observed in *srrk1.1/1.2* (G) and *bzipS1* (H) compared to WT after 6h of extended night. Log2-fold changes are color-coded. Data obtained from 5 biological replicates were *p<0.05, ** p<0.01, *** p<0.001

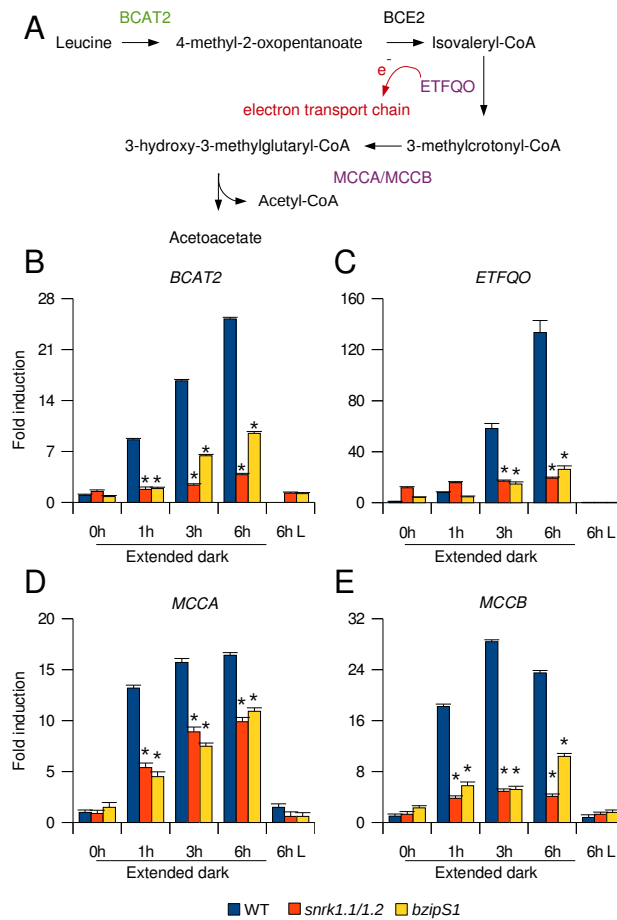


Figure 2. SnRK1 and S1-bZIPs regulate the branch chain amino acid degradation pathway

(A) Representation of the Leu degradation pathway. Enzymes involved are highlighted according to their subcellular localization: green for gene products with a chloroplastic localization, purple for those localized in the mitochondria (Binder, 2010).

(B-E) RT-qPCR validation of the expression of *BCAT2*, *ETFQO*, *MCCA*, and *MCCB* in 4-weeks old WT (blue), *snrk1.1/1.2* (orange) and *bzipS1* (yellow) plants. 0h was defined at the end of the dark period; 1h, 3h, 6h time points correspond to extended dark, 6h L refer to plants cultivated for 6h in light. Given are mean expression level (\pm st.d.) (n=3) relative to WT at 0h. *t*-test to WT at the same time point, * $P < 0.01$.

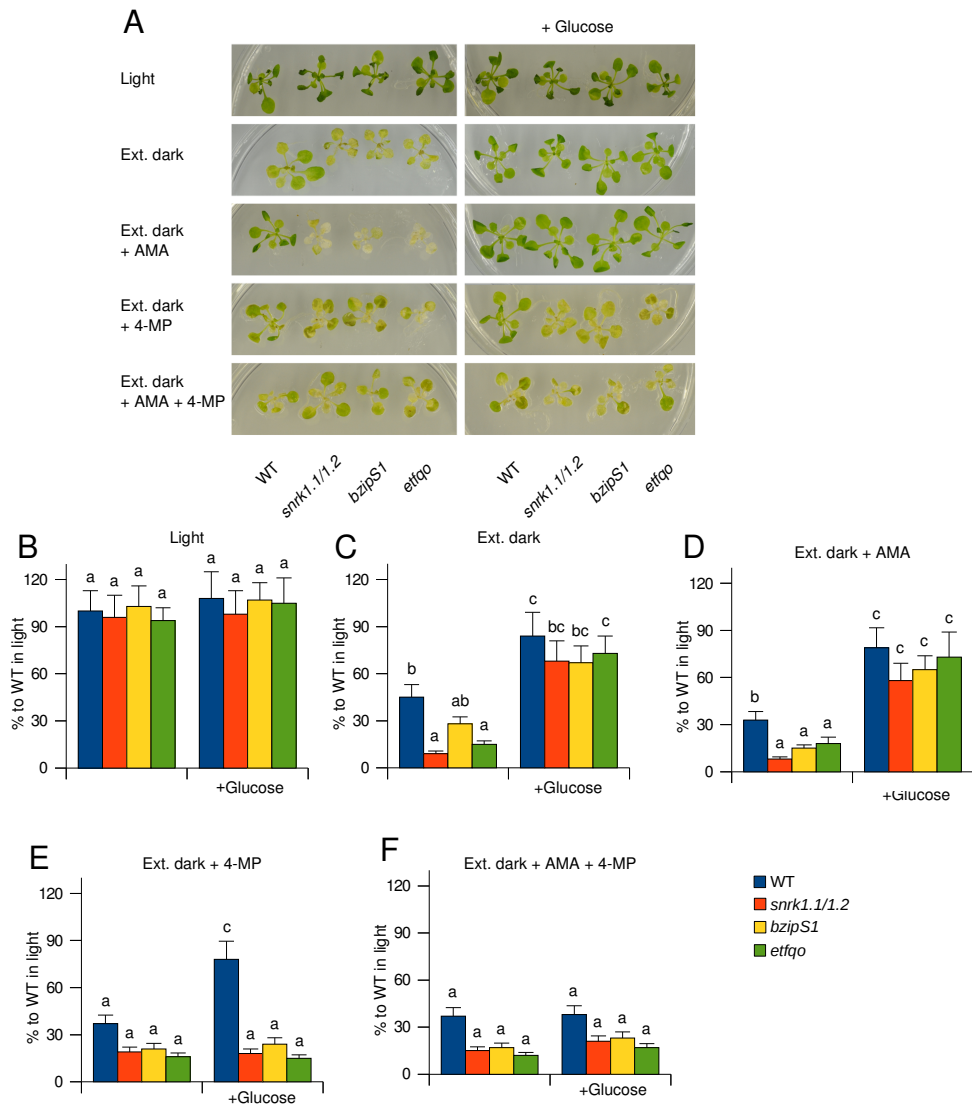


Figure 3. SnRK1 and S1-bZIPs regulate mitochondrial metabolism via the expression of *ETFQO*

Phenotype (left: - sugar; middle: + 2% glucose) and chlorophyll content (right) of WT (blue), *snrk1.1/1.2* (red), *bzipS1* (yellow), and *etfqo* (green) plants measured under the following conditions: (A) 12h/12h light/dark photoperiod; (B) 6 days of extended darkness; (C) 6 days of extended darkness and antimycin-A (AMA) treatment; (D) 6 days of extended dark and 4-methylpyrazole (4MP) treatment; (E) 6 days of extended dark, AMA, and 4MP treatment. Given are mean values (\pm se) ($n > 17$) expressed as percentage to WT plants growing under 12h/12h light/dark photoperiod. ANOVA, post-hoc test: Fisher's test.

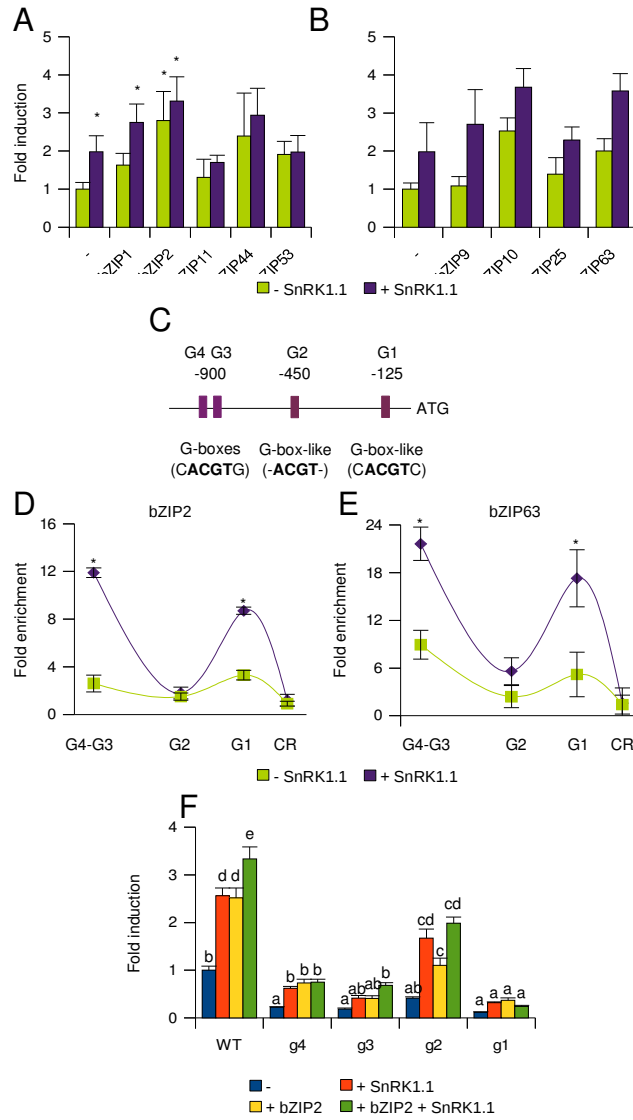


Figure 4. bZIP2 and bZIP63 regulate the expression of *ETFQO*

(A, B) Activation of the Pro_{ETFQO}:GUS reporter by HA-tagged fusion proteins of group S1- and C-bZIPs in *Arabidopsis* protoplasts (green) and after co-expression (purple) of SnRK1.1. (C) Schematic representation of the *ETFQO* promoter: positions of G-box and G-box-like motifs are highlighted relative to the start of translation (ATG). (D, E) ChIP_{PCR} of HA-bZIP2 (D) and HA-bZIP63 (E) in *Arabidopsis* protoplasts using the indicated *ETFQO*-specific primers to detect binding at the G-boxes G1-G4. CR: control corresponding to the coding sequence; αHA- and αGFP: specific antibodies; *t*-test, * *P* < 0.01. (F) Activation of mutated versions (g1 – g4) of the Pro_{ETFQO}:GUS reporter by SnRK1.1 (red), HA-bZIP2 (yellow) or the combination of both (green). Given values are mean values (± st.d.) (n=3), *t*-test, * *P* < 0.01. ANOVA, post-hoc: Tukey's.

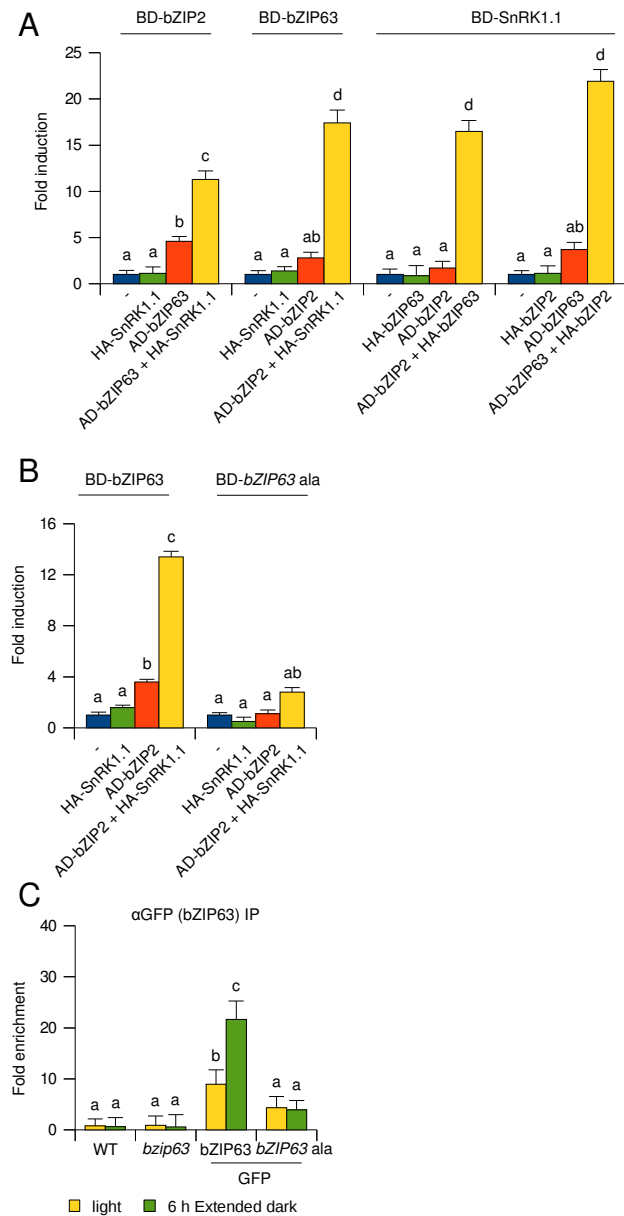


Figure 5. Complex formation between SnRK1.1, bZIP2, and bZIP63

(A) Protoplasts-3-hybrid (P3H) assay: interaction between Gal₄BD- and AD-fused proteins indicated in the presence or absence of the third partner (HA-fusion protein). (B) P3H assay: interaction between AD-bZIP2 with BD-bZIP63 or BD-*bzip63ala* (S/A exchange mutant of the SnRK1-specific phosphorylation sites: S29/294/300A). (C) ChIP_{PCR} in 4-week old GFP-bZIP63 or GFP-*bzip63ala* plants using specific primers for the G3-G4 site on the *ETFQO* promoter. αGFP: specific antibody; 6h in the light (yellow) or 6h in extended dark (green). Given are mean values (± st.d.) (n=3). ANOVA, post-hoc: Tukey's.

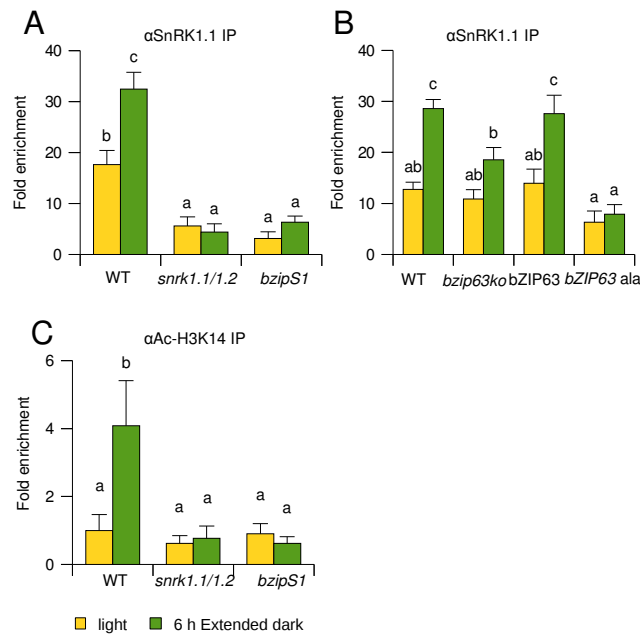


Figure 6. Recruitment of SnRK1 to the *ETFQO* promoter

(A) ChIP_{PCR} of WT, *snrk1.1/1.2* and *bzipS1* plants using primers amplifying the G3-G4 site of the *ETFQO* promoter and a SnRK1.1-specific antibody.

(B) ChIP_{PCR} of WT, *bzip63* mutant and *bzip63* complemented with a genomic bZIP63 fragment fused to GFP (bZIP63) or bZIP63 fragment fused to GFP carrying S/A exchange mutant of the SnRK1-specific phosphorylation sites (bZIP63ala). α GFP: specific antibody.

(C) Acetylation of the *ETFQO* promoter. ChIP_{PCR} using an Ac-H3K14 antibody.

All analyses are performed with 4-week old plants in light (yellow) or 6 h extended dark (green). Given are mean values (\pm st.d.) (n=3). ANOVA, post-hoc: Tukey's.

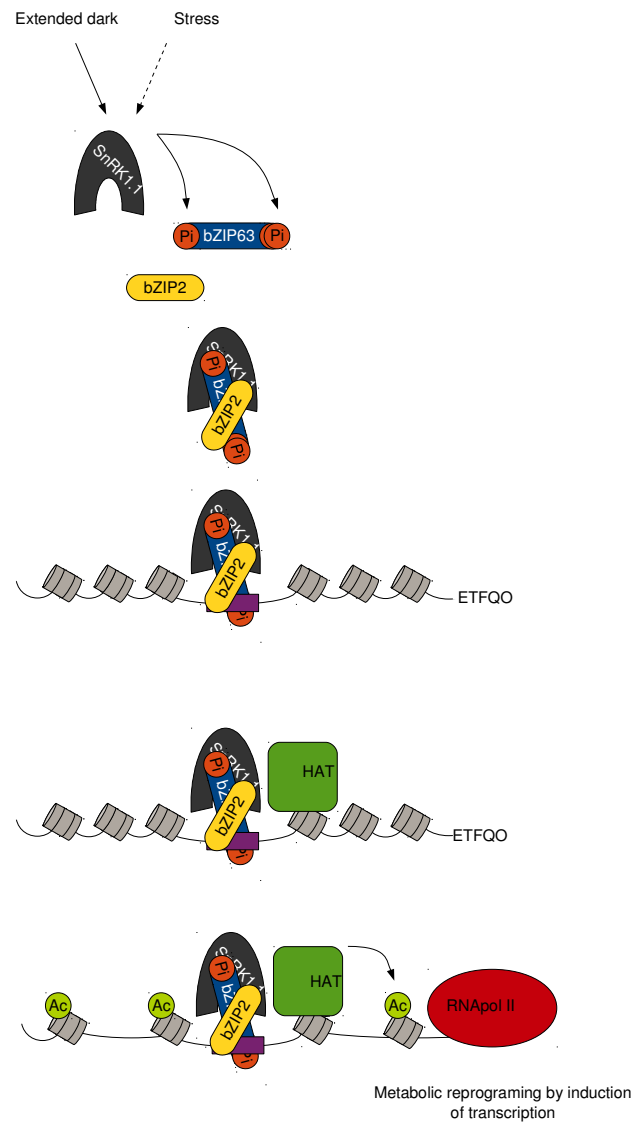


Figure 7. Model summarizing starvation-induced transcriptional control via the SnRK1-C/S1-bZIPs pathway

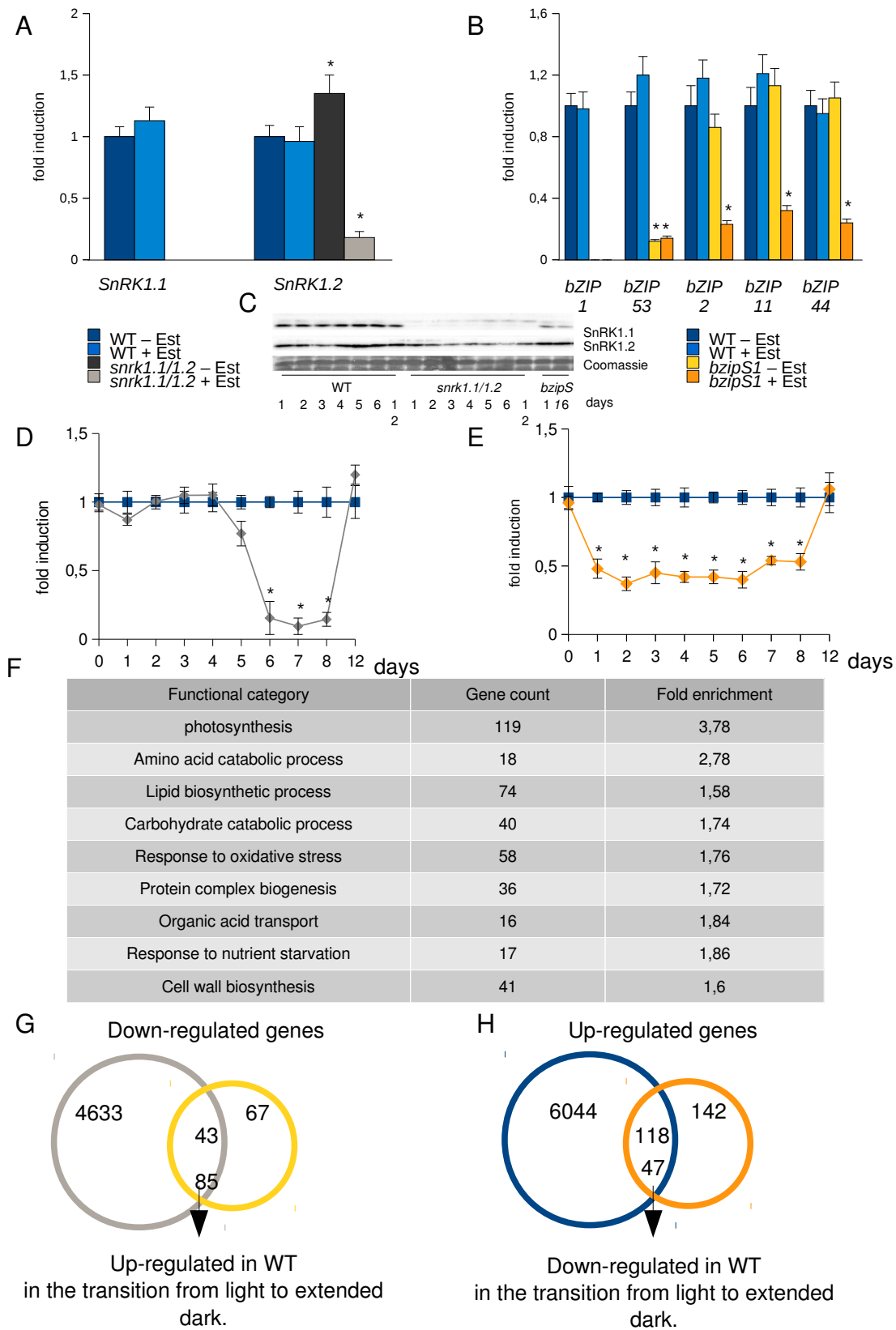


Figure S1. Characterization of *snrk1.1/1.2* and *bzipS1* mutant lines

(A) RT-qPCR analysis of *SnRK1.1* and *SnRK1.2* expression in WT (blue) or *snrk1.1/1.2* mutant (grey) without (dark) or with 16 h Est treatment (light color). T-test to WT – Est.

(B) RT-qPCR analysis of *bZIP1*, *bZIP53*, *bZIP2*, *bZIP11*, and *bZIP44* expression in WT without (blue) or with Est (light blue) and in *bzipS1* plants without (yellow) or with 16 h Est-treatment.

(C) Immuno-blot: expression of SnRK1.1 and SnRK1.2 in WT, *snrk1.1/1.2*, and *bzipS1* plants grown. The time Est of treatment is indicated in days. Although a rapid decrease in *SnRK1.2* RNA has been observed in (A), the protein is relatively stable and its level decreases 5-6 days after Est treatment (quantified relative to the “1 day” time point using ImageLab, Biorad). Equal loading is verified by coomassie staining.

(D) RT-qPCR analysis of the expression of the SnRK1 target gene *ASN1* (Dietrich et al., 2011) in WT (blue) or *snrk1.1/1.2* (grey) plants in response to 6h of extended dark. The length of pre-treatment with Est is given in days and reflects the stability of the SnRK1.2 protein (C). Values are normalized to the relative WT values..

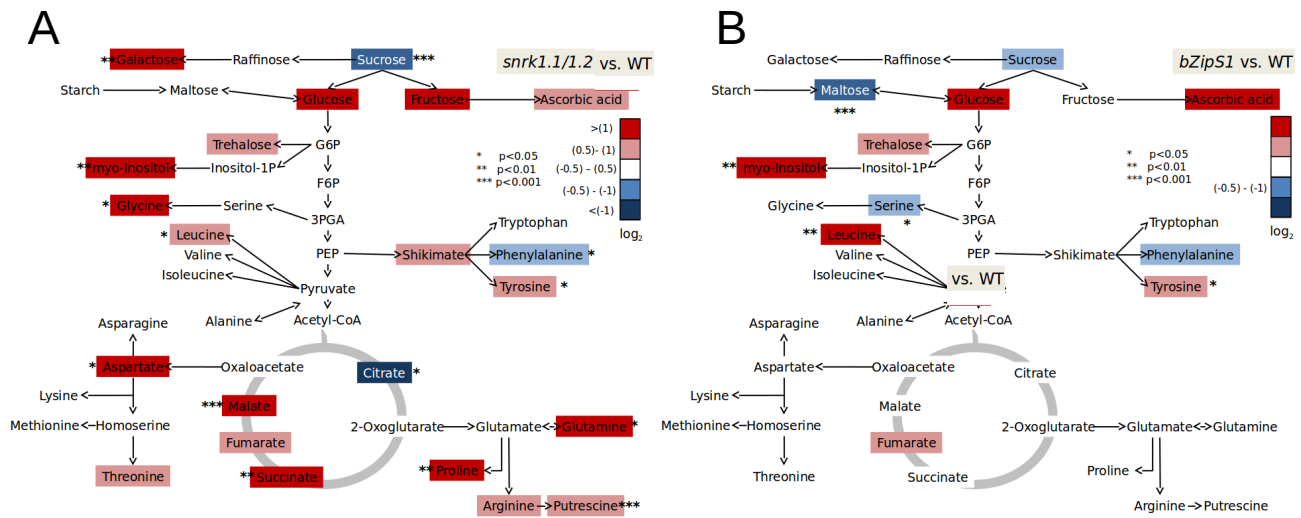
(E) RT-qPCR analysis of the expression of the bZIP target gene *GH3.3* (Weiste and Dröge-Laser, 2014) in WT (blue) or *bzipS1* (orange) plants in response to 6h of extended dark. The length of pretreatment with Est is given in days. Values are normalized on WT at day 0.

For (A, B, D, and E) given are mean values (\pm st.d.) (n=3). * P.value < 0.05.

(F) Selection of GO enrichment annotation of RNAseq results of *snrk1.1/1.2* (for detailed overview see Figure SX).

(G, H) Venn-diagram displaying the number of down- and up-regulated genes in *snrk1.1/1.2* (grey and blue) and *bzipS1* (yellow and orange). The respective overlap provides the number of DEGs shared by both mutants (see Figure 1 C,D). Numbers of genes that have an opposite behavior in WT in transition from light to extended dark are highlighted.

For (A, B, D, and E) given are mean values (\pm st.d.) (n=3). * P.value < 0.05.



FigureS2. SnRK1 and S1-bZIPs reprograms the primary metabolism.

A) Comparison of the metabolome between WT and *snrk1.1/1.2* plants. B) Comparison of the metabolome between WT and *bzipS1* plants. GC measurements of the metabolite indicated in the figures. Relative quantification using WT as reference. At least 5 different repetitions were used. pValue are indicated in the figures.

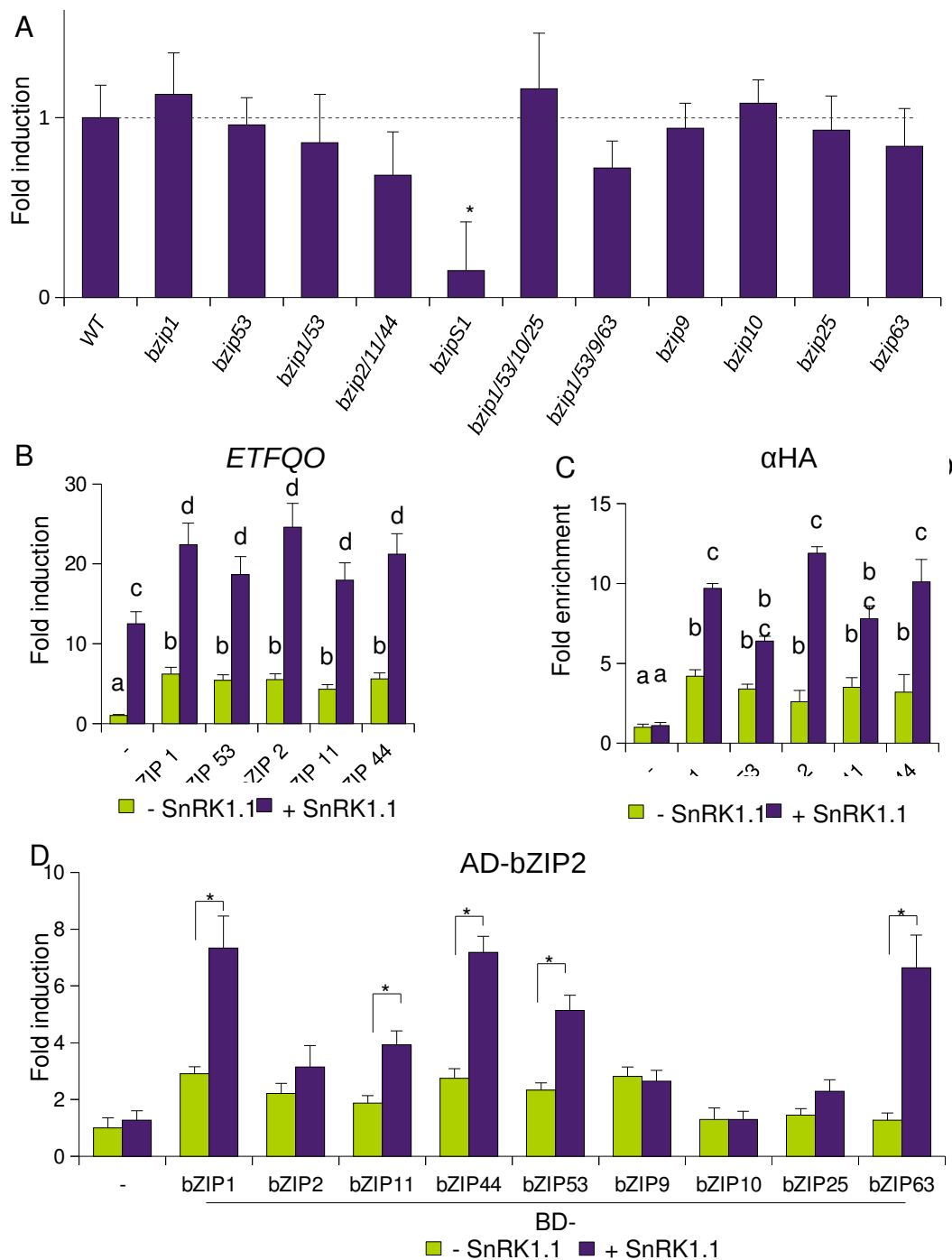


Figure S3. Regulation of the expression of *ETFQO* by C- and S1-bZIPs

(A) RT-qPCR experiment to assess the expression of *ETFQO* in different C- and S1-bZIP loss-of-function mutant plants. Expression was normalized on WT plants exposed to 6h of extended darkness. *t*-test to WT, $P < 0.05$.

(B) RT-qPCR experiment to assess the transcript abundance of *ETFQO* in response to

overexpression of S1-bZIPs in protoplasts (green) or after co-expression of SnRK1.1 (purple). Values are normalized to non-expressing controls.

(C) P2H: changes of the dimerization properties of BD-bZIP2 with other AD-fusions of the bZIP TFs indicated (green), depending on co-expression of SnRK1.1 (purple). Given are mean values (\pm st.d.) (n=3). * *t*-test to “-SnRK1.1” $P < 0.05$.

(D) ChIP_{PCR} experiment: binding of HA-bZIPs of the S1 group in protoplasts to *ETFQO* promoter. An HA-tag antibody and primers specific for the G3-4 sites have been used.

(B, D) Given are mean values (\pm st.d.) (n=3). ANOVA, post-hoc test: Tukey's.

SUPPLEMENTARY METHODS

RT-qPCR

1 μ g of plant total RNA isolated according to Dietrich et al. (2011) was used for cDNA synthesis. First strand synthesis was done using DNaseI (EN0521, Thermo-Scientific, Germany) and RevertAid H Minus Reverse Transcriptase (Thermo-Scientific, Germany) according to the manufacturer's protocol. RT-qPCR was performed with BIOTAQ DNA Polymerase (BIO-line, Germany) using the following cycling conditions: 10 min at 95°C, 40 cycles of 20 s at 95°C, 10 s at 55°C, and 30 s at 72°C. Amplification products were visualized by SYBR green. The Ubiquitin 5 gene (At3g62250) was used as internal standard for relative quantification.

RNAsequencing and data analysis

Total plant RNA was cleaned-up using a RNeasy Mini Kit (Qiagen, Germany) according to the manufacturer's protocol. 5 μ g of total RNA was used for library preparation. mRNA was isolated using Sera-Mag Magnetic Oligo (dT) Particles (Thermo-Scientific, Germany) and cDNA library was prepared using the NEBNext mRNA Library Prep Master Mix Set for Illumina (New England BioLabs) in combination with the NEBNext Multiplex Oligos for Illumina (New England BioLabs). Quality of RNA and fragmentation size was checked using Experion RNA HighSens Analysis Kit (BIORAD, Germany). Quality of the cDNA at the end of the library preparation was checked using Experion DNA Chips (BIORAD, Germany). During library preparation products were isolated with the QIAquick PCR Purification Kit (Qiagen, Germany). One library was constituted by 12 samples. For sequencing one library was distributed on 2 lanes. High-throughput sequencing was performed on an Illumina GAIIx platform following the manufacturer's instructions. Quality control of the sequencing data was done using fastQC

(<http://www.bioinformatics.bbsrc.ac.uk/projects/fastqc/>). Mapping of the reads was performed using Bowtie 0.12.8 (Langmead et al., 2009) onto the *A. thaliana* genome release TAIR9. The resulting BAM files were then sorted and indexed using samtools 0.1.18. For analysis of differentially expressed genes R was used with GenomicRanges (Lawrence et al., 2013), rtracklayer (Lawrence, Gentleman, & Carey, 2009), samtools and edgeR (Robinson, McCarthy, & Smyth, 2010) libraries. Only genes with a p.Adjust (BH⁺ correction) <0.01 were used for further analysis. DAVID was used for GO enrichment analysis (Jiao et al., 2012), Venny (Oliveros, 2007-2015) to obtain the list of genes commonly regulated by SnRK1 and S1-bZIPs.

Chlorophyll content measurement

Around 100 mg of frozen material was pulverized using a Mixer Mill (MM400, Retsch, Germany) and metal beads in a 2 ml reaction tube. 1 ml of methanol was used for the extraction. Extract was incubated at 60°C for 30 min and for 10 min at RT. Clarification of the supernatant was obtained by centrifugation in a bench-top centrifuge. Absorption of a 1:10 dilution of the clarified supernatant was measured at 650 and 665 nm in a spectrophotometer. Total chlorophyll content was obtained applying the formula: $A_{650} \times 0.025 + A_{665} \times 0.005 = \text{mg total chl./ml extract}$ (Holden, 1965). At least 17 replicates were used.

Protoplast transformation

Protoplast transformation was performed according to Yoo et al. (2007) with small modifications. Protoplasts were obtained from 3-week old plants grown on soil. 1 h after dawn leaves were cut into tiny stripes and digested for 30 min under vacuum and 3 h at atmospheric pressure with enzyme solution (1.25% (w/v) Cellulase R-10, 0.3% Macerozyme R-10, 0.4 M Mannitol, 20 mM KCl, 10 mM CaCl₂, 20 mM MES, pH 5.7). Protoplast suspension was filtered through a metal net to remove leaf debris and washed twice with 10 ml of W5 solution (2 mM MES, 154 mM NaCl, 125 mM CaCl₂, 5 mM KCl, pH 5.7). Afterwards, the protoplasts were resuspended in 10 ml of W5, incubated on ice for at least 1 h and subsequently resuspended to a final concentration of 1×10^5 cell/ml in MMg buffer (4 mM MES, 0.4 M mannitol, 15 mM MgCl₂, pH 5.7). 200 μ l of protoplast suspension was then gently mixed with DNA in a 2 ml reaction tube. 220 μ l of PEG (40% PEG4000, 0.2 M mannitol, 100 mM CaCl₂) were added to the reaction tube and gently mixed, followed by 10 min of incubation at RT. 800 μ l of W5 buffer were used to wash the

protoplasts, followed by centrifugation (300 *g*) for 1 min. A syringe was used to remove the supernatant. The protoplasts were incubated for 16 hours in 200 μ l of WI solution (4 mM MES, 0.5 M mannitol, 20 mM KCl, pH 5.7) in the growth incubator in order keep diurnal growth conditions. For ChIP and CoIP assays the incubation time was 8 h to reduce unspecific binding of the proteins.

In protoplast-2/3-hybrid (P2/3H) assays (Ehlert et al., 2006), 10 μ g of effector plasmid, 7 μ g of reporter (ProGal₄:GUS or ProGal₄:LUC) and 3 μ g of transfection control reporter (Pro35S:NAN or Pro35S:REN) were used. For ChIP experiments and Co-IP, 10 μ g of effector plasmid were used. If not stated otherwise, 3 independent transfections were used to one data point.

ChIP using protoplasts

A modified protocol according to (Fode et al., 2008) was used. 12 samples of transformed protoplasts were pooled, centrifuged for 1 min at 300 *g* and resuspended in 200 μ l of WI solution. Formaldehyde was added to a final concentration of 1% and the suspension was incubated for 10 min at RT. Addition of 250 μ l of 2.5 M glycine was followed by 5 min incubation at RT. Protoplasts were washed twice with 800 μ l of ice-cold W5 and finally resuspended in 500 μ l of extraction buffer 1 (1 M hexylenglycol, 50 mM PIPES-KOH (pH 7.2), 10 mM MgCl₂, 5 mM β -mercaptoethanol, one tablet per 10 ml complete protease inhibitor cocktail tablets (Roche, Germany)). After 20 min of incubation on ice, extraction buffer was removed by centrifugation for 5 min at 150g (). The pellet was resuspended in 500 μ l of RIPA buffer (50 mM HEPES (pH 7.9), 140 mM NaCl, 1 mM EDTA, 1% Triton-X100, 0.1% Na-deoxycholate, 0.1% SDS) and incubated on ice for 10 min. Lysate was sonicated (28 times for 15 sec, 100 Hz) while kept on ice. Chromatin was cleared by centrifugation for 15 min at 11,000 *g* at 4 °C. The DNA fragment size was checked on a 2% agarose gel after de-crosslinking and chloroform/phenol extraction. Chromatin was incubated with 2 μ g of ChIP grade HA-antibody (ab9110, AbCam, UK) for 6h at 4°C and subsequently over night after addition of 70 μ l of protein A-coated magnetic beads dissolved in BSA-PBS (5 mg/ml) (Invitrogen, Germany). Subsequently, the beads were washed with 1 ml of the wash buffers 1 (20 mM Tris-HCl (pH 8.1), 150 mM NaCl, 2 mM EDTA, 1% Triton-X100, 0.1% SDS), 2 (20 mM Tris-HCl (pH 8.1), 500 mM NaCl, 2 mM EDTA, 1% Triton-X100, 0.1% SDS), 3 (20 mM Tris-HCl (pH 8.1), 250 mM LiCl, 1 mM EDTA, 1% NP40, 1% Na-deoxycholate) and finally 1 ml of TE buffer (5 mM Tris-HCl (pH 8.5)).

Each washing step was performed for 5 min at 4°C. The chromatin was eluted twice using 150 µl of elution buffer (1% SDS, 100 mM NaHCO₃) each time for 15 min at RT. Finally, DNA was purified by phenol/chloroform extraction and quantified by qPCR using the input DNA for normalization.

ChIP from plant material.

Plant material was incubated for 30 min under vacuum in 20 ml cross-linking buffer (50 mM KH₂PO₄/K₂HPO₄ buffer, pH 5.8; 1% (v/v) formaldehyde). Cross-linking was stopped by incubating the samples in 20 ml of 2.5 M glycine for 15 min under vacuum. Afterwards, plant material was washed twice with ice-cold water and subsequently frozen and pulverized. For nuclei isolation plant material was re-suspended in 10 ml ice-cold extraction buffer (1 M hexylenglycol, 50 mM PIPES- KOH, pH 7.2; 10 mM MgCl₂, 5 mM β-mercaptoethanol, protease inhibitor cocktail (Roche, Germany) and filtrated by gravity through two layer of miracloth. 0.5 ml of 25% Triton X-100 was added to the extract and stirred for 15 min at 4°C. Nuclei were isolated by density-gradient centrifugation using a 35% percoll solution. From this step on material was treated as described in the protocol for ChIP from protoplasts. The following antibodies were used: α-HA-antibody (ab9110, AbCam, UK), α-HA:α-SnRK1.1 (AS10 919, Agrisera, Vännäs, SWEDEN), α-SnRK1.2 (AS10 920, Agrisera, Vännäs, SWEDEN) and α-Ac-H3K14 (AB4729, Abcam, Cambridge, UK).

Immuno Blot

Western analysis was performed making use of a primary polyclonal xxx antibody from rabbit (1:700 dilution) (cat. no.) or a monoclonal α-xxx antibody from mouse (1:1,000 dilution) (cat. no.) and a secondary anti-rabbit (1:10,000 dilution) (cat. no. NA934) or anti-mouse (1:7,500 dilution) (cat. no. RPN4201) immunoglobulin G conjugated with a horseradish peroxidase (GE Healthcare, Freiburg, Germany). Protein loading was quantified by Ponceau S staining or by determining ACTIN11 (At3g12110) abundance using an α-ACTIN11 antibody from mouse (1:1,000 dilution) (cat. no. AS10702, Agrisera, Sweden).

GC-MS Metabolite analysis

Metabolite extraction was performed by adding 1ml of -20°C cold methanol/chloroform/H₂O (2.5/1/0.5) mixture to 50-80 mg of ground plant material. Samples were vortexed, incubated on ice for 8 - 10min and centrifuged for 4 minutes at 4°C. 500µl H₂O were added to the supernatant, followed by brief vortexing and 2 minutes of

centrifugation. The polar phase was split into two equal aliquots and 10µl of a 0.1 g L⁻¹ solution of C¹³-labelled sorbitol was added as an internal standard. Samples were dried for derivatization. The dried pellets were resolved at 30°C for 90 minutes in 20µl of a 40mg ml⁻¹ methoxyamine hydrochloride in pyridine solution. 80µl of N-methyl-N-trimethylsilyltrifluoroacetamid (MSTFA), spiked with 30µl/ml of a mix of even-numbered alkanes, were added, and the samples were incubated for 30 minutes at 37°C under constant shaking, followed by 2 minutes of centrifugation. The supernatant was transferred into a glass vial for measurement. GC-MS measurements were performed on an Agilent 6890 gas chromatograph coupled to a LECO Pegasus ® 4D GCxGC-TOF mass spectrometer (LECO® Corporation, Michigan, USA). For GC analysis, the initial oven temperature was set to 70°C for 1 minute, followed by a 9°C/min ramp with 350°C end temperature which was set constant for 8 minutes. In the MS method, the data acquisition rate was set to 20 spectra sec⁻¹ at a detector voltage of 1550V. The acquisition delay was set to 5.5 minutes and the detected mass range was set from 40 to 600 m/z. Raw data were processed with the LECO Chroma-TOF ® software (LECO® Corporation, Michigan, USA). Peak areas were normalised by the peak area of the internal standard, and by the sample fresh weight.

SUPPLEMENTARY REFERENCES

Ehlert, A., Weltmeier, F., Wang, X., Mayer, C.S., Smeekens, S., Vicente-Carbajosa, J., and Dröge-Laser, W. (2006). Two-hybrid protein-protein interaction analysis in Arabidopsis protoplasts: establishment of a heterodimerization map of group C and group S bZIP transcription factors. *Plant J* 46, 890–900.

Fode, B., Siemsen, T., Thurow, C., Weigel, R., and Gatz, C. (2008). The Arabidopsis GRAS protein SCL14 interacts with class II TGA transcription factors and is essential for the activation of stress-inducible promoters. *Plant Cell* 20, 3122–3135.

Holden M. (1965): Chlorophylls. *Chemistry and Biochemistry of Plant Pigments* (T. W. Goodwin, ed.), Academic Press, New York, 461-488.

Langmead, B., Trapnell, C., Pop, M., and Salzberg, S.L. (2009). Ultrafast and memory-efficient alignment of short DNA sequences to the human genome. *Genome Biol.* 10, R25.

Oliveros, J.C. (2007-2015). Venny. An interactive tool for comparing lists with Venn's diagrams. <http://bioinfogp.cnb.csic.es/tools/venny/index.html>

Yoo, S.-D., Cho, Y.-H., and Sheen, J. (2007). Arabidopsis mesophyll protoplasts: a versatile cell system for transient gene expression analysis. *Nat. Protoc.* 2, 1565–1572.

Table S1: Primer used in this study**RT-qPCR Primer**

Primer	Forward sequence (5'-3')	Reverse sequence (5'-3')
<i>BCAT2</i>	QuantiTect® Primer QT00854875	QuantiTect® Primer QT00854875
<i>ETFQO</i>	AGATGTATCAGCAGTGAAGCG G	AATGGCCAAGCCAGGAAGTA GC
<i>MCCA</i>	AGAGGCAATGAAGATGGAGCA C	AGGTCCTGTATGCTTCCAGAG G
<i>MCCB</i>	GCCAAACGCCAGAATTGGCAT C	TCTTCCTCTTCCTCAGTCCAC TTG
<i>SnRK1.1</i>	ACTGGATTTGCAGAGAGTACA AGGTCC	TCAGAGGACTCGGAGCTGAG CA
<i>SnRK1.2</i>	GCTCGTAACTTTTCCAGCAG A	TTCAGGTCTCTATGGACAACC A
<i>bZIP1</i>	TCAGCGTTAAACTCGTCGTAG CAA	AACGCGGGTCTTAGATCGGA GAAG
<i>bZIP2</i>	TGATCGGAAACTGATGACTCC	GAGCAGATTTGACCGTGAGC
<i>bZIP11</i>	CGATTCAAACGTCGTCAGG	TCCGTTTACGTTTCCTCTGC
<i>bZIP44</i>	CATCTACGTAAAGAAAACGCT CAG	CCGGTCTCCATACCGAATC
<i>bZIP53</i>	TGGGGTCGTTGCAAATGCAAA CAA	CCGTGGCGTACCTCGGATCAT TAT
<i>ASN1</i>	TTCTTGAGCTTTCTCGCAGAT	CCGTTCTGATATAAGCCACTC C
<i>GH3.3</i>	CATCACAGAGTTCCTCACAAG C	GTCGGTCCATGTCTTCATCA

ChIP Primer

Primer	Forward sequence (5'-3')	Reverse sequence (5'-3')
<i>ETFQO CR</i>	CATAGAAGAAACATTTGGAC AATCT	GGAGGATGATCCAAGGAG GA

<i>ETFQO G1</i>	CAAGTCGTAGCTTGCCAACA	CATCACTCTTCTTACGTTG CTTT
<i>ETFQO G2</i>	TCCAAACCTTTTCATTCAACA A	CACTGATGTTGCTTTTCTT ACACA
<i>ETFQO G3-4</i>	TTCTCTTCTTTTCTTTTCTCT TAGG	TGTGGGGACGGTTTATCTT T

Primer for amiRNA construction

Primer	sequence (5'-3')
amiSnRK1.2 I miR-s	gaTTATCAGATAGTACGTCACATtctctcttttgta ttcc
amiSnRK1.2 II miR-a	gaATGTGACGTACTATCTGATAAtcaaagagaa tcaatga
amiSnRK1.2 III miR*s	gaATATGACGTACTAACTGATATtcacaggtcgt gatatg
amiSnRK1.2 IV miR*a	gaATATCAGTTAGTACGTCATATtctacatatat tcct

Primer for promoter:GUS reporter construction

Primer	Forward sequence (5'-3')	Reverse sequence (5'-3')
<i>ProETFQO-1000bp</i>	AAAATCTAGATAAGCCTA TCCAAACCTTTTC	TTTTTCCATGGCATGATCA CTGAGTAATTAGGAGGA
<i>ProETFQO_{G1mut}</i>	GAATGAGCTTGCCAATC ATCGCCGAGTC	GACTCGGCGATGATTTGGC AAGCTCATTC
<i>ProETFQO_{G2mut}</i>	CATGAATATAAAGCAAAA TAAGAAGAGTGATGTAG	CTACATCACTCTTCTTATTT TGCTTTATATTCATG
<i>ProETFQO_{G3mut}</i>	GAAAACACGCACGTGTC AAATGTGTGTGCGTGTAT ATATG	CATATACACGCACACAC ATTTGACACGTGCGTGTTT TC
<i>ProETFQO_{G4mut}</i>	CAAAGAAAACACGCAA TGTCACGTGTGTGTGCG	CGCACACACACGTGACAT TTGCGTGTTTTCTTTG

Chapter 5: Crosstalk between two basic leucine ZIPPER signaling pathways orchestrates salt-induced metabolic reprogramming in *Arabidopsis* roots

Laura Hartmann^a, Lorenzo Pedrotti^a, Christoph Weiste^a, Agnes Fekete^a, Jasper Schierstaedt^a, Jasmin Göttler^a, Stefan Kempa^b, Markus Krischke^a, Katrin Dietrich^{a‡}, Martin J. Müller^a, Jesus Vicente-Carbajosa^c, Johannes Hanson^{d,e}, Wolfgang Dröge-Laser^{a,1}

^aJulius-von-Sachs-Institut, Pharmazeutische Biologie, Universität Würzburg, Julius-von-Sachs-Platz 2, 97082 Würzburg, Germany.

^bBSIO Berlin School of Integrative Oncology, Charite - Universitätsmedizin Berlin (CVK), Augustenburger Platz 1, D-13353 Berlin, Germany.

^cCentro de Biotecnología y Genómica de Plantas (UPM-INIA). Campus de Montegancedo, Autopista M40 (km 38). Universidad Politécnica de Madrid. 28223 - Pozuelo de Alarcón, Madrid, Spain.

^dDepartment of Molecular Plant Physiology, Utrecht University, Padualaan 8, 3584 CH Utrecht, the Netherlands.

^eUmeå Plant Science Center, Department of Plant Physiology, Umeå University, SE-901 87 Umeå, Sweden.

¹For correspondence: wolfgang.droege-laser@uni-wuerzburg.de

[‡]Present address: Metanomics GmbH, Tegeler Weg 33, D-10589 Berlin, Germany.

The author responsible for distribution of materials integral to the findings presented in this article in accordance with the policy described in the Instructions for Authors (www.plant-cell.org) is Wolfgang Dröge-Laser (wolfgang.droege-laser@uni-wuerzburg.de).

ABSTRACT

Soil salinity increasingly impacts crop loss world-wide. Although roots are the primary targets of salt stress, the signaling networks facilitating metabolic reprogramming to provoke stress tolerance are less understood than in leaves. Here, a combination of transcriptomic and metabolic approaches was performed in salt-treated *Arabidopsis* roots, which identifies the group S1 basic leucine zipper transcription factors bZIP1 and bZIP53 to reprogram primary C- and N-metabolism. In particular, gluconeogenesis and amino acid catabolism are affected. Importantly, *bZIP1* expression reflects information on the cellular stress and energy status. In addition to the well-described abiotic stress response pathway initiated by the hormone abscisic acid (ABA) and executed by SnRK2 (Snf1-RELATED-PROTEIN-KINASE2) and AREB-like bZIP factors, we identify a structurally related ABA-independent signaling module consisting of SnRK1s and S1 bZIPs. Crosstalk between these signaling pathways recruits particular bZIP factor combinations to establish at least four distinct gene expression patterns. Understanding this signaling network provides a framework to secure future crop productivity.

INTRODUCTION

Salt (NaCl) stress is a serious threat to food production affecting around 30% of the agricultural land world-wide (Kronzucker and Britto, 2011). However, plants have established efficient mechanisms to avoid or adapt to salt stress conditions (for review see Krasensky and Jonak, 2012; Huang et al., 2012; Deinlein et al., 2014; Golldack et al., 2014). Gaining insight into resistance mechanism will be essential for developing strategies to enhance tolerance and, consequently crop yield (Schroeder et al., 2013).

Salt stress is intrinsically complex since it implies both ion toxicity and an osmotic component (Huang et al., 2012; Verslues et al., 2006). Although sensing of these cues is believed to take place at the membrane (Christmann et al., 2013), the respective sensors are not well-defined, yet (Osakabe et al., 2013; Kumar et al., 2013). After stress perception, a burst of Reactive Oxygen Species (ROS) mediated by NADPH oxidases (Chung et al., 2008) triggers an increase of cytosolic Ca² (Laohavisit et al., 2013) and the synthesis of the phytohormone Abscisic Acid (ABA) (Fujita et al., 2009, 2006; Huang et al., 2012; Umezawa et al., 2010).

Recent discoveries provide a detailed view on ABA-mediated stress signaling pathways (Fujii et al., 2009) sensed by the PYR/PYL/RCAR (PYRABACTIN RESISTANCE1/PYR1-like/REGULATORY COMPONENT OF ABA RECEPTOR1) co-receptors (Ma et al., 2009; Park et al., 2009). ABA bound to the receptor recruits members of the redundant PP2C (PROTEIN PHOSPHATASE 2C) family (Hao et al., 2011), thereby impeding their inhibitory action over a crucial regulatory kinases belonging to the SnRK2 (SUCROSE-NON-FERMENTING1-RELATED PROTEIN KINASE2) family (Fujita et al., 2009). The active SnRK2 kinases phosphorylate different cellular targets such as AREB1 (ABA-RESPONSE-ELEMENT BINDING1) (Furihata et al., 2006), a member of the group A basic leucine Zipper (bZIP) transcription factor (TF) family (Jakoby et al., 2002). Three related bZIPs, namely AREB1, AREB2 and ABF3, co-operate as master regulators of ABA-dependent transcription through their binding to ABRE (ABA-RESPONSIVE ELEMENT) promoter *cis*-elements (Yoshida et al., 2010).

Transcriptome studies provided a valuable overview on the massive transcriptional reprogramming in response to abiotic stresses (Kilian et al., 2007). Osmotic stress imposed by salt or drought share common signaling networks which are in part ABA-dependent and ABA-independent (Huang et al., 2012). Whereas ABA-dependent transcriptional changes

are controlled by AREB1-like bZIPs, ABA-independent responses are mediated by other TFs, e. g. DREB2 (DROUGHT-RESPONSIVE ELEMENT BINDING2) (Lata and Prasad, 2011).

Salt-induced defenses are energy-dependent. As photosynthesis is strongly impaired under these conditions, a metabolic change is required to serve the plant's energy demands. Nevertheless, the impact of salt stress on respiration is not fully understood and controversially discussed (for review see Jacoby et al., 2011). In *Arabidopsis* leaves, dramatic salt-induced metabolic changes were discovered with respect to carbohydrate and amino acid (aa) metabolism (Kempa et al., 2008). Although roots are the primary targets of salt stress, metabolome studies in salt-treated *Arabidopsis* roots are currently not available and little is known about the regulatory signaling network particularly within the root.

TFs involved in metabolic reprogramming in salt-treated roots have not been characterized, yet. *Arabidopsis* bZIP1 was found to be transcriptionally induced by salt treatment (Weltmeier et al., 2009) leading to enhanced or reduced tolerance to salt and drought stress when over-expressed or knocked-out, respectively (Sun et al., 2012). However, the precise mechanism of action remains elusive. bZIP1 belongs to the group S1 bZIP factors (bZIP1, -2, -11, -44, -53) which preferentially forms heterodimers with group C (bZIP9, -10, -25, -63) (Ehlert et al., 2006; Weltmeier et al., 2006). This so-called C/S1 network of bZIP TFs has been shown to control metabolic reprogramming under low energy stress (Ma et al., 2011; Hanson et al., 2008; Dietrich et al., 2011). In particular, bZIP1 and its closest homologue bZIP53 display a partially redundant function. Under starvation induced by extended night, bZIP1 directly targets genes in aa metabolism, such as *ASPARAGINE SYNTHETASE1* (*ASN1*) and *PROLINE DEHYDROGENASE1* (*PRODH1*) (Dietrich et al., 2011). Likewise, genome-wide binding studies in protoplasts revealed bZIP1 as a major regulator of N-related genes (Para et al., 2014).

In *Arabidopsis*, the kinases SnRK1.1 (AKIN10) and SnRK1.2 (AKIN11) belonging to the SnRK1-family of protein kinases and have been shown to function as central integrators of plant stress and low energy signaling (Baena-Gonzalez et al., 2007). It was proposed that SnRK1 responses were mediated by C and/or S1 bZIPs, but direct phosphorylation of any of these TFs remains to be demonstrated. Moreover, the impact of SnRK1s in salt stress responses has not been studied to date.

In addition to their function as energy supply, sugars are also important signaling molecules (Hanson and Smeekens, 2009). In *Arabidopsis* HEXOKINASE1 (*HXK1*) functions as a major glucose sensor (Moore et al., 2003). Interestingly, *bZIP1* transcription in seedlings is repressed by glucose and depends on *HXK1* (Kang et al., 2010; Dietrich et al., 2011). These findings support the view that *bZIP1* transcription responds to the glucose status of the cell. Along this line, all group S1 members are translationally repressed by sucrose due to a conserved upstream open reading frame (uORF) (Wiese et al., 2004; Weltmeier et al., 2009). Although plants' energy resources are assumed to impact an efficient stress response, the nature of relevant metabolic parameters, their sensing and a functional connection to group S1 TFs has not been disclosed, yet.

Here, we provide several lines of evidence to elucidate the function of bZIP1 and its interlinked C/S1 bZIP partners in salt-stressed *Arabidopsis* roots. (I) We demonstrate that *bZIP1* transcription integrates signals on metabolic and/or energy status of stressed cells. (II) Using combined transcriptome and metabolic approaches we define the function of bZIP1 in reprogramming carbohydrate and aa metabolism. (III) Besides the well-described SnRK2/AREB signaling module, we identify a second, structurally related SnRK1/group S1 bZIP signaling module functioning in salt-treated roots. (VI) Crosstalk of these bZIP factors allows to build up a regulatory circuit providing means to integrate information on the metabolic situation of the cell into salt stress response programs.

RESULTS

***bZIP1* transcription in roots is induced by ionic or osmotic stimuli**

To gain insight into the function of group C and S1 TFs in plant stress responses, quantitative real-time PCR (RT-qPCR) experiments were performed on salt-treated, hydroponically grown *Arabidopsis* Col-0 plants. We could reproduce public transcriptome data (Weltmeier et al., 2009) demonstrating that specifically *bZIP1* and to a minor extend *bZIP53* were transcriptionally induced by NaCl treatment (Figure 1A). In comparison to well-described markers of abiotic stress responses such as *RD29B* (Msanne et al., 2011), a relatively slow transcriptional activation kinetic was observed showing the strongest increase later than 6 h post treatment (Supplemental Fig. 1A). Transcription of all group C members showed only minor salt-induced changes (Supplemental Figure 1B). Importantly, the response was found only in roots, but not in leaves (Supplemental Figure 1C). We therefore focused our study on bZIP1 and bZIP53 in the *Arabidopsis* root system.

To further characterize conditions inducing *bZIP1* transcription, we treated roots with several salts (NaCl, KCl, Na₂SO₄, MgCl₂) and the osmotically active sugar mannitol using identical osmotic strength in all experiments. All treatments induced *bZIP1* transcription (Figure 1B). Whereas, NaCl and KCl led to similar induction patterns, stronger activation was triggered by multivalent ions, suggesting that besides osmotic cues, ionic stimuli are sensed in a specific manner.

***bZIP1/bZIP53* mutants show reduced salt tolerance**

To address a putative function of C/S1 bZIPs in salt responses, seeds of *bzip1* and *bzip53* single and double mutants (Dietrich et al., 2011, Sun et al., 2012) were germinated on 175 mM NaCl (Figure 1C). Whereas *bzip1* and *bzip53* showed no significantly reduced germination rates, the correspondent double mutant was clearly impaired. Although group C bZIPs are known hetero-dimerization partners of S1 bZIPs in abiotic stress responses (Weltmeier et al., 2006; Alonso et al., 2009), the *bzip10/bzip25* double mutant was not affected in germination. Nevertheless, a quadruple *bzip1/bzip53/bzip10/bzip25* line showed a tendency to be less salt-tolerant than the *bzip1/bzip53* double mutant. We therefore concluded that bZIP1 and bZIP53 are important, potentially redundant players in salt stress responses, which are functionally supported by bZIP10 and bZIP25.

Transcriptomic analyses reveal functions of bZIP1 and bZIP53 in metabolic reprogramming under salt stress

In order to get mechanistic insights into bZIP1 and bZIP53 function in salt-stressed roots genome-wide transcriptome analyses were performed. As *bzip1* single mutants showed only minor transcriptional alterations (Obertello et al., 2010), we chose the *bzip1/bzip53* double mutant for further studies to disclose significant changes in salt-induced gene expression. It needs to be noted, that the mutants did not show any visible growth phenotypes in comparison to WT.

In our experimental set-up, we compared transcriptome profiles of hydroponically grown, 6-week-old wild-type (WT) and mutant roots, salt-treated for 0 h, 1 h, 3 h and 6 h. To minimize the input of the circadian clock, plant material was harvested simultaneously 1 h before the end of the light period. In a parallel approach, roots were harvested for metabolite analyses. The complete data is provided in Supplemental Data sets 1-4.

The WT plants showed substantial transcriptional up-regulation upon salt stress (1 h: 851 genes, 3 h: 1415 genes, 6 h: 2016; log \geq 2-fold, $p \leq 0.01$) which is in agreement with

previously published data sets (Kilian et al., 2007). Hence, the used system is suitable to perform the proposed study. In contrast to this high number of differentially expressed genes (DEGs), only 5 or 4 genes were down- or up-regulated 1 h after salt stress when *bzip1/bzip53* and WT were compared (Fig. 2, Supplemental Data set 1). In particular, *bZIP1* and *bZIP53* transcription were reduced as it is expected for the double mutant. Nevertheless, more DEGs could be observed after 3 h and 6 h of salt treatment, as displayed by the Venn diagram shown in Figure 2A ($\log_2 \geq 0.7$ -fold, $p \leq 0.01$). This kinetic is in concurrent with the relatively slow induction of *bZIP1* and *bZIP53* which increases significantly only after 3 - 6 h of salt treatment. It has to be noted that almost no overlap within the set of DEGs was observed at the 3 h and 6 h time points indicating a sequential regulatory activity of the TFs involved.

In order to define the functional impact of bZIP1 and bZIP53, GENE ONTOLOGY (GO) annotation and MAPMAN (Thimm et al., 2004) analyses were performed. As pointed out in Figure 2B, the most significantly down-regulated genes 3 h after salt-treatment correspond to fermentation, response to low-oxygen-stress and carbohydrate metabolism. After 6 h of salt treatment, expression of several known stress-related marker genes such as *SENESCENCE-ASSOCIATED1 (SEN1)* (Yu et al., 2005), *DARK-INDUCED2 (DIN2)* (Fujiki et al., 2005), *EARLI1* (Zhang and Schläppi, 2007) and *RD29B* (Msanne et al., 2011) were found to be down-regulated in the *bzip1/bzip53* mutant (Figure 2B, Supplemental Data Set 1). Strikingly, a set of genes involved in catabolism of specific aa was identified supporting a function of these bZIPs in reprogramming the root metabolism to respond adequately to the applied stress.

The *bzip1/bzip53* mutant is affected in primary carbohydrate metabolism

As highlighted in Figure 2B, most of the genes found to be down-regulated in *bzip1/bzip53* roots 3 h of salt treatment are connected to fermentation and low-oxygen response. In particular, this can be observed for the whole set of anaerobic core genes as defined by Pucciariello et al. (2012) (e.g. *NODULIN 26 INTRINSIC PROTEIN2.1, NIP2.1; ALCOHOL DEHYDROGENASE1, ADH1; PYRUVATE DECARBOXYLASE, PDC; SUCROSE-SYNTHASE4, SUS4; HYPOXIA-RESPONSIVE UNKNOWN PROTEIN 43, HUP43; LOB-DOMAIN-CONTAINING PROTEIN, LBD43*). Altogether, these data support the view that a major shift to non-oxidative energy metabolism occurs in salt-treated roots, which is partially impaired in the *bzip1/bzip53* double mutant.

To further support this hypothesis, transcriptome data were correlated with detailed carbohydrate measurements. Indeed, salt treatment led to major quantitative and qualitative alteration in carbohydrate composition. Most prominent within 3 – 6 h after stress, glucose (glc), fructose (fru) and sucrose (suc) levels rose significantly (Figure 3A, B). Strikingly, the pattern of mono- and disaccharides differed between *bzip1/bzip53* and WT (Figure 3B). E.g. whereas the glc levels of the WT strongly increased 3 h to 6 h after salt-stress, similar levels were already present in the mutant under unstressed conditions. Moreover, although the initial suc level in the mutant was significantly higher in comparison to the WT, a further increase was observed within the first 3 h of treatment. Hence, bZIP1 and bZIP53 have a major impact on carbohydrate homeostasis during the onset of the salt stress response program.

One of the most significantly DEGs in primary carbohydrate metabolism in the array data set is *SUS4*, encoding a SUCROSE SYNTHASE participating in sucrose breakdown, in particular under low oxygen stress (Pucciariello et al., 2012; Baroja-Fernández et al., 2012). Validation of these results by RT-qPCR studies revealed that *SUS4* expression is partially impaired in the *bzip1/bzip53* mutant (Figure 3C).

Carbohydrate measurements showed that 6 h after onset of salt stress glc, fru and suc levels stayed constant or slowly decreased whereas the concentrations of these sugars were more rapidly reduced in the mutant (Figure 3B, Supplemental Data Set 3). Interestingly, this correlated with a reduced induction of gluconeogenesis-associated genes that were partially impaired in the *bzip* double mutant. In particular, *PYRUVATE ORTHOPHOSPHATE DIKINASE (PPDK)* and *FRUCTOSE-1,6-BISPHOSPHATASE (FBP)* encode key enzymes in this pathway, which is important under metabolic situations where lipids are remobilized via the glyoxylate cycle to shuttle the C-backbones into carbohydrates (Hsu et al., 2011). In agreement with this finding, *MALATE ENZYME*, which is associated with the glyoxylate cycle, was also down-regulated (Supplemental Data Set 1). Finally, *SWEET4* was found as one of the strongest misregulated genes, belonging to a gene family encoding sugar transporters (Chen et al., 2012; Xuan et al., 2013) (Figure 2B). Salt-induced expression profiles of selected genes (*PPDK*, *FBP*) were confirmed by RT-qPCR (Figure 3 D, E). As previous work demonstrated that hetero-dimerization with group C bZIPs is significantly enhancing target gene activation (Weltmeier et al., 2006) we also tested the quadruple mutant (*bzip1/bzip53/bzip10/bzip25*) including potential group C hetero-dimerization

partners. Indeed, salt-induced transcription of *PPDK* was reduced in *bzip1/bzip53* and completely abolished in the quadruple mutant supporting the importance of group C heterodimers at least for this target gene.

Finally, acting as compatible solutes, sugars such as raffinose are implicated in establishing salt stress tolerance (Krasensky and Jonak, 2012). Whereas the raffinose concentration increased steadily in the WT, this increase was impaired 6 h after salt treatment in the *bzip1/bzip53* mutant (Supplemental Figure 2). These findings corresponded with a reduction in *RAFFINOSE SYNTHASE (DIN10)* expression, though the transcriptional changes were minor. Altogether, the bZIPs under investigation have an important impact on the salt-induced metabolic shift in carbohydrate metabolism.

A metabolic switch to fermentation should be reflected on the level of the Tricarboxylic Acid (TCA) Cycle. Indeed, all measured intermediates accumulated immediately after salt stress peaking within 6 and 24 h (Supplemental Figure 3, Supplemental Data Set 4). Whereas transcription of TCA cycle genes was not significantly altered in the *bzip1/bzip53* mutant (Supplemental Data Set 1), the amount of the TCA cycle intermediates citrate, succinate, 2-ketoglutarate and fumarate accumulated in the *bzip1/bzip53* mutant to higher levels than in the corresponding WT. The amounts of these metabolites eventually returned to WT levels within the first 24 h. In comparison to WT the malate concentrations remained at high levels within the 48 h period of the performed measurements. Taken together, although the TCA cycle is affected in the *bzip1/bzip53* mutant, this is not due to bZIP specific gene regulation.

The *bzip1/bzip53* mutant is affected in the catabolism of a specific subset of amino acids

As pointed out in Figure 2B, *bzip1/bzip53* mainly affect genes involved in aa catabolism. Overall eight genes coordinating degradation of Branched-Chain Amino Acids (BCAA: Val, Leu, Ile) (Binder, 2010) as well as Met and Tyr were partially impaired in the mutant. This indicates a major function of these bZIPs in aa breakdown (Figure 4A). The array results of DEGs were confirmed by independent RT-qPCR experiments (Figure 4B). Interestingly, for all analysed genes (*BRANCHED-CHAIN AMINO ACID TRANSFERASE2*, *BCAT2*; *METHYLCROTONYL-COA-CARBOXYLASE*, *MCCA*; *HOMOGENISATE 1,2-DIOXYGENASE*, *HGO*; *METHIONINE- γ -LYASE*, *MGL*) (Binder, 2010; Mentzen et al., 2008), the use of a quadruple *bZIP* mutant

(*bzip1/bzip53/bzip10/bzip25*) did not further reduce the expression found in the *bzip1/bzip53* double mutant. We therefore assume that regulation of the genes involved in BCAA degradation differs from that of *PPDK*.

Salt treatment led to a transient increase in the overall aa levels. However, the effect of bZIP1 and bZIP53 was restricted to particular aa. Whereas in WT Val, Leu, Ile and Tyr concentrations decreased after 6 h of salt treatment which correlated with the activation of the metabolic genes encoding enzymes in aa degradation, this process was blocked in the *bzip* double mutant under study. Down-regulation on gene expression level could clearly be correlated with aa levels (Figure 4C).

ASN1 is the only up-regulated gene in aa biosynthesis, which is in line with the hypothesis that Asn functions in C/N transport under stress (Lam et al., 1994). However, in the *bzip1/bzip53* mutant, *ASN1* transcription was only slightly reduced. Importantly, the quadruple mutant has a much stronger effect indicating differences in gene regulation when compared to that of genes involved in aa degradation. Overall, based on these results bZIP1 and bZIP53 are major regulators of stress-induced metabolic reprogramming of aa degradation, presumably to support metabolism with an alternative energy resource (Araújo et al., 2010; Ishizaki et al., 2006).

The ABA-SnRK2-AREB pathway is dispensable for salt-induced bZIP1 expression

The phytohormone ABA is an important signaling molecule in abiotic stress responses. Thus, we studied *bZIP1* transcription in salt-treated roots of mutants that are affected in stress-induced ABA biosynthesis (*aba2*) (Cheng et al., 2002) or ABA signaling (*snrk2.2/3/6*, *areb1/areb2/abf3*) (Supplemental Figure 4). The latter have been demonstrated to block the ABA response on the level of SnRK2 kinases (Fujita et al., 2009) or group A bZIP TFs (Yoshida et al., 2010), respectively. Although at early time points a minor impact on *bZIP1* expression cannot be excluded, later around 19 h post salt-treatment no significant difference between WT and mutants could be observed. Hence, the ABA-SnRK2-AREB pathway has no major impact on salt-induced *bZIP1* activation (Figure 5A). Nevertheless, as demonstrated in Figure 5B, *bZIP53* transcription partially depends on the SnRK2/AREB pathway demonstrating a unique regulatory mechanism.

Mutant analyses position bZIP1 both in ABA-dependent and -independent abiotic stress signaling networks

Although the ABA-SnRK2-AREB pathway is dispensable for salt-induced *bZIP1* transcription, the transcriptome studies revealed that several well-described ABA responsive genes are down-regulated in the *bzip1/bzip53* mutant, such as *EARLI1*, *RD29B* or *LEA76*. To assess how bZIP1 crosstalks with the ABA-SnRK2-AREB pathway, we studied the expression of these genes in *aba2*, *snrk2.2/3/6* and *areb1/areb2/abf3* as well as *bzip1/bzip53* and *bzip1/bzip53/bzip10/bzip25* mutants. These mutant-based expression studies allowed us to group the array-derived genes into four classes.

Class 1 genes (e.g. *LEA76*, *EARLI*) are group A bZIP targets and depended on all components of the ABA pathway (Figure 5C, Supplemental Figure 5). As these genes were transcriptionally induced more rapidly than *bZIP1* and as activation was unchanged in the C/S1 quadruple mutants (Figure 5D), they are probably no direct C/S1 target genes. Hence, minor differences in expression observed in the array data set are most likely due to indirect crosstalk during the salt stress response.

Class 2 genes such as the BCAA catabolic genes *BCAT2* and *MCCA* clearly dependent on bZIP1 and bZIP53 as demonstrated by the respective mutant analyses. Interestingly, group C bZIPs appear to have no impact in the respective gene regulation. In accordance with the induction profile of *bZIP1*, these genes were less rapidly induced as described for class 1 genes. Moreover, class 2 genes depend on both AREB1/AREB2/ABF3 TFs and SnRK2s. These data indicate that both group A and group S1 bZIP signaling pathways merge to regulate class 2 transcription.

Class 3 genes such as *TAT7* and *HGO* do not depend on the ABA-AREB-SnRK2 pathway but on group S1 bZIPs. Again group C has no or only minor impact.

Finally, mutant analyses studying class 4-gene expression, such as *PPDK*, *DIN2* or *ASN1* clearly showed no dependency on group A bZIPs but regulation by group S1 which was further enhanced in the C/S1 quadruple mutant (Figure 5D, Supplemental Figure 5). Interestingly, kinases of the SnRK2 family interfered with *class 4*-gene expression in a not yet well-defined manner.

ChIP analysis reveals binding of bZIP1 to the *BCAT2* and *TAT7* target promoter

In agreement with previous data, we could detect strong binding of HA-tagged bZIP1 to the *BCAT2* promoter using Chromatin Immunoprecipitation coupled to PCR (ChIP-PCR). Promoter scanning revealed a strong binding to a G-box rich region close to the TATA-box (designated ProBCAT2-3) (Figure 5E) whereas promoter regions more upstream were

hardly or not at all bound by bZIP1. As salt treatment did not lead to enhanced ChIP signals, binding is constitutive. In contrast, salt-induced ChIP signals were detected for all tested TAT7 promoter primers, supporting a stimulus-induced bZIP1 binding mechanism. The *LEA76* and the *PPDK* promoters showed limited background binding, indicating that these are no or low-affinity targets.

SnRK1 signaling is required for salt-induced *bZIP1* transcription

Due to its proposed function in metabolic reprogramming, we focused on potential upstream signaling compounds to deduce which metabolic inputs are mediated via bZIP1 activity. SnRK1.1 and SnRK1.2 kinases are known to mediate responses upon energy deprivation (Baena-Gonzalez et al., 2007). Due to redundancy, single *snrk1.1* knock-out lines show only limited phenotypical and molecular alterations, whereas double knock-out mutants are lethal (Baena-Gonzalez et al., 2007). We therefore established a β -Estradiol (Est)-inducible *snrk1.2* artificial micro RNA (ami) approach in a *snrk1.1* background, designated *snrk1*. Immunoblot analyses confirmed the loss-of-function approach (Supplemental Figure 6). In comparison to salt-treated WT roots, *bZIP1* transcription was strongly reduced in *snrk1* (Figure 6A). These data indicate that SnRK1 signaling is required for salt-induced *bZIP1* transcription.

Ca²⁺ signaling induces *bZIP1* transcription

Ca²⁺ signaling is important in controlling various stress responses. Indeed, salt-induced *bZIP1* transcription was strongly impaired by the Ca²⁺ blocker LaCl₃ (Figure 6C). In contrast to LaCl₃, the calmodulin antagonist N-(6-aminohexyl)-5-chloro-1-naphthalenesulfonamid-hydrochloride (W7) has been shown to generate cytosolic Ca²⁺ transients in *Arabidopsis* (Kaplan et al., 2006). Indeed, W7 treatment partially substituted for the salt stress to induce *bZIP1*. Altogether, stress and metabolic signaling events are integrated into *bZIP1* transcription which is further relayed into salt-specific gene regulation.

DISCUSSION

In order to cope with salt-stress, plants produce protective compounds, adjust their ion homeostasis and remodel primary metabolism to serve the energy demand under stress (Deinlein et al., 2014; Müller et al., 2014). Focusing on *Arabidopsis* roots which are the primary targets of salt stress, this study reports a rapid and substantial reprogramming of the transcriptome leading to metabolic adaptation. Here, we demonstrate that the group S1

bZIP TFs bZIP1 and bZIP53 play an important role in the root specific response to salt. As summarized in the model in Figure 7, this study provides a mechanistic view how bZIP1 signaling is controlled by stress and metabolic cues, reprograms C- and N-metabolism to promote the plant's survival under stress conditions and is integrated in abiotic stress signaling networks.

***bZIP1* transcription integrates cues from stress- and energy-dependent signaling pathways**

Salt or mannitol treatment led to an activation of the *bZIP1* promoter specifically in *Arabidopsis* roots. As transcriptional responses to mannitol and several ionic sources of equal osmolarity differ considerably, it is tempting to speculate that both ionic and osmotic cues are sensed and transmitted into *bZIP1* transcription. In comparison to classical salt response marker genes, *bZIP1* is induced relatively slowly showing the strongest induction later than 6 h post salt treatment. In contrast, the other members of the C/S1 network of bZIPs are not regulated by salt in roots, indicating a specific function of bZIP1. Nevertheless, the closest homologue bZIP53 is also transcriptionally induced, but only to a minor extent. Mutant analysis demonstrates that germination of *bzip53* and *bzip1/bzip53* are increasingly impaired by salt treatment. Although in our assay system *bzip1* mutants displayed comparable germination rates as WT plants, Sun et al. (2012) demonstrated in several phenotypical assays that two independent *bzip1* T-DNA insertion mutants are less tolerant to salt and drought treatments. Taken together, these data support the view that both TFs share partially redundant functions in salt-treated roots, as it has been previously described in the dark-induced starvation response (Dietrich et al., 2011).

Pharmacological evidence support the view, that cytosolic Ca²⁺ bursts observed in response to salt are sufficient to induce *bZIP1*. In contrast, an active ABA/SnRK2/AREB signaling pathway is not required for *bZIP1* induction. However, it has to be stressed that genetic approaches do not eliminate indirect effects, which might explain minor changes in *bZIP1* expression. Interestingly, mutations in the ABA signaling pathway partially impair salt-induced *bZIP53* transcription indicating TF specific differences. Further studies need to unravel the mechanistic differences in regulation of these genes.

Generally, stresses such as salt treatment are believed to interfere with plant energy homeostasis (Baena-Gonzalez and Sheen, 2008). The *Arabidopsis* SnRK1s are evolutionary conserved kinases which facilitate metabolic adaption to stress and energy

starvation (Baena-Gonzalez et al., 2007). Applying an inducible knock-down approach, SnRK1s were found to be crucial for full-level *bZIP1* transcription. Although the C/S1 bZIP TFs have been implicated as likely targets of these kinases, experimental proof for direct phosphorylation is still missing. The metabolic cues related to energy starvation and the upstream components regulating SnRK1 activity are not yet well defined (Crozet et al., 2014). As we could measure substantial sugar resources within the salt-stressed roots, further studies are needed to unravel whether rapid changes in carbohydrate concentrations or other metabolic cues are relayed into SnRK1 activity and ultimately *bZIP1* transcription. In summary, metabolic and stress-related signaling pathways merge on the *bZIP1* promoter. Whether the promoter itself acts as a signal integration platform or whether crosstalk occurs further upstream remains elusive.

bZIP1 and bZIP53 reprogram primary carbohydrate and amino acid metabolism to adapt roots to salt stress conditions

Bioinformatic and systems biology approaches implicate several group S1 bZIP factors as crucial regulators in metabolic reprogramming (Usadel et al., 2008; Gutiérrez et al., 2008). As recently described in dark-treated leaves (Dietrich et al., 2011), *bZIP1* shows strong transcriptional responses in salt-treated roots whereas activation of *bZIP53* is marginal under both stress conditions. We therefore assume that bZIP1 serves as the main transcriptionally regulated “driver” of these responses, although bZIP53 may partially substitute for a loss of bZIP1 in the mutant plant. Here, we demonstrate that these TFs control carbohydrate energy metabolism (fermentation, gluconeogenesis) and catabolism of specific aa providing the enzymatic frame to remobilize carbon skeletons of proteins to satisfy stress-related energy demands. Moreover, our studies propose a connection between hypoxia and salt/osmotic responses. Indeed recent studies demonstrated that HRE2, an important TF in hypoxia-related transcription is also required for growth on salt-containing medium (Park et al., 2011). However, further studies are needed to evaluate the biological impact of this crosstalk.

Interestingly, both transcriptome and metabolic studies propose two phase transitions in primary C-metabolism in salt-treated roots. Within the first 3 h, WT roots show hypoxia-/fermentation-related gene expression, which is partially impaired in the *bzip1/bzip53* mutant. A reduction in oxidative energy metabolism is in line with the proposed function of the SnRK1-bZIP1 pathway in starvation response (Baena-Gonzalez et

al., 2007; Dietrich et al., 2011). In particular, regulation of the hypoxia marker gene *SUS4* depends on bZIP1/bZIP53 and encodes a sucrose-degrading enzymatic activity (Baroja-Fernández et al., 2012) which might explain the increase in monosaccharides 3-6 h upon onset of stress. In leaves of salt-treated plants, the shift in sugar levels is fed by starch breakdown (Kempa et al., 2008). Accordingly, the transcriptome data set shows α -*AMYLASE* (*BAMs*) gene activation in roots. Moreover, sink-driven transport processes to the root may occur (Ludewig and Flügge, 2013). *SWEET4* and *SWEET2* provide examples for genes misregulated in *bzip1/bzip53* which encode putative sugar transporters (Chen et al., 2012; Xuan et al., 2013).

In a second phase, the transient increase in glc, fru and suc returns to initial levels around 24 h after onset of stress. Transcriptome data 6 h after salt stress support a metabolic shift to gluconeogenesis. Key genes like *PPDK* and *FBP* are transcriptionally down-regulated in the *bzip1/bzip53* mutant. Again, both genes are typically expressed under anaerobic conditions (Pucciariello et al., 2012; Hsu et al., 2011). As carbohydrate-driven fermentation provides only limited ATP production under non-oxidative conditions, non-carbohydrate substrates like lipids or proteins are used for energy metabolism (Mentzen et al., 2008; Araújo et al., 2011). Here, we demonstrate that breakdown of specific aa is regulated by bZIPs under investigation in order to provide C-skeletons to the gluconeogenesis pathway. Moreover, recently *FBP* has been proposed to function as a fructose sensor (Cho and Yoo, 2011). Hence, via altered sugar sensing reduced *FBP* expression in the bZIP mutant might lead to a perturbed carbohydrate metabolism.

Proteins can function as alternative respiratory substrates under stress (Araújo et al., 2010; Ishizaki et al., 2005; Araújo et al., 2011). After salt treatment, a transient increase in the concentration of most aa is measured which presumably is due to protein degradation. After 6 h, aa concentration decreases again which is correlated with the degradation of a specific set of aa. Importantly, transcriptional up-regulation of the cognate bZIP TFs precedes the onset of the expression of aa catabolic genes. In particular, a set of genes involved in degrading BCAA (Leu, Val, Ile), Met and Lys is activated which feeds into the Acetyl-CoA pool (AcCoA pool) (Araújo et al., 2011; Binder, 2010). AcCoA can provide intermediates for the TCA cycle, which is perturbed during stress. More strikingly, recent studies disclosed that BCAA breakdown can provide electrons both directly to the electron transport chain via the Electron Transfer Flavoprotein (ETF) complex as well as indirectly

feeding the TCA cycle with metabolic intermediates (Araújo et al., 2010; Ishizaki et al., 2005). Moreover, Tyr degradation is also regulated by the bZIPs under study and feeds into the TCA cycle via fumarate (Dixon and Edwards, 2006). The TCA cycle often operates in a modular fashion in plants, meaning that parts of the cycle are involved in distinct metabolic pathways. Consequently, not all reactions in the pathway carry the same flux (Sweetlove et al., 2010). Although TCA cycle gene expression in *bzip1/bzip53* mutants is not affected, this issue is well documented on the level of several TCA cycle intermediates of the second half of the TCA cycle (succinate, malate, fumarate), which significantly increase in the mutant after salt treatment. This fragmented TCA cycle has been demonstrated to take place in *Lotus japonicus* roots under anoxia, where alanine aminotransferase links glycolysis to the TCA cycle (Rocha et al., 2010).

In contrast to genes involved in aa catabolism, *ASN1* transcription leads to Asn biosynthesis which is controlled by bZIP10 and bZIP25 (group C) and to a minor extent by bZIP1 and/or bZIP53. Accordingly, Asn levels increase both in dark-treated leaves and in salt-stressed roots. Asn has been proposed to function as transported form of C and N (Lam et al., 2003, 1998). In darkened leaves, it has been shown to be derived from pyruvate by PPK activity (Lin and Wu, 2004). Consistently, *PPDK* is also up-regulated in roots and partially depends on bZIP53. As bZIP1 and bZIP53 co-ordinate an alternative metabolic program which provides means to support survival under low energy stress in leaves as well as salt-stress in roots, it is tempting to speculate that these bZIPs may have a broad function in general stress management.

ABA-independent SnRK1/S1-bZIP- and ABA-dependent SnRK2/AREB- signaling pathways regulate specific and overlapping sets of target genes

Group A bZIPs have been demonstrated to control a substantial set of genes responsive to salt stress (Yoshida et al., 2010). Importantly, only a limited number of these genes was found to be differentially expressed in the *bzip1/bzip53* transcriptome data set (e.g. *EARL11*, *RD29B*; depicted as class 1 genes). Indeed, almost no bZIP1 promoter binding was observed for the ABA response gene *LEA76* and mutant analysis demonstrated that this “classical” ABA-dependent gene is not strongly dependent on C and S1 bZIPs.

In contrast, class 2 genes functioning in aa degradation (e.g. *BCAT2*) are direct S1 targets in salt-stressed roots. Promoter scanning by ChIP-PCR reveals that HA-tagged bZIP1 directly and constitutively targets the *BCAT2* promoter in close vicinity to the

transcriptional start site. Here, a number of G-box related *cis*-elements are located, which are known to function as bZIP binding sites. Due to constitutive promoter occupancy of the 35S-driven bZIP1, a transcriptional and/or post-translational salt-stimulated bZIP1 activation mechanism can be anticipated. Interestingly, class 2 transcription depends on group A and S1 bZIPs but not on group C signaling. Whether bZIP1 forms homo- or heterodimers with group A or a yet unknown hetero-dimerization partner needs to be studied. Nevertheless, salt-induced phosphorylation of group A might provide a possible activation mechanism. Alternatively, both bZIP signaling pathways may integrate their cues via independent G-box *cis*-elements.

Class 3 genes depend only on group S1 factors but not on group A or C bZIPs. More strikingly, bZIP1 binding is induced after salt treatment indicating a regulatory mechanism, which is distinct from the constitutive binding of *BCAT2* (class 2). Although formation of bZIP1 homodimers has been described *in vitro* (Kang et al., 2010), it needs to be demonstrated whether homo- or heterodimers are formed *in vivo*. Interestingly, similar to class 2 genes, class 3 genes belong to the same functional context (Tyr degradation). This indicates that functional related genes may share the same transcriptional regulation.

Finally, class 4 genes such as *PPDK* or *ASN1* are regulated by group S1 and C bZIPs, but not by AREB-like bZIPs. Beside these well-defined genes in primary metabolism, stress responsive genes such as *DIN2* and *SEN1* belong to this class (Figure 5, Supplemental Figure 5). Focusing on *PPDK*, bZIP1 did not show substantial binding to this promoter at least at the time point analysed. However, recent ChIP_{seq} studies propose a transient promoter occupancy of bZIP1 which complicates the interpretation of ChIP data (Para et al., 2014). As *bzip1/bzip53* show partially impaired *PPDK* transcription, the alternative explanation that bZIP53 is more important for regulating *PPDK* transcription should be taken into consideration. Previous results demonstrated that S1 bZIPs preferentially heterodimerize with group C bZIPs, thus potentiating target gene expression (Ehlert et al., 2006; Weltmeier et al., 2006). Along this line the *bzip1/bzip53/bzip10/bzip25* mutant is completely impaired in target gene expression supporting the impact of C and S1 bZIPs on transcription of class 4 genes. Interestingly, although class 4 *PPDK* transcription is not depending on AREB-like bZIPs, it is impaired in the SnRK2-triple mutant. Here, the limitations of mutant approaches become obvious as indirect effects are difficult to evaluate. Observations such as phosphorylation of SnRK1 by SnRK2 which has been

found in phosphoproteomic studies (Umezawa et al., 2013) or crosstalk via PP2C phosphatases (Rodrigues et al., 2013) might explain these findings.

Taken together, two structurally related SnRK - bZIP signaling modules orchestrate salt-responsive gene expression in roots (Figure 7). Whereas the SnRK2-AREB pathway responds to ABA and regulates general defense-related functions, the SnRK1-bZIP module is involved in metabolic reprogramming by integrating information on the plant's energy and carbohydrate resources. Importantly, both pathways control specific sets of genes but display substantial crosstalk on the level of bZIP-type transcriptional regulators. Elaborated genetic, ChIP and hetero-dimerization studies are required to address this additional layer of regulatory complexity. Importantly, unraveling the sophisticated network of salt stress response will gain knowledge on how to precisely manipulate plants to engineer stress tolerant crops.

METHODS

Plants lines and culture: Two *Arabidopsis* Columbia (*Col-0*) *bzip1* T-DNA insertion lines, *bzip1-1* (Salk_059343) and *bzip1-2* (SALK_069489) have been characterized in Dietrich et al. (2011). The identical lines were used by Sun et al. (2011) showing highly related phenotypes after salt-treatment. These findings indicate that the T-DNA insertion in the *bZIP1* gene causes the observed alterations. The following mutant lines have been used: *bzip1/bzip53*, *bzip1/bzip53/bzip10/bzip25*, Pro_{35S}::HA:bZIP1 (Dietrich et al., 2011), *aba2* (Cheng et al., 2002), *snrk2.2/3/6* (Fujita et al., 2009), *areb1/areb2/abf3* (Yoshida et al., 2010), *snrk1.1* (Baena-Gonzalez et al., 2007). *snrk1* lines were constructed by floral-dip transformation (Weigel and Glazebrook, 2002) of the *snrk1.1* mutant with an amiRNA targeting SnRK1.2 (<http://wmd3.weigelworld.org/cgi-bin/webapp.cgi>) making use of the vector pMDC7 (Curtis and Grossniklaus, 2003).

Plants were cultured hydroponically (8/16 h day/night regime) according to (Gibeaut et al., 1997). Roots of 6-week-old plants were treated with 150 mM NaCl or equimolar concentrations of salts (KCl, MgSO₄, Na₂SO₄) or mannitol, respectively (final osmolarity 0.25 mosM/l). To minimize the effect of circadian regulation, root material from salt-treated WT and mutant lines utilized for RT-qPCR and transcriptome studies was harvested simultaneously 1 h before the end of the light period.

Alternatively, roots of 3-week-old aseptically grown plants cultured on MS-media (Murashige and Skoog, 1962) were treated with NaCl (final concentration: 250 mM (Ler),

450 mM (Col-0)) for the time periods indicated. In this system chemical compounds such as Est (10 μ M), LaCl_3 (300 μ M), and W7 (N-(6-aminohexyl)-5-chloro-1-naphthelenesulfonamid-hydrochloride) (100 μ M) (Kaplan et al., 2006) can be easily applied.

Molecular Biology Methods: Immunoblot and RT-qPCR techniques were performed as described in Dietrich et al. (2011). The following antibodies were used: AKIN10 (Agrisera Ab10919, Vämäs, Sweden) and anti HA-tag (Abcam ab9110, Cambridge, UK). Cycling conditions were as follows: 10 min at 95th C, 40 cycles of 20 s at 95th C, 10 s at 55th C and 30 s at 72°C, linked to a default dissociation stage program to detect non-specific amplification. The ubiquitin (*UBI5*) gene was used for sample normalization. PCR primers are given in Supplemental Table 1. If not stated differently calculated values are derived from 2-3 biological and 3 – 4 technical replicates. Methods related to ChIP-PCR, transcriptome and metabolomic studies are provided in Supplemental Methods online

Bioinformatic and statistical analyses were performed with GraphPad Prism, Origin and Excel software using the statistic tests indicated in the figure legend.

Accession Numbers: *Arabidopsis* Genome Initiative identifiers for the genes mentioned in this article are as follows: *bZIP53* (At3g62420), *bZIP1* (At5g49450), *bZIP63* (At5g28770), *bZIP10* (At4g02640), *bZIP25* (At3g54620), *bZIP9* (At5g24800), *ASN1* (At3g47340), *BCAT2* (At1g10070), *LEA76* (At3g15670), *RD29B* (At5g52300), *PPDK* (At4g15530), *DIN2* (At3g60140), *SEN1* (At4g35770), *DIN10* (At5g20250), *TAT7* (At5g53970), *HGO* (At5g54080), *MCCA* (At1g03090), *MGL* (At1g64660), *SUS4* (At3g43190), *SWEET4* (At3g28007), *SWEET2* (At3g14770), *KIN10* (At3g01090), *KIN11* (At3g29160), *UBI5* (At3g62250), *ACTIN7* (At5g09810), *ACTIN8* (At1g49240).

Supplemental Data

The following materials are available in the online version of this article.

Supplemental Figure 1: Transcription of group C and S1 bZIPs after salt-treatment.

Supplemental Figure 2: Carbohydrate metabolism in salt-treated WT and *bzip1/bzip53* roots.

Supplemental Figure 3: Metabolites of the TCA cycle but not transcription of the related genes is altered in the *bzip1/bzip53* mutant.

Supplemental Figure 4: RT-qPCR validation of salt-induced expression of *SnRK2* and *AREB* genes in WT and the respective *snrk2.2/3/6*, *areb1/areb2/abf3* multiple T-DNA insertion mutants.

Supplemental Figure 5: RT-qPCR analysis of bZIP1 regulated class 1 – 4 genes.

Supplemental Methods: ChIP-PCR, transcriptome and metabolomic studies

Supplemental Table 1: List of primers used in this study

Supplemental Data Set 1: Summary of transcriptome results comparing salt-treated WT and *bzip1/bzip53* roots.

Supplemental Data Set 2: Summary of aa concentrations comparing salt-treated WT and *bzip1/bzip53* and *bzip1/bzip53/bzip10/bzip25* roots

Supplemental Data Set 3: Summary of carbohydrate concentrations comparing salt-treated WT and *bzip1/bzip53* roots.

Supplemental Data Set 4: Relative amount of selected metabolites comparing salt-treated WT and *bzip1/bzip53* roots.

ACKNOWLEDGMENTS

We are grateful to Drs. J.K. Zhu, K. Shinozaki, E. Baena-Gonzalez and N.H Chua for providing mutants and Susanne Gillig for proof reading. The Research was supported by DFG DR273/11-2 and FP7 Marie Curie ITN MERIT (GA 264474).

AUTHOR CONTRIBUTIONS

L.H. performed most of the research, with exception of generation *snrk1* (L.P.), ChIP-PCR (C.W.), aa analyses (J.S., A.F.), carbohydrate analyses (M.K., M.M.), metabolic profiling (S.K.), transcriptomics and data analysis (J.H.), a part of the RT-qPCR studies (J.G.) and

characterization of particular bZIP mutants (J.V.-C.). The work was supervised and designed by K.D. and W.D.-L. The manuscript was written by W.D.-L.

REFERENCES

- Alonso, R., Onate-Sanchez, L., Weltmeier, F., Ehlert, A., Diaz, I., Dietrich, K., Vicente-Carbajosa, J., and Dröge-Laser, W. (2009). A pivotal role of the basic leucine zipper transcription factor bZIP53 in the regulation of Arabidopsis seed maturation gene expression based on heterodimerization and protein complex formation. *Plant Cell* 21: 1747–1761.
- Araújo, W.L., Ishizaki, K., Nunes-Nesi, A., Larson, T.R., Tohge, T., Krahnert, I., Witt, S., Obata, T., Schauer, N., Graham, I. a, Leaver, C.J., and Fernie, A.R. (2010). Identification of the 2-hydroxyglutarate and isovaleryl-CoA dehydrogenases as alternative electron donors linking lysine catabolism to the electron transport chain of Arabidopsis mitochondria. *Plant Cell* 22: 1549–63.
- Araújo, W.L., Tohge, T., Ishizaki, K., Leaver, C.J., and Fernie, A.R. (2011). Protein degradation - an alternative respiratory substrate for stressed plants. *Trends Plant Sci.* 16: 489–98.
- Baena-Gonzalez, E., Rolland, F., Thevelein, J.M., and Sheen, J. (2007). A central integrator of transcription networks in plant stress and energy signalling. *Nature* 448: 938–942.
- Baena-Gonzalez, E. and Sheen, J. (2008). Convergent energy and stress signaling. *Trends Plant Sci* 13: 474–482.
- Baroja-Fernández, E., Muñoz, F.J., Li, J., Bahaji, A., Almagro, G., Montero, M., Etxeberria, E., Hidalgo, M., Sesma, M.T., and Pozueta-Romero, J. (2012). Sucrose synthase activity in the *sus1/sus2/sus3/sus4* Arabidopsis mutant is sufficient to support normal cellulose and starch production. *Proc. Natl. Acad. Sci. U. S. A.* 109: 321–6.
- Binder, S. (2010). Branched-Chain Amino Acid Metabolism in Arabidopsis thaliana. *Arabidopsis Book* 8: e0137.
- Chen, L.-Q., Qu, X.-Q., Hou, B.-H., Sosso, D., Osorio, S., Fernie, A.R., and Frommer, W.B. (2012). Sucrose efflux mediated by SWEET proteins as a key step for phloem transport. *Science* 335: 207–11.

- Cheng, W., Endo, A., and Zhou, L. (2002). A unique short-chain dehydrogenase/reductase in *Arabidopsis* glucose signaling and abscisic acid biosynthesis and functions. *Plant Cell* ... 14: 2723–2743.
- Cho, Y.-H. and Yoo, S.-D. (2011). Signaling role of fructose mediated by FINS1/FBP in *Arabidopsis thaliana*. *PLoS Genet.* 7: e1001263.
- Christmann, A., Grill, E., and Huang, J. (2013). Hydraulic signals in long-distance signaling. *Curr. Opin. Plant Biol.* 16: 293–300.
- Chung, J.-S., Zhu, J.-K., Bressan, R. a, Hasegawa, P.M., and Shi, H. (2008). Reactive oxygen species mediate Na⁺-induced SOS1 mRNA stability in *Arabidopsis*. *Plant J.* 53: 554–65.
- Crozet, P., Margalha, L., Confraria, A., Rodrigues, A., Martinho, C., Adamo, M., Elias, C. , and Baena-Gonzalez, E. (2014). Mechanisms of regulation of SNF1/AMPK/SnRK1 protein kinases. *Front. Plant Sci.* 5: 1–17.
- Curtis, M.D. and Grossniklaus, U. (2003). A Gateway Cloning Vector Set for High-Throughput Functional Analysis of Genes in *Planta*. *Plant Physiol.* 133: 462–469.
- Deinlein, U., Stephan, A.B., Horie, T., Luo, W., Xu, G., and Schroeder, J.I. (2014). Plant salt-tolerance mechanisms. *Trends Plant Sci.* 19: 371–9.
- Dietrich, K., Weltmeier, F., Ehlert, A., Weiste, C., Stahl, M., Harter, K., and Dröge-Laser, W. (2011). Heterodimers of the *Arabidopsis* transcription factors bZIP1 and bZIP53 reprogram amino acid metabolism during low energy stress. *Plant Cell* 23: 381–95.
- Dixon, D.P. and Edwards, R. (2006). Enzymes of tyrosine catabolism in *Arabidopsis thaliana*. *Plant Sci.* 171: 360–6.
- Ehlert, A., Weltmeier, F., Wang, X., Mayer, C.S., Smeekens, S., Vicente-Carbajosa, J., and Dröge-Laser, W. (2006). Two-hybrid protein-protein interaction analysis in *Arabidopsis* protoplasts: establishment of a heterodimerization map of group C and group S bZIP transcription factors. *Plant J* 46: 890–900.
- Fujiki, Y., Nakagawa, Y., Furumoto, T., Yoshida, S., Biswal, B., Ito, M., Watanabe, A., and Nishida, I. (2005). Response to darkness of late-responsive dark-inducible genes is positively regulated by leaf age and negatively regulated by calmodulin-antagonist-sensitive signalling in *Arabidopsis thaliana*. *Plant Cell Physiol.* 46: 1741–6.
- Fujita, M., Fujita, Y., Noutoshi, Y., Takahashi, F., Narusaka, Y., Yamaguchi-Shinozaki, K., and Shinozaki, K. (2006). Crosstalk between abiotic and biotic stress responses: a

- current view from the points of convergence in the stress signaling networks. *Curr Opin Plant Biol.* 9: 436–42.
- Fujita, Y. et al. (2009). Three SnRK2 protein kinases are the main positive regulators of abscisic acid signaling in response to water stress in *Arabidopsis*. *Plant Cell Physiol.* 50: 2123–32.
- Furihata, T., Maruyama, K., Fujita, Y., Umezawa, T., Yoshida, R., Shinozaki, K., and Yamaguchi-Shinozaki, K. (2006). Abscisic acid-dependent multisite phosphorylation regulates the activity of a transcription activator AREB1. *Proc Natl Acad Sci U S A* 103: 1988–1993.
- Gibeaut, D.M., Hulett, J., Cramer, G.R., and Seemann, J.R. (1997). Maximal biomass of *Arabidopsis thaliana* using a simple, low-maintenance hydroponic method and favorable environmental conditions. *Plant Physiol.* 115: 317–9.
- Golldack, D., Li, C., Mohan, H., and Probst, N. (2014). Tolerance to drought and salt stress in plants: Unraveling the signaling networks. *Front. Plant Sci.* 5: 151.
- Gutiérrez, R.A., Stokes, T.L., Thum, K., Xu, X., Obertello, M., Katari, M.S., Tanurdzic, M., Dean, A., Nero, D.C., McClung, C.R., and Coruzzi, G.M. (2008). Systems approach identifies an organic nitrogen-responsive gene network that is regulated by the master clock control gene CCA1. *Proc. Natl. Acad. Sci. U. S. A.* 105: 4939–44.
- Hanson, J., Hanssen, M., Wiese, A., Hendriks, M.M.W.B., and Smeekens, S. (2008). The sucrose regulated transcription factor bZIP11 affects amino acid metabolism by regulating the expression of ASPARAGINE SYNTHETASE1 and PROLINE DEHYDROGENASE2. *Plant J* 53: 935–949.
- Hanson, J. and Smeekens, S. (2009). Sugar perception and signaling--an update. *Curr. Opin. Plant Biol.* 12: 562–567.
- Hao, Q., Yin, P., Li, W., Wang, L., Yan, C., Lin, Z., Wu, J.Z., Wang, J., Yan, S.F., and Yan, N. (2011). The molecular basis of ABA-independent inhibition of PP2Cs by a subclass of PYL proteins. *Mol. Cell* 42: 662–72.
- Hsu, F.-C., Chou, M.-Y., Peng, H.-P., Chou, S.-J., and Shih, M.-C. (2011). Insights into hypoxic systemic responses based on analyses of transcriptional regulation in *Arabidopsis*. *PLoS One* 6: e28888.

- Huang, G.-T., Ma, S.-L., Bai, L.-P., Zhang, L., Ma, H., Jia, P., Liu, J., Zhong, M., and Guo, Z.-F. (2012). Signal transduction during cold, salt, and drought stresses in plants. *Mol. Biol. Rep.* 39: 969–987.
- Ishizaki, K., Larson, T.R., Schauer, N., Fernie, A.R., Graham, I.A., and Leaver, C.J. (2005). The Critical Role of Arabidopsis Electron-Transfer Flavoprotein : Ubiquinone Oxidoreductase during Dark-Induced Starvation. *Plant J.* 17: 2587–2600.
- Ishizaki, K., Schauer, N., Larson, T.R., Graham, I. a, Fernie, A.R., and Leaver, C.J. (2006). The mitochondrial electron transfer flavoprotein complex is essential for survival of Arabidopsis in extended darkness. *Plant J.* 47: 751–60.
- Jacoby, R.P., Taylor, N.L., and Millar, a H. (2011). The role of mitochondrial respiration in salinity tolerance. *Trends Plant Sci.* 16: 614–23.
- Jakoby, M., Weisshaar, B., Dröge-Laser, W., Vicente-Carbajosa, J., Tiedemann, J., Kroj, T., and Parcy, F. (2002). bZIP transcription factors in Arabidopsis. *Trends Plant Sci* 7: 106–111.
- Kang, S.G., Price, J., Lin, P.-C., Hong, J.C., and Jang, J.-C. (2010). The arabidopsis bZIP1 transcription factor is involved in sugar signaling, protein networking, and DNA binding. *Mol. Plant* 3: 361–73.
- Kaplan, B., Davydov, O., Knight, H., Galon, Y., Knight, M.R., Fluhr, R., and Fromm, H. (2006). Rapid transcriptome changes induced by cytosolic Ca²⁺ transients reveal ABRE-related sequences as Ca²⁺-responsive cis elements in Arabidopsis. *Plant Cell* 18: 2733–48.
- Kempa, S., Krasensky, J., Dal Santo, S., Kopka, J., and Jonak, C. (2008). A central role of abscisic acid in stress-regulated carbohydrate metabolism. *PLoS One* 3: e3935.
- Kilian, J., Whitehead, D., Horak, J., Wanke, D., Weinl, S., Batistic, O., D'Angelo, C., Bornberg-Bauer, E., Kudla, J., and Harter, K. (2007). The AtGenExpress global stress expression data set: protocols, evaluation and model data analysis of UV-B light, drought and cold stress responses. *Plant J.* 50: 347–63.
- Krasensky, J. and Jonak, C. (2012). Drought, salt, and temperature stress-induced metabolic rearrangements and regulatory networks. *J. Exp. Bot.* 63: 1593–608.
- Kronzucker, H.J. and Britto, D.T. (2011). Tansley review Sodium transport in plants : a critical review.: 54–81.

- Kumar, M.N., Jane, W.-N., and Verslues, P.E. (2013). Role of the putative osmosensor *Arabidopsis* histidine kinase1 in dehydration avoidance and low-water-potential response. *Plant Physiol.* 161: 942–53.
- Lam, H.M., Hsieh, M.H., and Coruzzi, G. (1998). Reciprocal regulation of distinct asparagine synthetase genes by light and metabolites in *Arabidopsis thaliana*. *Plant J* 16: 345–353.
- Lam, H.M., Peng, S.S., and Coruzzi, G.M. (1994). Metabolic regulation of the gene encoding glutamine-dependent asparagine synthetase in *Arabidopsis thaliana*. *Plant Physiol* 106: 1347–1357.
- Lam, H.M., Wong, P., Chan, H.K., Yam, K.M., Chen, L., Chow, C.M., and Coruzzi, G.M. (2003). Overexpression of the *ASN1* gene enhances nitrogen status in seeds of *Arabidopsis*. *Plant Physiol* 132: 926–935.
- Laohavisit, A., Richards, S.L., Shabala, L., Chen, C., Colaço, R.D.D.R., Swarbreck, S.M., Shaw, E., Dark, A., Shabala, S., Shang, Z., and Davies, J.M. (2013). Salinity-induced calcium signaling and root adaptation in *Arabidopsis* require the calcium regulatory protein annexin1. *Plant Physiol.* 163: 253–62.
- Lata, C. and Prasad, M. (2011). Role of DREBs in regulation of abiotic stress responses in plants. *J. Exp. Bot.* 62: 4731–48.
- Lin, J.F. and Wu, S.H. (2004). Molecular events in senescing *Arabidopsis* leaves. *Plant J* 39: 612–628.
- Ludewig, F. and Flüggé, U.-I. (2013). Role of metabolite transporters in source-sink carbon allocation. *Front. Plant Sci.* 4: 231.
- Ma, J., Hanssen, M., Lundgren, K., Hernández, L., Delatte, T., Ehlert, A., Liu, C.-M., Schlupepmann, H., Dröge-Laser, W., Moritz, T., Smeekens, S., and Hanson, J. (2011). The sucrose-regulated *Arabidopsis* transcription factor bZIP11 reprograms metabolism and regulates trehalose metabolism. *New Phytol.* 191: 733–45.
- Ma, Y., Szostkiewicz, I., Korte, A., Moes, D., Yang, Y., Christmann, A., and Grill, E. (2009). Regulators of PP2C phosphatase activity function as abscisic acid sensors. *Science* 324: 1064–8.
- Mentzen, W.I., Peng, J., Ransom, N., Nikolau, B.J., and Wurtele, E.S. (2008). Articulation of three core metabolic processes in *Arabidopsis*: fatty acid biosynthesis, leucine catabolism and starch metabolism. *BMC Plant Biol.* 8: 76.

- Moore, B., Zhou, L., Rolland, F., Hall, Q., Cheng, W.H., Liu, Y.X., Hwang, I., Jones, T., and Sheen, J. (2003). Role of the Arabidopsis glucose sensor HXK1 in nutrient, light, and hormonal signaling. *Science* 300: 332–336.
- Msanne, J., Lin, J., Stone, J.M., and Awada, T. (2011). Characterization of abiotic stress-responsive Arabidopsis thaliana RD29A and RD29B genes and evaluation of transgenes. *Planta* 234: 97–107.
- Müller, M., Kunz, H.-H., Schroeder, J.I., Kemp, G., Young, H.S., and Neuhaus, H.E. (2014). Decreased capacity for sodium export out of Arabidopsis chloroplasts impairs salt tolerance, photosynthesis and plant performance. *Plant J.* 78: 646–58.
- Murashige, T. and Skoog, F. (1962). A revised medium for rapid growth and bioassays with tobacco tissue cultures. *Physiol. Plant.* 15: 473–497.
- Obertello, M., Krouk, G., Katari, M.S., Runko, S.J., and Coruzzi, G.M. (2010). Modeling the global effect of the basic-leucine zipper transcription factor 1 (bZIP1) on nitrogen and light regulation in Arabidopsis. *BMC Syst Biol* 4: 111.
- Osakabe, Y., Yamaguchi-Shinozaki, K., Shinozaki, K., and Tran, L.-S.P. (2013). Sensing the environment: key roles of membrane-localized kinases in plant perception and response to abiotic stress. *J. Exp. Bot.* 64: 445–58.
- Para, A. et al. (2014). Hit-and-run transcriptional control by bZIP1 mediates rapid nutrient signaling in Arabidopsis. *Proc. Natl. Acad. Sci. U. S. A.* 111.
- Park, H.-Y., Seok, H.-Y., Woo, D.-H., Lee, S.-Y., Tarte, V.N., Lee, E.-H., Lee, C.-H., and Moon, Y.-H. (2011). AtERF71/HRE2 transcription factor mediates osmotic stress response as well as hypoxia response in Arabidopsis. *Biochem. Biophys. Res. Commun.* 414: 135–41.
- Park, S.-Y. et al. (2009). Abscisic acid inhibits type 2C protein phosphatases via the PYR/PYL family of START proteins. *Science* 324: 1068–71.
- Pucciariello, C., Parlanti, S., Banti, V., Novi, G., and Perata, P. (2012). Reactive oxygen species-driven transcription in Arabidopsis under oxygen deprivation. *Plant Physiol.* 159: 184–96.
- Rocha, M., Licausi, F., Araújo, W.L., Nunes-Nesi, A., Sodek, L., Fernie, A.R., and van Dongen, J.T. (2010). Glycolysis and the tricarboxylic acid cycle are linked by alanine aminotransferase during hypoxia induced by waterlogging of *Lotus japonicus*. *Plant Physiol.* 152: 1501–13.

- Rodrigues, A. et al. (2013). ABI1 and PP2CA Phosphatases Are Negative Regulators of Snf1-Related Protein Kinase1 Signaling in Arabidopsis. *Plant Cell* 25: 3871–84.
- Schroeder, J.I., Delhaize, E., Frommer, W.B., Guerinot, M. Lou, Harrison, M.J., Herrera-Estrella, L., Horie, T., Kochian, L. V, Munns, R., Nishizawa, N.K., Tsay, Y.-F., and Sanders, D. (2013). Using membrane transporters to improve crops for sustainable food production. *Nature* 497: 60–6.
- Sun, X., Li, Y., Cai, H., Bai, X., Ji, W., Ding, X., and Zhu, Y. (2012). The Arabidopsis AtbZIP1 transcription factor is a positive regulator of plant tolerance to salt, osmotic and drought stresses. *J Plant Res* 125: 429–438.
- Sweetlove, L.J., Beard, K.F.M., Nunes-Nesi, A., Fernie, A.R., and Ratcliffe, R.G. (2010). Not just a circle: flux modes in the plant TCA cycle. *Trends Plant Sci.* 15: 462–70.
- Thimm, O., Bläsing, O., Gibon, Y., Nagel, A., Meyer, S., Krüger, P., Selbig, J., Müller, L.A., Rhee, S.Y., and Stitt, M. (2004). MAPMAN: a user-driven tool to display genomics data sets onto diagrams of metabolic pathways and other biological processes. *Plant J.* 37: 914–939.
- Umezawa, T., Nakashima, K., Miyakawa, T., Kuromori, T., Tanokura, M., Shinozaki, K., and Yamaguchi-Shinozaki, K. (2010). Molecular basis of the core regulatory network in ABA responses: sensing, signaling and transport. *Plant cell Physiol.* 51: 1821–39.
- Umezawa, T., Sugiyama, N., Takahashi, F., Anderson, J.C., Ishihama, Y., Peck, S.C., and Shinozaki, K. (2013). Genetics and phosphoproteomics reveal a protein phosphorylation network in the abscisic acid signaling pathway in *Arabidopsis thaliana*. *Sci. Signal.* 6: rs8.
- Usadel, B., Blasing, O.E., Gibon, Y., Retzlaff, K., Hohne, M., Gunther, M., and Stitt, M. (2008). Global transcript levels respond to small changes of the carbon status during progressive exhaustion of carbohydrates in *Arabidopsis* rosettes. *Plant Physiol.* 146: 1834–61.
- Verslues, P.E., Agarwal, M., Katiyar-Agarwal, S., Zhu, J., and Zhu, J.K. (2006). Methods and concepts in quantifying resistance to drought, salt and freezing, abiotic stresses that affect plant water status. *Plant J.* 45: 523–539.
- Weigel, R. and Glazebrook, J. (2002). *Arabidopsis: A Laboratory Manual* (Cold Spring Harbour Laboratory Press: New York).

- Weltmeier, F. et al. (2009). Expression patterns within the Arabidopsis C/S1 bZIP transcription factor network: availability of heterodimerization partners controls gene expression during stress response and development. *Plant Mol Biol* 69: 107–119.
- Weltmeier, F., Ehlert, A., Mayer, C.S., Dietrich, K., Wang, X., Schutze, K., Alonso, R., Harter, K., Vicente-Carbajosa, J., and Droge-Laser, W. (2006). Combinatorial control of Arabidopsis proline dehydrogenase transcription by specific heterodimerisation of bZIP transcription factors. *EMBO J* 25: 3133–3143.
- Wiese, A., Elzinga, N., Wobbes, B., and Smeekens, S. (2004). A conserved upstream open reading frame mediates sucrose-induced repression of translation. *Plant Cell* 16: 1717–1729.
- Xuan, Y.H., Hu, Y.B., Chen, L.-Q., Sosso, D., Ducat, D.C., Hou, B.-H., and Frommer, W.B. (2013). Functional role of oligomerization for bacterial and plant SWEET sugar transporter family. *Proc. Natl. Acad. Sci. U. S. A.* 110: E3685–94.
- Yoshida, T., Fujita, Y., Sayama, H., Kidokoro, S., Maruyama, K., Mizoi, J., Shinozaki, K., and Yamaguchi-Shinozaki, K. (2010). AREB1, AREB2, and ABF3 are master transcription factors that cooperatively regulate ABRE-dependent ABA signaling involved in drought stress tolerance and require ABA for full activation. *Plant J.* 61: 672–85.
- Yu, C., Hou, X.L., and Wu, P. (2005). [The effects of phosphorus, glucose and cytokinin on SEN1 gene expression in Arabidopsis]. *Zhi Wu Sheng Li Yu Fen Zi Sheng Wu Xue Xue Bao* 31: 85–89.
- Zhang, Y. and Schläppi, M. (2007). Cold responsive EARLI1 type HyPRPs improve freezing survival of yeast cells and form higher order complexes in plants. *Planta* 227: 233–43.

FIGURES

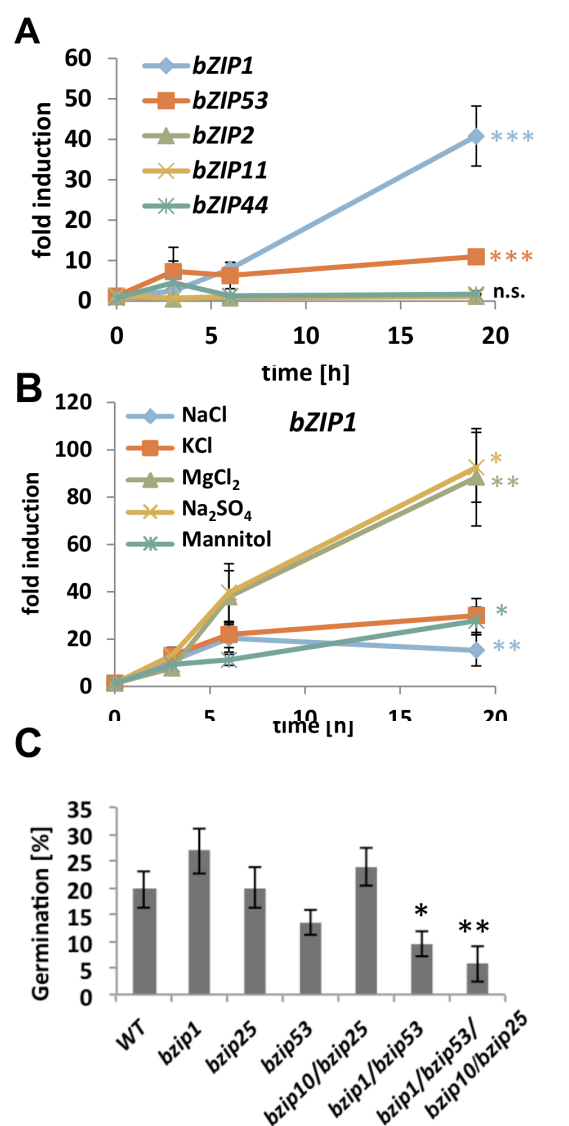


Figure 1. Stress-induced transcription of bZIP1 and bZIP53 and their functional impact on germination. (A) Transcript abundance of the indicated group S1-bZIP genes was analyzed by RT-qPCR in roots of hydroponically grown Col-0 plants treated with 150 mM NaCl. (B) Induction of bZIP1 by equiosmotic concentrations of salt (NaCl, KCl, MgCl₂, Na₂SO₄) or mannitol solutions. Osmolarity was adjusted to 0,25 mosM/l. Given are mean values (\pm SE). WT and respective mutants 19 h post-treatment (A) and untreated and treated WT after 19 h (B) are compared by Students t-Test. (C) Germination rate of WT and the indicated bZIP single and multiple T-DNA insertion mutants grown on MS-medium supplemented with 175 mM NaCl. Germination rates of stressed mutants are calculated in percent of the respective untreated line. Given are mean values (n=170 -350; \pm SD); * p < 0.05, ** p < 0.01, *** p < 0.001.

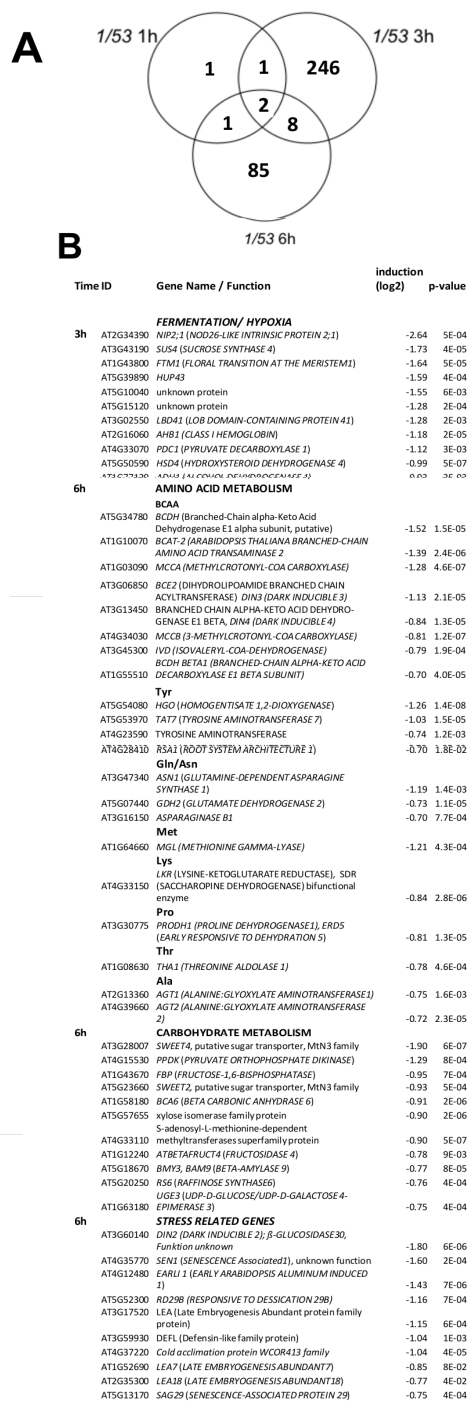


Figure 2. Transcriptome analysis comparing roots of NaCl-treated (150 mM) hydroponically grown Col-0 WT and bzip1/bzip53 plants. (A) Venn-diagram presenting the number of down-regulated genes comparing WT and bzip1/bzip53 mutant plants 1, 3 and 6 h after salt-treatment ($\log_2 \geq 0.7$; $p < 0.01$). (B) List of selected genes (selected by function and time of salt-treatment) down-regulated in bzip1/bzip53 in comparison to WT roots. Given are differential expression levels (\log_2) and p-values.

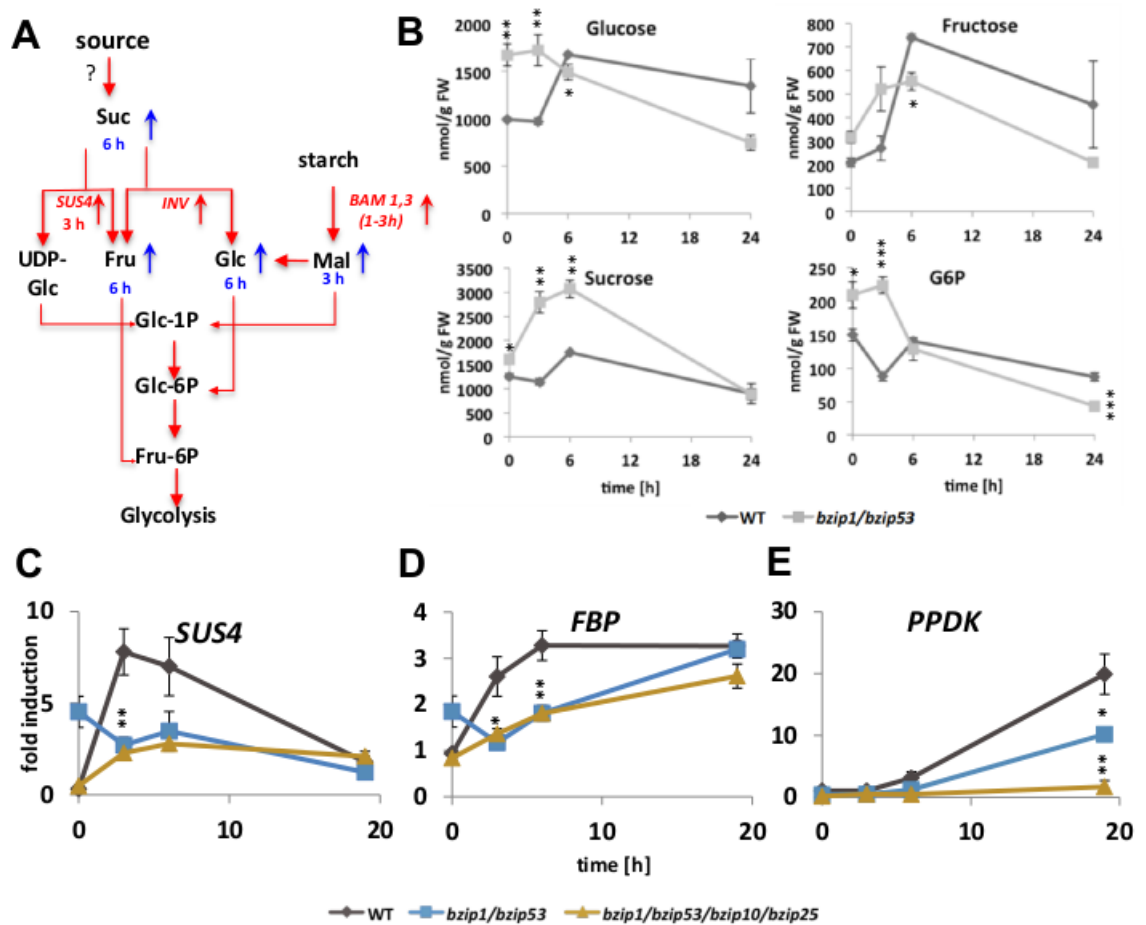


Figure 3. Changes in carbohydrate metabolism comparing NaCl-treated hydroponically-grown roots of WT and *bzip1/bzip53* mutants. (A) Simplified overview of carbohydrate metabolism. Changes in sugar concentrations or gene expression are indicated by blue or red arrows, respectively (see Supplemental Data Set 3, Figure 3B). Times (in h) indicate maxima of metabolites (blue) or transcript abundance (red). (B) Changes in carbohydrate concentrations (nmol/g fresh weight) after salt treatment in WT (black) and *bzip1/bzip53* (grey). Given are mean values (\pm SD) of 3 biological replicates. (C-E) RT-qPCR analysis of *SUS4* (C), *FBP* (D), and *PPDK* (E) expression in WT (black), *bzip1/bzip53* (blue) and *bzip1/bzip53/bzip10/bzip25* (brown) plants. Given are mean expression values (\pm SD). *SUS4*: SUCROSE SYNTHASE4; *INV*: INVERTASE; *BAM*: β -AMYLASE, *PPDK*: PYRUVATE ORTHOPHOSPHATE DIKINASE; *FBP*: FRUCTOSE-1,6-BISPHOSPHATASE; *Glc*: glucose; *Fru*: fructose; *Suc*: sucrose; UDP-Glc: Uridine-diphosphate-glucose. Significant differences between WT and mutants have been defined by Student's t-test for each time-point. Test: * $p < 0.05$, ** $p < 0.01$, *** $p < 0.001$.

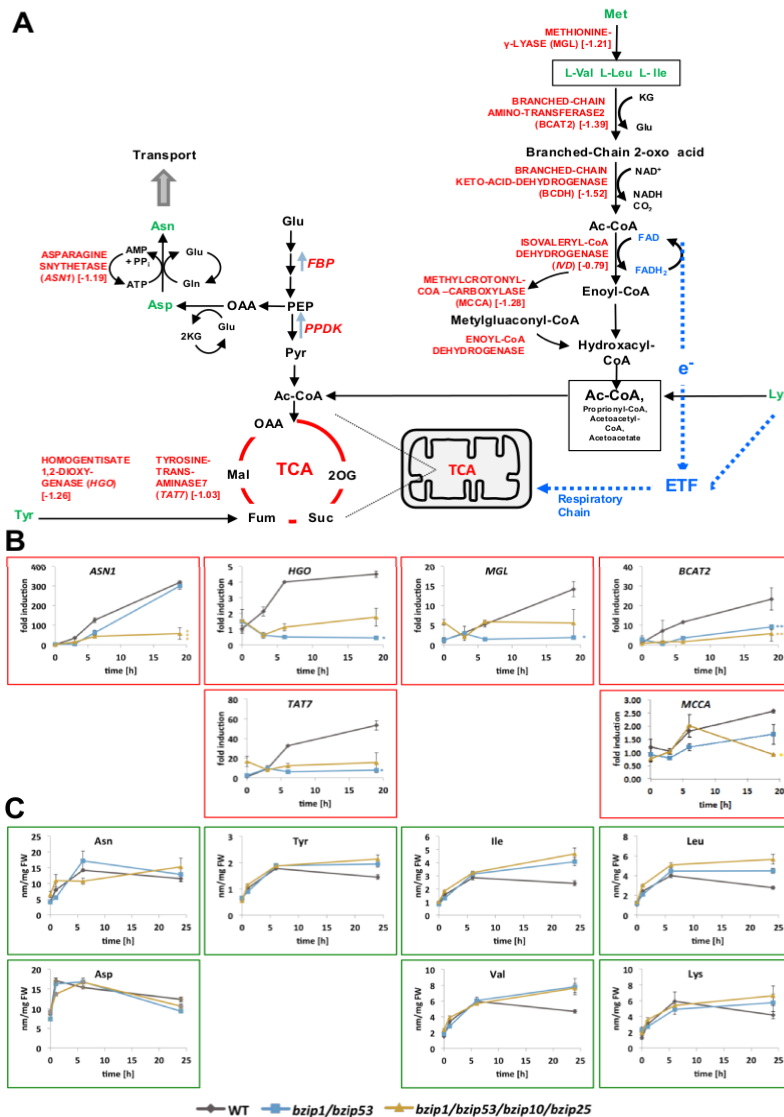


Figure 4. Impact of C and S1 bZIP factors on aa metabolism of salt-treated roots. (A) Simplified overview of the catabolism of Branched Chain Amino Acids (BCCA: Ile, Leu, Val), Met, Lys, and Tyr and biosynthesis of Asn. Relevant enzymes are indicated in red and array data of the correspondent genes differentially regulated in bzip1/bZIP53 are given in brackets. TCA: Tricarboxylic Acid Cycle; ETF: ELECTRON-TRANSFER-FLAVOPROTEIN. (B) RT-qPCR analysis of the salt-induced gene expression comparing WT (black), bzip1/bzip53 (blue) and bzip1/bzip53/bzip10/bzip25 (brown) plants. Given are mean fold (± SE) induction values. Students t-Test compares WT and mutant at the respective time-point: * p < 0.05, ** p < 0.01, *** p < 0.001. (C) Quantification of selected aa concentrations (green) observed in the mutants indicated in (B). Given are mean values (± SE) of n=5 replicates.

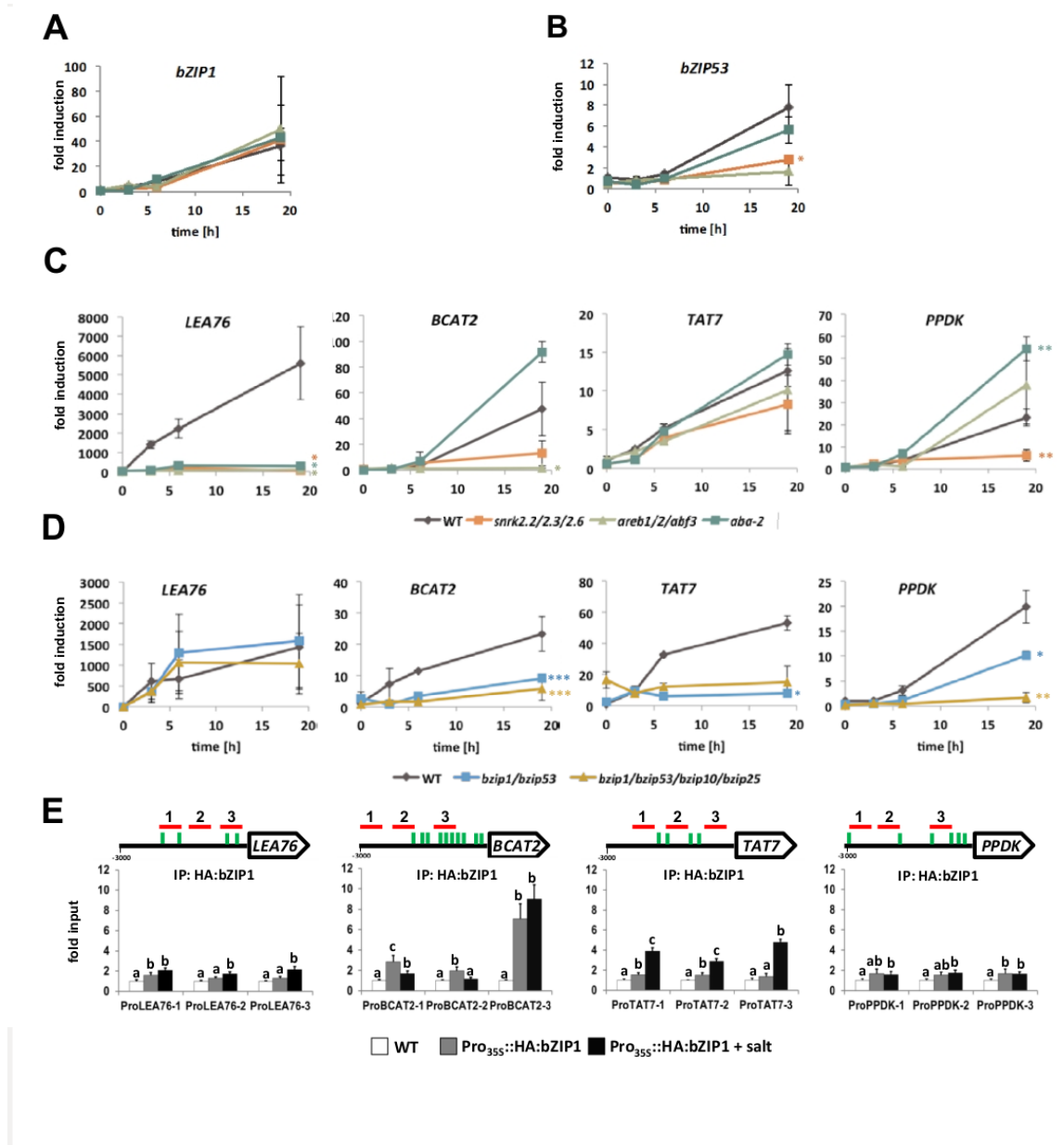


Figure 5. Mutant and ChIP analysis to study regulation of bZIP1, bZIP53 and potential target genes in salt-treated roots. (A-C) RT-qPCR analysis of salt-treated mutant roots impaired in defined components of the ABA-SnRK2-AREB pathway studying bZIP1 (A), bZIP53 (B) and the potential targets PPKD, TAT7, BCAT2 and LEA76 (C). WT (black), *aba2* (blue), *snrk2.2/3/6* (orange) and *areb1/2/abf3* (light green) (see Figure 7 for details). (D) RT-qPCR analysis of the same target genes in WT (black), *bzip1/bzip53* (blue) and *bzip1/bzip53/bzip10/bzip25* (brown) mutant plants. Given are mean fold (\pm SE) induction values. Students t-Test compares WT and mutants at the respective time-point: * $p < 0.05$,

** $p < 0.01$, *** $p < 0.001$. (E) ChIP-PCR analyses for the indicated promoters using an α -HA-antibody to detect binding of HA:bZIP1. Upper panel describes the promoter scanning experiments indicating localization of the primer derived PCR products (red) and putative G-box related binding sites (green). Lower panel: Compared are fold input levels calculated relative to WT (white; set to 1) and Pro 35S ::HA:bZIP1 plants untreated (grey) and induced with salt (black). Significant differences have been determined by one-way ANOVA followed by a Bonferroni post-hoc test and are labeled with individual letters.

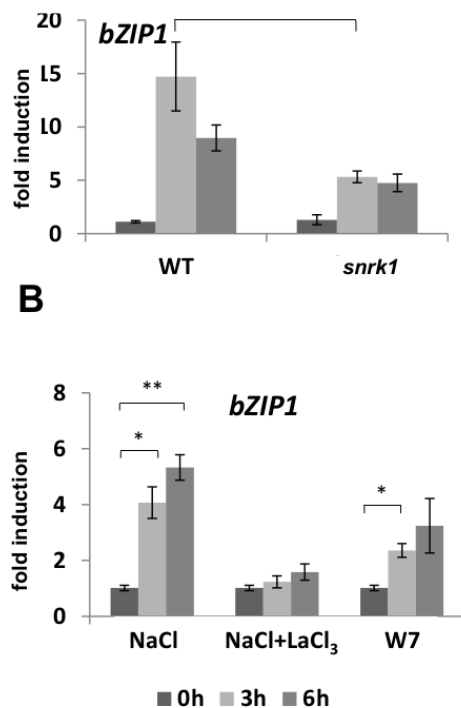


Figure 6. Transcription of bZIP1 in roots depends on various signaling pathways. (A) RT-qPCR analysis of WT and inducible snrk1 loss-of-function plants. (B) Ca²⁺ signaling was manipulated using the inhibitor La³⁺ or the Ca²⁺ agonist W7, respectively. 3-week-old plants were grown on MS medium and treated with NaCl for 0h, 3h or 6h. Duration of treatments are indicated by a colour code. Given are mean fold (\pm SE) induction values of 4-6 replicates. All experiments are repeated at least three times. Students t-Test: * $p < 0.05$, ** $p < 0.01$, *** $p < 0.001$, n. s.: not significant.

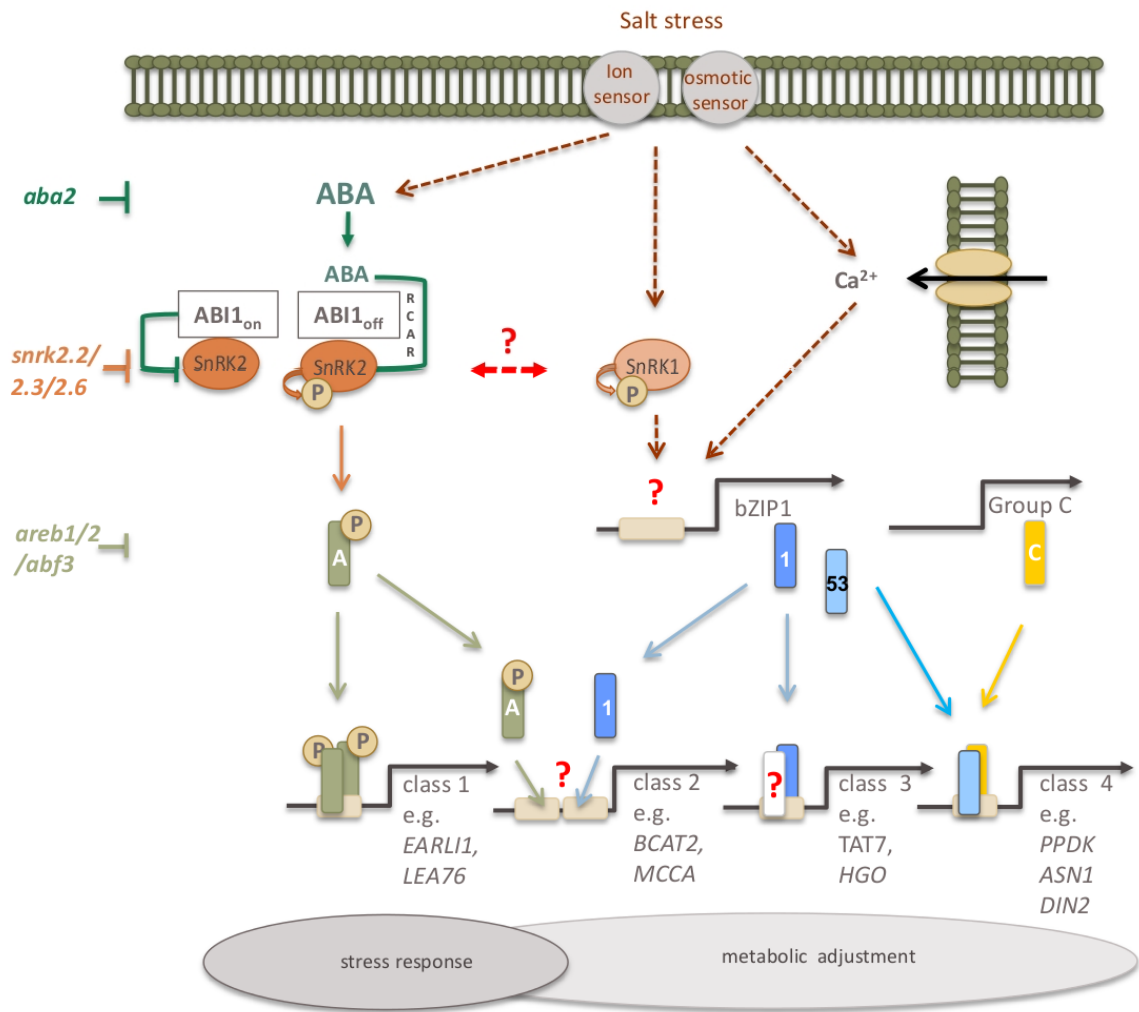
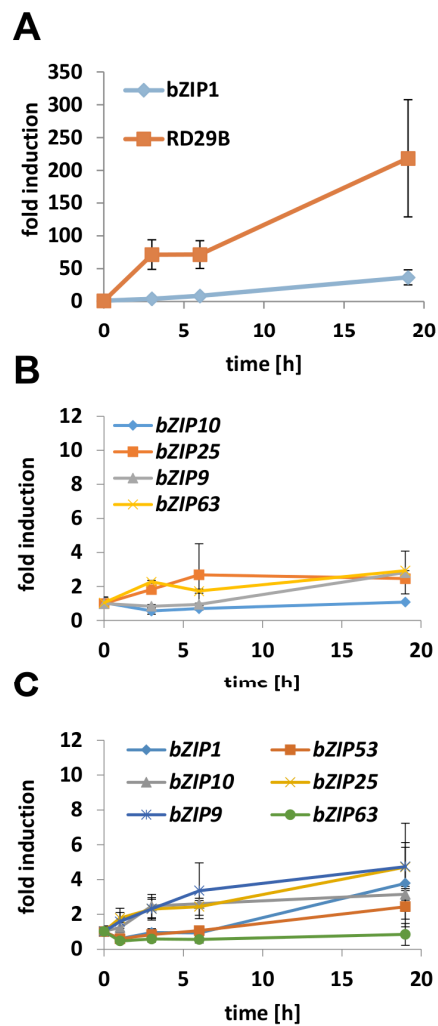
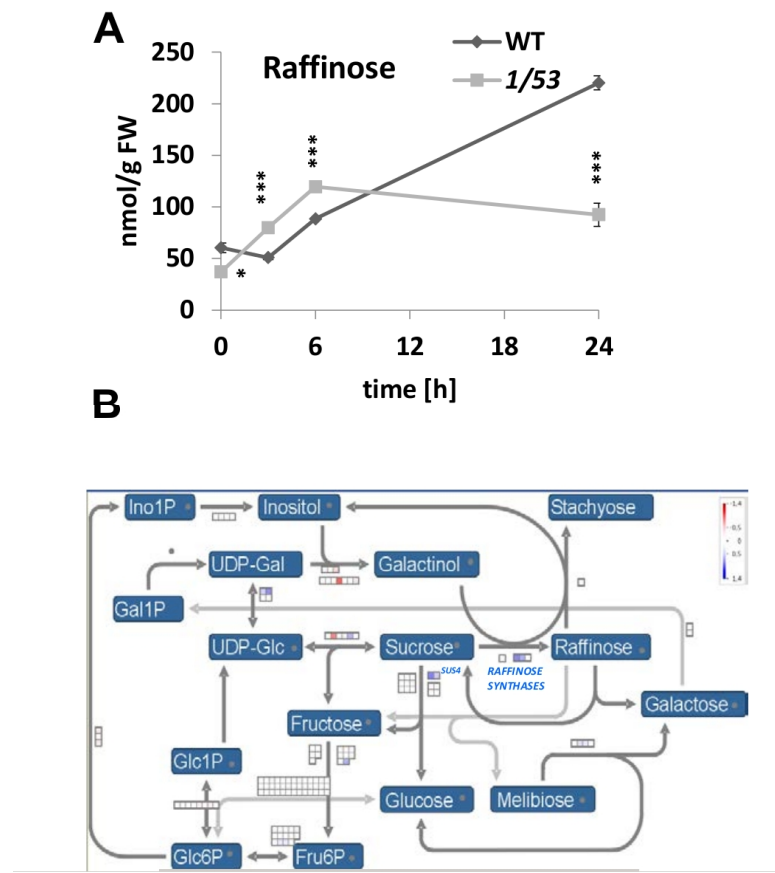


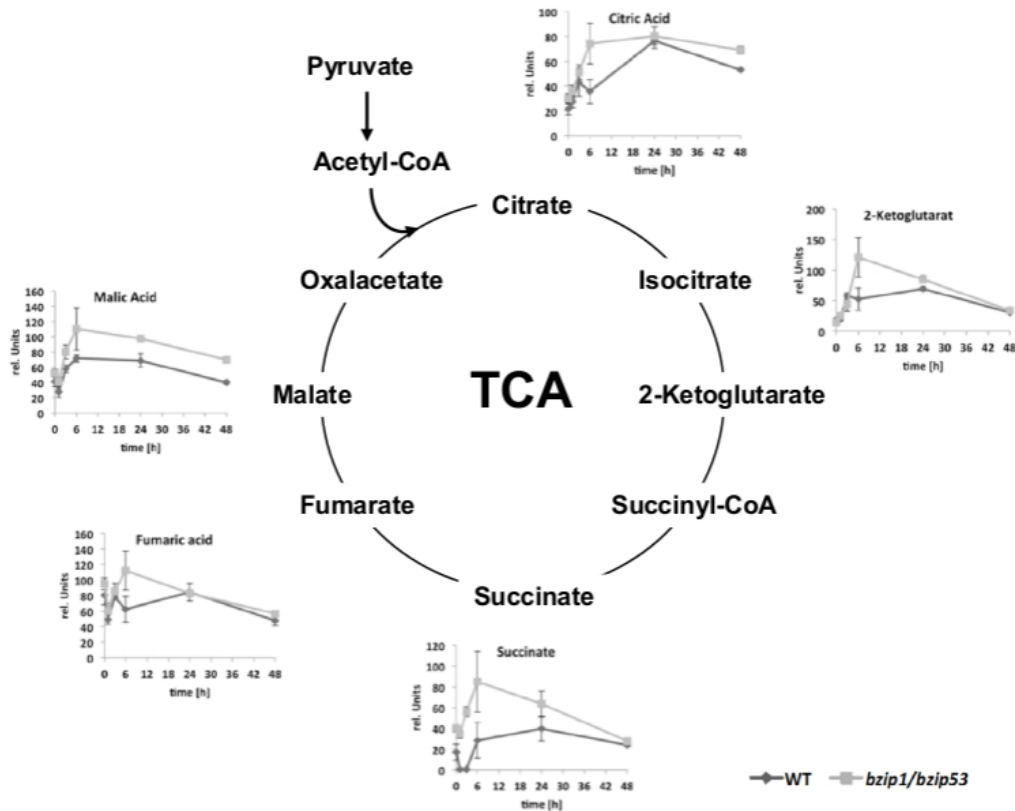
Figure 7. Model summarizing the findings on the regulation of bZIP1 transcription in salt stress response in Arabidopsis roots and the crosstalk of the ABA-independent SnRK1-bZIP1 pathway and ABA-dependent SnRK2-AREB pathway. Due to the mutant and ChIP PCR analysis, putative bZIP1 target genes can be classified as dependent on the ABA/SnRK2/AREB pathway (class I), the SnRK1/bZIP1 pathway (class III) or both (class II). Class IV genes depend on group C and S1 bZIPs and are independent of AREB-like TFs. A potential interaction between SnRK1 and SnRK2 kinases is proposed by (Umezawa et al., 2013; Rodrigues et al., 2013).



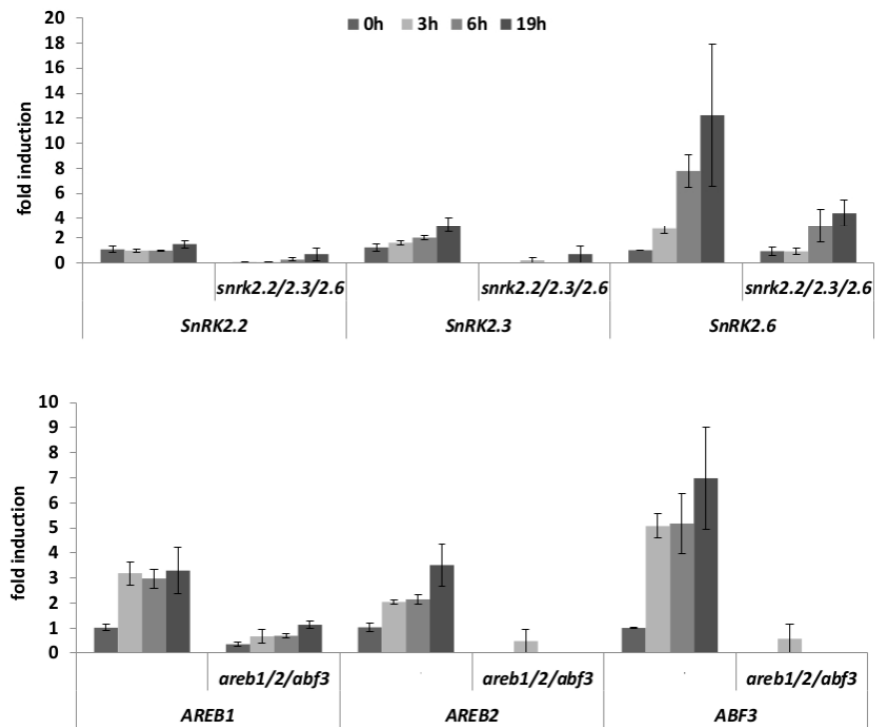
Supplemental Figure 1. Transcription of group C and S1 bZIPs after salt-treatment. RT-qPCR analysis of bZIP1 and RD29B in roots (A), group C bZIPs in roots (B) or group C and S1 bZIPs in leaves (C) at the time-points indicated. Given are mean fold (\pm SD) induction values.



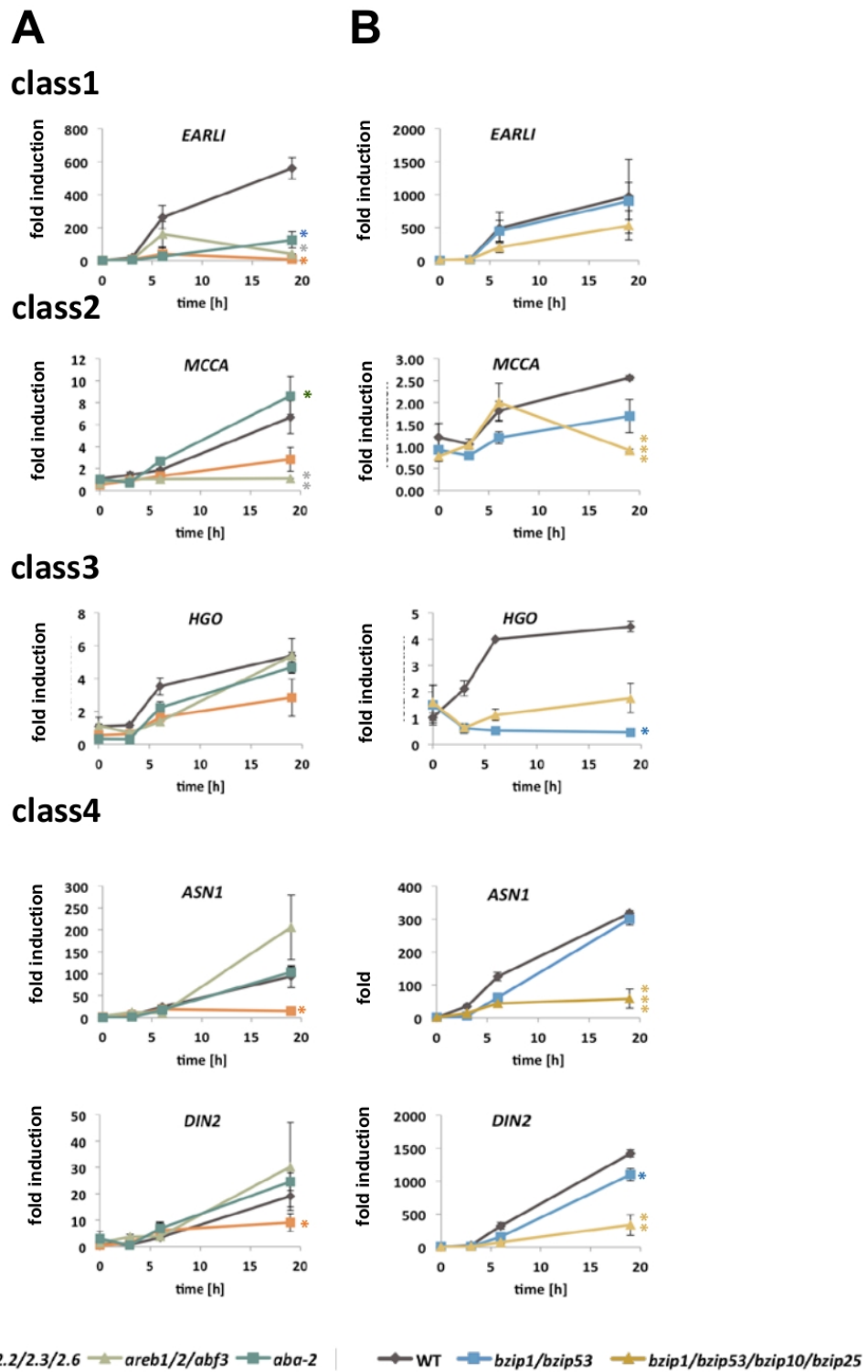
Supplemental Figure 2. Carbohydrate metabolism in salt-treated WT and *bzip1/bzip53* roots. (A) Measurement of raffinose (nmol/g fresh weight). Given are mean fold (\pm SD) values. Students t-Test: * $p < 0.05$, ** $p < 0.01$, *** $p < 0.001$. (B) MAPMAN representation of cell wall sugars. Downregulated genes comparing WT and *bzip1/bzip53* roots 3 h after salt treatment are colour-coded in blue, upregulated in red. RAFFINOSE SYNTHASE6 (DIN10) is marked as down-regulated in *bzip1/bzip53* roots.



Supplemental Figure 3. Metabolites of the TCA cycle but not transcription of the related genes is altered in the *bzip1/bzip53* mutant. Schematic overview summarizing changes in TCA cycle intermediates relative to the un-induced situation. WT (black) *bzip1/bzip53* (grey).

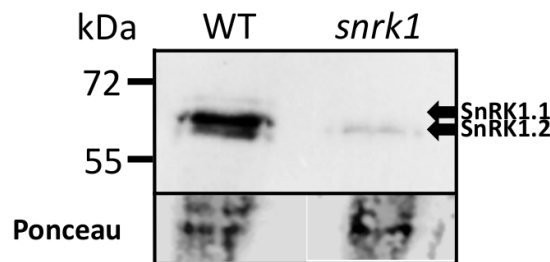


Supplemental Figure 4. qRT-PCR validation of salt-induced expression of SnRK2 and AREB genes in WT and the respective *snrk2.2/3/6* (Fujita et al., 2009), *areb1/areb2/abf3* (Yoshida et al., 2010) multiple T-DNA insertion mutants. Hydroponically-grown plants were cultivated on MS-medium treated with NaCl for the times indicated. Given are mean fold induction values (\pm SD).



Supplemental Figure 5. RT-qPCR analysis of bZIP1 regulated class 1 – 4 genes in WT (black), *aba2* (blue), *snrk2.2/3/6* (orange) and *areb1/2/abf3* (light green) mutants (A) and in

WT (black), *bzip1/bzip53* (blue) and *bzip1/bzip53/bzip10/bzip25* (brown) plants (B). Given are mean fold (\pm SE) induction values. Significance is calculated relative to the corresponding time-point of the WT; Students t-Test: * $p < 0.05$, ** $p < 0.01$, *** $p < 0.001$.



Supplemental Figure 6. Characterisation of *snrk1* mutant plants. Expression of SnRK1.1 and SnRK1.2 was analysed by immunoblotting applying root protein extracts from 2-weeks-old WT and *snrk1* mutant plants, which were cultivated on MS medium supplemented with NaCl and β -Estradiol. Arrows indicate the position of the respective SnRK1 kinases. Equal amounts of protein was loaded as confirmed by Ponceau S staining.

SUPPLEMENTAL METHODS

ChIP-PCR Root material (~ 5 g) was harvested from 3-week-old plants grown on 1xMS without sugars after a 6 h NaCl (400 mM) or mock treatment. Subsequently samples were incubated with crosslinking buffer (50 mM KH₂PO₄ /K₂HPO₄ buffer [pH 5.8], 1 % (v/v) formaldehyde) for 30 min under vacuum. Crosslinking was stopped by incubating the samples in glycine buffer (50 mM KH₂PO₄ /K₂HPO₄ buffer [pH 5.8], 0.3 M glycine) for 15 minutes under vacuum followed by further washing with ice-cold water. Samples were frozen in liquid nitrogen and subsequently grinded. Nuclei extraction was performed in a cooling chamber at 4°C. Therefore root material was re-suspended in 24 ml ice-cold extraction buffer (1 M hexylenglycol, 50 mM PIPES-KOH [pH 7.2], 10 mM MgCl₂, 5 mM β -mercaptoethanol, 1 tablet/10ml complete protease inhibitor cocktail tablets, Roche) and was cleared by filtration through two layers of miracloth. 1 ml 25% Triton X-100 was added dropwise to the extract. After incubation for 15 min nuclei were isolated by density

gradient centrifugation using a 35 % percoll cushion. The nuclei pellet was re-suspended in sonication buffer (10 mM Tris/HCl [pH 7.4], 1 mM EDTA [pH 8.0], 0.25 % SDS and protease inhibitor) prior to sonification for 20 x 20 sec. Chromatin was cleared by centrifugation for 15 min at 11.000g, 4°C and frozen in aliquots. For each IP, 15 µg chromatin and 4 µg ChIP grade α-HA (ab9110) antibody (Abcam Cambridge, UK) were used. 70 µl of protein A coated magnetic beads (Invitrogen, Karlsruhe, Germany) dissolved in ice-cold extraction buffer, supplemented with protease inhibitor (Roche, Mannheim, Germany) were applied to each sample. Antibody-antigen binding was achieved during a 2 h incubation step at 4°C and slow rotation on an Intellimixer. To remove unspecifically bound proteins, beads were washed 4 times with washing buffer supplemented with protease inhibitor, before precipitated protein-DNA complexes were dissolved in elution buffer. Precipitated DNA was quantified by RT-qPCR using the oligonucleotide primers summarized in Supplemental Data Set 1. Data was normalized to DNA input, which was quantified by ACTIN8 transcript abundance. Results were obtained from 2 independent plant pools per line from which 2-4 independent ChIP experiments were performed.

Transcriptome studies: Transcriptome analysis was performed on root material from hydroponically grown Col-0 WT and bzip1/bzip53 plants 1 h, 3 h, and 6 h after treatment with 150 mM NaCl. RNA purity and integrity were confirmed by using a RNA 6000 Nano Assay (Agilent, <http://www.home.agilent.com>) and gel electrophoresis. cRNA labeling, hybridization, washing and scanning of Affymetrix Arabidopsis ATH1 GeneChips® (Affymetrix, <http://affymetrix.com>) was performed according to Affymetrix OneCycle Lab protocols. Data were analysed statistically using the R language environment for statistical computing (<http://www.r-project.org>) version 2.9 and Bioconductor release 2.4 (Gentleman et al., 2004). Data were normalized using the Robust Multichip Average (RMA) expression measure in the Affy package (Gautier et al., 2004). Differentially expressed genes were identified using the LIMMA package. The obtained p-values were corrected for multiple testing errors using the BH procedure (Benjamini and Hochberg, 1995) and transferred to Microsoft Excel™. The probe set sequences were aligned to the TAIR9 gene model database of transcripts (www.arabidopsis.org). Data analyses (triplicate) were performed using MAPMAN (Thimm et al., 2004).

Metabolic studies The metabolic profile from treated and untreated root material was determined 1, 3, 6, 24 and 48 h post-treatment using GC-MS (Kempa et al., 2008). Amino

acid levels were determined by UPLC-ESI-qTOF-MS (Acquity UPLC, Synapt HDMS G2, Waters, Milford, MA, USA) prior derivatization with the AccQ Ultra Kit (Waters, Eschborn, Germany) as described (Salazar et al., 2012). Sugars were analyzed using a Waters Acquity ultra-high-performance liquid chromatograph coupled to a Waters Micromass Quattro Premier triple quadrupole mass spectrometer (Milford, MA, USA) with a electrospray interface (ESI). Chromatographic separation was carried out according to application note WA60126 with a modified flow rate of 0.2 mL/min. Sugars were detected in the negative electrospray mode (ESI⁻) at a source temperature of 120°C and a capillary voltage of 3.25 kV. Nitrogen was used as desolvation and cone gas with flow rates of 800 L h⁻¹ at 350°C and 25 L h⁻¹. The mass spectrometer was operated in the multiple reaction monitoring (MRM) mode using Argon as collision gas at a pressure of approximately 3 × 10⁻³ bar.

Supplemental References:

- Benjamini, Y. and Hochberg, Y. (1995). Controlling the False Discovery Rate: A Practical and Powerful Approach to Multiple Testing. *J. R. Stat. Soc. Ser. B* 57: 289 – 300.
- Fujita, Y. et al. (2009). Three SnRK2 protein kinases are the main positive regulators of abscisic acid signaling in response to water stress in Arabidopsis. *Plant Cell Physiol.* 50: 2123–32.
- Gautier, L., Cope, L., Bolstad, B.M., and Irizarry, R.A. (2004). Affy - Analysis of Affymetrix GeneChip data at the probe level. *Bioinformatics* 20: 307–315.
- Gentleman, R.C. et al. (2004). Bioconductor: open software development for computational biology and bioinformatics. *Genome Biol* 5: R80.
- Kempa, S., Krasensky, J., Dal Santo, S., Kopka, J., and Jonak, C. (2008). A central role of abscisic acid in stress-regulated carbohydrate metabolism. *PloS One* 3: e3935.
- Thimm, O., Blasing, O., Gibon, Y., Nagel, A., Meyer, S., Kruger, P., Selbig, J., Muller, L.A., Rhee, S.Y., and Stitt, M. (2004). MAPMAN: a user-driven tool to display genomics data sets onto diagrams of metabolic pathways and other biological processes. *Plant J* 37: 914–939.
- Yoshida, T., Fujita, Y., Sayama, H., Kidokoro, S., Maruyama, K., Mizoi, J., Shinozaki, K., and Yamaguchi-Shinozaki, K. (2010). AREB1, AREB2, and ABF3 are master transcription factors that cooperatively regulate ABRE-dependent ABA signaling involved in drought stress tolerance and require ABA for full activation. *Plant J.* 61: 672–85.

Chapter 6: The crucial metabolic kinase SnRK1 controls lipid degradation to support phase transition from heterotrophy to autotrophy during Arabidopsis seedling establishment

Lorenzo Pedrotti¹, Agnes Fekete¹, Elmar Wolf², Martin Eilers², Martin J. Müller¹ and Wolfgang Dröge-Laser¹

Author's affiliation.

¹Department of Pharmaceutical Biology, Julius-von-Sachs-Institute, Biocenter, Julius-Maximilians-Universität Würzburg, Würzburg, 97082, Germany;

²Department of Biochemistry and Molecular Biology, Theodor-Boveri-Institute, Biocenter, Julius-Maximilians-Universität Würzburg, Würzburg, 97074, Germany;

Contact: wolfgang.droege-laser@uni-wuerzburg.de

This chapter is to consider as a first incomplete version of a manuscript. More effort has to be done to implement this draft before having it ready for a publication. It was included in this thesis to emphasize the importance of this argument and to stimulate future investments to carry forward the project.

INTRODUCTION

The onset of plant life is characterized by a major metabolic phase transition. Seed germination and subsequent seedling establishment are, indeed, entirely heterotrophic (Theodoulou & Eastmond, 2012). Seed reserves need to be rapidly converted to soluble metabolites that can be transported throughout the seedling to be used to sustain growth and to establish the photosynthetic apparatus (ref). Subsequently, the plant's life style changes based on an autotrophic metabolism.

Proteins, lipids, and sugars are the three major compounds stored in seeds. In particular, lipids are stored in the form of triacylglycerols (TAGs) and TAGs represent about the 45% of the seed weight of the oil-seed plant *Arabidopsis thaliana* (Graham, 2008). After germination, specialized programs have evolved to ensure the rapid and efficient conversion of TAGs to sugars. The first step in the TAGs usage is their remobilization from the oil bodies. Oil bodies are spherical cytoplasmatic organelles of 0.5-2 μm in diameter, consisting of a TAGs matrix covered by a phospholipids monolayer in which proteins are embedded that prevent oil body coalescence (Chapman, Dyer, & Mullen, 2012). Oleosins and caleosins are the predominant proteins sharing a crucial role in lipid remobilization from oil bodies during seed germination (Ref 3 seed storage give and take). After remobilization TAGs are hydrolyzed to produce free fatty acids (FAs) and glycerol. FAs are degraded by β -oxidation to yield acetyl-CoA which subsequently is condensed into 4-carbon compounds via the glyoxylate cycle localized in the peroxisomes (T. G. Cooper, 1969). Products of the glyoxylate cycle can either be used by the mitochondrial respiration or transported to the cytoplasm and enter the gluconeogenesis which is of crucial importance for seedling establishment. In contrast to non-plant eucaryotes, which rely on PHOSPHOENOLPYRUVATE CARBOXYKINASE (PCK) to fuel gluconeogenesis, recent findings disclosed a second enzymatic route to exist in plants, making use of PYRUVATE ORTHOPHOSPHATE DIKINASE (PPDK) (Eastmond et al., 2015). Whereas PCK mainly uses compounds derived by lipid breakdown, PPDK uses pyruvate, which is derived from amino acid (aa) breakdown. SnRK1 kinases are master regulator of plant metabolism, activated in multiple and different situations when catabolic activity is needed to sustain plant life. SnRK1 kinases reprograms plant metabolism regulating enzymes, transcription factors or miRNAs (Confraria, Martinho, Elias, Rubio-Somoza, & Baena-González, 2013). Recently, we have demonstrated that SnRK1 controls alternative

mitochondrial respiration during starvation via transcription of *ELECTRON-TRANSFER FLAVOPROTEIN: UBIQUINONE OXIDO-REDUCTASE (ETFQO)* part of the ETF/ETFQO electron transfer complex (Pedrotti et al., Chapter 4). As germination and subsequent seedling establishment rely only on mitochondrial respiration, we investigated the involvement of SnRK1 in the regulation of seed establishment. We applied a combination of chemical, genetics, genomics and cell-based analyses to dissect the SnRK1 signaling network in TAGs remobilization. We discovered that SnRK1 controls the expression of oleosin and caleosin genes, interfering with the complete lipid remobilization from the oil bodies. This SnRK1 regulated molecular framework provides energy, metabolites and biomass necessary to fuel seedling establishment until the complete development of the photosynthesis apparatus and the beginning of the “eternal” autotrophic plant life.

RESULTS

SnRK1 has a central role in the regulation of the early stage of seed establishment.

Baena-González and colleagues showed that SnRK1 is an important activator of catabolic processes (Baena-González, Rolland, Thevelein, & Sheen, 2007). Therefore, we speculated about its involvement in the activation of seed storage degradation necessary to sustain plant life in the early stage of seedling establishment. To test this hypothesis, we applied the phenotypical growth assays recently described by Xiong and colleagues (Xiong & Sheen, 2013) to study phase transition from heterotrophic to autotrophic seedling growth. Accordingly, 3-day-old *Arabidopsis* seedlings developed green cotyledons but soon entered a mitotic quiescent state, characterized by arrested root growth (Figure 1). Exogenous glucose taken up by the root (Xiong & Sheen, 2012) was sufficient to fully substitute for photosynthetic support of root meristem activation and growth (Figure 1). This assumption was further supported, as WT plants plant treated with the photosynthesis inhibitor DCMU show glucose dependent activation of the root meristem (Xiong & Sheen, 2013). To study the impact of SnRK1 in this model system, we made use of the *snrk1* loss-of-function approach (Pedrotti et. al., Chapter 4). Recent work established, that a double knock-out in the redundantly active *Arabidopsis* SnRK1 genes (*SnRK1.1/AKIN10* and *SnRK1.2/AKIN11*) is lethal. We therefore expressed an estradiol (Est) inducible artificial microRNA (ami) construct targeting *SnRK1.2* in a *snrk1.1* T-DNA knock-out line. As demonstrated in our growth system, we can significantly reduce the amount of SnRK1

protein after Est-treatment.

Focusing on phenotypical changes, we observed that *snrk1.1/1.2* plants were unable to establish functional, green-colored cotyledons (Figure 1A). 6 days after germination the majority of the seedlings appeared with white cotyledons and root primordia shorter than 2 mm as quantified in Figure 1B, C. This phenotype resembles plants impaired in lipids remobilization or degradation (Ref). Surprisingly, glucose treatment induced cotyledon establishment had no effects on root growth of the *snrk1.1/1.2* mutant (Figure 1 A, B). On the contrary, SnK1.1 over expressing seedlings (SnRK1.1 o.e) showed green cotyledons and well developed root (Figure 1A, B), even when plant were treated with DCMU in absence of glucose. Apparently, SnRK1.1 o.e. plants avoid the quiescent meristem state, but continuously grew careless of the presence of glucose or DCMU in the medium. These results revealed that SnRK1 signaling actively contributes to seedling establishment. Importantly, Moreover, SnRK1 kinases appears to have a double and distinct functionality: firstly with respect to cotyledon development, glucose supplementation can compensate for absence of SnRK1 in the mutant, whereas this is not the case for secondly root development.

SnRK1 is an important activator of catabolic processes at the onset of plant life.

To better understand the molecular landscape of the SnRK1 signalling network during seed establishment, we performed genome-wide expression profiling in WT and *snrk1.1/1.2* 3 days old seedlings. Based on stringent statistic (P_{adjust} (“BH” correction) < 0.01) we defined 1470 activated and 2215 repressed genes differentially regulated by SnRK1 (Supplemental material 1). In line with the expected function of SnRK1 on the activation of catabolic processes, GO enrichment analysis showed that *snrk1.1/1.2* had severe problems in gaining energy from seed storage compounds. In particular we observed that generation of precursor metabolites and energy was depleted due to the down-regulation of the major energy providing pathways such as fatty acid degradation, carbohydrate and amino acid catabolism. The inability of degrading lipids and carbohydrates resulted in the down-regulation of several anabolic processes, such as cell growth, root and leaves development. Viceversa, the expression of genes involved in protein catabolism, proteolysis, and cellular respiration was up-regulated. They probably were exploited as the last attempt to provide energy and precursors indispensable for the development of a functional photosynthetic apparatus. Notably, also the expression of genes involved in

regulation of cell death were up-regulated in *snrk1.1/1.2* in comparison to WT plants. These findings further demonstrate a primary function of SnRK1 in the orchestration of seed storage compounds catabolism (Figure 2).

SnRK1 contributes to the catabolism of seed storage lipids.

In order to investigate further how SnRK1 contributes to the catabolism of seed storage lipids during germination, lipid analysis in three days old WT and *snrk1.1/1.2* seedlings grown on mineral medium were performed using liquid chromatography coupled to mass spectrometry (Supplementary Figure 1A). Orthogonal partial least square discriminant analysis (OPLS-DA) revealed significant higher level of 25 from 2061 lipid features in *snrk1.1/1.2* seedlings compared to the WT (Supplementary Figure 1B).

Structure elucidation of the differentiating lipids were performed by comparing their accurate masses with the Database of Lipid Metabolites and Pathways Strategy (LIPID MAPS). In accordance of the expectation, 19 from 25 differentiating lipid features were annotated as ammonium adducts of TAGs. In addition, their collision induced fragmentation revealed a loss of fatty acyls resulting in abundant formation of diacylglycerol ions and protonated fatty acid fragments that are characteristic for TAGs (lit: Murphy et al (2002) Analytical and Bioanalytical Chemistry 366:59-70). The identified TAG species consisted of fatty acyls with 52-58 carbon and 2-9 double bonds (Supplementary Table 1).

To investigate if the altered TAG content in *snrk1.1/1.2* seedlings was specific to the identified differentiating lipids, endogenous TAGs were determined using an in-house developed database (unpublished). Retention-time aligned molecule ion and fragment ions led to identification of 49 TAGs specified by the number of carbons and double bonds of the three fatty acids esterified to glycerol. The most abundant TAG species were identified as differentiating lipids in *snrk1.1/1.2* seedlings using OPLS-DA analysis (Supplementary Figure 2 and Figure 3A). In addition, all identified TAGs were determined to be at least 2-fold higher in *snrk1.1/1.2* comparing to WT. Our result suggest that TAG accumulation in the mutant seedlings was not species specific and thus total TAG content was used to characterize the contribution of SnRK1 in changes of energy storage lipid content during germination. The determined contents of TAGs were 5.7 $\mu\text{g}/\text{mg}$ and 14.1 $\mu\text{g}/\text{mg}$ in three days old WT and *snrk1.1/1.2* seedlings, respectively (Figure 3 B).

SnRK1 controls the lipid remobilization process.

Because of the strong accumulation of TAGs in *snrk1.1/1.2* plants, we investigated the possibility of an aberrant lipid usage. Oleosin and caleosin are known important proteins for the regulation of lipids remobilization from oil bodies. RT-qPCR experiments showed a reduced expression of *OLEOSIN* 1, 2, 3, and 4 and partially of *CALEOSIN* 1 in *snrk1.1/1.2* (Figure 4 A-E).

By feeding glucose or a short chain fatty acid, sodium-octanoate, the cotyledons phenotype of *snrk1.1/1.2* plants could be rescued (Figure 1 and 5). As expected an high concentration of Na-octanoate resulted toxic for WT, *snrk1.1/1.2*, and SnRK1.1 o.e. plants, although the last one could develop a longer root than the other tested genotypes. Lower concentration of Na-octanoate promote root growth of WT seedlings, probably by providing enough energy to overcome the meristematic quiescent phase. These results strictly indicated that SnRK1 controls an upstream process of the lipids degradation pathway.

SnRK1 has a primary role in the regulation of plant transcriptome in response to sugar treatment and energy conditions.

In WT seedlings glucose application was able to induce the reactivation of the root meristem and the subsequent root growth. Similarly to what already described by Sheen and colleagues, glucose treatment induced the expression of 1014 genes and simultaneously repressed that of 741 genes (Supplementary table 2). Remarkably, the glucose induced genes belonged to a myriad of different GO categories (Figure 6A). Beside metabolism-related GO classes, several development-related category were induced by glucose treatment, such as cell growth, shoot and root development, post-embryonic development, and transcription. Despite the ability of external applied glucose to induce cotyledons establishment in *snrk1.1/1.2* plantlets (Figure 1), glucose treatment affected the expression of only 128 genes in the *snrk1.1/1.2*. Interestingly, glucose treatment activated, the carbohydrate metabolism, lipids mobilization and metabolism. The expression of oleosin 1, 2, 3, and 4 and caleosin 1 was also induced by glucose treatment (Figure 4) as well as the expression of several seed storage albumin protein (Supplementary table 3) involved in the remobilization of lipids. Compatible with a primary role of SnRK1 in the regulation of seed establishment, none of the development-related GO category activated by glucose in WT seedlings were induced in *snrk1.1/1.2* plantlets (Figure 6.B-F). Taken together, these results revealed the centrality of SnRK1 in the regulation of plant transcriptome in response to sugar, or more in general energy, conditions.

DISCUSSION

The results presented in this paper clearly demonstrate the primary role of SnRK1 during the onset of plant life. Depending on the tissue or the developmental state, SnRK1 signaling respond to specific stimuli by triggering transcriptional changes which are generally accompanied by a down-regulation of energy consuming processes and an induction of ATP-producing pathways (Baena, Zhang 2009). We showed that SnRK1 orchestrates oil seed degradation in order to fuel the early postgerminative growth prior to photosynthetic establishment.

From results here presented it is clear that SnRK1 has a primary role in the activation of seed storage catabolism. Genome wide expression profiling shows that SnRK1 regulates the expression of several genes which encodes for protein involved in the metabolism of fatty acids, carbohydrates, and amino acids. Thus, SnRK1 controls the metabolism of the major source of energy, carbon, and nitrogen that can be used by the seedlings to sustain their growth. We suggest that the mechanism by which SnRK1 controls lipids metabolism is by regulating their remobilization from oil-bodies. TAGs represent the 45% of the weight of *Arabidopsis* seed, being the most abundant energy source presents in seeds. Therefore, controlling their metabolism means regulating the complete seedling metabolism. We observed that SnRK1 regulates the expression of oleosin 1, 2, 3, and partially of oleosin 4 and caleosin 1. This resulted in the inability of *snrk1.1/1.2* seedlings to degrade the majority of the TAGs and therefore the incapacity of establishing themselves due to energy deficiency. Controlling such an up-stream process in lipid metabolism represents an “elite” regulation to control the complete seed establishment process. Beside the remobilization of TAGs, SnRK1 positively regulates the expression of other 65 genes involved in lipid metabolism. Several studies have reported the importance of lipid metabolism for seed establishment (Some reference about it), indeed, many mutation in genes involved in the lipid metabolism are lethal already at early stages of plant development. Lipid profiling revealed altered levels of all identified TAG species in *snrk1.1/1.2* comparing to WT seedlings three days after seed germination.

Addition of glucose or Na-ocatanoate to *snrk1.1/1.2* seedlings allow their normal development of cotyledons. This indicate that carbohydrates and lipids metabolism could be reactivated when they are present at cellular level, even in the absence of SnRK1. Sheen and colleagues indicated that glucose or sucrose act as pivotal nutrient signals able to

reactivate the root meristem growth. They based this conclusion on the observation that neither amino acids or hormones could reactivate the meristem quiescence and root growth. Here, we show that also a short chain fatty acid (Na-octanoate) is able to reactivate the root meristem and induce root development (Figure 5). It is tempt to speculate that is not the signal molecule nature of glucose or sucrose that induces root growth but either their ability to provide energy.

When looking at gene expression, glucose induces the expression of about thousand genes in WT seedlings. In particular glucose activate the expression of 54 transcription factors, indicating a strong correlation between energy availability and transcription ability (Ref Magda paper 2014). The re-activation of plant transcriptome is accompanied by the co-activation of shoot and root developmental program and cell growth (Figure 6.B-F). From the box-plot in Figure 6B is clear that without SnRK1 the global transcription program activated by glucose does not take place. Our study also reveals that SnRK1 activity is important for root development. It is known that sugar metabolism could interfere with cell-cycle regulation (Ref: Sugar Control of the Plant Cell Cycle), it is likely that SnRK1 plays a crucial role in the regulation of cell-division, necessary for the complete development of a plant. Further work has to be done to confirm this hypothesis and to elucidate the possible cross-talk with TOR kinase signalling.

In conclusion with our results we demonstrate that SnRK1 kinases are important regulator of all the most energy costly developmental phase transitions, from juvenile to adult and vegetative to reproductive (Tsai & Gazzarrini, 2014) but also from the eterotrophic to autotrophic transition that occurs at the onset of plant life.

MATERIALS AND METHODS

Plant growth conditions

All seeds were sown in a 24 well plate with 1 ml of MS medium (MS: M0222, Duchefa-Biochemie, Germany) per well. Col-0 WT, WS WT, *snrk1.1/1.2*, and SnRK1.1 o.e. seeds were grown for 3 days in the dark at 20°C and 60% of relative humidity in a plant growth incubator (BINDER, Tuttlingen, Germany). After 3 days the different treatments were applied. Samples were harvested at different time points accordingly to their purpose: i) phenotyping, 3 days after treatment (6 days after germination); ii) metabolites measurments, 1 day after treatment (4 days after germination); iii) RNAseq experiments, 1 days after treatment (4 days after germination); RT-qPCR experiments 1 days after treatment (4 days after germination).

Induction of amiRNA expression was performed by supplementing b-Est to MS medium after sterilization ($T < 40^{\circ}\text{C}$) to a final concentration of $10\ \mu\text{M}$. b-Est was applied from day 0 on. DCMU was applied to a final concentration of $10\ \mu\text{M}$.

Plant lines

Col-0 and WS were used as WT *Arabidopsis* lines. *snrk1.1/1.2* mutant is described in Chapter 4 (Pedrotti et. al.). SnRK1.1 o.e. plants were kindly provided by Elena Baena-Gonzales and previously described by Baena-Gonzales and colleagues (Baena-González et al., 2007).

RT-qPCR.

RNA was isolated using Trizol. cDNA synthesis was performed using $1\ \mu\text{g}$ of total RNA as starting material. DNase treatment and first strand cDNA synthesis were done using DNase I (EN0521, Thermo-Scientific, Germany) and RevertAid H Minus Reverse Transcriptase (EP0451, Thermo-Scientific, Germany) according to manufacturer's protocol. qPCR was performed using BIOTAQ DNA Polymerase (BIO-line, Germany) and the relative protocol. Cycling conditions were as follows: 10 min at 95°C , 40 cycles of 20 s at 95°C , 10 s at 55°C , and 30 s at 72°C , followed by a default dissociation stage program to detect nonspecific amplification. Amplification products were visualized by SYBR green. The Ubiquitin 5 gene (AT3G62250) was used as internal standard for relative quantification. All the primers used for RT-qPCR determination of gene expression are safely stored by our internal database.

RNAseq.

For RNAseq experiment RNA has been isolated using Trizol and subsequently cleaned-up on RNeasy Mini Kit (Qiagen, Germany) according to manufacturer's protocol. RNA was treated with DNase I within the RNeasy Mini Kit. $5\ \mu\text{g}$ of total RNA was used for library preparation. mRNA was isolated using the Sera-Mag Magnetic Oligo (dT) Particles (2815-2103, ThermoScientific, Germany). cDNA library was prepared using the NEBNext mRNA Library Prep Master Mix Set for Illumina (#E6110, New England BioLabs) in combination with the NEBNext Multiplex Oligos for Illumina (#E7335, New England BioLabs). Quality of RNA and fragmentation size was checked using Experion RNA HighSens Analysis Kit (700-7105, BIORAD, Germany). Quality of the cDNA at the end of the library preparation was checked using Experion DNA Chips (700-7163, BIORAD, Germany). During library preparation products were isolated with the QIAquick PCR

Purification Kit (28106, Qiagen, Germany). One library was constituted by 12 samples. For the sequencing one library was distributed on 2 lanes.

High-throughput sequencing was performed on an Illumina GAIIX platform following the manufacturer's instructions. Quality control of the sequencing data was done using fastQC (<http://www.bioinformatics.bbsrc.ac.uk/projects/fastqc/>). Mapping of the reads was performed using Bowtie 0.12.8 (Langmead, Trapnell, Pop, & Salzberg, 2009) onto the *A. thaliana* genome release TAIR9. The resulting BAM files were then sorted and indexed using samtools 0.1.18. For analysis of differentially expressed genes R was used with GenomicRanges (Lawrence et al., 2013), rtracklayer (Lawrence, Gentleman, & Carey, 2009), samtools and edgeR (Robinson, McCarthy, & Smyth, 2010) libraries. Only genes with a pAdjust („BH“ correction) <0.01 were used for further analysis. DAVID was used for GO enrichment analysis (Jiao et al., 2012).

BIBLIOGRAPHY

- Baena-González, E., Rolland, F., Thevelein, J. M., & Sheen, J. (2007). A central integrator of transcription networks in plant stress and energy signalling. *Nature*, *448*(7156), 938–42. doi:10.1038/nature06069
- Chapman, K. D., Dyer, J. M., & Mullen, R. T. (2012). Biogenesis and functions of lipid droplets in plants: Thematic Review Series: Lipid Droplet Synthesis and Metabolism: from Yeast to Man. *Journal of Lipid Research*, *53*(2), 215–26. doi:10.1194/jlr.R021436
- Confraria, A., Martinho, C., Elias, A., Rubio-Somoza, I., & Baena-González, E. (2013). miRNAs mediate SnRK1-dependent energy signaling in Arabidopsis. *Frontiers in Plant Science*, *4*(June), 197. doi:10.3389/fpls.2013.00197
- Graham, I. a. (2008). Seed storage oil mobilization. *Annual Review of Plant Biology*, *59*, 115–42. doi:10.1146/annurev.arplant.59.032607.092938
- Jiao, X., Sherman, B. T., Huang, D. W., Stephens, R., Baseler, M. W., Lane, H. C., & Lempicki, R. a. (2012). DAVID-WS: a stateful web service to facilitate gene/protein list analysis. *Bioinformatics (Oxford, England)*, *28*(13), 1805–6. doi:10.1093/bioinformatics/bts251
- Langmead, B., Trapnell, C., Pop, M., & Salzberg, S. L. (2009). Ultrafast and memory-efficient alignment of short DNA sequences to the human genome. *Genome Biology*, *10*(3), R25. doi:10.1186/gb-2009-10-3-r25
- Lawrence, M., Gentleman, R., & Carey, V. (2009). rtracklayer: an R package for interfacing with genome browsers. *Bioinformatics (Oxford, England)*, *25*(14), 1841–2. doi:10.1093/bioinformatics/btp328

- Lawrence, M., Huber, W., Pagès, H., Aboyoun, P., Carlson, M., Gentleman, R., ... Carey, V. J. (2013). Software for computing and annotating genomic ranges. *PLoS Computational Biology*, 9(8), e1003118. doi:10.1371/journal.pcbi.1003118
- Robinson, M. D., McCarthy, D. J., & Smyth, G. K. (2010). edgeR: a Bioconductor package for differential expression analysis of digital gene expression data. *Bioinformatics (Oxford, England)*, 26(1), 139–40. doi:10.1093/bioinformatics/btp616
- T. G. Cooper, H. B. (1969). and Glyoxysomes. *The Journal of Biological Chemistry*, (13), 3507–3513.
- Theodoulou, F. L., & Eastmond, P. J. (2012). Seed storage oil catabolism: a story of give and take. *Current Opinion in Plant Biology*, 15(3), 322–8. doi:10.1016/j.pbi.2012.03.017
- Tsai, A. Y.-L., & Gazzarrini, S. (2014). Trehalose-6-phosphate and SnRK1 kinases in plant development and signaling: the emerging picture. *Frontiers in Plant Science*, 5(April), 119. doi:10.3389/fpls.2014.00119
- Xiong, Y., & Sheen, J. (2012). Rapamycin and glucose-target of rapamycin (TOR) protein signaling in plants. *The Journal of Biological Chemistry*, 287(4), 2836–42. doi:10.1074/jbc.M111.300749
- Xiong, Y., & Sheen, J. (2013). Glucose-TOR signaling in the transcriptional control of cell cycle, 1989–1990.

FIGURES AND SUPPLEMENTAL FIGURES

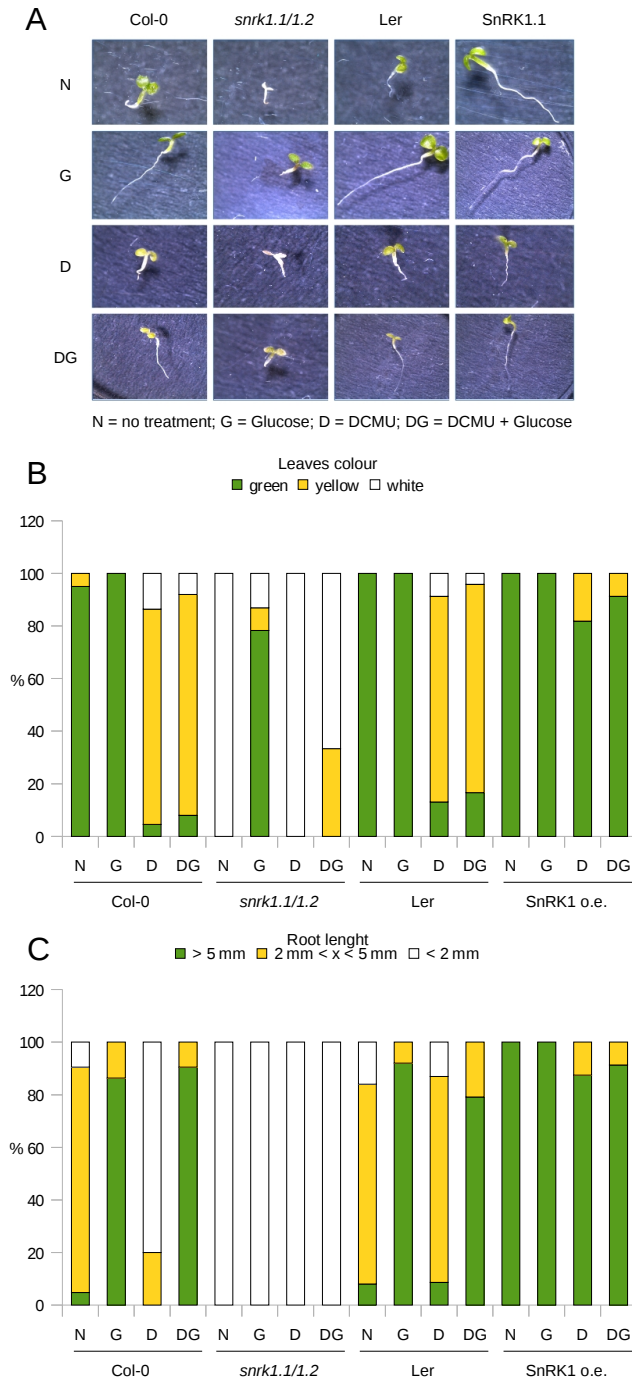


Figure 1: SnRK1 controls cotyledons development and root growth during the early stage of seed establishment.

A. Seed germinated and grown for 3 days in a photosynthesis-constrained and sugar-free medium and 3 more days under the indicated conditions. N: normal light; G: normal light, glucose supplied to the medium (final concentration 3 %); D: normal light, DCMU (10

μM); DG: normal light, DCMU (10 μM), glucose (3 %). B. Percentage of Col-0, *snrk1.1/1.2*, Ler, SnRK1.1 seedling with green, yellow, or white cotyledons in the different growing conditions. At least 17 seedling were considered for each genotype and condition. C. Percentage of Col-0, *snrk1.1/1.2*, Ler, SnRK1.1 seedling with root length > 5 mm, comprised between 2 and 5 mm, smaller than 2 mm. At least 17 seedling were considered for each genotype and condition.

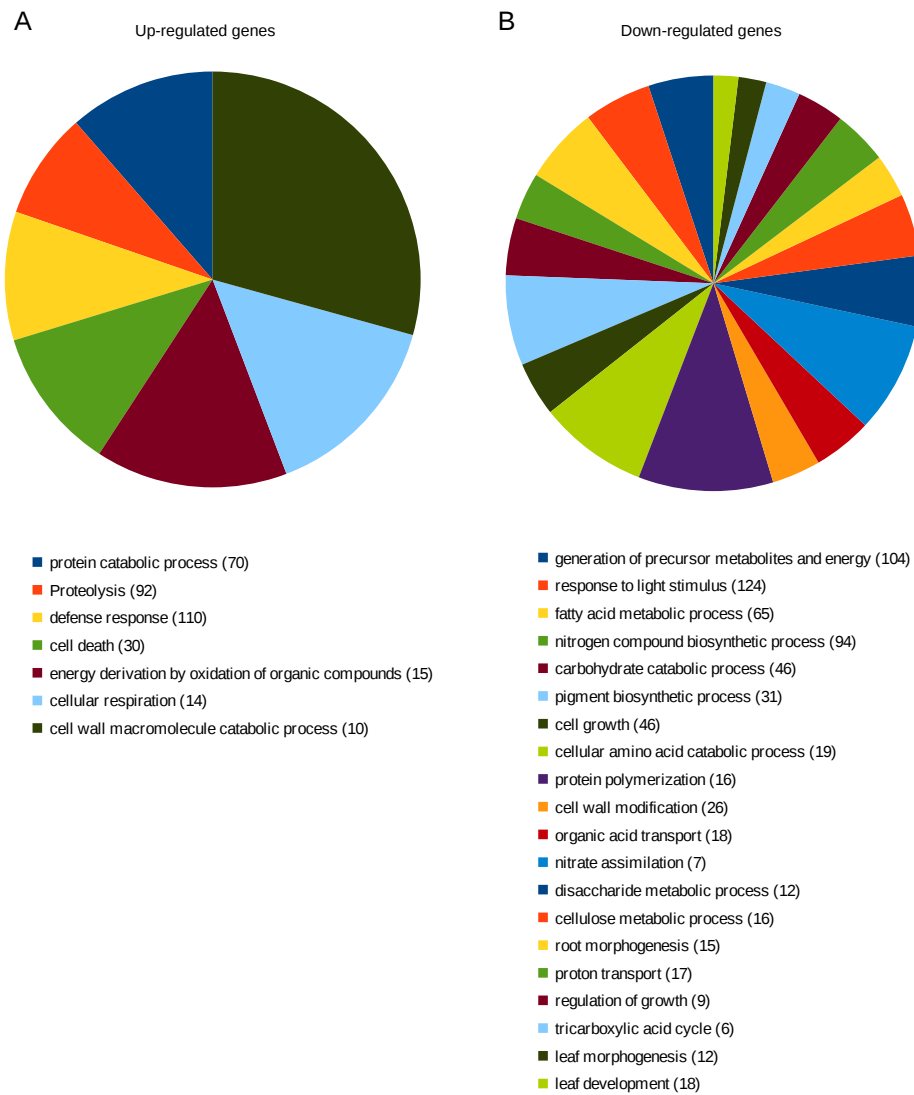


Figure 2: SnRK1s control a large set of catabolic genes.

GO enrichment of DEG in *snrk1.1/1.2* compared to WT. A. up-regulated genes. B. down-regulated genes. Pie-charts represent the fold enrichment, all included categories had a benjamini value < 0.05 , in bracket: number of genes in each category.

A,

		Number of double bonds of the fatty acyls									
		0	1	2	3	4	5	6	7	8	9
Number of carbons of the fatty acyls	48					4					
	50				3	4	3	3	2	3	nd
	52			2	2	2	3	4	3	5	14
	54	16	7	3	2	2	2	2	3	3	4
	56		4	6	3	2	2	2	3	4	
	58		nd	11	5	2	2	2	2	3	
	60			14	11	5	3	2	3		
	62					11					

B,

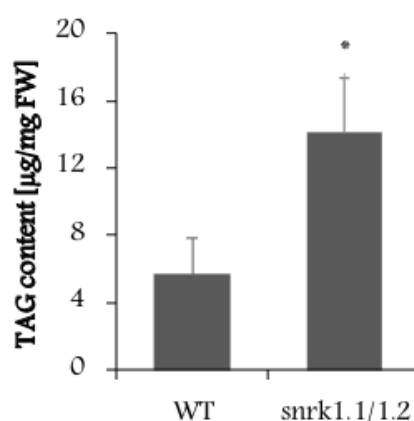


Figure 3: TAG content in *snrk1.1/1.2* and WT seedlings. A: Numbers indicate the fold change of TAG species according to the number of carbons and double bonds of the fatty acyls in *snrk1.1/1.2* compared to the WT. The color indicates the relative contribution of the identified lipid species in WT (dark red: >5%, light red: 5-0.5%, white: <0.5%). TAG species identified as differentiation lipids using OPLS-DA were highlighted in blue bold letters. B, TAG content in total lipid extracts of three days old seedlings determined by LC-MS.

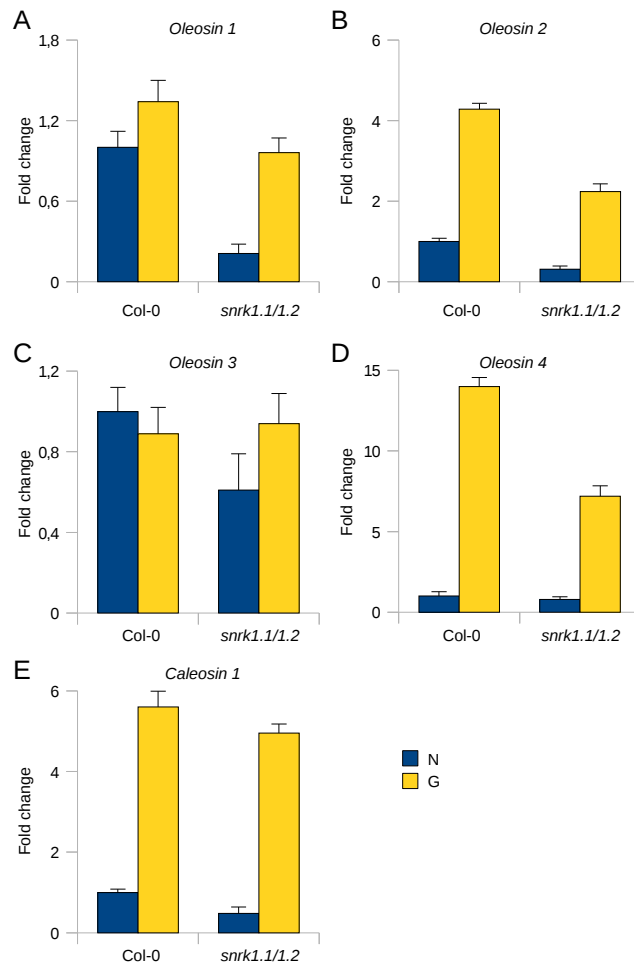


Figure 4: SnRK1s affect the expression of genes involved in lipid remobilization from oil droplets.

RT-qPCR. Expression of *OLEOSIN 1* (A), *OLEOSIN 2* (B), *OLEOSIN 3* (C), *OLEOSIN 4* (D), *CALEOSIN 1* (E) in WT (blue) or *snrk1.1/1.2* (yellow) seedlings. N: normal light; G: normal light, glucose supplied to the medium (final concentration 3 %).

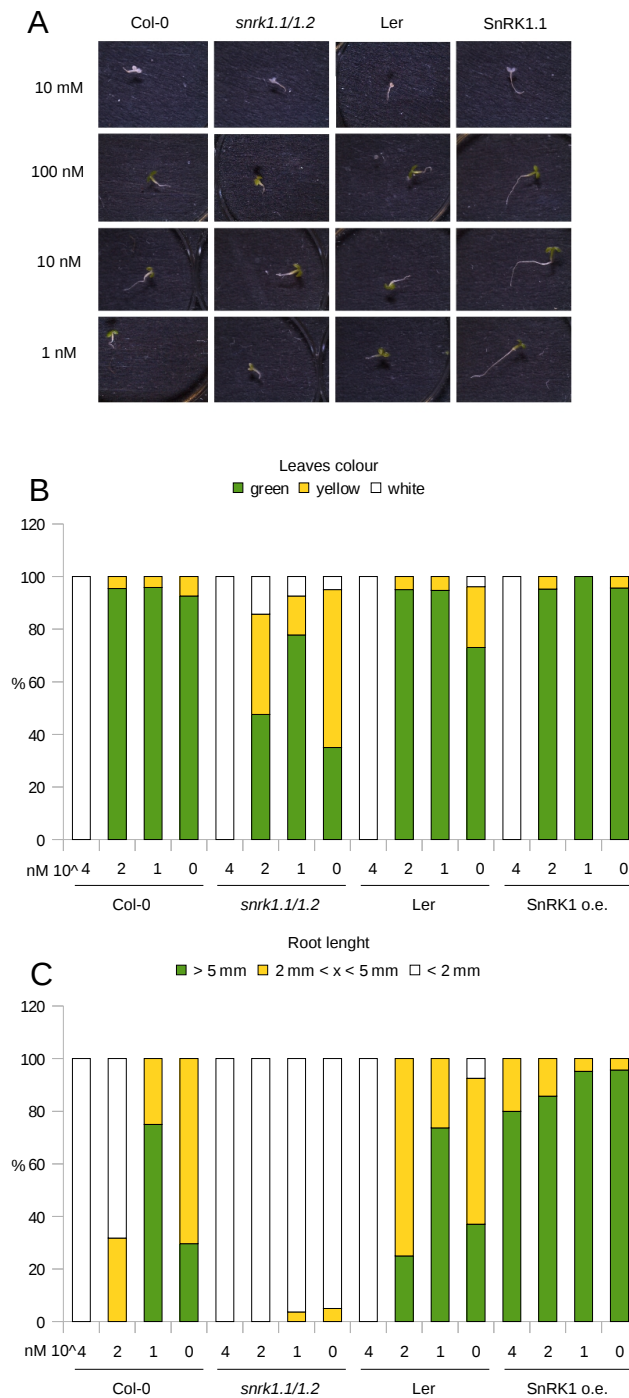


Figure 5: Short chain fatty acid could rescue the phenotype observed for *snrk1.1/1.2* seedlings in a dose dependent manner.

A. Seed germinated and grown for 3 days in a photosynthesis-constrained and sugar-free medium and 3 more days under normal light conditions. Sodium-octanoate added to the

medium a different concentrations, as indicated on the left side. B. Percentage of Col-0, *snrk1.1/1.2*, Ler, SnRK1.1 seedling with green, yellow, or white cotyledons. At least 15 seedling were considered for each genotype and condition. C. Percentage of Col-0, *snrk1.1/1.2*, Ler, SnRK1.1 seedling with root length > 5 mm, comprised between 2 and 5 mm, smaller than 2 mm. At least 17 seedling were considered for each genotype and condition.

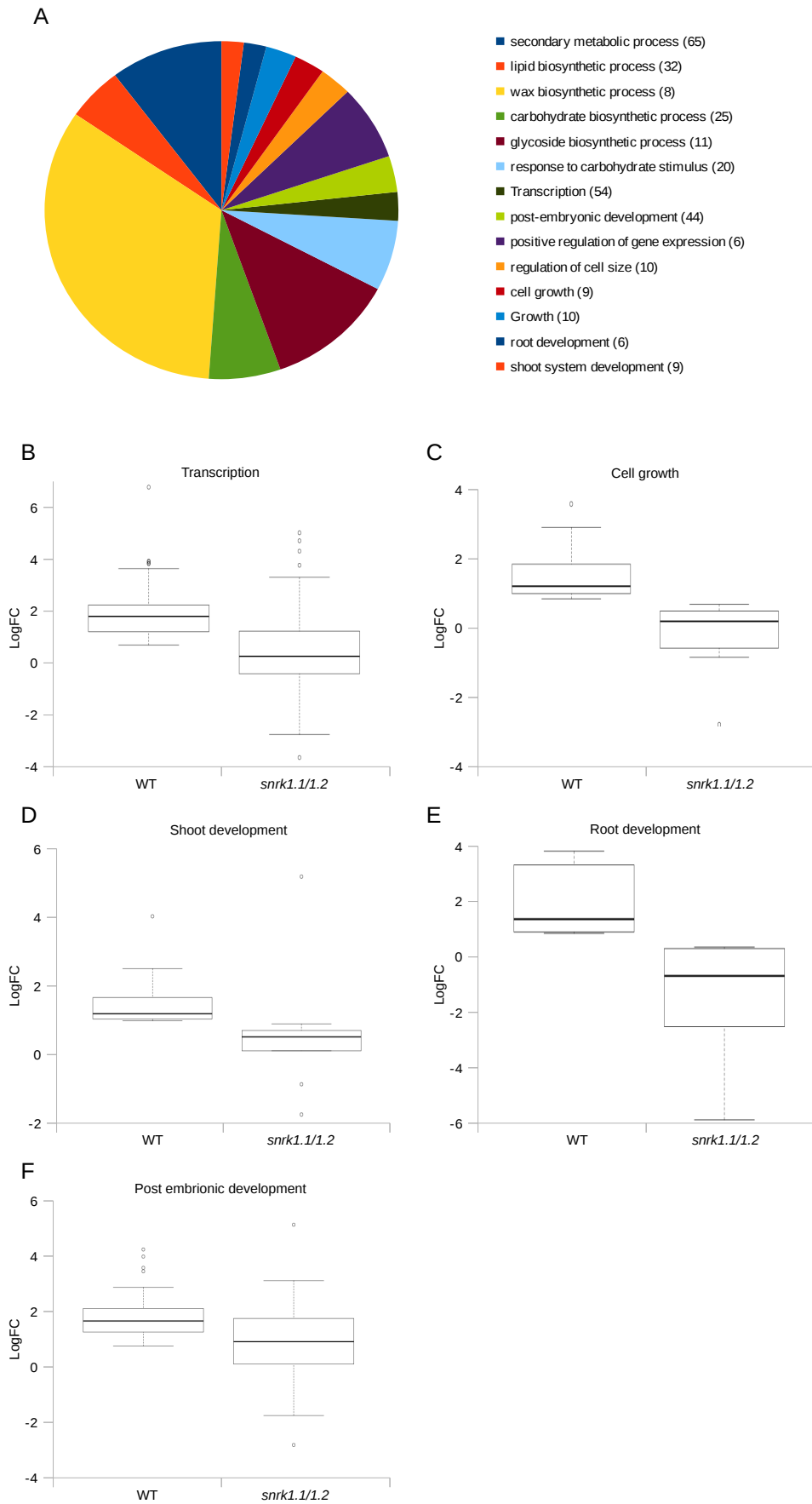
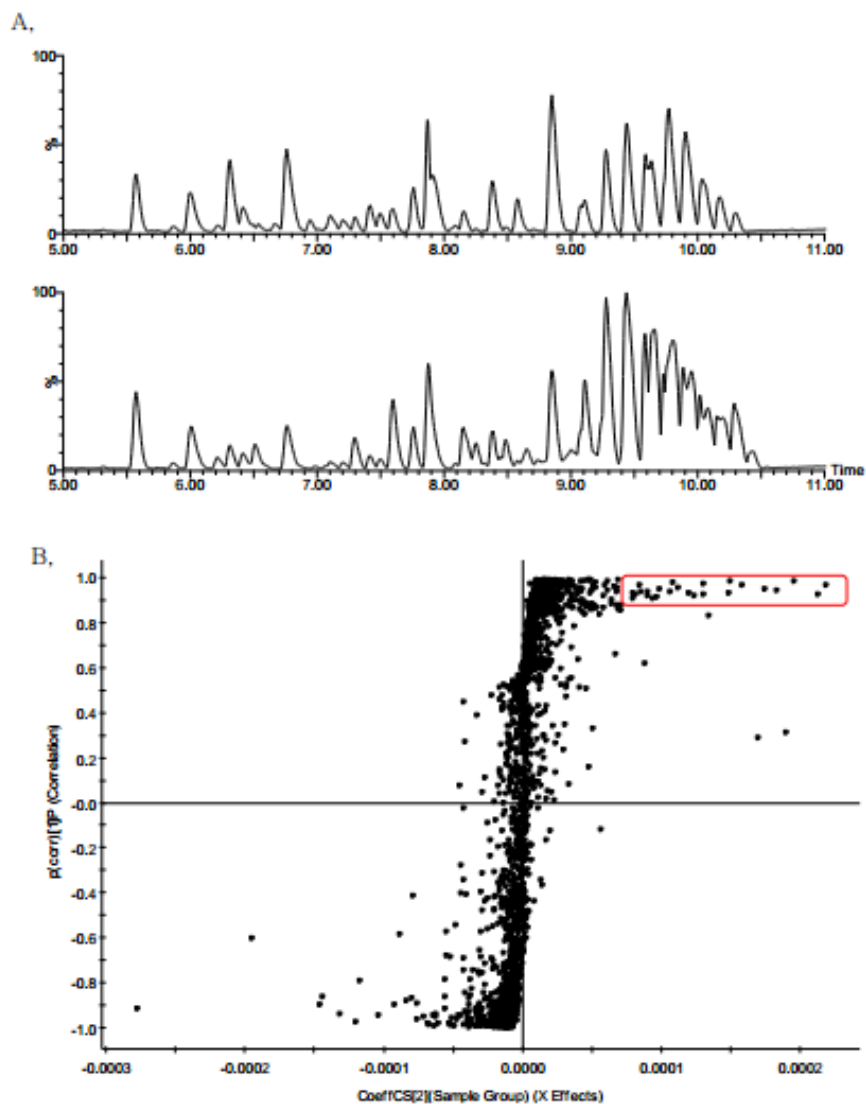
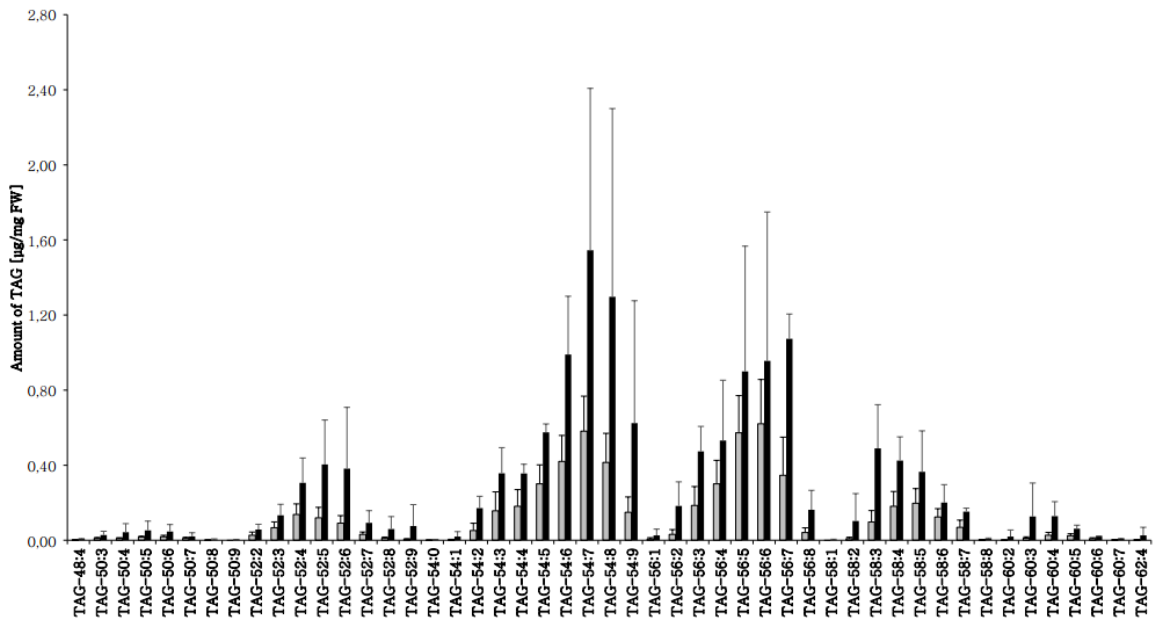


Figure 6: Glucose reactivate the expression of many catabolic genes in WT but not in *snrk1.1/1.2* seedlings.

RNA-seq experiment. A. GO enrichment of DEG in WT seedlings grown on medium supplied with glucose 3 % compared with WT seedling grown under normal light conditions. Pie-charts represent the fold enrichment, all included categories had a benjamini value < 0.05, in bracket: number of genes in each category. B, C, D, E, boxplots describing the expression of genes belonging to the different GO categories in WT or *snrk1.1/1.2* seedlings.



Supplementary Figure 1: Lipid profiling of three days old *snrk1.1/1.2* seedlings. A. Base peak ion chromatogram of total lipid extracts of WT (top) and *snrk1.1/1.2* (bottom). B. Identification of differentiating lipids in *snrk1.1/1.2* seedlings compared to the WT using OPLS-DA statistical analysis. Lipid features that were significantly elevated in the mutant is marked in red box.



Supplementary Figure 2: Endogenous TAG level in the total lipid extracts of three days old *snrk1.1/1.2* (black column) and WT (white column) seedlings.

Supplementary Table 1: RNAseq experiment. DEG between *snrk1.1/1.2* and WT seedlings. GO analysis of down and up-regulated genes.

Supplementary Table 2: Identification of the differentiating lipids in *snrk1.1/1.2* compared to WT.

Supplementary Table 3: RNAseq experiment. DEG between WT seedling grown on medium supplied with glucose 3 % and under normal light conditions. GO analysis of up down and up-regulated genes.

Chapter 7: General discussion and conclusion.

Stress could severely affect plant growth and development, reducing crop yield and productivity (Tomé et al., 2014). Understanding the molecular mechanisms underlying plant stress response will be important to sustain the increasing worldwide food demand. In recent years it has been postulated that the response to a specific stress could be separated in two components: a generic one, that confers basal tolerance, and a stress specific one. Plants subjected to stress grow less than plant growing under optimal conditions, since mounting an adequate response to environmental cues is an energy costly process. Although the work of Bolton is centered on plant-pathogen defense, the concept emerging from this work could be valid for any other stress: plant growth and yield are negatively correlated with plant stress, more a plant is stressed, less energy could be invested to increase its biomass (Bolton, 2009). In the past years many progresses have been made to unravel the components and mechanisms that enable and control the energy metabolism in response to plant stress. However, “...an intriguing and comparatively understudied phenomenon is how plants are able to recruit energy for the defense response.” (Cit. Bolton, 2009).

Driven by this aim we investigated the role of SnRK1s and bZIP transcription factors of the C/S1 network in *Arabidopsis* response to stress.

Extended dark is one of the most efficient stress to induce energy deprivation in plants

Energy deprivation seems to be a shared consequence of different kind of stresses, independently of their origins (Baena-González, 2010; Tomé et al., 2014). The more drastic stress that we could think about to induce energy depletion was to expose growing plants to extended dark (Baena-González & Sheen, 2008; Lastdrager, Hanson, & Smeekens, 2014; Rolland, Baena-González, & Sheen, 2006). Despite eclipses, extended dark rarely happen in nature. However many situations could decrease the photosynthesis potential. Extended dark could then be seen as the outermost stress able to rapidly induce energy deprivation. Indeed, by the end of the night starch is almost completely degraded (Sulpice et al., 2009) and is easy for the plant to run out of carbohydrate. Previous studies reported that a short extension of the night period is able to consume completely the starch residues and, therefore, to induce a strong adaptive response.

To identify SnRK1 and S1-bZIPs target genes we decided to perform genome-wide

expression profiling experiments. To identify the best time point to use for these experiments we combined literature knowledge with trial experiments. Of particular help was the work of Usadel and colleagues (Usadel et al., 2008) where they traced a detailed gene expression kinetic of many SnRK1.1 target genes in response to extended dark. Moreover, by RT-qPCR we measured the expression of SnRK1.1 target genes presented in the supplementary table 2 of the work of Baena-Gonzales and colleagues (Baena-González, Rolland, Thevelein, & Sheen, 2007). The model genes taken into consideration in these trial experiments presented different kinetics of regulation upon extended dark treatment (see also the work of Dietrich and colleagues (Dietrich et al., 2011)). However, most of them had a significantly different expression at 6h of extended dark compared to their expression level at the end of the night. Usadel and colleagues reported that the expression of transient induced or repressed genes occurred already within 1 h of extended dark. Although many of these genes could be important SnRK1 and S1-bZIP target genes, we thought that the high variability registered during the very early response could invalidate all our attempt to identify SnRK1 and S1-bZIP target genes. 6h of extended dark represented the best compromise between the high variability of the early response and the unwanted secondary effects.

The use of amiRNA and b-estradiol inducible approach provide a good tool to study *snrk1* and *s1-bzips* mutants

A strong functional redundancy between SnRK1.1 and 1.2 have already been reported (Baena-González et al., 2007), therefore, we decided that the best way to identify SnRK1s target genes was to generate a *snrk1.1* and *snrk1.2* double mutant. Similarly, S1-bZIPs have been reported to have a certain functional overlap and/or redundancy (Alonso et al., 2009; Dietrich et al., 2011; Weiste & Dröge-Laser, 2014), forcing us to use a multiple mutant to study their influence on gene expression. Because of the lethality of a double *snrk1.1/1.2* mutant and of a *bzip11* mutant (Hanson, Hanssen, Wiese, Hendriks, & Smeekens, 2008), we decided to make use of the combination of b-estradiol inducible system (Ref) and artificial micro RNA technology (amiRNA).

The definition of the right b-est induction timing was a “thorn in the side” for the first year of my work. As reported in Supplementary.Figure.1 of the Chapter 4, we could measure a drastic reduction of *SnRK1.2*, *bZIP2*, *bZIP11*, and *bZIP44* expression already 12 hours after b-est application. In line with this, S1-bZIPs known target genes also undergo a

similar reduced induction. This indicated that not only the expression of *S1-bZIPs* was reduced within 12 hours from b-est induction, but also that *S1-bZIPs* proteins were not present after that time. Strangely, we could not observe the same for SnRK1. SnRK1-target genes expression, indeed, was clearly unaffected by 12 hours of b-est treatment. Only an exposition to b-est for 5 to 6 days gave appreciable results in terms of reduced expression. From those experiments we deduced that SnRK1.2 protein has a long stability: around 6 days in our experimental conditions.

Of course, by using our experimental setup we could not control the effects of long term b-est exposition on *snrk1.1/1.2*. Although is true that SnRK1.2 was not anymore detectable only after 6 days of b-est induction and the material for our experiments was harvested on the 7th day, small interferences with the normal plant physiology could be present, and not estimable for us. In our experimental design we decided to compare gene expression at 6 h of extended dark between the different genotypes. Including further experimental conditions such as 0h (end of the night) or 6 h in light, could have provide more valuable data on genes whose expression change only in response to extended dark and is directly regulated by SnRK1 and *S1-bZIPs*. To compensate the lack of these data, we compare the data of our RNAseq experiment with those present in Genevestigator database (Supplementary figure 1, Chapter 4).

The combinatorial usage of b-est inducible system and amiRNA technology allowed us to obtain 2 important tools. These 2 plant lines, indeed, could be of fundamental help for many other laboratories interested, as we are, to unravel the complicated role of SnRK1 and bZIP C/S1 network.

The expression of *bZIP1*, *bZIP53*, and *bZIP63* is regulated in a SnRK1-dependent manner

Several bZIPs of the C/S1 network appear to be regulated at transcriptional level by different kind of stresses. It is the case for example of *bZIP1* and *bZIP53*. These two bZIPs seems to be regulated in a coordinated way since in many stresses they present a similar kinetic of induction (despite the different magnitude). Their expression is strongly induced by extended dark and salt stress (Dietrich et al., 2011) Hartmann et al., Chapter 5). The expression of *bZIP63* reflects those of *bZIP1* and *bZIP53* in response to extended dark (Mair et al., Chapter 3). Accordingly, the expression of *bZIP1*, *bZIP53*, and *bZIP63* measured in our RNAseq in Chapter 4, is affected by SnRK1. In the *snrk1.1/1.2* mutant,

indeed, we did not observed anymore the induction of the expression of these three bZIPs. In the experiment presented in Chapter 5, we saw that upon salt stress, the induction of the expression of *bZIP1* is reduced in the *snrk1.1/1.2* mutant. Furthermore, we saw that not only SnRK1 has an impact on the expression of *bZIP1* but also the ABA-SnRK2 pathway is involved. Therefore it seems that many pathways are converging on the regulation of bZIPs expression.

It would be Interesting to investigate deeper what are the pathways directly influencing *bZIPs* expression. In this direction we have already started to test the activation of the construct *Prom(bZIP1):LUC* against the TFs collection present in our lab making use of the high-throughput protoplast transactivation system (Wehner et al., 2011) A good candidate seems to be bZIP25. The confirmation of this data will lead to the design of an innovative model, where a bZIP is responsible of the regulation of the expression of other bZIPs, depicting an intra C/S1 network regulatory loop.

Other bZIPs of the C/S1 network, however, do not appear to be regulated on transcriptional level. It is the case of *bZIP2*, *bZIP11*, and *bZIP44*. All the members of the S1 group are post-transcriptionally regulated by the so called sucrose induced repression of translation (SIRT) (Rahmani et al., 2009). Therefore, transcription is not the only mechanism that regulates bZIP proteins. At the moment most of the data that we have are based on expression profiling experiment, and often we do not distinguish between bZIPs expression and the effective presence of the protein.

Because of the absence of more detailed data regarding bZIP proteins it is very difficult to draft an accurate model and to discriminate which bZIPs are involved in the response to a particular stress.

bZIP63 is the only TF directly phosphorylated in vivo by SnRK1 identified so far

Evidence collected in the past years revealed that several bZIP TFs are under the control of various post-translational mechanisms, that are crucial for the control of their function. Among these, phosphorylation plays an important role with respect to the regulation of bZIPs transactivation potential, cellular localization, stability and DNA binding (Schütze, Harter, & Chaban, 2008). Concerning bZIPs of the C/S1 network, only bZIP63 and bZIP9 were found to be phosphorylated by crude plant extract in vitro (Kirchler et al., 2010) and only for bZIP63 phosphorylation was confirmed in vivo (Chapter 3, Mair et al.). The analysis of the sequence of bZIP63 revealed the presence of several serines, potential target

of phosphorylation, distributed all over the protein. Interestingly, we showed that bZIP63 phosphorylation is related to energy availability, varying from almost negligible in the light to a multiple phosphorylation in extended dark. Mair et al. could show that different kinases are responsible for the post-translational modification of specific serines (data unpublished) and only S29, S294, and S300 were identified as targets of SnRK1.1. Accordingly, all three sites match the SnRK1.1 consensus sequence. Several other bZIPs of the C/S1 network have a high sequence similarity to bZIP63 and a strong conservation of the SnRK1 target site. None of them, however, has been found to be phosphorylated so far.

Confirming bZIP63 role in the regulation of the response to energy deprivation, *bzip63* and bZIP63 o.e. plants exhibited opposite phenotype when exposed to several days of extended dark. *bzip63* showed a retarded dark-induced senescence whereas bZIP63 o.e. plants an earlier one. When the phenotype of *bzip63* is compared with that of *snrk1.1/1.2*, and *s1-bzips* mutants, it seems that these proteins have an opposite influence on dark-induced senescence. As shown in Chapter 4, indeed, both *snrk1.1/1.2* and *s1-bzips* show an earlier yellowing of the leaves in comparison to WT when exposed to extended dark. Accordingly, SnRK1 o.e. plants showed an enhanced resistance to energy deprivation (Baena-González et al., 2007). The phenotype of these mutants after extended dark argue that SnRK1 and S1-bZIPs have an opposite function to that of bZIP63 in the reprogramming of the plant metabolism in response to energy deprivation. In the absence of more detailed data on the genes regulated by bZIP63 in response to extended dark, it seems that bZIP63 has a double function depending on its phosphorylation status, and (as discussed later) by its dimerization properties. An interesting possibility is that phosphorylated bZIP63 is involved in the activation of the SnRK1-driven energy saving program, whereas the non-phosphorylated bZIP63 could have an important role in the restoring of the normality once the stress is gone. bZIP63 could therefore be an important post-stress protein.

The SnRK1-dependent phosphorylation of bZIP63 regulates its dimerization properties and its activation potential

As mentioned before, protein phosphorylation could exert several regulatory function. Kirchler and colleagues (Kirchler et al., 2010) showed that the phosphorylation of S in the DNA-binding domain of bZIP63 (named S11, S15, and S19) alters its binding potential. In their model, S15 and S19 were in close proximity to a phosphodiester oxygen of the DNA

helix and could likely form an hydrogen bond. The usage of a phosphomimicking aspartate (D) in substitution of S15 and S19 induced a conformational change in the structure of the DNA-binding domain of bZIP63, increasing the distance between S15 and S19 and the DNA, inhibiting the formation of a hydrogen bond. Moreover, the negative charge of aspartate or phosphorylated serines is likely to prevent bZIP63 binding to DNA (Kirchler et al., 2010). The amino acid residues identified by Mair et al. (Chapter 3) are localized outside of the DNA binding domain of bZIP63. We therefore investigated the possible function of these post-translational modifications. Dietrich K. showed that the phosphorylation of S29, S294, or S300 did not affect the stability of bZIP63 (unpublished data). By generating single point mutation of bZIP63 we showed in protoplasts that the substitution of S29 with an alanine resulted in a weaker activation of the *ASN1:GUS* and *PRODH:GUS* reporter. Given that this could be due to changes in dimerization preferences, we tested the effect of SnRK1-mediated phosphorylation on bZIP63 dimers formation with bZIP1 and bZIP11. Using the protoplast 2 hybrid assay (P2H) we could demonstrated that the phosphorylation of the above mentioned serines (and in particular of S29) affects the dimerizations properties of bZIP63. In particular we showed that depending on its phosphorylation, bZIP63 prefers the formation of specific dimers. For example, we observed that the dimerization between bZIP63 and bZIP11 is enhanced by the co-expression of SnRK1. Based on the experimental evidences collected so far, we suggest that the reduced activation potential of bZIP63 observed on *ANS1:GUS* and *PRODH:GUS* reporter is due to its inability to form the right dimer to activate those promoters.

bZIP dimer formation is an highly dynamic process

Ehlert and colleagues (Ehlert et al., 2006) investigated the interactions between bZIPs of the C/S1 network. What has been shown is a statical overview of the interaction among these bZIPs without considering the effect of post-translational modification, and neither the presence of the proteins in a particular situation, such as the response to a specific stress. We start to widen our knowledges on the dynamism of the C/S1 network introducing a stimulus on top of the dimerization assay (typically P2H). We tested the influence of the o.e. of SnRK1.1 on the interaction among bZIP63 and bZIP1, bZIP11, or bZIP63 it self. We could show that the dimerization was strongly influenced by the presence of SnRK1 and preliminary data (not showed in this thesis) showed us that the o.e.

of SnRK1.1 not only affect the interaction which includes bZIP63 but also others. In line with these results, I argue that specific dimers are involved in the response to particular stresses.

Each bZIPs of the S1 group has its own subset of target genes (or different bZIPs respond to different stresses?)

Many evidences have been collected in the last years aiming to identify bZIPs target genes but the data that we have so far are not sufficient to solve this question. The study of bZIP target genes is particularly difficult because of the redundancy and/or functional overlap seen in many experiments. It has been observed in many cases that the mutation of a single bZIP TF does not have any (or negligible) impact on the expression of supposed target genes. Vice versa, when bZIP dimers are removed simultaneously from the cellular environment, there is a stronger impact on gene expression. As observed by Dietrich and colleagues (Dietrich et al., 2011)) for example, the expression of *ASN1* in single *bzip1* or *bzip53* mutant is similar to that in WT plants, whereas in quadruple *bzip1/53/9/63* or *bzip1/53/10/25* mutants there is a more pronounced difference. To be able to identify as many genes regulated by S1-bZIPs in response to energy deprivation as possible we decided to ko all the five members of the S1-group (to be precise, *bZIP1* and *bZIP53* were ko, for *bZIP2*, *bZIP11*, and *bZIP44* we made use of a b-est inducible amiRNA). With hindsight, this approach was probably not the best. In particular because we are still not able to assign a certain “bZIP specificity” to genes regulation. As already observed previously, for example, bZIP2, bZIP11, and bZIP44 do not play any role in the regulation of *ASN1* expression in response to extended dark. However, the expression of *ASN1* seems to be under the control of one of the dimer between bZIP1 (or bZIP53) and bZIP63 (or bZIP9).

It would be of crucial importance to investigate which bZIPs are physically present in the response to a certain stress, or in a developmental program etc. So far, we based all our models and conclusions on transcriptomic data but other kind of regulatory mechanism (e.g. post.translational modifications) should be taken into account to have a complete picture. Because of the high homology between bZIPs it is impossible to produce an antibody against a specific bZIP. Therefore alternative solutions have to be taken in consideration. Ella Nukarinen (group of Wolfram Weckwerth, Uni-Vienna) started to use mass-spec proteome analysis to investigate the presence of specific bZIPs during the plant

response to energy deprivation. However, proteome analysis could only provide information about the presence of a certain bZIP but could not help to investigate which are its target genes. An efficient way to examine this would be to introduce in *Arabidopsis* genome a tagged version of the studied bZIP under its endogenous promoter. We already started to build the different constructs. Our idea is to produce plants having two bZIPs differentially tagged: ideally the two components of a dimer (a S1-bZIP with one tag and a C-bZIP with another tag). Following this strategy we will be able to check the presence of the bZIPs, the localization, the timing of induction, the stability of the protein etc. Furthermore, we will be able to perform single and sequential ChIP-seq analysis. In this way we will have a more detailed overview of the genes specifically regulated by single bZIPs and dimers.

SnRK1 are central regulators of the plant response to energy deprivation

To confirm that S1-bZIPs are mediator of the transcriptional reprogramming driven by SnRK1 upon energy limiting conditions, we decided to compare the transcriptome of WT, *snrk1.1/1.2* and *bzipS1* exposed to extended dark. This approach allowed us to identify a gene set commonly regulated by SnRK1s and S1-bZIPs. In our approach we observed that SnRK1 affect the expression of 10'677 genes, of which 4'633 were down regulated in the *snrk1.1/1.2* mutant in response to extended dark and 6'044 up-regulated. Probably, many of these genes are not direct targets of SnRK1 but their expression is indirectly affected by the absence of SnRK1 from the cellular environment. It has been often reported that SnRK1 has strong connection with the ABA-SnRK2 pathway, with the TOR pathway, etc. and therefore is likely that the absence of SnRK1 affects many other processes. Nevertheless, we observed that our data are in line with the data presented by Baena-Gonzalez and colleagues (Baena-González et al., 2007) The different amount of identified differentially expressed genes (DEG) between our approach and the approach of Baena-Gonzalez and colleagues are due to different factors. First of all the two approaches used different systems. In our experiments we used an in-vivo study, collecting data from the total rosette of the plant, without discrimination between the different tissues. The study presented by Baena-Gonzalez and colleagues was done in protoplast o.e. SnRK1.1. Therefore in our investigation we took into consideration the complete aerial part of the plant and so all the developmental and physiological processes regulated by SnRK1. This approach, however, could suffer of many secondary effects that are hard to determine. It

has to be mentioned that to obtain a sufficient degree of suppression of SnRK1.2, we had to induce the plants with b-est for 5 days and it is impossible for us to determine what are the consequence of this prolonged exposition. However, the effects of b-est exposition have been quantified by RNAseq: only 12 DEG were found between un-treated WT and b-est exposed plants. Protoplast experiments provide data from single cell, without any information on the complete system. The overexpression of a protein could also enhanced the discovery of false positive. On the other side, the approach used by Baena-Gonzalez and colleagues suffer less of the secondary effects mentioned before. To skim the indirect target of SnRK1 other conditions could have been included in the design of the experiment. For example, since we were interested in the study of genes which are important in the response to extended dark (energy deprivation), the non-stressed situation could have been compared with the 6h time point that we decided to use. In this way, all the genes that were not changing their expression in response to the stress would have been left out of our analysis. Because genome-wide expression profiling experiments are still expensive, we made use of public available data to compensate the lack of non-stress situation data.

Despite the different approach, we come to a similar conclusion as Baena-Gonzalez and colleagues (Baena-González et al., 2007). We observed that SnRK1 is very important for the activation of all the energy saving programs needed for survival under energy deprivation conditions, such as the catabolism of protein, of sugars and amino acids. We observed as well that SnRK1 is an important repressor of protein synthesis, amino acids synthesis, glycolysis and more in general of all the anabolic processes (a more detailed overview is presented in Chapter4.Fig1.Supplementary).

S1-bZIPs are mediator of part of the SnRK1-driven response to extended dark

Analzing the genome-wide expression profile of the *bzipS1* plant line generated by us, we saw that there is a substantial overlap between genes regulated by SnRK1 and those who had a miss regulated expression in the quintuple S1-bZIPs mutant. This evidence supported our hypothesis that S1-bZIPs are mediator of part of the SnRK1-driven response to energy deprivation. We observed that the number of DEGs in *bzipS1* mutant was much more limited than those found in the *snrk1.1/1.2* mutant. Therefore we guess that S1-bZIPs are mediator of a part of the SnRK1 driven response and more effort should be taken to identify other TFs involved in the SnRK1 signaling cascade.

As mentioned before, bZIPs normally act as dimers in the regulation of the expression of a

particular gene. Although it is true that they can bind to the DNA as monomers, the activity of a dimer is stronger than the one of a monomer. Taken into consideration that S1-bZIPs preferentially form dimers with C-bZIPs, and that we remove from the cellular environment only S1-bZIPs and therefore only a part of the dimer, my opinion is that we underestimate the genes that are controlled by the C/S1 network. Moreover, we did not consider the presence of conflicts between the different bZIPs. It could be possible that a bZIP regulates the expression of another *bZIP* (as it seems the case of bZIP25 regulating the expression of *bZIP1*) or that different bZIPs have different effects on the expression of a specific target genes. It seems the case for example of the regulation of *GH3.5*. Weiste C. identified this gene as activated by bZIP2, bZIP11, or bZIP44 in response to energy deprivation. However, in our RNAseq experiment we did not observe any alteration of its expression in our quintuple mutant. Many other explanations could be found to explain this discrepancy. Again, I guess that in future it will have more sense to focus the attention on single dimers and create mutants dedicated to the identification of dimer targets. As well it is valid also in this case what mentioned before, it is of crucial importance to define the presence of a bZIP on a protein level to understand its involvement in the response to a particular stress or physiological process.

bZIPs dimer recruit SnRK1.1 on the double helix of the DNA

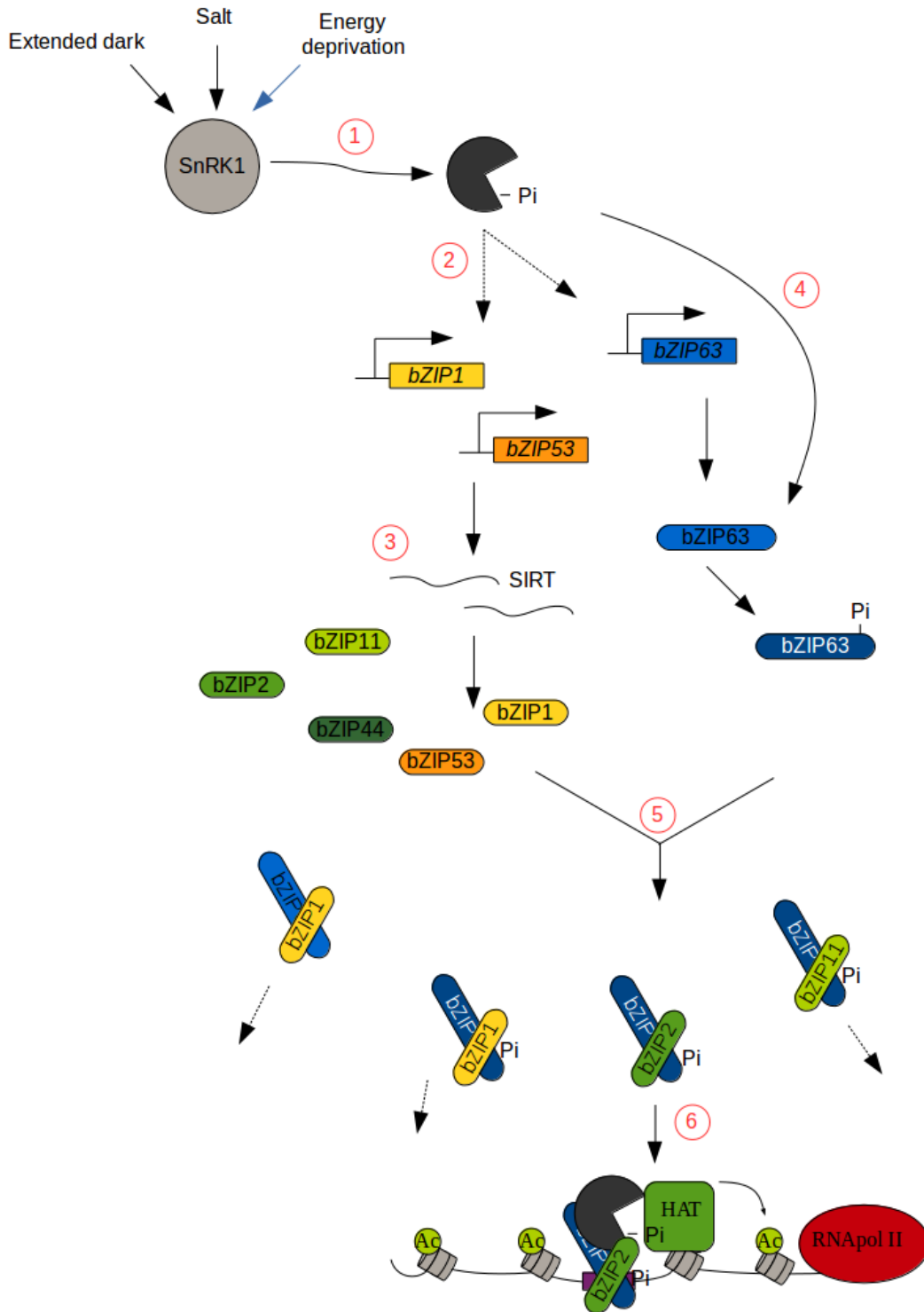
Recently it has been demonstrated that also the SNF1 plant homolog (SnRK1) has both a cytoplasmic and nuclear localization (Bitrián, Roodbarkelari, Horváth, & Koncz, 2011). The double localization of SnRK1 is compatible with its associated function. Indeed, SnRK1 has been observed to be able to directly phosphorylate cytoplasmic enzymes but also to be involved in the regulation of the activity of TFs with a nuclear localization. In yeast the nuclear localization of SNF1 was already known and it has been observed that SnRK1 is often associated to the chromatin (Lo et al., 2001). SNF1 was purified as part of a histone 3- serine 10 kinase complex and was identified as the catalytic subunit of the complex (Lo et al., 2001). It has been shown that SNF1-introduced modification serves as recognition sites for the histone acetyltransferase complex Gcn5. Thus SNF1 and Gcn5 function in an obligate sequence to enhance specific gene transcription. The recruitment of the SNF1 and Gcn5 complexes is particularly important for the derepression of the glucose repressed genes (Tachibana, Biddick, Law, & Young, 2007). On the well studied *ADH2* gene in yeast, indeed, glucose repression is associated with chromatin remodeling on the

promoter that could be reverted by the recruitment and activation of SNF1. Although an RNA pol II complex is already associated with the gene, it shown that the activation of its expression occurs only after SNF1 activation and SNF1-induced chromatin modification. Similarly to what observed in yeast we found SnRK1.1 associated with the chromatin around the *ETFQO* gene promoter. Importantly we observed that SnRK1.1 recruitment on *ETFQO* promoter was dependent on S1-bZIPs and bZIP63. Crucial for the recruitment was also the phosphorylation of bZIP63. In the alanine mutant of bZIP63, indeed, we observed a reduced recruitment of SnRK1. Accordingly to SNF1 function in yeast, we observed that a reduced recruitment of SnRK1 corresponded to a lower acetylation of the *ETFQO* promoter. Weiste and Dröge-Laser (Weiste & Dröge-Laser, 2014) recently found Gcn5 associated with bZIP2, bZIP11, and bZIP44. Therefore we speculated that the observed acetylation of the *ETFQO* promoter was dependent on the same acetyl transferase complex.

Because of the high similarity of the proteins and complex involved in the derepression of glucose repressed genes between yeast and *Arabidopsis*, we think that the observation made on the *ETFQO* promoter could be extended to other genes. Probably other bZIPs are involved in the recruitment of SnRK1 on those promoters, accordingly to our expectations that different dimers have different target genes.

A model for SnRK1-activated transcriptional response mediated by bZIP63 and S1-bZIPs

1. Different kind of stresses sharing a low energy perception induce SnRK1 activation.
2. The activation of SnRK1 induce the expression of *bZIP1*, *bZIP53*, and *bZIP63* but does not affect the expression of other S1-bZIPs.
3. Among other mechanisms, SIRT regulates the translation of S1-bZIPs.
4. SnRK1 directly phosphorylates bZIP63, regulating its dimerization properties (5).
5. Accordingly to their compatibility, S1-bZIPs and bZIP63 dimerize. The different dimers have a different subset of target genes.
6. bZIP2 and bZIP63 dimer recruits SnRK1 on the *ETFQO* promoter. The introduced phosphorylation on H3S10 could be the recognition motif for the HAT complex, that subsequently introduces acetylation on the H3 and promotes *ETFQO* transcription.



SnRK1 is an important regulator of the metabolic reprogramming occurring during seedling establishment

During seed germination and establishment there is an extraordinary usage of seed storage compounds in order to support seedling growth until reaching the autotrophic stage, characterized by photosynthetic independence. In our attempt to obtain a comprehensive picture of catabolic processes regulated by SnRK1, we extended the analysis of the role of SnRK1 out of stress-related fields considered before. Because of the inability of *snrk1.1/1.2* seedling to grow and establish we speculated on the importance of SnRK1 as a regulator of the metabolic reprogramming associated with seed germination and establishment. In particular, we observed that in the absence of SnRK1s *Arabidopsis* seeds were able to germinate but seedlings quickly wilt before establishment. *snrk1.1/1.2* seedling germinated in liquid MS medium appeared without roots and with white cotyledons 6 days after germination. When grown in MS medium with glucose they still did not present any roots but cotyledons appeared similar to WT seedlings. Because of the ability of glucose to recover the cotyledon phenotype but not the root development we decided to treat the two parts of the plants separately. Recently it has been shown that TOR is a master regulator that links photosynthesis and root meristem activation (Sheen 2014). The root phenotype of *snrk1.1/1.2* mutant was pretty similar to that of *tor* mutant described by Xiong and colleagues (Xiong et al., 2013). We therefore suspected that because of the high cross-regulation between the SnRK1 and TOR pathways, what we observed at root level was due to a misregulation of TOR. However, cotyledons of the *tor* mutant were not wilting during establishment. We therefore investigated deeper the apparently TOR-independent phenotype of the *snrk1.1/1.2* mutant.

It was possible to rescue leaf development of *snrk1.1/1.2* by adding sucrose or a short fatty acid to the medium, indicating that this aberration was mainly related to energy availability. In line with the expected function of SnRK1 in the activation of catabolic processes, GO enrichment analysis executed on RNAseq-derived data showed that *snrk1.1/1.2* had severe problems in gaining energy from seed storage compounds. In particular we observed that generation of precursor metabolites and energy was depleted due to the down-regulation of the major energy providing pathways such as fatty acid degradation, carbohydrate and amino acid catabolism. According to that, a higher amount of TAGs was measured in *snrk1.1/1.2* than in WT seedlings. Surprisingly, addition of

glucose could partially bypass the SnRK1 pathway. Glucose treatment, indeed, induced the normal cotyledons development also in *snrk1.1/1.2* seedlings but had no effect on root growth. Glucose could reactivate the TAGs remobilization, as showed by the induction of the expression of genes such as oleosin, caleosin, and albumin, involved in seed lipid mobilization.

The idea emerging from our work is that SnRK1 has a predominant role in the regulation of seed storage catabolism and the crosstalk between SnRK1 and TOR could have an important function in the regulation of root development. In other eukaryotic systems it has been shown that one point of cross communication between the TOR and SnRK1 pathways is represented by the RAPTOR protein. We therefore think that the possibility of the presence of this regulation in plants should be explored.

In our conditions S1-bZIPs had no visible effect on seedling establishment. The phenotype of *bzipS1* line was wholly similar to that of WT seedlings. Because RNAseq data showed that SnRK1s are regulating the expression of several hundred genes, we think that further effort has to be made to identify the TFs responsible for such regulation. A way to study this would be to use the promoter of one of the SnRK1 genes involve in lipids catabolism fused to a reporter genes (*GUS* or *LUC*) and screen its activation against our TFs library.

Bullet-points conclusion

1. bZIP63 is directly phosphorylated by SnRK1;
2. SnRK1-mediated phosphorylation of bZIP63 alters its dimerization properties, inducing the formation of specific dimers only under stress situations;
3. S1-bZIPs are mediator of the transcriptional response induced by SnRK1 upon LES;
4. C and S1 bZIPs form a complex together with SnRK1 on the chromatin of specific genes, able to recruit acetylases that open the chromatin to allow gene transcription;
5. bZIP-SnRK1 complex regulates the expression of several genes involved in the metabolism of amino acids and in the respiration of substrates other than glucose;
6. SnRK1 regulates the expression of several bZIP TFs of the C/S1 network, among which bZIP1, bZIP53 and bZIP63;
6. bZIP1 (and bZIP53) merge energy stress and salt stress by reprogramming the expression of many genes involved in the plant primary metabolism;
7. SnRK1s have an important role in the regulation of the degradation of seed storage compounds, necessary to sustain seedling life before the acquisition of photosynthetic

capacity.

BIBLIOGRAPHY

- Alonso, R., Oñate-Sánchez, L., Weltmeier, F., Ehlert, A., Diaz, I., Dietrich, K., ... Dröge-Laser, W. (2009). A pivotal role of the basic leucine zipper transcription factor bZIP53 in the regulation of Arabidopsis seed maturation gene expression based on heterodimerization and protein complex formation. *The Plant Cell*, 21(6), 1747–61. doi:10.1105/tpc.108.062968
- Baena-González, E. (2010). Energy signaling in the regulation of gene expression during stress. *Molecular Plant*, 3(2), 300–13. doi:10.1093/mp/ssp113
- Baena-González, E., Rolland, F., Thevelein, J. M., & Sheen, J. (2007). A central integrator of transcription networks in plant stress and energy signalling. *Nature*, 448(7156), 938–42. doi:10.1038/nature06069
- Baena-González, E., & Sheen, J. (2008). Convergent energy and stress signaling. *Trends in Plant Science*, 13(9), 474–82. doi:10.1016/j.tplants.2008.06.006
- Bitrián, M., Roodbarkelari, F., Horváth, M., & Koncz, C. (2011). BAC-recombineering for studying plant gene regulation: developmental control and cellular localization of SnRK1 kinase subunits. *The Plant Journal : For Cell and Molecular Biology*, 65(5), 829–42. doi:10.1111/j.1365-313X.2010.04462.x
- Bolton, M. (2009). Primary metabolism and plant defense-Fuel for the fire. *Molecular Plant-Microbe Interactions*, 22(5), 487–497. Retrieved from <http://apsjournals.apsnet.org/doi/pdf/10.1094/MPMI-22-5-0487>
- Dietrich, K., Weltmeier, F., Ehlert, A., Weiste, C., Stahl, M., Harter, K., ... Dröge-Laser, W. (2011). Heterodimers of the Arabidopsis Transcription Factors bZIP1 and bZIP53 Reprogram Amino Acid Metabolism during Low Energy Stress. *The Plant Cell Online*, 23(January), 381–395. doi:10.1105/tpc.110.075390
- Ehlert, A., Weltmeier, F., Wang, X., Mayer, C. S., Smeekens, S., Vicente-Carbajosa, J., & Dröge-Laser, W. (2006). Two-hybrid protein-protein interaction analysis in Arabidopsis protoplasts: establishment of a heterodimerization map of group C and group S bZIP transcription factors. *The Plant Journal : For Cell and Molecular*

Biology, 46(5), 890–900. doi:10.1111/j.1365-313X.2006.02731.x

Hanson, J., Hanssen, M., Wiese, A., Hendriks, M. M. W. B., & Smeekens, S. (2008). The sucrose regulated transcription factor bZIP11 affects amino acid metabolism by regulating the expression of ASPARAGINE SYNTHETASE1 and PROLINE DEHYDROGENASE2. *The Plant Journal : For Cell and Molecular Biology*, 53(6), 935–49. doi:10.1111/j.1365-313X.2007.03385.x

Kirchler, T., Briesemeister, S., Singer, M., Schütze, K., Keinath, M., Kohlbacher, O., ... Chaban, C. (2010). The role of phosphorylatable serine residues in the DNA-binding domain of Arabidopsis bZIP transcription factors. *European Journal of Cell Biology*, 89(2-3), 175–83. doi:10.1016/j.ejcb.2009.11.023

Lastdrager, J., Hanson, J., & Smeekens, S. (2014). Sugar signals and the control of plant growth and development. *Journal of Experimental Botany*, 1–9. doi:10.1093/jxb/ert474

Lo, W. S., Duggan, L., Emre, N. C., Belotserkovskya, R., Lane, W. S., Shiekhattar, R., & Berger, S. L. (2001). Snf1--a histone kinase that works in concert with the histone acetyltransferase Gcn5 to regulate transcription. *Science (New York, N.Y.)*, 293(5532), 1142–6. doi:10.1126/science.1062322

Rahmani, F., Hummel, M., Schuurmans, J., Wiese-Klinkenberg, A., Smeekens, S., & Hanson, J. (2009). Sucrose control of translation mediated by an upstream open reading frame-encoded peptide. *Plant Physiology*, 150(3), 1356–67. doi:10.1104/pp.109.136036

Rolland, F., Baena-González, E., & Sheen, J. (2006). Sugar sensing and signaling in plants: conserved and novel mechanisms. *Annual Review of Plant Biology*, 57, 675–709. doi:10.1146/annurev.arplant.57.032905.105441

Schütze, K., Harter, K., & Chaban, C. (2008). Post-translational regulation of plant bZIP factors. *Trends in Plant Science*, 13(5), 247–55. doi:10.1016/j.tplants.2008.03.002

Sulpice, R., Pyl, E.-T., Ishihara, H., Trenkamp, S., Steinfath, M., Witucka-Wall, H., ... Stitt, M. (2009). Starch as a major integrator in the regulation of plant growth. *Proceedings of the National Academy of Sciences of the United States of America*, 106(25), 10348–53. doi:10.1073/pnas.0903478106

- Tachibana, C., Biddick, R., Law, G. L., & Young, E. T. (2007). A poised initiation complex is activated by SNF1. *The Journal of Biological Chemistry*, 282(52), 37308–15. doi:10.1074/jbc.M707363200
- Tomé, F., Nägele, T., Adamo, M., Garg, A., Marco-Llorca, C., Nukarinen, E., ... Gamm, M. (2014). The low energy signaling network. *Frontiers in Plant Science*, 5(July), 353. doi:10.3389/fpls.2014.00353
- Usadel, B., Bläsing, O. E., Gibon, Y., Retzlaff, K., Höhne, M., Günther, M., & Stitt, M. (2008). Global transcript levels respond to small changes of the carbon status during progressive exhaustion of carbohydrates in *Arabidopsis* rosettes. *Plant Physiology*, 146(4), 1834–61. doi:10.1104/pp.107.115592
- Wehner, N., Hartmann, L., Ehlert, A., Böttner, S., Oñate-Sánchez, L., & Dröge-Laser, W. (2011). High-throughput protoplast transactivation (PTA) system for the analysis of *Arabidopsis* transcription factor function. *The Plant Journal : For Cell and Molecular Biology*, 68(3), 560–9. doi:10.1111/j.1365-313X.2011.04704.x
- Weiste, C., & Dröge-Laser, W. (2014). The *Arabidopsis* transcription factor bZIP11 activates auxin-mediated transcription by recruiting the histone acetylation machinery. *Nature Communications*, 5(May). doi:10.1038/ncomms4883
- Xiong, Y., McCormack, M., Li, L., Hall, Q., Xiang, C., & Sheen, J. (2013). Glucose-TOR signalling reprograms the transcriptome and activates meristems. *Nature*, (15 mM). doi:10.1038/nature12030

Lorenzo Pedrotti, own contribution to the thesis

Chapter 1: Lorenzo Pedrotti (LP), together with Alessia Peviani and Abhroop Garg wrote the paragraph “SnRK1 regulates stress responses upon low energy”.

Chapter 2: LP wrote the entire chapter

Chapter 3: LP actively participate in the design of the experiments and in the discussion of the project. LP performed the protoplasts experiments. Results of the experiments performed by LP are depicted in:

Figure 4- figure supplement 2;

Figure 5.C

Figure 5- figure supplement 4;

Figure 7.A and B

Figure 7-figure supplement 1.A and B

Chapter 4: LP together with Wolfgang Dröge-Laser and Christoph Weiste designed all the experiments. LP performed all the experiments except those whose results are depicted in:

Figure 4.A and B → Christoph Weiste

Figure S2 → Thomas Nägele

Chapter 5: LP together with Katrin Dietrich generated the *snrk1.1/1.2* mutant lines used in this work. LP performed the experiments whose results are depicted in

Figure 6.A

Chapter 6: LP design and performed all the experiments except the metabolomics measurements whose results are depicted in

Figure 3 → Agnes Fekete

Figure S1 → Agnes Fekete

Figure S3 – Agnes Fekete

Chapter 7: LP wrote the entire chapter

More information about contribution to every chapter could be find in the “Author contribution” paragraph.

Lorenzo Pedrotti, *Curriculum Vitae*

Lorenzo Pedrotti was born in Rovereto on the 27th of February 1987. He lived and grown up in the surrounding area. After attending the technical high school “I.T.I.S. M. Buonarroti” in Trento he received the High School Diploma in 2006. After that, he moved to Padova, where he studied molecular biology. He achieved the Bachelor degree in “Molecular Biology” in 2009 and the Master degree in 2011. Via the ERASMUS program he spent the 5th year of the university studies at the University of Wuerzburg. In August 2011 he started the research activities for the achievement of his PhD title in the lab of Prof. DR. Wolfgang Dröge-Laser. From April 2015 Lorenzo is assistant of Microbiology and Fermentation Technology at Sandoz Industrial Product S.p.a., Rovereto (Italia).

Acknowledgment

I would like to thank all the people with whom I worked in the last three and a half years. In particular I would like to thank first of all Wolfgang for the guidance. I would like to thank Katrin, which left me a very well-running project. Thanks Christoph, for the scientific conversations we had, for your immense help, supervision, and patience. Thank you Jasmine, for the very friendly and relaxed coffee-breaks (and help with the protoplasts), and thanks Elisabeth, especially for your moral support during the last months. Thanks Christian, for the happy environment. I would like to thank Frank, it was because of you that I got in contact with Würzburg. Thank you Agnes to be there always at the right time. Special thanks go to the MERIT friends, and to all the friends old and new.

I would like to express my deepest gratitude towards my family and Francesca, who have supported me during my university years, the PhD and in all the decisions I have taken.

Thank you to all the people that made these years so special:

I feel so grateful to have met you all!

Lorenzo Pedrotti
fraz. Savignano n.48/a
38060 Pomarolo (TN)
Italy

Tel.: 0039-3488730386
E-Mail: lorenzo.pedrotti@virgilio.it

Erklärungen nach §4 Abs. 3 Satz 3, 5, 8 der Promotionsordnung der Fakultät für Biologie

Affidavit

I hereby declare that my thesis entitled: „**The SnRK1-C/S1-bZIPs network: a signalling hub in *Arabidopsis* energy metabolism regulation** ” is the result of my own work.

I did not receive any help or support from commercial consultants. All sources and / or materials applied are listed and specified in the thesis.

Furthermore I verify that the thesis has not been submitted as part of another examination process neither in identical nor in similar form.

Eidesstattliche Erklärung

Hiermit erkläre ich an Eides statt, die Dissertation: „**The SnRK1-C/S1-bZIPs network: a signalling hub in *Arabidopsis* energy metabolism regulation** ”, eigenständig, d. h. insbesondere selbständig und ohne Hilfe eines kommerziellen Promotionsberaters, angefertigt und keine anderen, als die von mir angegebenen Quellen und Hilfsmittel verwendet zu haben.

Ich erkläre außerdem, dass die Dissertation weder in gleicher noch in ähnlicher Form bereits in einem anderen Prüfungsverfahren vorgelegen hat.

_____, den _____

Unterschrift